THE ASTROPHYSICAL JOURNAL

AN INTERNATIONAL REVIEW OF SPECTROSCOPY AND ASTRONOMICAL PHYSICS

VOLUME 93 MARCH 1941 NUMBER 2

FREDERICK EUGENE FOWLE

C. G. ABBOT

Frederick Eugene Fowle, son of Frederick E. and Mary Proctor Fowle, was born at Arlington, Massachusetts, on November 20, 1869. He died after a long illness at Washington, D.C., on April 22, 1940.

As a youth he spent much time out of doors, taking long walks and familiarizing himself with fauna and flora. Precocious at school, he was keen at mathematics but was also deeply interested in languages and music—avocations which continued to attract him greatly through his later years. Another hobby was the association with people a little different from others. Throughout his life he took much enjoyment in seeking out and becoming intimate with eccentric persons whom most people would pass by.

For several years in his youth he was an assistant at Harvard College Observatory, where Professors E. S. King and W. Gerrish were among his close friends. George E. Hale's early work there with the spectroheliograph was done at that time. This preliminary astronomical service led to Fowle's entering the Massachusetts Institute of Technology several years older than his classmates. He was graduated as B.Sc. in physics, with high honors, in the year 1894. Through Professor C. R. Cross's recommendation he was engaged immediately by Secretary S. P. Langley as assistant at the Astrophysical Observatory of the Smithsonian Institution at Washington. A year later his classmate at Massachusetts Institute of Technology, the present writer, was also engaged there, and we remained associated for nearly forty years.

Fowle's early work at the Astrophysical Observatory does not seem to have been adequately appreciated by Langley. To him Fowle was merely a photographer, although photography was only an avocation with Fowle and one of many sidelines in which he was proficient. Langley's lack of appreciation of Fowle was largely due to Fowle's cautious Scotch way of answering. He was always chary of committing himself, whereas Langley wanted an immediate answer—yes or no. Besides this Fowle had a slight impediment of speech, which was aggravated by embarrassment.

It was not until after Langley's death, in 1906, that Fowle began to have due recognition, either in salary or in scientific reputation. By that time we were already launched on the measurement of the solar constant of radiation and in determinations of the variation of the sun, which are still the chief features of the Observatory work.

Fowle and I, though conscious that we were doing exact observing— as, for instance, in our determination of the dispersion of rock salt—were troubled in those times by an

inferiority complex. We were but young assistants and worked in a temporary shed, while others occupied famous observatories. Hence it proved a real and very helpful stimulation to conduct a large eclipse expedition to Wadesboro, North Carolina, in 1900. Professor E. C. Pickering had loaned some apparatus, including a 12-inch lens of 135-foot focus, and an objective prism of equal size. One day at Washington I had gone home early, leaving Fowle to put away the apparatus. He had unluckily tripped on a tent peg and, falling, had chipped a small piece out of Pickering's lens. Hence we went to Wadesboro feeling more downcast than usual, and very small indeed compared to the famed astronomers of Yerkes Observatory, of Princeton, and those from England who were to be there also. What bucked us up was something that happened the night before the eclipse.

We had set up our objective-prism spectroscope with a reflecting mirror and intended to obtain spectrum lines parallel to the center of the vanishing crescent. But it suddenly occurred to one of us that we had not correctly considered the effect of the mirror reflection. When we felt sure, we called in the late C. E. Mendenhall, and after two hours of hot discussion we convinced him. But Hale and Goodwin were evidently in the same predicament as ourselves. So we called them in about midnight and after another long discussion convinced them also. It was, as may well be understood, a triumph for us boys, and ever after we felt more on an equality with the astronomical world! Hale and Goodwin made a hurried readjustment as soon as the sun appeared, but we contented ourselves with cusp spectra.

It is hard to separate the work on the solar constant done by Fowle and by myself over many years. But I did most of the expeditionary work and Fowle had charge of the measurement and computing at Washington. I relied heavily on his attainments in physics and mathematics, his reserved judgment, his knowledge of men's characters, and his great skill in measurement and computation. His work on the reduction of my observations on the contrast of brightness along a diameter of the sun's disk was especially careful and laborious.

Fowle became greatly interested in the study of the absorption of solar radiation by water vapor and ozone and in the scattering of radiation by small particles within the atmosphere. In the year 1914, from our measures of atmospheric transmission he computed the number of molecules per cubic centimeter of dry air at standard pressure as 2.68×10^{19}, in close agreement with the best present values by other methods. As his greatest individual investigation, he made many infrared spectral measurements through long columns of air containing known quantities of water vapor. Thereby, in the first instance, he was able to discover a valuable method for determining the total thickness of precipitable water between the observer and the sun, from bolographs of the solar spectrum. We use this method constantly as a fundamental feature of solar constant determination. Some years ago, with a special portable apparatus for measuring precipitable water by Fowle's method, our Mr. Moore examined the relative merit of a half-dozen stations in Africa for solar observations. The Weather Bureau became interested, and the Smithsonian Institution has recently constructed for them an improved instrument of that type.

Fowle's further experiments with the long tube related to the absorption of atmospheric vapors at great wave lengths. They resulted in a great increase of our knowledge of the absorption of water vapor and ozone in the solar spectrum and the terrestrial spectrum, up to wave lengths of 14 microns.

He also turned his attention to the absorption of ozone in the yellow-green region of the solar spectrum and published several papers giving indications of the variation of ozone from place to place and from time to time.

Still better known, and more generally useful, were Fowle's labors as editor of the *Smithsonian Physical Tables*. He carried them through four editions, always amplifying and taking great pains toward correctness. Physicists and engineers well know how

much they are indebted to Fowle for putting in their hands this brief compendium of knowledge culled from world-wide sources. They will be glad, I am sure, to know that the Institution has arranged with Fowle's successor, W. H. Hoover, to continue the editorship of these invaluable tables.

Fowle was twice married—first in 1894 to Susie Gates, of Arlington, Massachusetts, by whom he had two children, Elsa and Walter, who survive him. He married, in 1930, Juliana Thomasson, of North Dakota, who survives him.

He was a fellow of the American Association for the Advancement of Science, the American Astronomical Society, the American Physical Society, and of the Optical Society of America. He also held membership in the Washington Philosophical Society, the Washington Academy of Science, the National Geographic Society, the American Museum of Natural History, and the Sons of the American Revolution.

His principal papers are the following:

"The Absorption of Water Vapor in the Infra-red Solar Spectrum," *Smith. Misc. Coll.*, **47**, 1, 1904.
"The Discrepancy between Solar Radiation Measures by the Actinometer and by the Spectrobolometer," *ibid.*, p. 399, 1905.
"The Spectroscopic Determination of Aqueous Vapor," *Ap. J.*, **35**, 149, 1912.
"The Determination of Aqueous Vapor above Mount Wilson," *ibid.*, 1913.
"The Nonselective Transmissibility of Radiation through Dry and Moist Air," *ibid.*, **38**, 393, 1913.
"Avogadro's Constant and Atmospheric Transparency," *ibid.*, **40**, 435, 1914.
"Die Durchlässigkeit der Atmosphäre für Strahlung," *Met. Zs.*, p. 270, 1914.
"Atmospheric Transparency for Radiation," *M. Weather Rev.*, p. 1, 1914.
"The Transparency of Aqueous Vapor," *Ap. J.*, **42**, 394, 1915.
"Smithsonian Physical Tables: Second Reprint of the Sixth Revised Edition with Further Changes," *Smith. Misc. Coll.*, **63**, No. 6, 1916.
"Water-Vapor Transparency to Low-Temperature Radiation," *ibid.*, **68**, No. 8, 1917.
"The Atmospheric Scattering of Light," *ibid.*, **69**, No. 3, 1918.
"Smithsonian Physical Tables: Third Reprint of the Sixth Revised Edition with Further Additions," *ibid.*, **63**, No. 6, 1918.
"Smithsonian Physical Tables: Seventh Revised Edition," *ibid.*, **71**, No. 1, 1920.
"Ozone in the Northern and Southern Hemispheres," *J. Mag. and Atm. Elect.*, No. 3, p. 151, 1928.
"Atmospheric Ozone: Its Relation to Some Solar and Terrestrial Phenomena," *Smith. Misc. Coll.*, **81**, No. 11, 1930.
"Ozone: Is It Due to Corpuscular or Ultra-violet Emission from the Sun or Both?" *Trans. of the Amer. Geophys. Union*, p. 73, 1930.
"Atmospheric Turbidity," *ibid.*, p. 87, 1931.
"Smithsonian Physical Tables: Eighth Revised Edition," *Smith Misc. Coll.*, **88**, 1934.

THE LUMINOSITIES OF THE NONVARIABLE c STARS*

RALPH E. WILSON

ABSTRACT

The mean absolute magnitudes of nonvariable c stars have been determined from radial velocities (205 stars) and proper motions (241 stars). The value derived from all the stars is $\bar{M} = -4.40$. It is found, however, that the stars with early-type spectra are much brighter than those of late type, the values of $\bar{M}$ decreasing continuously from -5.4 for type Bo to -2.0 for type K5.

The spectrum-luminosity relation for the Cepheids, the spectra of which on low-dispersion spectrograms are quite similar to those of the nonvariable c stars, runs in the opposite direction. The conclusion is that within this rather rare class of stars there exist two luminosity sequences, in one of which the stars are essentially nonvariable, while in the other all are subject to a single type of light-variation.

The stars of division c of Miss Maury's classification[1] of spectra form an interesting and definite, though far from homogeneous, group. They are differentiated from other stars of the same general spectral types by the narrowness and sharpness of the lines and in the later types by increasingly abnormal intensity of the hydrogen lines. These characteristics are accompanied in certain types by abnormal intensity and sharpness of lines of *O* II and *N* II and of certain metals, notably *Fe* II, *Si* II, *Si* III, and *Sr* II.

These stars are supergiants, many fold brighter intrinsically than the normal stars of early type and the normal giants of late type. They are probably representative of the high-luminosity stars in general, although absolutely bright stars are also found among stars with normal spectra. They constitute a large proportion of the high-luminosity stars whose parallaxes and corresponding luminosities, either as individuals or as members of clusters, have been determined with some degree of accuracy. Owing to their intrinsic brightness they can be recognized at distances much greater than can the normal stars. Thus, when their mean absolute magnitudes are known, they become useful in the estimation of great cosmic distances.

The Cepheid variables, all of which are probably c stars, are especially important in this connection because they can be recognized, even in extragalactic nebulae, from their light-curves. Certain, at least, of the nonvariable stars are known to be intrinsically much brighter than the Cepheids. That these have not been extensively used in the estimation of extragalactic distances is due primarily to the fact that recognition of the c characteristics must be by means of individual spectra, and these are difficult to obtain with sufficient dispersion for stars at great distances and with correspondingly faint apparent magnitudes. Within the galactic system, however, the nonvariable c stars should enable us to reach distances comparable to those reached by the Cepheids.

The earlier attempts to determine the mean absolute magnitudes of the c stars did not differentiate between the variables (Cepheids) and the nonvariables. From the parallactic motions of 400 stars, selected upon a broad definition of c characteristics and including the Cepheids, J. Schilt[2] in 1922 found $\bar{M} = -3.2$. He reached two additional conclusions which have been somewhat misleading. Finding no difference between the mean parallactic motions of the stars of early and of late types, he concluded that there was no difference between their respective absolute magnitudes. Evidence contradicting this is presented later in this paper. He also contended that the early-type c stars are not found at distances greater than 1.0 kpc—a conclusion logically untenable and prob-

* *Contributions from the Mount Wilson Observatory, Carnegie Institution of Washington*, No. 643.

[1] *Harvard Ann.*, **28**, Part 1, 1897. [2] *B.A.N.*, **2**, 47, 1922.

ably due, as Miss Payne[3] points out, to the difficulty of recognizing the c characteristics on faint spectra of low dispersion.

From a similar study of the proper motions of 109 stars K. F. Bottlinger[4] in 1931 found $\bar{M} = -3.4$, confirming Schilt's earlier value. It was even then clear that typical stars, such as β Orionis and α Cygni, must be considerably brighter than the mean values of Schilt and Bottlinger, and in 1935 P. W. Merrill[5] wrote concerning the early-type stars, "although the absolute magnitudes of these stars are not accurately known, it seems to be the consensus of opinion that -5.0 is a useful approximation." From a distance-intensity relation in the interstellar lines of calcium and sodium, established partly upon the mean absolute magnitudes of normal B and A stars and partly upon the assumption that $\bar{M} = -5.0$ for the c stars, Merrill and Sanford[6] in 1938 determined the absolute magnitudes of 58 early-type c stars, in whose spectra the intensities of the interstellar lines had been measured. From the mean values they concluded that the A stars were slightly brighter than the B's, the mean being -4.9.

Up to 1938 there had been no attempt of which the writer is aware to apply to the nonvariable c stars as a group the statistical methods quite successfully used to determine the mean absolute magnitudes of the Cepheids. It was clear at that time that we still had little definite knowledge of values of $\bar{M}$, especially for the late-type stars, and that an attempt should be made to obtain them.

METHOD

Several factors contribute to make these stars a rather ideal group to which to apply statistical methods. Many of them are apparently bright, and the radial velocities of the majority of those north of declination $-20°$ have been measured. Because few are spectroscopic binaries, two or three spectrograms usually suffice to give reliable radial velocities. Moreover, good proper motions are available for most of them; hence, mean angular parallactic and peculiar motions can be accurately determined. They are strongly concentrated toward the galaxy and therefore should give a good determination of the galactic rotation. And, finally, trigonometric and cluster parallaxes are available for a representative number, sufficient at least to give a reasonably accurate check upon the mean absolute magnitudes derived from the rotation factors and comparisons of parallactic and peculiar motions.

Let

V' = radial velocity, corrected for solar motion,
l, b = galactic longitude and latitude of star,
l_0 = galactic longitude of rotation center,
K = residual term,
$\bar{r}$ = mean distance,
A = constant of galactic rotation,
$\bar{m}_1$ = mean apparent magnitude, radial-velocity stars,
$\bar{M}_r$ = mean absolute magnitude from rotation,
$5C_1 = 5(\overline{\log r} - \log \bar{r})$, correction for dispersion in distance,
a = constant of galactic absorption,
$q = \dfrac{\Sigma v \sin \lambda}{\Sigma \sin^2 \lambda}$, the secular parallax, in seconds of arc,

[3] *The Stars of High Luminosity*, p. 57, 1930.

[4] *Veröff. Univ. Stern. Berlin-Babelsberg*, **8**, Heft 5, 4, 1931.

[5] *Mt. W. Contr.*, No. 512; *Ap. J.*, **81**, 354, 1935.

[6] *Mt. W. Contr.*, No. 585; *Ap. J.*, **87**, 123–124, 1938.

v = parallactic motion, in seconds of arc,
τ = peculiar motion, in seconds of arc,
V_0 = solar motion, in kilometers per second,
θ = mean peculiar motion, in kilometers per second,
$\bar{\pi}$ = mean parallax,
$\bar{\pi}_q$ = mean parallax from parallactic motion,
p_1 = weight of $\bar{\pi}_q$,
$\bar{\pi}_\tau$ = mean parallax from peculiar motions,
p_2 = weight of $\bar{\pi}_\tau$,
$\bar{m}_2$ = mean apparent magnitude of proper-motion stars,
$\bar{M}_\pi$ = mean absolute magnitude from mean parallax,
$5C_2 = 5(\overline{\log \pi} - \log \bar{\pi})$, correction for dispersion in parallax,
$c = \bar{\pi} \cdot \bar{r} > 1$.

The determinations of the mean absolute magnitudes then employ the following relations:

$$\overline{V'} = \bar{r}A \overline{\sin 2(l - l_0) \cos^2 b} + K , \tag{1}$$

$$\bar{M}'_r = \bar{m}_1 + 5 - 5 \log \bar{r} , \tag{2}$$

$$\bar{M}_r = \bar{M}'_r - 5C_1 - \frac{a\bar{r}}{1000} , \tag{3}$$

$$\bar{\pi}_q = 4.74 \frac{q}{V_0} , \qquad \bar{\pi}_\tau = 4.74 \frac{|\bar{\tau}|}{\theta} , \tag{4}$$

$$\bar{\pi} = \frac{p_1\bar{\pi}_q + p_2\bar{\pi}_\tau}{p_1 + p_2} , \tag{5}$$

$$\bar{M}'_\pi = \bar{m}_2 + 5 + 5 \log \bar{\pi} , \tag{6}$$

$$\bar{M}_\pi = \bar{M}'_\pi + 5C_2 - \frac{ac}{1000\bar{\pi}} , \tag{7}$$

$$\bar{M}' = \tfrac{1}{2}(\bar{M}'_r + \bar{M}'_\pi) , \tag{8}$$

$$\bar{M} = \tfrac{1}{2}(\bar{M}_r + \bar{M}_\pi) . \tag{9}$$

The most troublesome factor in the determination of mean absolute magnitudes arises from the fact that all the stars are not at the same distance. While the dispersions in $\log r$ and $\log \pi$ may be approximately equal, those in r and π involved in equations (2) and (6) are not. Exact calculations of the corrections necessary to eliminate the effects of these dispersions are impossible; and when the values of $\bar{M}$ are dependent upon but one of the co-ordinates, $\bar{r}$ or $\bar{\pi}$, assumptions as to the dispersions have to be made. Since $\log \bar{r} > \overline{\log r}$, the values of $\bar{M}'_r$ given by equation (2) are too bright. Likewise, since $\pi = 1/r$, the values of $\bar{M}'_\pi$ given by equation (6) are too faint. If the data suffice to make these values of $\bar{M}'_r$ and $\bar{M}'_\pi$ significant, the true value of $\bar{M}$ must lie between them. If identical stars are used in the calculations of $\bar{r}$ and $\bar{\pi}$, $\bar{m}_1 = \bar{m}_2$ and the dispersions in $\log r$ and $\log \pi$ are equal. If the distribution in $\log \pi$ or $\log r$ is Gaussian, $C_1 = C_2$, and the effects of dispersion disappear in the means, equations (8) and (9). If, as in the

present case, a large proportion of the stars are common to both sets of data—radial velocities and proper motions—the difference between the corrections for dispersion is small[7] and has little effect upon $\bar{M}$. A good approximation to the value of $\bar{M}$ is, therefore, given by the relation

$$\bar{M} = \tfrac{1}{2}(\bar{M}'_r + \bar{M}'_\pi) - \frac{a\bar{r}}{1000}\,. \qquad (10)$$

Though the difference, $\bar{M}'_r - \bar{M}'_\pi$, which is approximately equal to $5(C_1 + C_2)$, is sensitive to differences in data and departures from the assumptions involved, it enables one to obtain an estimate at least of the "index of dispersion" c, since $\log c = -(C_1 + C_2)$ approximately.

DATA

A decision had to be made at the start as to what constitutes a c star. Notes in the *Henry Draper Catalogue*, summarized in Miss Payne's "Catalogue of c Stars,"[8] contain

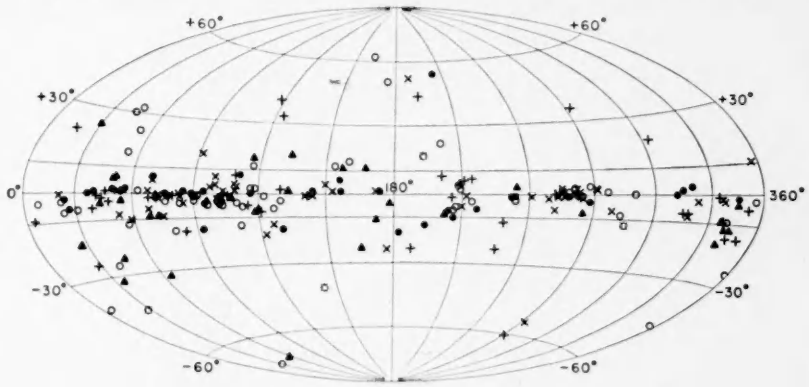

FIG. 1.—Galactic distribution of nonvariable c stars. Spectral classes are indicated as follows: B, dots; A, crosses; F, plus signs; G, circles; and K, filled triangles.

the comments concerning the spectral lines, "very narrow," "narrow," "somewhat narrow," "appear narrow," and "probably narrow." Examinations, mainly at Mount Wilson, of the lines on plates taken with slit spectrographs showed that, while nearly all the stars of the first two categories could be safely classified as c stars, those of the last three contained an appreciable number of miscellaneous spectra which should be eliminated from the list. The selection was, therefore, based for the most part on observations with slit spectrographs and compiled mainly from P. W. Merrill's "Partial List of c Stars of Classes A and B"[9] and those designated as c stars in the Mount Wilson catalogue of spectroscopic absolute magnitudes.[10] To these were added a few stars from J. H. Moore's *Catalogue of Radial Velocities*,[11] mainly far south and presumably classified from slit spectrograms taken by the Mills Expedition. Finally from Miss Payne's catalogue were added 25 stars not observed with slit spectrographs but having spectra described from objective-prism observations as "very narrow" or "narrow," for which radial velocities or proper motions are available.

The catalogue in Table 1 gives the observed data for 246 nonvariable c stars. The

[7] R. E. Wilson, *Mt. W. Contr.*, No. 615; *Ap. J.*, **90**, 361–362, 1939.

[8] *Op. cit.*, pp. 287–307.

[9] *Mt. W. Contr.*, No. 512; *Ap. J.*, **81**, 352, 1935.

[10] Adams, Joy, Humason, and Brayton, *Mt. W. Contr.*, No. 511; *Ap. J.*, **81**, 187, 1935.

[11] *Pub. Lick Obs.*, **18**, 1932.

TABLE 1

CATALOGUE OF NONVARIABLE c STARS

HD No.	α 1900	δ 1900	m_v	Sp.	V	μ	l	b	π_h	π_t	π_s	Remarks
					km/sec							
571	$0^h\ 5^m1$	+45° 31′	5.1	cF2	− 6.	0″.005± 1	84°	−16°	0″.0013	−0″.006	0″.010	
698	6.3	+57 39	7.1	cB8	−24.5	.013 9	85	− 4	.....	.....	.....	
2885	27.0	−63 31	4.5	cA2	+10.4	.120 4	272	−54	.....	+ .036	.015	β_2 Tuc* 1
2905	27.3	+62 33	4.2	cB0	− 4.1	.005 1	89	0	.0015	.....	.003	
3980	37.2	−57 3	5.8	cF0	+ 9.8	.095 4	271	−61	.....	.....	.....	ξ Phe*
4362	0 40.9	+59 2	6.5	cF9	.....	.009 4	90	− 3	.0011	.....	.002	
4817	45.2	+61 16	6.4	cK5	.....	.008 6	91	− 1	.002	.....	.001	
4841	45.4	+63 14	7.1	cB5	−29.6	.020 8	90	− 1	.....	.....	.....	
6226	58.2	+47 6	6.7	B5s	−63.9	.006 5	93	−15	.....	.....	.....	a
7902	1 13.6	+57 40	7.9	cB5	.....	.002 4	95	− 4	.....	.....	.....	
7927	1 13.8	+57 42	5.5	cF7	−24.7	.002 2	95	− 4	.002	− .006	.002	φ Cas
8065	15.0	+78 12	6.1	cA2	−76.	.008 3	92	+16	.....	.....	.....	
9105	24.6	+62 51	7.5	cB5	−39.9	.016 5	95	+ 1	.0005	.....	.....	†?
9352	27.0	+57 49	6.0	cK1	− 0.6	.006 9	96	− 4	.002	.....	.003	
12301	55.6	+63 54	5.6	cB8	−20.4	.004 2	98	+ 3	.0010	.....	.005	
12953	2 1.7	+57 57	5.9	cA2	−37.2	.012 2	101	− 2	.0010	.....	.....	†
13267	4.6	+57 11	6.4	cB8	−34.4	.015 2	101	− 3	.0008	.....	.....	†
13476	6.6	+58 6	6.5	cA0	−38.	.026 9	101	− 2	.0008	.....	.....	†
13744	8.9	+57 50	7.8	cA0	−51.	.003 9	102	− 2	.0005	.....	.....	†
13841	9.8	+56 34	7.2	cB2	−39.4	.001 4	102	− 3	.0005	.....	.001	†
13854	2 9.9	+56 36	6.4	cB1	−40.0	.001 4	102	− 3	.0007	.....	.001	†
13866	10.0	+56 15	7.7	cB2	−47.6	.026 10	102	− 4	.0005	.....	.001	†
14010	11.1	+63 58	7.0	cB8	−47.0	.004 3	100	+ 4	.0006	.....	.....	†
14134	12.1	+56 40	6.7	cB3	−43.4	.006 3	102	− 3	.0006	.....	.....	†
14143	12.2	+56 43	6.7	cB1	−45.2	.006 4	102	− 3	.0006	.....	.001	†
14322	2 13.8	+55 27	6.8	cB9	−37.	.013 7	103	− 4	.0007	.....	.001	†
14433	14.8	+56 47	6.5	cA2	−46.1	.010 3	103	− 3	.0008	.....	.001	†
14489	15.3	+55 23	5.2	cA2	−16.	.001 2	103	− 4	.0013	.....	.001	
14535	15.8	+56 47	7.5	cA2	−53.	.007 4	103	− 3	.0006	.....	.....	†
14542	15.9	+56 56	7.0	cB9	−51.4	.001 3	103	− 3	.0006	.....	.....	†
14662	2 16.9	+54 55	6.5	cF8	−26.2	.032 8	104	− 4	.0011	.....	.001	†
14818	18.2	+56 10	6.2	cB1	−47.0	.010 2	103	− 3	.0007	.....	.001	†
14889	19.2	+56 47	7.4	cA0	−42.0	.017 6	103	− 3	.0006	.....	.....	†
14956	19.6	+57 14	7.3	cB1	−30.3	.017 8	103	− 3	.0005	.....	.....	†
15084	20.8	+66 57	4.7	cA4	+ 0.5	.021 1	100	+ 7	.002	+ .022	.019	ϵ Cas 2
15316	2 22.8	+57 22	7.3	cA2	−44.	.029 8	104	− 2	.0006	.....	.....	†
15963	28.9	+57 38	8.0	cA0	.....	.008 11	104	− 1	.....	.....	.....	†?
16778	36.3	+59 24	7.7	cB9	−36.	.010 9	104	+ 1	.0005	.....	.003	
16901	37.6	+43 52	5.6	cG0	− 3.5	.008 3	111	−13	.0013	.....	.....	
17378	42.2	+56 40	6.5	cA8	.....	.010 4	106	− 1	.0009	.....	.....	
17506	2 43.4	+55 29	3.9	cK4	− 1.1	.023 1	107	− 2	.007	+ .001	.005	η Per
18925	57.6	+53 7	3.4	cF7	+ 1.0	.005 1	110	− 4	.004	+ .011	.018	γ Per
19926	3 7.1	+ 6 17	6.1	cG2	.....	.004 3	142	−41	.0011	.....	.004	
20041	8.2	+56 45	5.9	cA0	−13.	.006 3	109	+ 1	.....	.....	.....	
20123	9.1	+50 34	5.3	cG2	+ 2.2	.017 3	113	− 5	.002	.....	.005	
20210	3 9.8	+34 19	6.4	A2	.....	.058 5	122	−18	.....	.....	.....	a
20902	17.2	+49 30	1.9	cF4	− 2.4	.035 1	115	− 5	.006	+ .009	.024	α Per
21291	21.0	+59 36	4.4	cB9	− 7.2	.001 1	109	+ 4	.002	.....	.004	
21389	21.9	+58 32	4.8	cA0	− 7.2	.007 2	110	+ 3	.0014	.....	.001	
21771	25.5	+44 30	7.8	cG8	.....	.008 8	118	− 8	.0010	.....	.002	
23082	3 37.2	+44 34	7.8	cK5	+ 8.2	.033 10	120	− 7	.0014	.....	.001	
23089	37.3	+63 2	5.3	cF5	− 2.8	.010 3	109	+ 8	.0015	− .001	.007	
23193	38.1	+36 9	5.6	cA3	+21.8	.060 4	126	−13	.0008	.....	.014	
23230	38.4	+42 16	3.9	cF4	−13.0	.010 1	121	− 8	.003	+ .016	.010	ν Per
23675	41.9	+52 21	6.8	cB1	− 1.9	.006 4	116	0	.....	.....	.....	
24398	3 47.8	+31 35	2.9	cB1	+20.9	.016 1	130	−15	.002	+ .010	.007	ζ Per 3
25056	53.8	+53 35	7.4	cG2	− 6.3	.004 8	116	+ 2	.0009	.....	.001	
25443	57.4	+61 48	6.8	cB2	− 1.6	.006 7	111	+ 8	.....	.....	.....	
25878	4 0.9	+53 6	7.1	cG1	+15.9	.006 6	118	+ 2	.0009	.....	.001	
26630	7.6	+48 9	4.6	cG2	+ 7.8	.024 1	122	− 1	.003	+ .013	.005	μ Per
26673	4 8.1	+40 14	5.2	cG3	+ 3.	.030 2	127	− 7	.002	+ .002	.006	
29094	29.8	+41 4	4.8	cG2	+ 3.7	.021 3	130	− 3	.002	+ .021	.006	
31767	53.4	+ 1 34	4.7	cK3	+14.0	.003 2	165	−23	.004	+ .014	.008	
31910	54.5	+60 18	4.2	cG2	− 1.7	.015 1	117	+12	.003	+ .014	.004	β Cam
31964	54.8	+43 41	3.3	cF2	− 4.1	0.006± 1	130	+ 2	0.003	+0.002	0.010	ϵ Aur

TABLE 1—*Continued*

HD No.	α 1900	δ 1900	m_v	Sp.	V	μ	l	b	π_h	π_l	π_s	Remarks
					km/sec							
32068	4h55m5	+40° 56′	4.4	cK4	+11.0	0″.027± 1	133°	+ 1°	0″.005	+0″.001	0″.004	ζ Aur
34085	5 9.7	− 8 19	0.3	cB8	+23.6	.005 1	177	−24	.009	+ .006	.006	β Ori 4
34255	11.0	+62 33	5.9	cK4	− 5.3	.004 6	116	+15	.003	.....	.003	c
34452	12.4	+33 39	5.4	Aop	+28.6	.031 3	141	− 1	.0011	.....	.006	
34578	13.4	+33 52	5.2	cA5	− 4.2	.012 3	141	− 1	.0013	.....	.022	
35600	5 20.8	+30 7	5.7	cB9	+13.6	.018 5	144	− 1	.0010	.....	.005	
36371	26.2	+32 7	4.9	cB3	− 0.2	.006 2	144	+ 1	.0012	.....	.004	χ Aur
36673	28.3	−17 54	2.7	cF3	+24.	.011 1	188	−24	.004	− .003	.019	α Lep
38771	43.0	− 9 42	2.2	cBo	+20.1	.008 1	182	−17	.003	.....	.006	κ Ori
39400	47.2	+ 1 50	5.0	cK2	+10.4	.005 2	172	−11	.003	+ .002	.005	
39070	5 50.9	+24 14	6.0	cB9	− 3.	.009 5	153	+ 1	.....	.....	.....	
40589	54.7	+27 35	6.1	B8p	.....	.005 4	150	+ 4	.....	.....	.....	b
41117	58.0	+20 8	4.7	cB1	+16.5	.010 2	157	+ 1	.0012	.....	.002	
43384	6 10.8	+23 46	6.3	cB3	+11.6	.007 2	156	+ 6	.0007	.....	.001	
44537	17.2	+49 20	5.1	K2	+ 4.2	.006 2	133	+17	.003	+ .003	.003	
44743	6 18.3	−17 54	2.0	cB1	+34.4	.001 1	194	−13	.004	+ .018	.009	β CMa
45348	21.7	−52 38	−0.9	cF1	+20.5	.030 2	228	−24	.020	+ .015	.016	α Car
45416	22.1	+ 0 22	5.3	cKo	+32.5	.011 3	178	− 4	.003	+ .002	.005	
46300	27.5	+ 7 24	4.5	cAo	+15.6	.006 2	172	+ 1	.002	+ .000	.005	
47129	32.0	+ 6 13	6.1	O8	+23.9	.009 7	174	+ 1	.....	.....	.....	a
47731	6 35.0	+28 17	6.5	cG5	− 4.3	.015 2	154	+12	.0012	.....	.002	
48329	37.8	+25 14	3.2	cG5	+ 9.9	.013 1	157	+11	.006	+ .008	.009	ε Gem
50877	50.0	−24 4	4.1	cK5	+30.3	.013 2	202	− 9	.006	− .001	.005	
52005	54.5	+16 13	5.9	cK4	+21.9	.007 2	167	+11	.003	.....	.002	
52089	54.7	−28 50	1.6	cB1	+27.4	.008 1	207	−10	.004	.....	.010	ε CMa 5
52497	6 56.3	+24 21	5.2	cG2	− 8.8	.002 2	160	+14	.002	+ .013	.005	ω Gem
53138	58.8	−23 41	3.1	cB3	+48.6	.006 2	204	− 7	.002	.....	.007	
54005	7 4.3	−26 14	2.0	cG3	+34.3	.006 1	206	− 7	.008	− .019	.007	δ CMa
57146	14.8	−26 24	5.4	cG5	+33.1	.016 5	207	− 5	.002	.....	.002	
58350	20.1	−29 6	2.4	cB7	+40.4	.007 1	210	− 5	.004	.....	.012	η CMa
59612	7 25.6	−22 49	4.8	cA7	+36.3	.005 6	205	− 1	.002	− .007	.017	b
60098	27.8	−35 56	6.5	B5p	.....	.024 8	217	− 7	.....	.....	.....	
61715	35.5	−48 22	5.6	cF5	+11.0	.009 5	229	−12	.....	.....	.....	
62058	37.0	−31 25	6.6	Gop	.....	.020 8	214	− 3	.....	.....	.....	a
62623	39.8	−28 43	4.1	cA2	+30.	.004 2	212	− 1	.002	+ .022	.....	
63700	7 45.1	−24 37	3.5	cG6	+ 3.7	.002 1	209	+ 2	.005	− .002	.005	ξ Pup
64238	47.7	−14 35	5.7	cF3	.....	.010 3	201	+ 8	.0013	.....	.006	
65228	52.6	−22 37	4.4	cG2	+13.8	.026 2	208	+ 4	.003	+ .023	.004	
65339	53.2	+60 36	6.0	cA8	− 3.	.033 1	124	+33	.....	.....	.....	
65099	54.8	−23 2	5.2	cK2	+10.7	.007 4	209	+ 5	.004	− .007	.....	
67523	8 3.3	−24 1	3.2	cF5	+46.6	.097 1	211	+ 6	.....	+ .034	.016	ρ Pup*
67594	3.6	− 2 42	4.4	cG6	+29.6	.016 2	193	+17	.003	− .002	.005	ζ Mon
70761	18.6	−26 2	5.9	cF5	+64.0	.009 3	215	+ 7	.0012	− .009	.004	
74180	37.3	−46 18	4.1	cF8	+25.3	.008 3	233	− 2	.003	+ .026	.....	
74371	38.5	−45 3	5.2	B5	+24.6	.008 5	232	− 1	.0011	.....	.002	a
74395	8 38.8	− 6 52	4.7	cG4	+31.4	.004 3	201	+22	.003	− .001	.006	
75149	43.1	−45 32	5.5	cB5	+25.2	.012 4	233	− 1	.....	.....	.....	
75276	43.9	−45 48	5.8	cFo	+32.0	.008 5	233	− 1	.....	.....	.008	τ UMa*
78362	9 2.7	+63 55	5.0	cF6	− 6.5	.117 2	118	+40	.....	.....	.013	λ Vel
78647	4.3	−43 2	2.2	cK4	+18.4	.024 2	234	+ 3	.014	+ .018	.....	
80558	9 15.4	−51 8	5.9	cB8	.....	.019 6	241	− 1	.....	.....	.....	
81471	20.6	−51 18	6.1	cFo	.....	.009 6	241	0	.....	.....	.....	
83808	35.8	+10 21	4.5	cF5	+27.0	.143 1	193	+43	.....	+ .028	.009	o Leo*
84441	40.2	+24 14	3.1	cG3	+ 5.1	.043 1	175	+50	.005	+ .002	.013	ε Leo
86441	53.4	−57 11	7.4	Bo	.....	.009 11	249	− 2	.....	.....	.....	a
86557	9 54.1	−62 55	8.0	Bop	.....	.014 9	252	− 7	.....	.....	.....	a
87737	10 1.9	+17 15	3.6	cAo	+ 2.2	.004 1	188	+52	.002	− .006	.005	η Leo
90772	23.7	−57 8	4.9	cF1	− 1.2	.005 5	252	0	.002	− .016	.....	
91054	25.5	−59 6	7.8	A2	.....	.026 8	253	− 1	.....	.....	.....	a
91316	27.5	+ 9 49	3.8	cBo	+42.2	.003 1	204	+54	.0014	+ .012	.004	ρ Leo
91533	10 29.0	−58 9	6.2	cA2	.....	.020 6	253	0	.....	.....	.....	
92125	33.1	+32 30	4.8	cG2	− 6.8	.007 2	163	+62	0.002	+0.015	0.005	
92207	33.6	−58 13	5.6	cA2	var.	.027 5	254	0	.....	.....	.....	a
92964	38.8	−58 42	5.4	B1s	− 1.7	.006 4	255	− 1	.....	.....	.....	a
93619	43.3	−56 48	7.2	Ao	.....	0.014± 9	255	+ 1	.....	.....	.....	

TABLE 1—*Continued*

HD No.	α 1900	δ 1900	m_v	Sp.	V	μ	l	b	π_h	π_t	π_s	Remarks
					km/sec							
93737	10h44m2	−59° 24′	6.1	cA2	.....	0″.012± 6	256°	− 1°	0″.0009	.....	0″.001	
94367	48.4	−56 43	5.6	cB9	−22.5	.003 5	255	+ 2	.....	.....	.....	
95707	57.6	−61 1	7.7	B1p	.....	.007 8	258	− 1	.....	.....	.....	*a*
96918	11 4.3	−58 26	4.0	F8p	+ 7.3	.008 4	258	+ 1	.003	−0″.008	.....	*b*
97534	8.3	−59 46	4.7	cF5	− 8.4	.001 5	259	0	.002	.000	.....	
100198	11 26.6	−60 43	6.4	cA2	.....	.003 7	261	0	.....	.....	.....	
100261	27.1	−58 53	5.0	cG4	−19.5	.011 4	261	+ 2	.....	.....	.....	
100262	27.1	−58 58	5.3	cA2	−16.8	.016 5	261	+ 2	.....	.....	.....	
100826	31.1	−60 44	6.2	cA0	.....	.016 6	262	0	.....	.....	.....	
101570	36.2	−61 32	4.9	cG6	+14.2	.017 5	262	0	.....	.....	.....	
101947	11 38.8	−61 56	5.2	cG4	+10.1	.008 4	263	− 1	.002	+ .032	.....	
102839	45.2	−69 40	4.9	cK2	+18.2	.016 5	265	− 8	.004	.....	.004	
102878	45.5	−62 5	5.6	cA2	.....	.014 4	264	+ 1	.....	.....	.....	
103516	50.0	−62 43	6.0	cA2	.....	.022 8	264	− 1	.....	.....	.....	
104035	53.7	−63 47	5.7	cA2	.....	.005 6	265	− 2	.....	.....	.....	
108002	12 19.4	−64 39	7.3	cB1	.....	.047 9	268	− 3	.....	.....	.....	
108968	26.1	−58 52	5.4	cG2	−19.6	.020 4	268	+ 3	.002	+ .006	.....	
111613	45.4	−59 47	5.9	cA2	−22.0	.023 5	271	+ 2	.....	.....	.....	*a*
111904	47.4	−59 47	5.8	B9p	−15.	.014 5	271	+ 2	.....	.....	.....	
112374	51.1	−25 55	6.8	cF6	−22.0	.023 4	273	+36	.0007	.....	.003	
119796	13 41.4	−60 26	6.2	G5p	.....	.026 7	277	+ 1	.....	.....	.....	*a*
125835	14 16.8	−67 44	5.7	cA2	var.	.019 3	279	− 7	.....	.....	.....	
133683	15 0.6	−66 42	5.8	F8p	.....	.012 6	283	− 8	.....	.....	.....	*a*
135153	8.5	−31 9	5.0	cFc	−22.8	.004 3	304	+21	.0013	+ .008	.....	
141767	45.6	−68 18	5.2	cG6	+ 4.8	.020 3	286	−12	.002	+ .002	.....	κ Tri
146143	16 9.6	−49 49	5.0	cG4	−18.5	.012 4	290	0	.003	− .006	.....	
151985	45.6	−37 51	3.6	B2	+ 2.0	.032 3	314	+ 2	.002	.....	.007	μ^2 Sco *a*
152236	47.0	−42 12	4.9	cB1	−26.2	.009 5	311	0	.0011	.....	.002	
154090	58.2	−33 59	4.9	cB1	+10.2	.009 3	319	+ 3	.0011	.....	.003	
159181	17 28.2	+52 23	3.0	cG2	−20.1	.013 1	46	+32	.005	+ .003	.011	β Dra
159532	17 30.1	−42 56	2.0	cF1	+ 1.4	.013 2	315	− 7	.006	.....	.024	θ Sco
160529	35.3	−33 27	6.7	cA4	−32.	.007 8	323	− 3	.....	.....	.....	
161471	40.6	−40 5	3.1	cF6	−27.6	.006 2	318	− 7	.004	.....	.009	ι′ Sco
161796	42.5	+50 5	7.3	F8p	.....	.022 6	44	+30	.....	.....	.....	*a*
161912	43.1	−40 4	4.9	cA3	−18.0	.013 4	318	− 8	.0014	− .006	.014	
163506	17 51.4	+26 4	5.5	cF5	−29.4	.005 1	19	+22	.0011	− .005	.004	
163770	52.8	+37 16	4.0	cK1	−28.	.009 1	30	+25	.005	− .001	.009	θ Her
164353	55.6	+ 2 56	3.9	cB7	− 4.3	.013 1	357	+11	.002	− .004	.006	
164514	56.4	−22 54	7.3	cA8	.....	.014 7	334	− 1	.0007	.....	.003	
165784	18 2.6	−21 28	6.6	cA2	−14.	.018 5	337	− 2	.0008	.....	.020	
166937	18 7.8	−21 5	4.0	cB8	− 9.2	.006 1	338	− 3	.002	+ .008	.006	μ Sgr
169454	19.6	−14 2	6.8	cBo	.....	.025 12	345	− 2	.....	.....	.....	
170975	27.0	−14 56	5.9	cK5	+ 1.6	.006 3	345	− 4	.003	.....	.002	
171115	27.8	−24 6	5.7	cK4	−14.2	.016 2	337	− 9	.003	.....	.003	
171237	28.4	−24 18	6.1	cF3	+ 9.2	.007 3	337	− 9	.0011	.....	.004	
171635	18 30.8	+56 58	5.0	cF8	−11.7	.011 2	53	+24	.002	+ .008	.004	
172052	32.9	−23 16	6.8	F8p	.....	.018 6	338	− 9	.....	.....	.....	*a*
173638	41.2	−10 14	5.8	cF4	+10.1	.008 4	351	− 5	.0013	.....	.005	
173764	41.9	− 4 51	4.8	cG7	−20.9	.025 2	256	− 3	.003	+ .018	.006	
174947	48.0	−21 29	5.8	cKo	− 4.3	.022 3	342	−12	.002	.....	.004	
174974	18 48.1	−22 52	5.0	cK2	−12.1	.018 2	340	−12	.004	+ .024	.003	
178524	19 3.8	−21 11	3.0	cF3	− 9.8	.043 1	343	−15	.004	.015	.....	π Sgr
179323	7.1	−26 4	5.9	cKo	.....	.014 3	339	−17	.002	.....	.004	
180028	9.8	+ 5 52	7.2	F8p	.....	.022 8	9	− 4	.....	.....	.....	*a*
181615	16.0	−16 8	4.6	cF2	+11.9	.005 2	350	−15	.002	.....	.003	υ Sgr
182835	19 21.4	+ 0 8	4.9	cF5	− 0.6	.003 2	5	− 9	.002	− .008	.004	ν Aql
183143	23.0	+18 5	6.9	cB9	+12.9	.013 8	21	− 1	.....	.....	.....	
184398	29.2	+55 31	6.5	cG6	− 5.7	.018 5	54	+16	.....	.....	.....	
185758	35.6	+17 47	4.4	cG8	+ 2.0	.031 2	22	− 3	.003	− .005	.007	κ Sge
185859	36.1	+20 15	6.4	cB1	+ 5.6	.029 6	24	− 2	.....	.....	.....	
188262	19 49.2	+16 31	7.6	cF8	− 1.1	.....	23	− 7	.0007	.....	.003	
190066	58.1	+21 52	6.6	cBo	+16.1	.006 8	27	− 6	.....	.....	.....	
190603	20 0.7	+31 56	5.7	cBo	+18.0	.022 3	37	0	.0009	.....	.002	
190919	2.2	+35 34	5.7	cBo	−14.	.007 9	40	+ 1	.....	.....	.....	
192577	10.5	+46 26	4.6	cK1	− 3.0	0.006± 1	50	+ 6	0.004	−0.006	0.005	

TABLE 1—*Continued*

HD No.	α 1900	δ 1900	m_v	Sp.	V	μ		l	b	π_h	π_l	π_s	Remarks
					km/sec								
192713	20h11m2	+23° 12′	5.7	cG4	−23.5	0″.020±	3	31	− 7°	0″.002	+0″.003	0″.003	
192876	12.1	−12 49	4.6	cG5	−25.9	.019	1	359	−26	.003	+ .003	.003	
192909	12.4	+47 24	4.5	cK5	−14.4	.001	2	51	+ 6	.005	+ .007	.004	
193370	14.8	+34 40	5.5	cF5	−17.	.014	2	41	− 1	.0014	.....	.004	
194093	18.6	+39 56	2.3	cF7	− 7.6	.006	1	46	+ 1	.006	− .004	.013	γ Cyg
195295	20 25.3	+30 2	4.1	cF4	−18.8	.011	2	39	− 6	.003	+ .004	.010	
195592	27.2	+43 59	7.2	cBo	−23.5	.016	6	50	+ 2	.....	.....	.....	
195593	27.2	+36 36	6.3	cF5	−22.4	.009	3	44	− 2	.0011	.....	.003	
196093	30.0	+34 54	4.8	cK4	− 4.4	.011	2	43	− 4	.004	+ .001	.003	
196725	34.0	+12 58	6.1	cK4	−14.2	.008	2	26	−18	.002	.....	.003	
197345	20 38.0	+44 55	1.3	cA2	− 5.	.003	1	52	+ 1	.006	− .007	.008	α Cyg
198287	44.2	+38 55	7.0	cA7	− 2.0	.....		48	− 3	.0007	− .014	.002	
198478	45.5	+45 45	4.9	cB2	− 6.6	.007	2	53	+ 1	.0012	+ .017	.004	
199216	50.7	+49 9	7.1	cB1	− 6.6	.002	3	56	+ 2	.....	.....	.....	
199478	52.4	+47 2	5.8	cB8	−17.1	.007	3	55	+ 1	.0009	.....	.004	
200905	21 1.3	+43 32	4.2	cK5	−19.9	.008	1	54	− 3	.006	+ .004	.006	ξ Cyg
201601	5.5	+ 9 44	4.8	cF1	−17.1	.171	2	28	−26	.....	+ .022	.010	γ Equ* 6
202850	13.5	+38 59	4.3	cAo	− 3.8	.008	1	52	− 8	.002	− .005	.003	σ Cyg
204075	21.0	−22 51*	4.2	cG4	+ 3.0	.019	1	355	−45	.003	− .015	.008	ζ Cap
204867	26.3	− 6 1	3.1	cG1	+ 6.7	.022	1	16	−39	.004	+ .006	.008	β Aqa
205114	21 28.1	+52 11	6.8	cG2	−24.0	.009	4	63	+ 1	.0011	.....	.002	
206165	35.2	+61 38	4.9	cB2	−14.3	.006	2	70	+ 7	.0012	− .010	.004	γ Cep
206778	39.3	+ 9 25	2.5	cKo	+ 5.2	.029	1	34	−32	.010	− .001	.011	ε Peg
206859	39.8	+16 53	4.5	cG3	−22.7	.021	3	40	−27	.003	+ .004	.007	
207089	41.5	+22 29	5.4	cK1	−11.9	.010	2	45	−24	.003	+ .005	.002	
207260	21 42.6	+60 40	4.5	cA2	−21.5	.005	1	70	+ 6	.002	+ .011	.003	ν Cep
207489	44.2	+38 29	7.2	cGo	−58.1	.009	3	56	−12	.0006	.....	.002	
207673	45.6	+40 40	6.5	cAo	+ 3.	.011	4	58	−10	.....	.....	.....	
208501	51.5	+56 8	6.0	cB8	−15.2	.009	1	68	+ 1	.0009	.....	.003	
209750	22 0.6	− 0 48	3.2	cG1	+ 7.6	.021	1	28	−43	.004	+ .004	.008	α Aqa
210221	22 3.8	+52 49	6.5	A5p	.....	.015	4	68	− 2	.....	.....	.....	c
210745	7.4	+57 42	3.6	cK5	−18.1	.010	1	71	+ 1	.008	+ .025	.007	ζ Cep
211971	15.9	+59 38	7.2	cAo	−17.	.005	6	73	− 2	.....	.....	.....	
212455	19.3	+54 44	8.4	cB3	−56.	.....		71	− 2	.....	.....	.....	
212593	20.4	+48 58	4.6	cB8	−26.4	.011	2	68	− 7	.0015	− .001	.004	
213310	22 25.4	+47 12	4.6	K2	−11.6	.011	4	68	− 9	.004	+ .004	.004	
213470	26.5	+56 43	6.7	cA2	−61.	.016	6	72	− 1	.....	.....	.....	
216411	47.6	+58 28	7.2	cB1	−43.8	.022	12	76	0	.....	.....	.....	
216946	52.0	+49 12	5.1	cK3	− 9.5	.007	3	72	− 9	.004	.000	.003	
217476	55.9	+56 25	5.5	cG3	−58.4	.005	4	76	− 3	.002	− .001	.002	
218356	23 2.2	+24 56	5.0	cKo	−26.9	.035	2	64	−32	.003	+ .002	.005	
218376	2.4	+58 53	4.9	cB1	− 8.5	.008	2	78	− 1	.0011	.....	.003	
218393	2.6	+49 40	6.8	cA5	.....	.015	9	74	− 9	.....	.....	.....	
220102	16.0	+59 44	6.7	cF3	−21.9	.011	5	80	− 1	.0009	.....	.004	
222574	36.6	−18 22	5.3	cG1	+ 4.8	.016	2	30	−72	.002	− .011	.004	
223047	23 41.1	+45 52	5.1	cG5	−24.8	.011	2	79	−15	.002	+ .002	.005	ψ And
223385	44.0	+61 40	5.6	cA2	−44.5	.006	3	83	0	.0011	.....	.....	7
223960	48.9	+60 18	7.0	cAo	−48.	.005	4	84	− 1	.....	.....	.....	
224014	49.4	+56 57	4.8	cGo	−42.6	.005	1	83	− 4	.002	+ .022	.003	ρ Cas
225094	58.3	+63 5	6.3	cB2	−45.	.040	10	85	+ 1	.....	.....	.....	
225212	59.4	−11 4	5.5	cK5	−41.6	0.012±	2	59	−70	0.003	+0.014	0.002	

NOTES

π_h Hypothetical parallaxes by equation (12).
* Rejected.
† In *h* and χ Persei cluster.
a Lines narrow.
b Lines very narrow.
c Lines narrow and sharp.

Dynamical Parallaxes

1. 0″.024
2. .014
3. .012
4. .005
5. .001
6. .011
7. 0.001

term "nonvariable" is taken to mean "not intrinsically variable," since several eclipsing systems, such as ϵ and ζ Aurigae, show the c characteristics. The distributions of these stars in type and galactic latitude and the numbers of radial velocities and proper motions available are shown in Table 2. Their distribution in galactic longitude and latitude is shown in Figure 1.

Ninety-two per cent of the stars lie within 30° of the galactic equator, while 74 per cent lie within 10°. Twenty-one stars are members of the h and χ Persei cluster. Treating the cluster members of type A, and also of type B, as single stars, we find the following percentages for stars lying in the galactic zone: B, 88; A, 87; F, 64; G, 61; and K, 57. The distribution is exceptionally favorable for the determination of motions in the galactic plane, i.e., galactic rotation and the longitude and declination of the solar apex, knowledge of which is essential to the determinations of mean parallax and distance.

TABLE 2

DISTRIBUTION OF NONVARIABLE c STARS

b	B	A	F	G	K	All
0°–10°	41	61	27	34	20	183
11 –20	4	4	4	9	9	30
21 –30	.....	1	5	5	3	14
31 –40	.....	.....	3	2	2	7
41 –50	.....	.....	1	4	.....	5
51 –60	1	2	.....	.....	.....	3
> 60	.....	.....	1	2	1	4
All	46	68	41	56	35	246
V	41	50	35	47	32	205
μ	44	68	39	55	35	241

In order to ascertain whether or not these stars as a group show systematic motions differing from those of the stars in general, a solution based upon all the radial velocities was made.

GENERAL SOLUTIONS

Radial velocities.—The 205 stars with radial velocities were arranged in 31 groups according to position. The mean velocities, weighted according to the number of stars in each group, were analyzed by means of the well-known general relation

$$V = K + X \cos b \cos l + Y \cos b \sin l + Z \sin b + du - ev\,, \qquad (11)$$

where

$$u = rA \cos 2l_0\,, \qquad d = \sin 2l \cos^2 b\,,$$

$$v = rA \sin 2l_0\,, \qquad e = \cos 2l \cos^2 b\,.$$

V denotes the observed radial velocity; X, Y, and Z, the galactic rectangular components of the solar motion; and the other symbols have the significance given in the section on method. The results of this analysis are given in Table 3.

The values derived for the co-ordinates of the solar motion and the longitude of the center of rotation show that the stars under discussion share closely the general drift of

the stars due to the motion of the sun and their rotation about the galactic center. In extending the investigations, therefore, we may safely adopt the conventional values: $A_0 = 270°$; $D_0 = +30°$; $V_0 = 20$ km/sec; and $l_0 = 325°$. The radial velocities were, therefore, corrected for the standard solar motion to give values of V' applicable in equation (1).

The fact that many of these velocities, especially in the early types, are large led, before the discovery of rotation, to the conclusion that sharp lines in these spectra were an indication of high velocity. The large velocities are, however, found almost without exception in those regions of the sky where the effect of rotation is large, and after correction for rotation the mean peculiar motion is but 13.0 km/sec, indicating that the large observed radial velocities connote great distance rather than high random speed.

TABLE 3

GENERAL RESULTS FROM RADIAL VELOCITIES

	km/sec				
K	-2.00 ± 0.80	l_a	$26°.5$	l_0	$324°.4$
X	$-17.00 \quad 1.14$	b_a	$+15°.2$	$\bar{r}A$	16.3 km/sec
Y	$-8.49 \quad 1.14$	A_0	$278°.1$	θ	13.0 km/sec
Z	$-5.15 \quad 2.24$	D_0	$+30°.1$	$\bar{m}_1$	5.14
u	$+5.14 \quad 1.08$	V_0	19.7 km/sec	No.	205
v	-15.15 ± 1.15				

In applying equations (1) and (3), values for the constants of rotation and absorption were taken from a recent investigation by the writer,[12]

$$A = 17.7 \text{ km/sec kpc},$$

$$a = 0.65 \text{ mag/kpc}.$$

To determine a value of the mean effective absorption a_e, the value of a was multiplied by the percentage of the reference stars located within the zone ($b = +10°$ to $-10°$), in which the absorption is assumed to be effective. From the value of $\bar{r}A$ in Table 3, $\bar{r} = 0.92$ kpc, and, since $\bar{m}_1 = 5.14$,

$$\bar{M}'_r = -4.68.$$

Proper motions.—Well-determined proper motions are available for 241 of the 246 stars. The corrections to the Newcomb precessions plus a constant rotation derived by Raymond and Wilson[13] were applied to the catalogue values to give the total motions in the seventh column in Table 1. All but six of these are less than $0''.061$ per annum. They may be represented by a skew frequency-curve with the mean at $0''.013$ and the mode at $0''.006$. The larger and definitely outstanding proper motions are listed in Table 4. Five stars are of type F; one, of A. Five lie well outside the galactic zone; in fact, this short list contains all the F stars for which $b > 40°$ and one of the two A stars for which $b > 24°$. The single star (ρ Pup), located near the galaxy, is bright; but its proper motion reduced to the approximate mean magnitude 5.0 would be $0''.042$, which is still large. Three are not found in Miss Payne's catalogue but have been classified as

[12] *Mt. W. Contr.*, No. 631; *Ap. J.*, **92**, 170, 1940. [13] *A.J.*, **47**, 57, 1938.

c stars at Mount Wilson. These six stars have been omitted in the determinations of mean parallactic and peculiar motions.

TABLE 4

LARGE PROPER MOTIONS

Star	m_v	μ	Sp.	b
γ Equ*	4.8	$0''.171 \pm 2$	F1	26°
o Leo	4.5	.143 1	F5	43
β^2 Tuc	4.5	.120 4	A2	54
τ UMa*	5.0	.117 2	F6	40
ρ Pup	3.2	.097 1	F5	6
ξ Phe*	5.8	0.095 ± 4	Fo	61

* Not in Miss Payne's catalogue.

The remaining 235 stars gave the following mean values of the components of the proper motions:

$100\,\bar{\mu}_0$	$1''.32$	$100\,\bar{\mu}$	$1''.24$
$100\,\lvert\bar{\tau}_0\rvert$	0.68	$100\,\lvert\bar{\tau}\rvert$	0.51
$100\,\bar{\rho}$	0.38	$100\,q$	0.77
$100\,\bar{v}$	0.57		

Using the values of the solar and peculiar motions in Table 3, we find by equation (4)

$$1000\,\bar{\pi}_q = 1''.85\,, \qquad 1000\,\bar{\pi}_\tau = 2''.03\,.$$

Since[14]

$$\sqrt{p_2} : \sqrt{p_1} :: 1.44\,\theta : V_0\,,$$

by equation (5)

$$1000\,\bar{\pi} = 1''.94\,.$$

Since $\bar{m}_2 = 5.37$, we find by equation (6) that

$$\bar{M}'_\pi = -3.19\,.$$

As 74 per cent of the stars lie within the galactic zone, the value of the effective absorption is $a_e = 0.48$ mag/kpc. From equations (3) and (7), then,

$$\bar{M}_\tau = -4.68 - 5C_1 - 0.44\,,$$

$$\bar{M}_\pi = -3.19 + 5C_2 - 0.25c\,.$$

Assuming that $C_1 = C_2$, we find by successive approximations

$$c = 1.95\,, \qquad C_1 = C_2 = -0.144\,,$$

[14] H. N. Russell, *Mt. W. Contr.*, No. 215; *Ap. J.*, **54**, 142, 1921.

and, finally,

$$\bar{M} = -4.40 .$$

From equation (10) we find $\bar{M} = -4.38$.

The value of c suggests a large dispersion in distance, which is not surprising among stars as bright intrinsically as those with which we are dealing. If the distribution of $\log \pi$ is Gaussian,

$$\log c = \frac{\sigma^2_{\log \pi}}{\text{Mod}} ,$$

and, for $c = 1.95$,

$$\sigma_{\log \pi} = \pm 0.355 .$$

The value of $\bar{M}'_\pi$ agrees very well with the earlier determinations of Schilt and Bottlinger based upon the parallactic motions. The difference between their values and our final value $\bar{M}$ is clearly due to the corrections for dispersion and absorption rather than to improved data and a more critical selection of stars. The value of $\bar{M}$ indicates that the nonvariable c stars are in the mean considerably brighter intrinsically than the Cepheids and that as a class they are probably the most luminous stars known, averaging about 5000 times the luminosity of the sun.

THE LUMINOSITY SEQUENCE

Among the Cepheids the well-known increase in luminosity with period is accompanied by progression in spectral type from A to K. Although Schilt found no evidence

TABLE 5

PRELIMINARY SEQUENCES

Sp.	$\overline{\text{Sp.}}$	$\bar{r}A$	$\bar{M}'_r$	θ	$100\bar{\tau}$	$100q$	$1000\bar{\pi}$	$\bar{M}'_\pi$	$\bar{M}'$
		km/sec		km/sec					
B0–B5	B2	24.4	−5.2	13.9	0".55	0".09	1".04	−4.2	−4.7
B7–A5	A0	20.3	4.7	14.5	.26	0.58	1.12	4.0	4.4
A6–F7	F3	14.9	5.0	10.1	.66	1.15	2.80	3.1	4.0
F8–G6	G2	8.6	3.6	11.8	.54	1.11	2.51	2.8	3.2
K0–K5	K3	3.0	−1.2	6.9	0.61	1.19	3.31	−2.4	−1.8

of a difference in $\bar{M}$ for stars of early and late types, the difference between the values obtained by Merrill and Sanford for the early types and the mean value derived above suggested the possibility of a correlation between luminosity and type among the nonvariable stars. Plots in longitude of the corrected radial velocities V' for the separate types showed beautifully the double sine-curve due to galactic rotation, except for class K, and revealed a definite decrease in the amplitude $\bar{r}A$ of the curve, with advance in type. The values significant in the determinations of $\bar{M}$ were therefore computed for each type separately. The results are shown in Table 5. The sequences in $\bar{r}A$ and hence in $\bar{r}$, in θ and q and hence in $\bar{\pi}$, resulting in sequences in $\bar{M}'_r$ and $\bar{M}'_\pi$, reveal a definite and marked decrease in luminosity with advance in spectral type.

To establish more definitely the character of this trend the data were subdivided in several ways and the significant quantities again determined. The details are given in Tables 6 and 7, in which the groups and mean types are the same, the first column

of Table 6 applying likewise to Table 7. The asterisks denote the five main groups referred to in Table 5. Owing to the undue influence of the occasional abnormal value upon the means of a small number of values taken regardless of sign, mean values of θ were used in the computations of $\overline{\pi}_r$ as follows: Bo–A4, 14.1; A5–G8, 10.8; and Ko–K5, 6.9 km/sec, respectively.

TABLE 6

SEQUENCE FROM GALACTIC ROTATION

Sp.	$\overline{\text{Sp.}}$	No.	$\overline{m}_z$	$\bar{r}A$	θ	$\bar{r}$	$\overline{M}'_r$
				km/sec	km/sec	kpc	
Bo–B3	B1	36	5.5	22.5	14.1	1.27	−5.0
Bo–B5	B2	41*	5.6	24.4	13.9	1.38	5.2
B5–B9	B7	25	5.6	26.6	10.7	1.50	5.3
B7–A5	A0	51*	5.6	20.3	14.5	1.15	4.7
A0–A4	A2	31	5.7	20.8	17.3	1.18	4.7
A5–F3	F0	18	4.6	13.6	8.6	0.77	4.8
A6–F7	F3	39*	4.6	14.9	10.1	0.84	5.0
F4–F7	F6	21	4.7	17.5	11.5	0.99	5.3
F8–G3	G1	29	5.0	11.6	11.8	0.66	4.1
F8–G6	G2	44*	4.8	8.6	11.8	0.49	3.6
G4–G8	G5	17	4.9	6.7	11.2	0.38	3.0
K0–K5	K3	30*	4.9	3.0	6.9	0.17	−1.2
Bo–G5	A7	172	5.18	19.5	12.7	1.10	−5.03
All	F0	205	5.14	16.3	11.9	0.92	−4.68

* The five principal solutions (see Table 5).

TABLE 7

SEQUENCE FROM PARALLACTIC AND PECULIAR MOTIONS

$\overline{\text{Sp.}}$	No.	$100\,\bar{\mu}$	$100\,\bar{v}$	$100q$	$100\lvert\bar{r}\rvert$	$1000\,\pi_q$	$1000\,\pi_r$	$1000\,\bar{\pi}$	$\overline{m}_z$	$\overline{M}'_\pi$
B1	38	1".08	0".02	0".08	0".48	0".19	1".60	0".91	5.6	−4.6
B2	45*	1.09	.05	0.09	.55	0.22	1.84	1.04	5.7	4.2
B7	31	0.85	.26	0.30	.34	0.72	1.14	0.94	5.9	4.2
A0	70*	1.16	.49	0.58	.26	1.39	0.87	1.12	5.8	4.0
A2	43	1.24	.55	0.62	.33	1.49	1.10	1.29	6.0	3.4
F0	21	1.22	.77	1.04	.60	2.50	2.59	2.54	4.9	3.1
F3	36*	1.21	.72	1.15	.66	2.76	2.84	2.80	4.7	3.1
F6	18	1.19	.61	1.20	.71	2.88	3.06	2.96	4.7	2.9
G1	35	1.56	.87	1.18	.45	2.83	1.94	2.41	5.2	2.9
G2	51*	1.48	.81	1.11	.54	2.66	2.33	2.51	5.2	2.8
G5	19	1.42	.78	1.04	.72	2.50	3.10	2.78	5.0	2.8
K3	33*	1.27	0.88	1.19	0.61	2.86	4.19	3.31	5.0	−2.4
A7	202	1.23	0.51	0.71	0.49	1.70	1.83	1.76	5.43	−3.34
F0	235	1.24	0.57	0.77	0.51	1.85	2.03	1.94	5.37	−3.19

* The five principal solutions (see Table 5).

Although the data have been rather finely divided, the clear progressions with type in the significant observed quantities, $\bar{r}A$, θ, $\bar{v}$, and q, leave little room for doubt that the change in luminosity with type is a real, continuous phenomenon which may be represented by a simple curve.

As has been noted in the description of methods, the effects of dispersion in distance and parallax are such as to make the computed values $\overline{M}'_r$ too bright and those of $\overline{M}'_\pi$

too faint. Except in the K stars the differences between the sequences in Tables 6 and 7 are in the direction in which dispersion is effective. The means of the two sets of values should give reliable values of $\bar{M}'$, since they are little affected by the assumption that the dispersions in the logarithms of distance and parallax are equal, i.e., $C_1 = C_2$. The differences between them, which give approximate values of c, the index of dispersion, may, however, be seriously affected by this assumption as well as by the accidental errors involved in dealing with small groups of data. While little confidence can be placed in the actual values of c computed in this way, they do indicate trends in the dispersions. They have been derived in two ways, first, by means of successive approximations for c and C from the differences $\bar{M}_r - \bar{M}_\pi$; and, second, after reduction of the values of $\bar{r}$ and $\bar{\pi}$ to a uniform system corresponding to $m = 5.0$, from the definition $c = \bar{\pi} \cdot \bar{r}$. The values check within the errors of computation. The means (Table 8) indicate fairly normal dispersion, for such bright stars, among types B, A, and G, but a very large dis-

TABLE 8

THE OBSERVED SEQUENCE

Sp.	$\bar{r}_{5.0}$	$1000\bar{\pi}_{5.0}$	c	$\bar{M}'$	a_e	$\bar{M}_0$
	kpc					
B1	1.00	1".20	1.20	−4.8	0.57	−5.4
B2	1.10	1.44	1.58	4.7	.57	5.3
B7	1.15	1.42	1.63	4.7	.57	5.4
A0	0.87	1.62	1.41	4.4	.57	4.9
A2	0.87	2.04	1.77	4.0	.57	4.5
F0	0.91	2.43	2.21	4.0	.42	4.4
F3	1.00	2.44	2.44	4.0	.42	4.4
F6	1.15	2.61	3.00	4.1	.42	4.6
G1	0.66	2.64	1.74	3.5	.40	3.8
G2	0.52	2.75	1.43	3.2	.40	3.4
G5	0.40	2.78	1.11	2.9	.40	3.1
K3	0.17:	3.31	0.56:	−2.0	0.38	−2.2
A7	1.01	2.15	2.18	−4.18	0.52	−4.63
F0	0.86	2.30	1.98	−3.94	0.49	−4.43

persion in class F. This is not altogether surprising, since among the F stars with normal spectra one finds the most abnormal motions, which are reflected in abnormal dispersions when these motions are used for determinations of mean distance. In this connection it may be recalled that of the six stars rejected because of large proper motions, five are of class F.

Since by definition $c > 1$, an impossible value for the K stars results from the improbably small value of $\bar{r}A$ derived from the rotation. In the first place, so small a value is hardly determinate from but 30 radial velocities, the accuracy of the derivation of $\bar{r}A$ being a simple function of the adequacy in amount and distribution of the data and the ratio $\bar{r}A/\theta$. Second, from an analysis of the proper motions of 7546 K stars, Raymond and Wilson[15] found no evidence of rotation, although it appeared definitely in the proper motions of stars of all the other types. They suggested that the mixture of K stars belonging to the two main star streams may be such as to make it appear that these stars do not partake in the general rotation. For these reasons little confidence can be placed in the values of $\bar{r}A$ and, consequently, in that of $\bar{M}'_r$ derived from the K stars. The latter has been given half-weight only in the derivation of $\bar{M}'$ for this group.

The mean values of the distances and parallaxes, reduced to visual magnitude 5.0,

[15] *Op. cit.*, p. 54.

of c, $\bar{M}'$, the effective absorption a_e, and the final observed values of $\bar{M}_0$ for the groups indicated in Table 6 are shown in Table 8. The values of $\bar{M}_0$ are plotted in Figure 2. The vertical lines show the differences between $\bar{M}_r$ and $\bar{M}_\pi$, which were used as indices of the relative dispersions. The smoothed curve passed through the observed points gives the

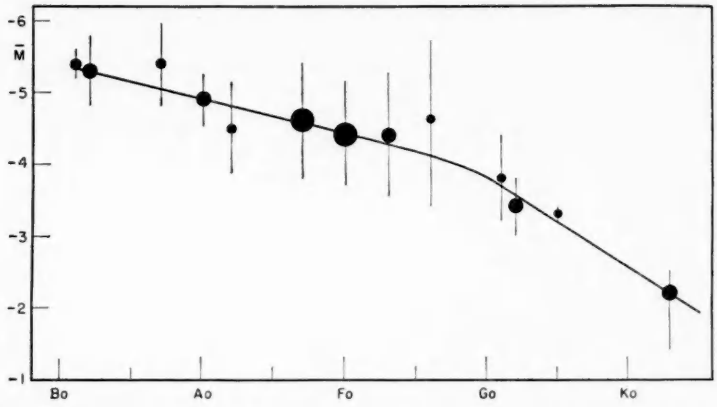

FIG. 2.—Relation between mean absolute magnitude and spectral type. The smallest dots represent the smallest divisions of the data; those of intermediate size, the five principal divisions; and the two largest, the mean values, one including and the other excluding stars of class K. The vertical lines indicate relative dispersions. The adopted values of $\bar{M}$ in Table 9 were read from the smoothed curve.

TABLE 9

ADOPTED VALUES OF $\bar{M}$

Type	$\bar{M}$	Type	$\bar{M}$	Type	$\bar{M}$
Bo–B1	−5.4	A8	−4.5	G2	−3.6
B2–B3	5.3	Fo	4.4	G5	3.2
B5	5.2	F2	4.3	G8	2.8
B7–B9	5.0	F5	4.2	Ko	2.6
Ao	4.9	F8	4.0	K2	2.3
A2–A3	4.8	Go	−3.8	K5	−2.0
A5	−4.7				

adopted values of $\bar{M}$ shown in Table 9.[16] These values represent luminosities ranging from 12,000 times that of the sun for type B to about 700 for K5.

[16] After this investigation had been completed a discussion appeared of the mean absolute magnitudes of the high-luminosity stars in general by J. L. Greenstein of Harvard (*Proc. Nat. Acad. Sci.*, **26**, 263, 1940). His results for the c stars may be summarized as follows:

Type	No.	$\bar{M}$
B–A	48	−6.3
B8–A5	22	5.4
A8–G4	24	5.1
Fo–G5	18	4.9
G5–K8	16	−2.2

His values are systematically brighter than ours, owing largely to his use of an absorption of 0.93 mag/kpc in the galactic zone and 0.50 outside of it, whereas we applied a maximum of 0.57 mag/kpc within the zone and no absorption outside it. His results, however, confirm the general decrease in luminosity with advance in spectral type.

COMPARISON WITH TRIGONOMETRIC AND OTHER PARALLAXES

A test of the validity of the adopted values of $\bar{M}$ may be obtained from comparisons of the means of the parallaxes computed upon the assumption that $M = \bar{M}$ with those secured in other ways. Hypothetical parallaxes on this assumption result from the relation

$$\log \pi_h - \frac{0.2a}{1000\pi_h} = 0.2\,(\bar{M} - m) - 1\,, \qquad (12)$$

where $a = 0$, except in the galactic zone.

Trigonometric and spectroscopic parallaxes are available for 82 of the stars in Table 1, while for 11 others we have the former only. The trigonometric parallaxes and the spectroscopic values for the early-type stars were found mainly in Schlesinger's catalogue,[17] a few more recent determinations being added. The spectroscopic parallaxes of the late-type stars are almost entirely from the Mount Wilson list.[10] The individual values of parallax are given in the last two columns of Table 1, and the mean values in Table 10. The results in the last three lines of this table indicate that the absolute magnitudes of Table 9 are in the mean satisfactorily adjusted to the system defined by the trigonometric parallaxes. The spectroscopic parallaxes in types A to G5 appear to be

TABLE 10

COMPARISONS OF MEAN PARALLAX

Type	No.	$\bar{m}_v$	$\bar{\pi}_h$	$\bar{\pi}_t$	$\bar{\pi}_s$	No.	$\bar{m}_v$	$\bar{\pi}_h$	$\bar{\pi}_t$
B0–B2	6	3.35	0".0023	0".0080	0".0063	6	3.35	0".0023	0".0080
B7–A4	11	3.69	27	16	72	12	3.72	26	33
A7–F5	14	3.96	37	06	105	17	4.12	33	00
F7–G6	28	4.30	31	37	63	34	4.39	30	46
G7–K5	23	4.41	52	63	55	24	4.45	51	57
Early	17	3.57	0.0025	0.0038	0.0069	18	3.60	0.0025	0.0049
Late	65	4.27	40	39	69	75	4.35	37	39
All	82	4.15	0.0037	0.0040	0.0069	93	4.23	0.0035	0.0041

systematically too large. This is probably due to difficulties in calibrating the curves relating M to line intensities for stars of small proper motion, the trigonometric parallaxes of many of which are negative in sign.

A second test, applicable in the case of the early-type stars, is afforded by the 21 stars in the h and χ Persei cluster. The distance of this twin cluster has been estimated in various ways, three of which may be mentioned. (1) Assuming that the mean corrected radial velocity is entirely due to galactic rotation, the distance is determined directly from the relation $\bar{V}' = \bar{r}A$. This method may be applied to both stellar and interstellar velocities. As an example of its application, we quote Oosterhoff's results: $\bar{r} = 2.10$ kpc (stellar), and 2.40 kpc (interstellar).[18] These distances, uncorrected for dispersion, correspond to parallaxes 0".00048 and 0".00042, respectively. The many estimates by this method are consistent because the mean radial velocity of the cluster is well determined and there has been fair unanimity of opinion as to the approximate value of the rotational constant. Some uncertainty, however, is introduced by the assumption that $\bar{V}' = \bar{r}A$.

Two other criteria were used by Trumpler,[19] namely, (2) mean absolute magnitudes of different spectral types and (3) the diameters of the clusters, both corrected for absorption. He finds for the h and χ Persei cluster that $\bar{r} = 1.30$ kpc (2) and 1.35 kpc (3),

[17] *General Catalogue of Stellar Parallaxes* 2d ed., 1935.

[18] *Leiden Ann.*, **17**, Part I, 31, 1937.

[19] *Lick Obs. Bull.*, **14**, 156, 1930.

the corresponding parallaxes being o".00074 and o".00077, respectively. These estimates are affected by the unknown dispersions in absolute magnitude and by uncertainties in the measured diameters of the clusters and in the amount of effective absorption. The mean of the four quoted values gives as the parallax of the cluster $\bar{\pi} = 0''.00060$.

Methods (1) and (2) may be applied to the c-star data, using the values of A, a, and $\bar{M}$ adopted above. The resulting values of the parallax of the cluster are given in Table 11. The agreement of the values derived from rotation with those of Oosterhoff is due to the fact that the mean radial velocity given by the c stars is essentially the same as that given by the stars with normal spectra. The parallaxes based upon mean absolute magnitudes are appreciably smaller than those of Trumpler. This difference was to be expected because Trumpler based his distances upon the mean absolute magnitudes of stars of normal spectra, disregarding the large proportion of c stars in this cluster. While emphasis cannot be placed upon the somewhat better agreement of the parallaxes based

TABLE 11

PARALLAX OF h AND χ PERSEI CLUSTER FROM C STARS

TYPE	$1000\bar{\pi}$ FROM			NO.
	Rotation	$\bar{M}$	Mean	
Bo–B5	o".48	o".58	o".53	8
B8–A2	0.46	0.68	0.57	12
All*	0.46	0.66	0.56	21

* Including one F8 star.

upon the mean absolute magnitudes of the c stars with those based upon the rotation factors, owing to the arbitrary assumption that $\bar{V}' = \bar{r}A$, the comparisons in Table 11 indicate that the adopted values of $\bar{M}$ for the early types (Table 9) are at least of the right order. In the mean, these values of $\bar{M}$ agree well with the value derived by Merrill and Sanford[6] from the intensities of the interstellar lines. Moreover, by superimposing the spectrum-luminosity-curve of the Perseus clusters upon that of the Pleiades at Class A, Miss Payne[20] finds a range in the absolute magnitudes of the individual stars from about -4 to -7, which would give a rough mean value again in satisfactory accord with those of Table 9.

CONCLUSION

The evidence of a correlation between luminosity and type among the nonvariable c stars is quite conclusive. The luminosity decreases continuously from Bo to K5. All the recent studies indicate very high luminosities for the early-type stars. The continued decrease through types F, G, and K, however, is contrary to the correlation found among the Cepheids. While the individual Cepheid presents an earlier-type spectrum at maximum light and thus follows the trend shown by the nonvariable c star, the mean spectrum-luminosity relation shows an increase in luminosity with advance in type. A comparison of the two correlations, both based on visual magnitudes, is shown in Figure 3. The two curves cross at type G5, while the separation at F2 is 3.2 mag. Both curves are too well determined to permit doubt that they represent real differences in luminosity. It appears, therefore, that, in spite of recognized similarities in their spectra, the Cepheids and nonvariable c stars form two separate groups, in one of which the stars are not variable, while in the other all are subject to a single type of light-variation. The presence among the F and early G stars of two such groups differing widely in luminosity

[20] *Op. cit.*, p. 108.

would naturally produce large values of the index of dispersion for these types (Table 8). It certainly offers an explanation of the departure of the mean spectroscopic parallaxes of these stars from their mean trigonometric values.

The third curve in Figure 3 is defined by the Mount Wilson spectroscopic absolute magnitudes. The calibration for stars of small proper motions appears to have been unduly influenced by the Cepheids with the result that the absolute magnitudes of the nonvariable c stars of types F and G are too faint and the mean spectroscopic parallaxes (Table 10) are too large. Around Ko the c-curve derived above and the Mount Wilson–curve are near together, and the mean hypothetical, trigonometric, and spectroscopic parallaxes agree.

The existence of two radically different luminosity sequences within a very uncommon class of stars is rather surprising. Yet studies of stellar temperatures indicate that the

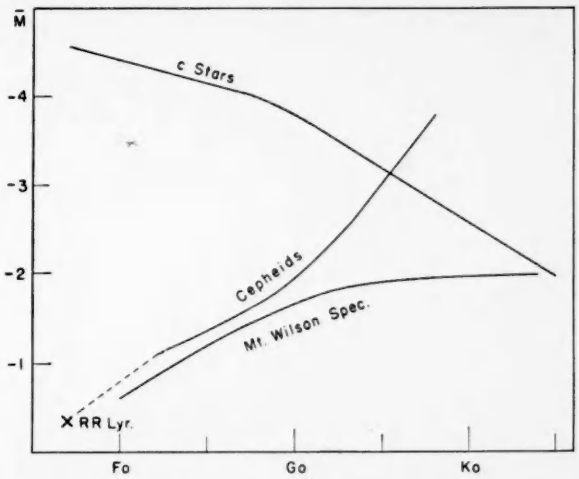

FIG. 3.—Comparison of the spectrum-luminosity sequences of the nonvariable c stars, Cepheid variables, and the Mount Wilson spectroscopic magnitudes.

supergiant is about 700° cooler, and the Cepheid only about 300° cooler, than the dwarf of corresponding spectral class. From this Miss Payne[21] concludes: "The suggestion is that the Cepheid is more luminous than the average, but not so luminous as the c star in classes F and G. This is in harmony with their spectral characteristics, which display a marked but not extreme c character." The last remark is suggestive, but it is not in harmony with the observation by Adams and Joy that the spectra of Cepheids and nonvariable c stars of the same spectral subtypes are practically identical. It may be true, however, that the most extreme degree of c characteristics is displayed by certain nonvariable stars rather than by the Cepheids, and detailed comparisons of corresponding spectra may reveal some significant differences. Certainly, a clearer definition of c characteristics is desirable. In this connection it may be noted that high-dispersion spectra secured at Mount Wilson by Adams and others show that the "narrow" and "sharp" lines observed in low-dispersion spectra of early-type c stars are mainly due to the sharpness of the borders rather than to actual lessened line width. Whereas the metallic lines in the normal spectrum are V-shaped, those in the c spectrum are U-shaped. A study of the line contours in high-dispersion spectra of some of the brighter c stars of different types would seem to promise interesting and valuable results.

CARNEGIE INSTITUTION OF WASHINGTON
MOUNT WILSON OBSERVATORY
October 1940

[21] *Ibid.*, p. 165.

PHYSICAL PROCESSES IN GASEOUS NEBULAE

XIII. THE ELECTRON TEMPERATURES OF SOME TYPICAL PLANETARY NEBULAE

DONALD H. MENZEL, LAWRENCE H. ALLER, AND MALCOLM H. HEBB

ABSTRACT

The electron temperatures of several typical planetary nebulae have been determined from the relative intensities of the line λ 4363 and the green nebular lines of *O* III. The values obtained range from about 6000° K to 10,000° K, and seem to be insensitive to the degree of excitation of the nebular spectrum and probably also of the temperature of the central star.

In a previous paper[1] we have shown how the electron densities for a number of planetary nebulae may be found when the intensity of the continuum at the Balmer limit is known and when T_e is known. In this paper we shall show how the electron temperature of a planetary nebula may be determined from the intensities of certain lines in the nebular spectrum and from the electron density.

The levels of the p^2 ground configuration of *O* III are, respectively, $^3P_{0,1,2}$, $^1D_2$, and $^1S_0$. The ground term is ^3P. Transitions from $^1D_2$ to $^3P_2$ and $^3P_1$ give the green nebular lines at λ 5007 and λ 4959, respectively. The transition from the highest level, $^1S_0$, to the $^1D_2$ level gives the λ 4363 auroral-type line. It was suggested by Bowen[2] that collisions of electrons with the *O* III ions in the ^3P term raised these ions to the metastable $^1S_0$ and $^1D_2$ levels. As the ions returned to the ground levels the nebular lines λλ 4363, 4959, and 5007 were emitted. Now, if the collisional cross-sections of *O* III are known, we may calculate the relative numbers entering the $^1S_0$ and $^1D_2$ levels as a function of the electron density and the temperature. Since the transition probabilities for λλ 4363, 4959, and 5007 are known, we may compute the electron temperature from the measured intensities of the relevant nebular lines.

If we assume that the electron velocities possess a Maxwellian distribution corresponding to some temperature T_e, the total number of transitions from the lower level A to the higher level B will be given by (X, 32)[1]

$$\mathfrak{F}_{AB} = 8.54 \times 10^{-6} \frac{N_A N_e \Omega_{AB}}{\bar{\omega}_A T_e^{1/2}} e^{-\chi_{AB}/kT_e}, \tag{1}$$

where $\frac{1}{2} mv_0^2 = \chi_{AB}$, the excitation potential in volts of level B with respect to level A, and $\bar{\omega}_A$ is the statistical weight of level A, while Ω_{AB} is a parameter calculated by wave mechanics and tabulated in Paper X for *O* III. Although only electrons with velocities greater than v_0 are effective in exciting atoms from level A to level B, it is apparent that electrons with any velocity whatever may be effective in de-exciting the atoms in the higher levels. Thus, from (X, 33) the number of de-excitations is given by

$$\mathfrak{F}_{BA} = 8.54 \times 10^{-6} \frac{N_B N_e \Omega_{AB}}{\bar{\omega}_B T_e^{1/2}}. \tag{2}$$

[1] "Physical Processes in Gaseous Nebulae. XII," *Ap. J.*, **93**, 195, 1941; X, *Ap. J.*, **92**, 408, 1940.

[2] *Ap. J.*, **81**, 1, 1935.

We set up the equations of statistical equilibrium for the levels of the p^2 configuration by equating the number entering each level by collisional and radiative transitions to the number leaving in a similar fashion. The problem is greatly simplified if we are permitted to suppose that the population of each of the levels of the ^3P term is proportional to its statistical weight. This will be the case, provided the collisions are sufficiently numerous to maintain a Boltzmann distribution, i.e., the probability of the collisional de-excitation of a level of the ^3P term is much greater than the probability of a radiative transition downward. As was shown in (X, 39), if the electron density is greater than about 4×10^3 electrons/cm^3 a Boltzmann distribution will obtain among the levels of the ^3P term.

Before setting up the general equations of statistical equilibrium we shall sketch a useful approximate method of treating the same problem. The number of atoms entering the $^1S_0$ level by collisions from the ground level will be

$$\mathfrak{F}_{PS} = 8.54 \times 10^{-6} N_{^3P_0} N_\epsilon \frac{\sum_i \Omega_{P_i S}}{T_\epsilon^{1/2}} e^{-\chi_{PS}/kT_\epsilon} \qquad \sum_i \Omega_{P_i S} = 3.53 . \quad (3)$$

By the use of the number of atoms in the $^3P_0$ level of unit weight we have avoided the necessity of introducing the weight factors in the other terms, since $N_{^3P_0} = N_{^3P_1}/3 = N_{^3P_2}/5$. Of the number arriving in $^1S_0$, the fraction

$$\frac{A_{SD}}{\sum_J A_{SJ}} ,$$

when J refers to the inner quantum numbers of both ^1D and ^2P, goes to form the line λ 4363.[3] According to the data of Pasternack,[3] $A_{SD} = 2.7$, $A_{SJ} = 2.84$, so that if there were no collisional de-excitation of the $^1S_0$ level, 95 per cent of the atoms in $^1S_0$ would go to produce the λ 4363 line. Similarly, the number of atoms arriving in $^1D_2$ by collision from ^3P will be

$$\mathfrak{F}_{PD} = 8.54 \times 10^{-6} N_{^3P_0} N_\epsilon \frac{\sum \Omega_{P_i D}}{T_\epsilon^{1/2}} e^{-\chi_{PD}/kT_\epsilon} \qquad \sum_i \Omega_{P_i D} = 20 . \quad (4)$$

We want to know what fraction of these will return to the ground state by collisions. According to Pasternack, $A_{^1D_2-^3P_2} + A_{^1D_2-^3P_1} = 0.0215$. The number of superelastic collisions will be

$$\mathfrak{F}_{DP} = 8.54 \times 10^{-6} \frac{N_{^1D_2} N_\epsilon}{5} \frac{20}{T_\epsilon^{1/2}} = 34.2 \times 10^{-6} \frac{N_\epsilon}{T_\epsilon^{1/2}} N_{^1D} .$$

If we take T_ϵ as 10,000° K, N_ϵ as 10^4 electrons/cm^3, we obtain $\mathfrak{F}_{DP} = 3.42\times10^{-3} N_D$, and the fraction of atoms collisionally de-excited will be only 0.14. Similarly, we find that an entirely negligible fraction of atoms in $^1S_0$ are collisionally de-excited at nebular densities. Thus, the intensity of λ 4363 will be proportional to the number of atoms entering the $^1S_0$ level multiplied by 0.95. Likewise, the intensity of the green nebular pair will be proportional to the number entering $^1D_2$ by collision from ^3P *plus* the number cascading from ^1S multiplied by $(1 - \beta)$, where β is the fraction of atoms in the $^1D_2$ level col-

[3] *Pub. A.S.P.*, **51**, 160, 1939; see also *Ap. J.*, **92**, 129, 1940.

lisionally de-excited. Therefore, the ratio of the intensity of the green nebular lines to λ 4363 will be given by

$$\left.\begin{aligned}\frac{I_{N_1+N_2}}{I_{4363}} &= \frac{[1-\beta]\{20e^{-\chi_{DP}/kT_e}+e^{-\chi_{PS}/kT_e}3.53\times 0.95\}h\nu_{5000}}{e^{-\chi_{PS}/kT_e}3.53\times 0.95\times h\nu_{4363}}\\ &= [1-\beta]\{5.97e^{\chi_{DS}/kT_e}+1\}0.875\,,\end{aligned}\right\} \tag{5}$$

where

$$\chi_{DS} = h\nu_{DS} = h\nu_{4363}\,,$$

$$\chi_{PD} = h\nu_{DP} = h\nu_{5000}\,,$$

$$\chi_{PS} = h\nu_{PS}\,.$$

If $\beta = 0.14$

$$\frac{I_{N_1+N_2}}{I_{4363}} = 4.4e^{33,000/T_e}+0.75\,. \tag{6}$$

In this equation we have neglected the effects of a number of processes that are not of great importance in the present case because of the particular values which the parameters assume for likely values of the electron density and temperature.

We shall now set up the general equations of statistical equilibrium for the terms of the p^2 configuration of *O* III. Ambarzumian has treated the problem of statistical equilibrium with four discrete states. We shall assume that the electron density is sufficiently high for the relative populations of the levels of the ^3P term to be proportional to their statistical weights.

As previously mentioned, we equate the number of atoms entering the $^1S_0$ level by collisions to the number leaving by collisions and radiative transitions,

$$\left.\begin{aligned}N_PN_e\frac{\Omega_{PS}}{\bar{\omega}_P}e^{-\chi_S/kT_e}C+N_DN_e\frac{\Omega_{DS}}{\bar{\omega}_D}e^{-(\chi_S-\chi_D)/kT_e}C&\\ = N_eN_S\frac{\Omega_{SP}\Omega_{SD}}{\bar{\omega}_S}C+N_S(A_{SD}+A_{SP})\,.&\end{aligned}\right\} \tag{7}$$

The number of atoms entering the $^1D_2$ term by collisions from the ^3P and ^1S terms and by radiative transitions from the ^1S term must equal the number collisionally de-excited to ^3P or collisionally excited to $^1S_0$ plus the number of radiative transitions from $^1D_2$ to ^3P.

$$\left.\begin{aligned}N_PN_e\frac{\Omega_{PD}}{\bar{\omega}_P}e^{-\chi_D/kT_e}C+N_SN_e\frac{\Omega_{SD}}{\bar{\omega}_S}C+N_SA_{SD}&\\ = N_DN_e\frac{\Omega_{DS}}{\bar{\omega}_D}e^{-(\chi_S-\chi_D)/kT_e}C+N_DN_e\frac{\Omega_{DP}}{\bar{\omega}_D}C+N_DA_{DP}\,,&\end{aligned}\right\} \tag{8}$$

where

$$C = \frac{8.54\times 10^{-6}}{T_e^{1/2}}\,,$$

$$\bar{\omega}_S = 2J_S+1 = 1\,,$$

$$\bar{\omega}_D = 2J_D+1 = 5\,.$$

If we eliminate N_P between these equations, we obtain for the relative populations of the S and D levels

$$\frac{N_S}{N_D} = \frac{\frac{\tilde{\omega}_S}{\tilde{\omega}_D} e^{-(\chi_S-\chi_D)/kT_e}\left\{1 + \frac{\Omega_{DS}e^{-(\chi_S-\chi_D)/kT_e}}{\Omega_{DP}\left(1+\frac{\Omega_{SD}}{\Omega_{SP}}\right)} + \frac{A_{DP}\tilde{\omega}_D}{\Omega_{PD}N_e\left(1+\frac{\Omega_{SD}}{\Omega_{SP}}\right)C}\right\}}{1 + \left(\frac{A_{SD}+A_{SP}}{\Omega_{SP}}\right)\frac{\tilde{\omega}_S}{\left(1+\frac{\Omega_{SD}}{\Omega_{SP}}\right)N_eC} + \frac{\Omega_{SD}e^{-(\chi_S-\chi_D)/kT_e}}{\Omega_{PD}\left(1+\frac{\Omega_{SD}}{\Omega_{SP}}\right)} + \frac{A_{SD}\tilde{\omega}_S e^{-(\chi_S-\chi_D)/kT}}{A_{PD}\left(1+\frac{\Omega_{SD}}{\Omega_{SP}}\right)N_eC}} . \quad (9)$$

When numerical values of the relevant parameters are substituted, we obtain

$$\frac{N_S}{N_D} = \frac{\frac{1}{5}e^{-Y}\left[1 + 0.0765e^{-Y} + \frac{A_{DP}}{N_e}T_e^{1/2}1.65 \times 10^4\right]}{1 + \left[0.0765 + T_e^{1/2}\frac{8.93 \times 10^3}{N_e}\right]e^{-Y} + \frac{A_{SD}+A_{SP}}{N_e}T^{1/2}1.88 \times 10^4} , \quad (10)$$

where

$$Y = \frac{\chi_S - \chi_D}{kT_e} .$$

To evaluate the quantities within the parentheses, we make use of formula (6) to estimate T_e, and we use the electron densities determined in XI. For a good approximation it is sufficient to take $T_e = 9000°$ and $N_e \sim 10^4$. Then $e^Y \sim 39$. The values of the A's are taken from the calculations of Pasternack and the collisional parameters from X. Then

$$\frac{N_S}{N_D} = 0.2e^{-Y}\frac{4.4}{508} ,$$

and the relative intensities of λ 4363 and the green nebular lines will be given by

$$\frac{N_D A_{DP} h\nu_{DP}}{N_S A_{SD} h\nu_{SD}} = 4.07e^{33,000/T_e} , \quad (11)$$

which is in good agreement with our formula (6) derived from elementary considerations.

As a check on equation (9) we note that as N_e becomes large, equation (9) approaches the form of the Boltzmann equation. This result is to be expected, since whenever the higher levels are excited and de-excited, principally by collisions, a Boltzmann distribution of the atoms among the various levels obtains. When N_e is low, we see that the Einstein A's play a very significant role.

An estimate of the electron temperature of any given planetary may be obtained from the use of equation (6). This estimated value of T_e may then be utilized in the calculation of the denominator of equation (10) and the terms inclosed in brackets in the numerator. We ultimately obtain an equation similar to equation (11) but with a different numerical coefficient.

The intensities of all of the stronger lines in a number of the brighter and more interesting planetaries have been determined by one of us from plates taken with the quartz slitless spectrograph attached to the Crossley Reflector of the Lick Observatory. In a

number of objects the sum of the intensities of the green nebular lines has been determined, and the intensity of the λ 4363 line has been measured whenever possible upon the slitless spectrograms. When λ 4363 was too faint to be measured we have used the intensity estimates of Wright[1] reduced to our system of intensities. In a number of the planetaries studied the λ 4363 line was blended with $H\gamma$, and it was necessary to disen-

TABLE 1

ELECTRON TEMPERATURES OF PLANETARY NEBULAE

Object	$N_1 + N_2$	4363	Ratio	$T_e(6)$	$T_e(11)$
NGC 6543	81	(0.08)	1000	6,100	6,000
6826	88	(0.22)	400	7,300	7,200
6572	129	0.90	143	9,500	9,200
7009	130	1.03	126	9,900	9,500
7027	187	1.46	128	9,800	9,500
7662	211	2.14	98.5	10,600	10,300
IC 418	16.9	(0.034)	497	7,000	6,800
NGC 1535	109	(1.0)	109	10,300	10,000
J 320	151	1.48	102	10,500	10,100
NGC 6210	126	(0.3)	420	7,300	7,100
IC 4997	72.3	5.3	13.6	31,800	27,000
IC 351	139	0.58	240	8,300	8,100
NGC 2440	236	0.83	284	7,900	7,700
2165	145	1.35	107	10,400	10,000
2392	130	2.65	49	13,900	13,200
3242	154	0.48	317	7,700	7,500
IC 4634	140	0.22	637	6,600	6,500
4776	57	0.19	300	7,800	7,600
NGC 6741	322	0.52	620	6,700	6,500
IC 4846	102	1.85	55.3	13,300	12,600
NGC 6790	263	1.24	212	8,500	8,300
6803	108	0.34	317	7,700	7,500
6807	106	0.50	212	8,500	8,300
6818	202	0.46	440	7,200	7,000
6833	86	0.55	157	9,300	9,000
6879	88	0.25	350	7,600	7,400
6884	204	0.57	355	7,500	7,400
6886	230	1.02	225	8,400	8,200
IC 5117	214	0.95	226	8,400	8,200
5217	106	0.48	218	8,500	8,200

The intensities of the nebular green lines in the upper part of the table are taken from the results of a photometric study of these planetaries. The intensities of λ 4363, when not inclosed in parentheses, are also obtained directly from the photometric observations. The values in parentheses are obtained from Wright's (*Lick Obs. Pub.*, **13**, 193, 1918) estimates reduced to our system of intensities.

The intensities of all the lines in the lower part of the table are taken from Wright's measures reduced to our system. They are uncertain.

tangle the effects of the overlapping images. A wave-length and intensity calibration of Wright's intensity scale was effected from the relative intensities of lines in objects common to our two lists. In this way approximate intensities for λλ 5007, 4959, and 4363 for nineteen objects observed by Wright but not by any of us were obtained, and electron temperatures were estimated by the application of equation (6).

The calculation of the electron temperatures is summarized in Table 1. The first column gives the NGC or IC number of the object. The second and third columns give the intensities of the green nebular pair and λ 4363. The column headed R gives the

ratio of intensities, and that headed T_e, (6) the electron temperatures computed by equation (6). The column headed T_e (11) gives the electron temperature as computed by the application of equation (11). The order of magnitude is unchanged if the temperature is computed by equation (10) with improved values taken from the results of the application of equation (6). At 6000° an error of 400 per cent in the ratio of the intensity of λ 4363 to that of the green nebular lines makes an error of about 30 per cent in T_e. At the higher temperatures, the line λ 4363 is stronger relative to the green nebular lines, and the ratio may be measured fairly accurately. The tabulated temperatures are probably good to within 10 or 20 per cent in even the worst cases.

The electron temperatures range from about 6000° for NGC 6543 to about 10,000° for NGC 7027. NGC 2392, observed by Wright, gives a temperature of about 14,000°, but this may easily arise from errors in the intensities of the relevant nebular lines. The case of the stellar planetary IC 4997 deserves special attention. With an assumed electron density of 10^4 electrons/cm^3, we obtain an electron temperature of about 27,000°. If we assume an electron density of 10^5 electrons/cm^3, the temperature is depressed to about 19,000°. If we assume an electron density of 10^6 electrons/cm^3, an electron temperature of 7500° is obtained. It would seem reasonable to suppose that the electron density in IC 4997 is relatively high, very likely between 10^5 and 10^6 electrons/cm.^{3} Widened spectra show a strong hydrogen continuum at the head of the Balmer series. Unfortunately, the angular size of this object is very small, and therefore we cannot obtain a good estimate of the electron density by use of the method described in XI.

The electron temperature seems to be relatively insensitive to the degree of excitation of the nebular lines or to the nuclear temperatures found by Zanstra. A glance at the table will show that the electron temperature of highly excited objects such as NGC 7027 is not much greater than that of objects such as NGC 6572. This discrepancy between the observed temperatures and those which one would be led to expect on the basis of the calculations for a purely hydrogenic nebula, as outlined in V, seems to arise from loss of energy by the electrons in the collisional excitation of the metastable levels of ions of *O* III, *O* II, *Ne* III, etc. The cooling effect of the presence of oxygen and other impurities upon the electrons photoelectrically ejected from hydrogen will be considered in a subsequent paper. It will there be shown that the density of *O* III in the planetaries is of the right amount to depress the electron temperatures to the observed values.

Miyamoto has attempted the calculation of the electron temperature by the same method as outlined here, but his collisional cross-sections were calculated upon the basis of plane wave functions for the impinging electron. As shown in X, it is necessary to take into account the distortion of the wave front by the field of the ion. His values of the electron temperature differ from ours and are somewhat higher. Page[4] attempted the determination of the electron temperature from the distribution of energy in the continuum beyond the limit of the Balmer series and obtained very low values. This method of the determination of the electron temperature is subject to very great systematic errors on account of photometric difficulties and space reddening. By the same method, one of us obtained an electron temperature for NGC 7662 much in excess of 10,000°.

The next paper of this series will be devoted to a discussion of the observational data upon which these and other theoretical calculations rest.

HARVARD COLLEGE OBSERVATORY
June 18, 1940

[4] *M.N.*, **96**, 604, 1936.

PHYSICAL PROCESSES IN GASEOUS NEBULAE

XIV. SPECTROPHOTOMETRY OF SOME TYPICAL PLANETARY NEBULAE

LAWRENCE H. ALLER

ABSTRACT

Total intensities of emission lines in the spectra of a number of typical planetaries have been determined from spectrograms made with the quartz slitless spectrograph attached to the Crossley reflector of the Lick Observatory. The plates have been measured with the microdensitometer of the Harvard Observatory. Intensities of all the strong lines between λ 5007 and λ 3133 are tabulated. Intensities of lines in the visual region of NGC 7027, 7662, and 7009 have also been measured.

The present paper deals with the results of a study undertaken to supply observational data for the theory, now being developed at the Harvard Observatory, of the gaseous nebulae. The objective is to establish a system of total intensities[1] for the stronger lines in the spectra of a number of the brighter and more interesting planetaries.

Eleven planetaries were observed with the quartz slitless spectrograph attached to the Crossley reflector of the Lick Observatory during the summers of 1938 and 1939. Of the 150 plates taken, the best 53 have been reduced. Particular attention was paid to the high-excitation objects NGC 7009, 7027, and 7662. For a detailed study the advantageous location of NGC 7662 in declination and galactic latitude minimizes atmospheric extinction and space reddening. Its angular dimensions—32″ × 28″—enable us to investigate the distribution of the various radiations. The irregular nebula NGC 7027 contains many strong lines and is also favorably placed for observation. NGC 7009 was included because of its brightness and interesting structural details.

Observations in the photographic region were secured for the objects of intermediate excitation—NGC 6210, 6543, 6572, and 6826—and for the objects of low excitation—BD + 30° 3639, NGC 40, and IC 418. The stellar nebula IC 4997 was studied because of the abnormal intensity of λ 4363. Plates taken by R. H. Stoy, of NGC 1535, Jonckheere 320, NGC 2022, and $18^h13^m + 10°.6$ were kindly made available to me by Director Wright of the Lick Observatory.

Eastman 33's were generally used for the photographic region, although for the ultraviolet lines and faint images faster emulsions were employed. I used Eastman Super Pancro Press plates for the visual regions of NGC 7009, 7027, and 7662. Photometric standards for various wave-length regions were impressed on the plates by means of a tube sensitometer. For the visual region Wratten No. 26 and No. 40 filters were used; for the photographic region a Wratten No. 50 filter was employed, and for the ultraviolet calibrations I found a Wratten 18A filter satisfactory. Early in the series, standards were impressed upon a plate taken from the same box as the one exposed on the planetary, and the two were developed together. Later, standards were placed on all plates of the nebulae and the comparison star. The plates were developed in a tank under constant agitation for seven minutes at 67° in D11.

The B3 comparison star π_1 Cygni (HD 206672), magnitude 4.78, used by Popper[2] in his study of Nova Lacertae, was likewise used here. Stebbins[3] finds for the former a

[1] Ideally, we should give total intensities and isophotic contours for each image in order to reduce our values to the rate of energy emission per unit volume. The unpublished material permits this to be done in some cases.

[2] "The Spectrum of Nova Lacertae," *Ap. J.*, **92**, 262, 1940.

[3] Unpublished.

color excess of 0.03 mag. from λ 4250 to λ 4750, but I have made no attempt to correct for space reddening. The spectral energy distribution was suggested by inference from the work of Barbier[4] and his colleagues. From λ 6600 to λ 3700, a Planckian energy distribution corresponding to 17,000° K is assumed. Because of the overlapping hydrogen lines, a discontinuity at λ 3700 amounting to a factor of 1.55 has been adopted. Beyond this point the energy-curve is supposed to correspond to a temperature of 20,000° K. Thus, on the redward side of λ 3700 the intensity of the continuum is taken as $A\,f(17{,}000^\circ\ \mathrm{K})$ and on the violet side as $A/1.55\,f(20{,}000^\circ\ \mathrm{K})$.

On each exposure on the comparison star the image was run back and forth twenty times by the slow-motion motor to widen the spectrum. Between successive exposures the brightness of the star was diminished by 1 mag. with the end of a diaphragm with circular holes placed over the end of the telescope. We readily see that it is then possible to obtain the plate-*plus*-instrument sensitivity and also to check the photometric calibration-curves derived from laboratory data.

To correct for atmospheric extinction we make use of the expression

$$\frac{I_\lambda}{I_{0\lambda}} = 10^{-f_\lambda \sec z}\ ,$$

where I_λ is the intensity at zenith distance z, $I_{0\lambda}$ is the intensity outside the earth's atmosphere, and f_λ is the atmospheric extinction factor given by

$$f_\lambda = a_\lambda + b\ ,$$

where a_λ depends on the wave length and b is a constant. The values of these quantities were taken from the unpublished work of Popper.

To calculate the relative amounts of energy falling upon the plate per millimeter along the dispersion, I assumed the aforementioned spectral energy distribution of the comparison star and computed the dispersion by Hartmann's formula from measures of the Balmer lines. By comparing these values with the observed intensity distribution corrected for atmospheric extinction, we may find the sensitivity of the plate-*plus*-instrument combination at once.

All spectrograms were analyzed with the new microdensitometer of the Harvard Observatory.[5] The procedure adopted for all except a few of the widened spectra of some of the smaller planetaries was to run the plates parallel to the dispersion and to set the beam over 0.05 mm or 0.10 mm (depending on the size of the planetary) between successive runs. The tracing of each plate consisted of from four to eight separate runs along the spectrum. Plates run in this manner, with a magnification of 25, resulted in about 2000 feet of tracings. The comparison-star spectra were analyzed with the same arrangements of slits, magnifications, and sensitivity adjustments.

The D–log I-curves for the different wave lengths were joined, on the assumption that the amount of light required to produce a density of 0.6 was the same for all colors. As both the comparison star and the nebula were reduced in a similar manner, I believe the errors tend to cancel out. A considerable change of contrast was noted between the visual and the photographic regions of the spectrum. The check provided by the diaphragmed exposures of the comparison star yielded reassuring results for the photographic region but did not turn out well for the visual region. In any case the intensities of the lines in the visual region are less accurate than those determined for the photographic region.

[4] *J. d. obs.*, **19**, 149, 1936, and *C.R.*, **210**, 99, 1940.

[5] Dimitroff and Menzel, *Harvard Ann.*, **105**, 99, 1937.

The total intensities were found in an obvious manner by the addition of the image sections supplied by successive tracings. Also, as was pointed out by Page,[6] we must subtract from each image the contribution of the continuous background, whose intensity may be inferred from the stronger exposures. Errors in the estimation of the continuous background are more serious for the weaker lines.

Vignetting, usually dependent on wave length in the slitless spectrograph, requires that the nebula and comparison star be photographed in the same part of the field. Variations of atmospheric extinction, especially in the far ultraviolet, and uncertainties in the energy-curve of the comparison star are also causes of concern. Likewise, nonuniform sky fog is hard to correct for. Because of the rapid variations in the sensitivity of the Eastman Super Pancro Press plates with wave length, especially near $H\alpha$, numerous uncertainties are introduced into the intensities of the visual lines. Finally, since the planetaries are Milky Way objects, they are affected by unknown amounts of selectively absorbing material in the line of sight.

The objects observed and plates reduced are listed in Table 1. Successive columns give the NGC or IC number, the α and δ for 1900, the plate number, the observation date, the exposure time in minutes, the spectral region, and the zenith distance. In Table 2 are listed the line intensities observed in the five planetaries NGC 2022, 7009, 7027, 7662, and 6572. Table 3 gives the total intensities of the lines observed in the other objects. Blends are inclosed in brackets, and the procedure here has been to measure and tabulate the sum of the intensities of the blended lines, unless the images were far enough apart for reliable estimates of the separate contributions to be made. For term designations and estimates of the relative intensities of the lines contributing to a blend, reference to the paper of Bowen and Wyse[7] is recommended. Ozone absorption introduces considerable uncertainty in the ultraviolet. The intensities of the lines beyond λ 3133 in the spectrum of NGC 7662 were obtained from only one plate and are to be regarded as very approximate.

A comparison of these results with those obtained by Plaskett,[8] by Page,[6] and by Berman[9] has been made for the objects common to our lists. The intensities found by Plaskett and Page from slit spectra are not immediately comparable. In some cases we might expect a better agreement, particularly in the visual region where the intensities tabulated here seem too low. It is more appropriate to compare our results with those of Berman, after his measures have been corrected for the error in dispersion pointed out by Page. Five objects—NGC 7027, 7009, 6572, 6826, and 6543—were common to the two lists. Usually, I find greater intensities for the green nebular lines than Berman found. Since the plate sensitivity is low in this region, slight errors in its determination are capable of producing relatively large errors in the measured intensities. The fainter lines seem to be measured systematically stronger by Berman than by the writer. This effect very likely arises from the method used in allowing for the general continuum. For intermediate intensities, ranging from 1 to 10 on the scale $H\beta = 10$, the two systems show no systematic differences depending on intensity or wave length, and the scatter of individual points amounts to less than 0.1 in $\log I$. For the weaker lines, even when the systematic difference is allowed for, the scatter is much greater because of random errors.

Since both Berman and I used the same telescope and spectrograph, the differences between our results show the size of the errors of observation. Although the same general method of photometry was used in both cases, the reductions were done by quite independent methods.

The eye-estimates of Bowen and Wyse for the fainter lines suggest intensities greater than those found here. Their intensity scale was calibrated with respect to the published

[6] *M.N.*, **96**, 604, 1936.

[7] *Lick Obs. Bull.*, **19**, 1, 1939.

[8] *Pub. Dom. Ap. Obs.*, **4**, 187, 1928.

[9] *Lick Obs. Bull.*, **15**, 86, 1930.

TABLE 1

LIST OF OBSERVATIONS

Object	α	δ	Plate	Date	Exp. (Min.)	Region	Z
				1938			
NGC 6210	$16^h40^m.3$	23° 59′	171	Sept. 15	12	Pg.	51°
6543	17 58.6	66 38	8	July 8	15	Pg.	36
			12	July 8	60	Pg.	45
			48	Aug. 5	30	Pg.	37
			49	Aug. 5	10	Pg.	41
6572	18 7.2	6 50	82	Aug. 15	5	Pg.	36
			90	Aug. 15	30	Pg.	51
			91	Aug. 15	10	Pg.	55
			114	Sept. 6	15	Pg.	14
BD 30°3639	19 30.8	30 18	122	Sept. 6	8	Pg.	44
			143	Sept. 13	12	Pg.	11
			149	Sept. 13	11	Pg.	39
NGC 6826	19 42.1	50 17	107	Sept. 5	20	Pg.	30
			108	Sept. 5	40	Pg.	35
			57	Aug. 6	25	Pg.	23
			59	Aug. 6	25	Pg.	21
			61	Aug. 6	12	Pg.	23
IC 4997	20 15.6	16 25	92	Aug. 15	17	Pg.	44
			94	Aug. 15	17	Pg.	47
			98	Aug. 15	13	Pg.	58
			99	Aug. 15	38	Pg.	64
			65	Aug. 6	87	Pg.	59
				1939			
			204	Sept. 6	61	Vis.	54
			206	Sept. 6	40	Vis.	51
NGC 7009	20 58.7	−11 46	208	Sept. 6	30	Pg.	57
			209	Sept. 6	20	Pg.	60
			228	Sept. 8	152	U.V.	49
			231	Oct. 5	60	U.V.	55
				1938			
			16	July 9	10	Pg.	34
			17	July 9	10	Pg.	32
			18	July 9	15	Pg.	27
			21	July 9	20	Pg.	16
NGC 7027	21 3.3	41 50	156	Sept. 13	25	Pg.	13
			157	Sept. 13	20	Pg.	9
				1939			
			220	Sept. 7	60	Vis.	7
			221	Sept. 7	20	Vis.	14
			244	Oct. 8	85	U.V.	34
				1938			
			23	July 9	10	Pg.	24
NGC 7662	23 21.1	41 59	24	July 9	18	Pg.	21
			26	July 9	10	Pg.	14
			50	Aug. 5	20	Pg.	13

TABLE 1—*Continued*

Object	α	δ	Plate	Date	Exp. (Min.)	Region	Z
				1938			
			51	Aug. 5	80	Pg.	5
			110	Sept. 5	150	U.V.	30
				1939			
NGC 7662	$23^h21^m.1$	41° 59′	194	Aug. 25	138	U.V.	34
			225	Sept. 7	130	Vis.	28
			237	Oct. 5	57	U.V.	45
			249	Oct. 8	177	U.V.	49
				1938			
NGC 40	0 7.6	71 32	125	Sept. 6	73	Pg.	39
			137	Sept. 7	11	Pg.	69
			138	Sept. 7	31	Pg.	65
IC 418	5 22.8	−12 46	140	Sept. 7	15	Pg.	58
			141	Sept. 7	5	Pg.	56
			168	Sept. 14	17	Pg.	60
				1934			
NGC 1535*	4 9.6	−13 0	S167	Nov. 2	70	Pg.	52
			S177	Nov. 11	120	Pg.	53
J 320*	5 0.0	10 36	.....	Dec. 14	120	Pg.	66
NGC 2022*	5 36.6	9 2	.....	.....	.....	Pg.	32
1813 10°.6*	.....	.....	S133	June 16	105	Pg.	47

* The asterisks refer to plates taken by R. H. Stoy in 1934.

intensities of Plaskett and Berman.[10] The intensities published by Wright[11] have been reduced to the present system by the following procedure: First, the wave-length variation was found from a comparison of the intensities of the stronger lines. Next, the lines in Wright's tables were corrected for the wave-length effect and plotted against the present measures. To effect this calibration the planetaries NGC 6543, 6572, 6826, 7009, 7027, 7662, and IC 418, common to our lists, were employed. The scatter of individual points was great, and the weaker lines were relatively stronger as measured by Wright. Since his work was done before the present techniques in photometry were available, it is not surprising that some discrepancies exist.

Objects observed by Stoy are indicated by an asterisk. Photometric standards were impressed on his plates in only the blue region, and different development was used for the individual plates of his series. I considered it impracticable to use his comparison stars in the reduction of his plates, since a different star was photographed on each plate and it would consequently have been hard to place the intensities on a uniform scale. Also, as the comparison star has been photographed on the same field as the nebula, pre-exposure effects may exist. Therefore, mean plate-*plus*-instrument sensitivity-curves for the types of plates used by Stoy have been employed. We may, therefore, expect larger errors in the line intensities derived from his plates.

[10] Apparently Bowen and Wyse have used the uncorrected Berman values for NGC 7027, so that their intensities for this object have a systematic error depending on wave length in the blue and violet spectral regions.

[11] *Lick Obs. Pub.*, **13**, 191, 1918.

TABLE 2

Line	Element	NGC 2022*	NGC 6572	NGC 7009	NGC 7027	NGC 7662
6583	*N* II					
6563	*H* I	.....	.....	14.5(?)	45(?)	17.5(?)
6548	*N* II					
6364	*O* I					
6312	*S* III	.....	.....	.....	5.7	.....
6300	*O* I					
5876	*He* I	.....	.....	1.35	2.4	1.1
5755	*N* II				1.0	
5412	*He* II				0.4	0.4
5007	*O* III	74	94	96	138	156
4959	*O* III	27	35	34	49	56
4861	*H* I	10.00	10.0	10.0	10.0	10.0
4740	*A* IV	.....	0.12	0.44	1.02	0.67
4712	*A* IV		0.13			
4686	*He* II	19.0	0.081	1.35	3.89	5.26
4659	C IV					
4650	C III	.....	0.16	0.38	0.58	0.32
4641	*N* III					
4634	*N* III					
4571	Mg I?	.....	0.044	.....	0.06	.....
4542	*He* II	.....	.....	.....	0.17	0.165
4471	*He* I	.....	0.58	0.43	0.27	0.25
4363	*O* III	8.7	0.90	1.03	1.46	2.14
4340	*H* I		3.60	3.42	2.71	4.29
4267	C II	.....	0.05	0.13	0.04	.....
4200	*He* II	.....	.....	.....	0.03	0.08
4144	*He* I	.....	0.034	.....	0.024	.....
4103	*N* III					
4101	*H* I	4.4	2.11	2.49	1.30	2.63
4097	*N* III					
4076	*S* II					
4069	*S* II	.....	0.24	.....	0.48	.....
4026	*He* I	.....	0.20	0.14	0.10	.....
3970	*H* I					
3967	*Ne* III	4.5	3.50	3.95	2.16	4.12
3924	*He* II	.....	.....	.....	0.02	.....
3889	*He* I, *H* I	9.8	1.43	9.85	0.80	11.4
3869	*Ne* III		5.85		4.43	
3835	*H* I	.....	0.60	.....	0.31	.....
3798	*H* I	.....	0.34	.....	0.22	.....
3771	*H* I	.....	0.23	.....	0.12	.....
3760	*O* III	.....	0.18	.....	0.15	.....
3750	*H* I	.....	.....	.....	0.12	.....
3728.6	*O* II	.....	3.53	1.66	1.19	2.4
3726.1	*O* II					
3712	*H* I	.....	.....	.....	0.05	.....
3444	*O* III	11.3	.....	0.47	0.72	2.0
3425	*Ne* V			0.11	2.98	1.2
3346	*Ne* V					
3343	*Ne* III	4.4	.....	0.36	1.36	1.57
3340	*O* III					
3312	*O* III	.....	.....	0.35	0.33	1.05
3299	*O* III	.....	.....	.....	0.07	0.26
3203	*He* II	4.6	.....	0.31	0.46	1.89
3178	*He* I	.....	.....	0.21	.....	.....
3133	*O* III	7.9	.....	1.23	1.35	7.10
3121	*O* III	.....	.....	.....	.....	0.66
3047	*O* III	.....	.....	.....	.....	2.08
3023	*O* III					very weak

As the theoretical discussion is taken up elsewhere in this series, no attempt at an ordered arrangement of the planetaries will be made. An empirical classification on the basis of their spectra was made by Wright, and there seems to be nothing further on that subject to add here. However, although he described most of their characteristics, a few remarks concerning certain of these planetaries may not be out of place.

NGC 1535 consists of an intense inner ring surrounded by a faint outer one. λ 4686 is represented only in the inner ring. λ 3727 has a fairly large but faint image. The lines of the Bowen fluorescent mechanism are present but very weak.

TABLE 3

Line	NGC 40	IC 418	NGC 1535	J 320	NGC 6210	NGC 6543	18^h13^m 10.6	BD $30^\circ3639$	NGC 6826	IC 4997
5007	.....	13.9	80.0	120.	92	60	.....	.....	80	54.3
4959	.....	5.0	28.6	31.0	34	21	.....	.....	27	18.9
4861	10.0	10.0	10.0	10.0	10.0	10.0	10.0	10.0	10.0	10.0
4686	.....	.....	1.3	.....	.....	.....	.....	.....	0.56	.....
4471	.....	0.4	0.21	.....	0.4	0.36	.....	.....	0.57	0.92
4363	.....	.....	[5.5]	1.5	[4.0]	[4.13]	.....	.....	[4.0]	5.6
4340	4.8	4.5		5.7			4.0	3.6		3.5
4101	2.5	2.4	3.1	3.4	1.8	2.14	2.1	2.0	1.9	1.78
4069, 76	.....	0.21	.....	.....	.....	.....	0.31	.....	.....	0.32
4026	.....	0.11	.....	.....	.....	0.21	.....	.....	.....	0.34
3967	1.3	1.50	4.5	7.9	3.0	2.33	1.2	1.26	2.3	4.50
3889	0.9	1.26	[11.8]	2.7	1.1	[5.3]	0.9	[1.51]	[5.1]	1.53
3868	.....	.....		15	5.6		.....			7.6
3835	.....	0.64	.....	.....	.....	.....	0.35	0.55	.....	0.92
3820	.....	.....	.....	.....	.....	.....	.....	.....	.....	0.29
3798	.....	0.34	.....	.....	.....	.....	0.34	.....	.....	0.53
3770	.....	.....	.....	.....	.....	.....	0.46	.....	.....	0.45
3750										0.38
3727	13.5	15.7	1.37	2.7	2.00	3.22	10.2	5.4	2.6	2.20

TABLE 4

(NGC 7009)

λ 5007	106	λ 4340	4	λ 3889	2
4959	40	4101	2	3868	11
4861	10	3967	4	3727	18

NGC 2022, a low-density object, seems to be the highest excitation planetary among the objects studied. It is a rather faint ring nebula, characterized by strong λ 4686 and lines of the Bowen fluorescent mechanism.

NGC 7009, a beautiful and interesting planetary, exhibits a spindle shape and a pair of faint extensions terminated by bright ansae. The ultraviolet hydrogen continuous spectrum is strong, and the Bowen fluorescent mechanism lines are not conspicuous.[12] A helium line at λ 3178 gives an image that seems to be diffuse and larger than the neighboring image of the λ 3203 line of *He* II. The mean relative intensities of the lines in the two ansae have been determined from plate 228. The degree of excitation in the two ansae is about the same and is much lower than in the main body of the planetary (cf. Table 2). The λ 4686 line and the lines of the Bowen fluorescent mechanism do not appear in the ansae.

[12] On the strongest plate the spectrum of the central star runs down to about λ 3000, and there is a faint suggestion of yet another line of the Bowen fluorescent mechanism.

The spectral characteristics of NGC 7662 and NGC 7027 will be discussed in some detail in later papers. The data on the continuous spectrum at the Balmer limit have been discussed in a previous paper[13] in connection with the determination of the electron density. In the later papers of this series these observational data will be subjected to further theoretical analysis. We shall discuss, among other topics, the ionization formula for gaseous nebulae, stratification, the Bowen fluorescent mechanism, and abundances.

I am very grateful to Director Wright of the Lick Observatory who make it possible for me to secure the observations for this investigation; and to Dr. A. B. Wyse I am grateful for many helpful suggestions. I am deeply indebted to Dr. Menzel whose interest in this investigation, constant encouragement, and valuable suggestions have made the tedious reductions much easier.

HARVARD COLLEGE OBSERVATORY
July 13, 1940

[13] Menzel and Aller, "Physical Processes in Gaseous Nebulae," XII, *Ap. J.*, **93**, 195, 1941.

PHYSICAL PROCESSES IN GASEOUS NEBULAE

XV. THE STATISTICAL EQUILIBRIUM OF NEUTRAL HELIUM

LEO GOLDBERG

ABSTRACT

The statistical equilibrium of an assembly of neutral helium atoms has been investigated with reference to the problem of gaseous nebulae. The helium atom was assumed to contain an infinite number of energy levels, but a single equation of equilibrium was written down for all triplet levels above $2\ ^3P^o$ and, similarly, for all singlets above $2\ ^1P^o$. Mean values are thus obtained for the populations of the high singlets and the high triplets. The population is given in terms of a quantity b_n, the ratio between the true population and the value for thermodynamic equilibrium at a temperature T_e. The temperature T_e refers to an assumed Maxwellian distribution of the free electrons.

The nebular atoms are assumed to be opaque to the stellar radiation field only in the frequencies corresponding to absorptions from levels $1\ ^1S$, $2\ ^1S$, and $2\ ^3S$. Numerical solutions of the equations are tabulated for stellar temperatures, T_1, of 50,000° and 100,000° and electron temperatures of 5,000°, 10,000°, 20,000°, 40,000°, and 80,000°, and also for the special case $T_1 = T_e = 20{,}000°$.

The procedure for calculating the distribution of atoms among their various energy levels when a gaseous assembly is not in thermodynamic equilibrium has been indicated by Rosseland.[1] In a nonvariable spectrum the condition of statistical equilibrium must be preserved. In order that a constant number of atoms may be maintained in a given level, the total number of atoms per second entering by radiative or by collisional processes must balance the total number leaving. The condition of statistical equilibrium for a given atom in a particular stage of ionization may be expressed as follows for a given level n:

$$\sum_{n''} F_{n''n} + \sum_{n'} F_{n'n} = \sum_{n'} F_{nn'} + \sum_{n''} F_{nn''} , \qquad (1)$$

where the F's denote the number of transitions per second between the involved levels. The subscript n' refers to levels with energy less than n, whereas n'' refers to higher levels, and the summations are to be taken over all possible levels n' and n'', including the continuous states. The F's are expressible in terms of the populations of the levels and the atomic and physical parameters that govern the assembly. Each atomic level yields an equation of the form of equation (1); and since, if we assume that the atomic and physical parameters are known, there is but one unknown per level—the population—the problem is theoretically soluble. In practice, however, difficulties arise from the fact that each atom has an infinite number of levels. The solution of the infinite determinant has been accomplished for hydrogen by Menzel and Baker,[2] but their solution cannot readily be adapted to more complex atoms. Other investigators[3] have avoided the difficulty by neglecting the higher atomic levels and treating the continuum as a single discrete state. Struve and Wurm, for example, have dealt with a six-state neutral helium atom comprising the five lowest levels and a discrete continuum.

The presence of two low-lying metastable levels makes the statistical equilibrium problem for *He* I of considerable interest. The influence of diluted radiation in over-

[1] *Ap. J.*, **63**, 218, 1926. [2] *Ap. J.*, **86**, 70, 1937.

[3] Cf. Plaskett, *Harvard Circ.*, No. 335, 1928; Carroll, *M.N.*, **90**, 558, 1930; Cillie, *M.N.*, **92**, 820, 1932; **96**, 771, 1936; Struve and Wurm, *Ap. J.*, **88**, 84, 1938.

populating the metastable levels and, indeed, all the triplet levels with respect to the singlets should be very much more pronounced in the nebulae than in the distended stellar atmospheres treated by Struve and Wurm.

In the present investigation we shall attempt to solve the equations of statistical equilibrium for an eight-state helium atom and at the same time allow in part both for the variation of the continuous absorption coefficient with frequency, and for the infinity in the number of discrete levels. We may write equation (1) for each of the five lowest levels: $1\ ^1S$, $2\ ^1S$, $2\ ^1P^o$, $2\ ^3S$, $2\ ^3P^o$, and for the continuum. The contribution of the higher levels may then be accounted for by the inclusion of two additional equations, one of which specifies the condition that the total number of atoms per second entering all the singlet levels above $2\ ^1P^o$ equals the number leaving, and similarly for the triplet levels above $2\ ^3P^o$. For the present only radiative processes will be considered.

We consider a source of black-body radiation at temperature T_1 shining on a distant unit volume of nebular material, whose temperature T_e is defined by a Maxwellian distribution of the free electrons. If the dilution factor is W, the intensity of radiation of a given frequency striking the nebular material will be $4\pi I_\nu W$. If we denote the lower of two atomic levels by n' and the upper by n, the total number of absorptions per second will be

$$F_{nn'} = 4\pi \int_0^\infty I_\nu W N_{n'} a_{n'n} \frac{d\nu}{h\nu} , \tag{2}$$

where $N_{n'}$ is the number of atoms in level n', and $a_{n'n}$ is the atomic absorption coefficient. The variation of I_ν/ν over the line width may be assumed to be so small that it may be removed from the integration sign. In terms of the oscillator strength $f_{n'n}$,

$$\int_0^\infty a_{n'n} d\nu = \frac{\pi e^2}{mc} f_{n'n} . \tag{3}$$

The number of emissions from n to n', including stimulated transitions, will be

$$F_{nn'} = N_n A_{nn'} + 4\pi \int_0^\infty I_\nu W N_n a_{nn'} d\nu , \tag{4}$$

where $A_{nn'}$ is the Einstein transition probability, and

$$a_{nn'} = \frac{\bar{\omega}_{n'}}{\bar{\omega}_n} a_{n'n} . \tag{5}$$

Following the procedure of Menzel,[4] we define a parameter b_n, which, for a given level n, is an index to the departure from thermodynamic equilibrium with respect to the ionized portion of the gas,

$$N_n = b_n N_i N_e \frac{h^3}{(2\pi m k T_e)^{3/2}} \frac{\bar{\omega}_n}{4} e^{I_n/kT_e} . \tag{6}$$

When $b_n = 1$, equation (6) reduces to the ionization equation for thermodynamic equilibrium. The factor 4 in the denominator is the product of the weights of the electron spin and of the ground level of ionized helium.

[4] *Ap. J.*, **85**, 330, 1937.

If we substitute equations (3) and (6) in equations (2) and (4) and replace I_ν by the Planck function, we get, for the number of absorptions,

$$F_{n'n} = K \frac{N_i N_e}{T_e^{3/2}} \tilde{\omega}_{n'} f_{n'n} b_{n'} \nu^2 \frac{W}{e^{h\nu/kT_1} - 1} e^{I_{n'}/kT_e}, \tag{7}$$

and for the number of emissions,

$$F_{nn'} = K \frac{N_i N_e}{T_e^{3/2}} \tilde{\omega}_{n'} f_{n'n} b_n \nu^2 e^{I_n/kT_e} \left(1 + \frac{W}{e^{h\nu/kT_1} - 1}\right), \tag{8}$$

where

$$K = \frac{h^3}{(2\pi mk)^{3/2}} \cdot \frac{2\pi^2 e^2}{mc^3}. \tag{9}$$

We number the eight states as follows: (1) 1 ^{1}S, (2) 2 ^{1}S, (3) 2 ^{1}P°, (4) high singlets, (5) 2 ^{3}S, (6) 2 ^{3}P°, (7) high triplets, and (8) continuum. The equations of statistical equilibrium may now be set down with the aid of equations (7) and (8) and solved for $b_1, b_2, \ldots, b_8$. Since the continuum is assumed to be in thermodynamic equilibrium, we set $b_8 = 1$. The values of b_4 and b_7 are mean values for the high levels. The presence of the Boltzmann factor in equation (6) tends to weight the lower levels in each group, for it is N_n that is actually averaged. The condition of statistical equilibrium leads to a seventh-order determinant that must be equated to zero:

$$\left.\begin{array}{cccccccc} b_1 & b_2 & b_3 & b_4 & b_5 & b_6 & b_7 & 1 \\ \hline D_{11} & D_{21} & D_{31} & \ldots & \ldots & \ldots & \ldots & D_{81} \\ D_{12} & D_{22} & \ldots & \ldots & \ldots & \ldots & \ldots & D_{82} \\ D_{13} & \ldots & \ldots & \ldots & \ldots & \ldots & \ldots & D_{83} \\ \ldots & \ldots & \ldots & \ldots & \ldots & \ldots & \ldots & \ldots \\ \ldots & \ldots & \ldots & \ldots & \ldots & \ldots & \ldots & \ldots \\ D_{18} & \ldots & \ldots & \ldots & \ldots & \ldots & \ldots & D_{88} \end{array}\right\} \tag{10}$$

The coefficients D_{ij} and D_{ji}, where $i < j$, are given, except for transitions involving states 4, 7, and 8, by

$$D_{ij} = \tilde{\omega}_i f_{ij} \nu^2 \frac{W}{e^{h\nu/kT_1} - 1} e^{I_i/kT_e}; \tag{11}$$

$$D_{ji} = \tilde{\omega}_i f_{ij} \nu^2 e^{I_j/kT_e} \left(1 + \frac{W}{e^{h\nu/kT_1} - 1}\right). \tag{12}$$

When $j = 4$ or 7,

$$D_{i4} = W \tilde{\omega}_i e^{I_i/kT_e} \sum_{n=3}^{\infty} f_{in} \frac{\nu^2}{e^{h\nu/kT_1} - 1}; \tag{13}$$

$$D_{4i} = \tilde{\omega}_i e^{I_i/kT_e} \sum_{n=3}^{\infty} f_{in} e^{-h\nu/kT_e} \left(1 + \frac{W}{e^{h\nu/kT_1} - 1}\right). \tag{14}$$

The index n refers to the total quantum number. When $j = 8$, the D's involve integrations over the continuous states:[4]

$$D_{i8} = \frac{1}{2R}\,\tilde{\omega}_i e^{I_i/kT_e}\int_{\nu_i}^{\infty}\frac{\kappa^3 f_{i\kappa}\nu^2}{e^{h\nu/kT_1}-1}\,d\nu\ ; \tag{15}$$

$$D_{8i} = \frac{1}{2R}\,\tilde{\omega}_i e^{I_i/kT_e}\int_{0}^{\infty}\kappa^3 f_{i\kappa}\nu^2 e^{-h\nu/kT_e}\left(1+\frac{W}{e^{h\nu/kT_1}-1}\right)d\nu\ . \tag{16}$$

In equations (15) and (16) κ is the continuous quantum number, defined by

$$E_\kappa = +\frac{R}{\kappa^2} = \tfrac{1}{2}mv^2\ , \tag{17}$$

where E_κ is the positive energy of a continuous state, in frequency units, and R is Rydberg's constant. When $i = 4$ or 7, equations (15) and (16) must be summed over all values of the total quantum number n from 3 to infinity. The coefficients D_{ii} are given by

$$\left.\begin{aligned} D_{11} &= -(D_{12}+D_{13}+\ldots.+D_{18})\ ,\\ D_{22} &= -(D_{21}+D_{23}+\ldots.+D_{28})\ ,\\ &\ldots\ldots\ldots\ldots\ldots\ldots\ldots\ldots\end{aligned}\right\} \tag{18}$$

Several simplifications may now be introduced. Because of the close adherence of *He* I to *LS* coupling, intersystem combinations are forbidden. Hence all values of D referring to transitions between singlets and triplets may be set equal to zero. In equations (12), (14), and (16) the right-hand term in the parenthesis represents the contribution of stimulated emissions. This term may obviously be neglected if it is small compared with unity, although it becomes important for small ν and large T_1. For the low-frequency transition $2\,{}^3\mathrm{P}^o - 2\,{}^3\mathrm{S}$, for example,

$$\frac{W}{e^{h\nu/kT_1}-1} \sim 3W, 7W\ , \tag{19}$$

when $T_1 = 50{,}000°$ and $100{,}000°$, respectively. The small values of W in the gaseous nebulae thus justify the neglect of stimulated emissions, even when W is as large as 0.001. We also neglect all absorptions other than those from $1\,{}^1\mathrm{S}$, $2\,{}^1\mathrm{S}$, and $2\,{}^3\mathrm{S}$.

The evaluation of the D_{ij} and D_{ji} requires a knowledge of the atomic transition probabilities. The exact values for helium are not known, but sufficiently good approximations have been derived by various investigators.[5] For the principal series a general expression derived by Vinti has been employed, with a very slight modification. Vinti made use of exact hydrogenic wave functions, with $Z = 1$, for the $n\,{}^1\mathrm{P}^o$ levels, whereas calculations based on the variation method suggest that $Z = 0.97$ is more ap-

[5] Cf. Hylleraas, *Zs. f. Phys.*, **106**, 395, 1937; Goldberg, *Ap. J.*, **90**, 414, 1939; Vinti, *Phys. Rev.*, **42**, 632, 1932.

propriate.[6] For the 2p − nd and 2s − np series, formulae given by the writer were used. For the 2p − ns series the following general expression was derived:

$$f(2p - ns) = \frac{2^{18}\pi^2 \nu m a_0^2}{27h} n^9 Z_1^3 Z_2^5 \frac{(nZ_2 - 2Z_1)^{2n-8}}{(nZ_2 + 2Z_1)^{2n+8}} \times [n^2(3Z_2^3 - 18Z_1Z_2^2 + 24Z_1^2Z_2 - 8Z_1^3) + 4Z_1^2(3Z_2 + 4Z_1)]^2 . \quad (20)$$

The formula (20) was obtained from hydrogenic wave functions with appropriate values of Z_1 and Z_2, the average effective charges:

$$\left.\begin{aligned} Z_1(2\,{}^3S) &= 1.22\,; & Z_2(n\,{}^3P^o) &= 1.10\,; \\ Z_1(2\,{}^1S) &= 1.22\,; & Z_2(n\,{}^1P^o) &= 0.97\,. \end{aligned}\right\} \quad (21)$$

The following asymptotic formulae for the f-values were found useful in carrying out the summations indicated in equations (13) and (14):

$$\left.\begin{aligned} f(1\,{}^1S - n\,{}^1P^o) &\sim [31.8146]n^{-3}\nu^{-2} \\ f(2\,{}^1S - n\,{}^1P^o) &\sim [30.3603]n^{-3}\nu^{-2} \\ f(2\,{}^3S - n\,{}^3P^o) &\sim [30.2191]n^{-3}\nu^{-2} \\ f(2\,{}^1P^o - n\,{}^1D) &\sim [45.1979]n^{-3}\nu^{-3} \\ f(2\,{}^3P^o - n\,{}^3D) &\sim [45.4570]n^{-3}\nu^{-3} \\ f(2\,{}^1P^o - n\,{}^1S) &\sim [43.9323]n^{-3}\nu^{-3} \\ f(2\,{}^3P^o - n\,{}^3S) &\sim [43.9698]n^{-3}\nu^{-3} \end{aligned}\right\} \quad (22)$$

The summations were performed accurately from $n = 3$ to $n = 10$; beyond that point the summation was replaced by an integral from $n = 11$ to infinity, and the asymptotic formulae (22) were employed. When n is replaced by the continuous quantum number κ, equation (22) applies to the bound-free transitions near the series limit and may be used to evaluate equations (15) and (16). Although the asymptotic formulae hold only close to the series limit, the integrations may be safely performed to infinity, because the exponential term in ν makes the contribution to the integral small when ν is large.

The coefficients D_{87} and D_{84}, which represent the rate of electron capture in the high triplet and singlet levels, may be obtained if we set $i = n'$ in equation (16), perform the indicated integration over the continuous states, and then sum over n' from 3 to infinity. For this purpose the levels of different l that belong to a given n' were assumed to be degenerate, and the hydrogenic formula for $f_{n'\kappa}$[7] was employed. The procedure is justified by the fact that the levels with large values of l are favored in the capture process and helium levels with $l = 1$, or greater, are practically hydrogenic. Since the integral in equation (16) reduces to an E_i function, which cannot be expressed analytically in simple form, the summations were performed numerically with the aid of the tables of E_i functions given by Menzel and Baker.[2]

The determinant, equation (10), was solved for two values of T_i: 50,000° and 100,000°, and for five values of T_e: 5,000°, 10,000°, 20,000°, 40,000°, and 80,000°. In addition, the special case $T_i = T_e = 20{,}000°$ was treated, to afford at least a rough comparison be-

[6] Goldberg and Clogston, *Phys. Rev.*, **56**, 696, 1939.

[7] Menzel and Pekeris, *M.N.*, **96**, 77, 1935.

tween the present results and those obtained by Struve and Wurm. The results are summarized in Table 1. Since the stellar radiation is absorbed only by the ground and metastable levels, the populations of these levels depend only upon the dilution factor. The preference of atoms for the metastable levels is clearly shown, as is the preponderance of triplets over singlets. The large values of b for $2\ ^3P^o$ are notable. Once an atom

TABLE 1

VALUES OF b FOR LEVELS OF *He* I AS A FUNCTION OF W, T_1, AND T_e

T_e	5,000°	10,000°	20,000°	40,000°	80,000°
	$T_1 = 100{,}000°$				
b_1W...	2.27×10^{-25}	1.05×10^{-12}	2.92×10^{-6}	6.66×10^{-3}	4.41×10^{-1}
b_2W...	4.25×10^{-6}	9.28×10^{-4}	1.76×10^{-2}	1.06×10^{-1}	3.64×10^{-1}
b_3....	5.05×10^{-5}	5.35×10^{-3}	6.93×10^{-2}	3.37×10^{-1}	1.02
b_4....	5.34×10^{-3}	6.96×10^{-2}	2.34×10^{-1}	5.35×10^{-1}	1.08
b_5W...	1.41×10^{-5}	8.14×10^{-3}	1.83×10^{-1}	1.24	3.67
b_6....	4.17×10^{-3}	6.42×10^{-1}	7.36	35.9	88.4
b_7....	2.02×10^{-2}	2.60×10^{-1}	7.96×10^{-1}	1.69	2.80
	$T_1 = 50{,}000°$				$T_1 = T_e = 20{,}000°$
b_1W...	8.04×10^{-24}	3.78×10^{-11}	1.04×10^{-4}	2.36×10^{-1}	5.67×10^{-1}
b_2W...	1.59×10^{-5}	3.58×10^{-3}	6.82×10^{-2}	4.05×10^{-1}	5.02×10^{-1}
b_3....	1.29×10^{-4}	1.39×10^{-2}	1.80×10^{-1}	8.82×10^{-1}	5.89×10^{-1}
b_4....	9.36×10^{-3}	1.18×10^{-1}	4.08×10^{-1}	9.74×10^{-1}	6.07×10^{-1}
b_5W...	6.02×10^{-5}	3.46×10^{-2}	7.80×10^{-1}	5.29	11.9
b_6....	6.20×10^{-3}	9.52×10^{-1}	10.95	53.4	35.5
b_7....	2.67×10^{-2}	3.35×10^{-1}	1.02	2.23	2.01

arrives in this level, it may exit only by a spontaneous transition to $2\ ^3S$. The probability of such a transition is small, because the frequency is low; hence this level becomes abundant at the expense of the higher triplet levels.

In a later paper the results derived here will be discussed in connection with observations of helium lines in the nebulae. The writer is indebted to Professor D. H. Menzel for many interesting discussions relating to the problem of statistical equilibrium.

HARVARD OBSERVATORY
December 5, 1940

THE STREAM-MOTIONS OF 92,656 STARS

W. J. LUYTEN

ABSTRACT

The estimated directions of motion of 92,656 stars in the southern hemisphere, mainly brighter than the sixteenth photographic magnitude, have been analyzed by means of the empirical methods of Kapteyn and Eddington and the analytical method of Schwarzschild. The apex of drift I is found to lie at $\alpha = 95^\circ$, $\delta = -15^\circ$; that of drift II at $\alpha = 228^\circ$, $\delta = -69^\circ$; the solar antapex at $\alpha = 104^\circ$, $\delta = -43^\circ$; and the vertex of star-streaming at $\alpha = 263^\circ$, $\delta = -17^\circ$. The ratio of the numbers of stars belonging to each drift is found to be 0.59 : 0.41, with a sampling error of less than 0.003.

A similar discussion dealing with 850 stars with $\mu > 0''.5$ gives for drift I: $\alpha = 99^\circ$, $\delta = -12^\circ$; for drift II: $\alpha = 241^\circ$, $\delta = -70^\circ$; for the solar antapex: $\alpha = 110^\circ$, $\delta = -38^\circ$, $q = 0''.61$; and a ratio of 2 : 1. A number of "odd" stars are singled out, for which the parallaxes should be larger than average.

Finally, the motions of 830 double stars with common proper motion are analyzed, and the apices of the two drifts are found to lie at $\alpha = 96^\circ$, $\delta = -9^\circ$, and $\alpha = 250^\circ$, $\delta = -71^\circ$, respectively, while a ratio of 0.63 : 0.37 is indicated.

1. The Bruce Proper-Motion Survey, undertaken in co-operation with the Harvard Observatory, was finished, in so far as the available plates are concerned, in December, 1936. Of the 1009 pairs of plates required to cover the southern hemisphere completely, 950[1] pairs were blinked by the writer; and a total of 94,300 proper-motion stars were found. The motions of all stars south of declination -60° were measured and reduced by 1937, and a preliminary discussion of these motions has appeared as No. 4 of the "Publications of the Bruce Proper-Motion Survey." In addition, the motions of all stars with an estimated motion exceeding $0''.45$ annually and of all double stars with common proper motion were measured; discussions of these have likewise been published as Nos. 3 and 5, respectively, of the above series. Since 1937 the motions of all 14,500 stars found between -60° and -50° were measured; and the motions of another 6000—slightly more than half the total number found between -50° and -45°—were measured. The motions of the remaining 55,000 stars cannot be measured until sufficient funds become available. As there appears to be little prospect of obtaining these in the near future, it is advisable to see what information can be obtained from the material at hand.

2. Discussions involving magnitude of proper motion are clearly out of the question, but fortunately the original records are such that a discussion of the directions of motion, i.e., an analysis of the stream-motions, may be attempted.

At this point the procedure followed in "blinking" may be conveniently described. All plates were blinked by the writer, and with very few exceptions all in the same position, such that, in the microscope, south was to the right, west up. The area on each pair of plates was blinked through systematically in narrow strips, about 10′ wide, beginning at the northeastern corner; and each star found to move was given a number and recorded in the observation book with an arrow indicating the estimated direction of its motion.

While this recording is admittedly only rough, especially for the smaller motions, it does make possible a preliminary analysis of the favored directions of motion. To this end, a circular glass protractor was made, divided into twenty-four sections corresponding to directions in position angle as follows: $352\frac{1}{2}^\circ$–$7\frac{1}{2}^\circ$–$22\frac{1}{2}^\circ$, etc. Arrows falling within each of these divisions were recorded as being "in" position angle 0°, 15°, etc., and it thus became an easy matter to determine for each plate the favored directions of motion and to construct diagrams similar to those given by Kapteyn and Eddington. The actual

[1] The single area centered at α $19^h.0^m$, δ $-12^\circ.5$ was blinked in 1939, after publication of the "First Report"; its results have been incorporated in the present paper.

scoring of the 92,656 arrows in the observation books was done by Federal Aid students assigned to the Department of Astronomy of the University of Minnesota.

It must be admitted at the outset that this method can lay no claim to great accuracy, but in the absence of precise measurements it is the only thing one can do. Moreover, the relative accuracy of the recorded arrows (i.e., the uncertainty in angle) should be at least as good as in similar investigations concerned with the proper motions of *all* stars in a limited area in the sky; for in the latter instance there is always a large percentage of stars with linear displacement of the same order of magnitude as the error of measurement.

In the present case it would seem difficult to commit an error of as much as 30° in any but the very smallest motions.

The procedure followed here is subject to considerable systematic error, but no more so than where reduction from relative to absolute motion is involved and magnitude error has its full scope. Both of these points—accuracy and systematic error—will automatically reveal themselves in the subsequent discussion, and the least that can be said for the present method is that it allows us to make use of a body of material larger than any other in existence, which otherwise would have to lie fallow until such time as the measurements and reductions can be completed.

3. The centers of the 1009 pairs of plates were located at the positions listed in the "First Report of the Bruce Proper-Motion Survey."[2]

In order to simplify the later calculations, these original regions, each of which covers about 30 square degrees, were combined into larger areas, called "Σ-regions," as used before.[3] The first Σ-region covers about two and one-half times as much area as the average of the others; but, owing to the distribution of the original regions, no other division seemed equitable. The overlap of adjacent pairs of plates, which is enormous in this first Σ-region and still large in the next 36 regions, becomes very small near the equator. No allowance has been made for this overlap, since (*a*) comparatively few stars in the overlapping regions were found in both regions and (*b*) the arrows recorded were wholly independent in the two cases. The earlier regions, thus, merely contain a certain percentage of stars which have been counted twice (or more); but it is evident that little or no selection has entered here, and accordingly nothing spurious is introduced.

4. A preliminary discussion of the data obtained from these Σ-regions has been given in the *Tercentenary Papers of the Harvard College Observatory*,[4] and the apex of the first drift was found to lie at $\alpha = 94^{\circ}.6 \pm 0^{\circ}.7$, $\delta = -15^{\circ}.4 \pm 0^{\circ}.7$ (1900). At that time the survey had not yet been completed north of declination −20°, and only 85,000 proper-motion stars were available; moreover, the directions of the second drift showed such a large scatter that it was decided to postpone their discussion until the remaining regions had been examined.

The preliminary discussion indicated that the originally recorded arrows are subject to a scatter due to errors of observation of about 15°, and it thus seemed profitable to combine the 157 Σ-regions into a smaller number of regions of larger area. The resultant loss in accuracy is very slight, and the saving in labor of computation is considerable. The arrows in any one region were corrected to the meridian of the center of the large area, naturally. Because of the original distribution of the Bruce regions, it did not seem feasible to make them all of the same area; and again the polar area differs markedly from the others, having now but half the average area of the others, viz., 0.0152 of the southern hemisphere, while that of the four areas with center at −69° amounts to 0.0297, that of the eight at −49° to 0.0280, and that of the twelve at −30° and −10° to 0.0250 and 0.0285, respectively.

[2] *Pub. A. Obs. U. Minnesota*, **2**, 73, 1938, sec. 3. Cf. also Harvard Tercentenary Volume, *Harvard Ann.*, **105**, 398, 1937.

[3] *Harvard Ann.*, **105**, 398, 1937, and *Pub. A. Obs. U. Minnesota*, **2**, 140, 1939.

[4] *Harvard Ann.*, **105**, 398, 1937.

Table 1 presents details of these larger areas, which will be referred to as "ΣΣ-regions." The first column gives the serial number, the second and third columns the center; the total number of Bruce regions contained in them, and the number of these still unblinked, are shown in the fourth and fifth columns, while the sixth column lists the total number of arrows scored in each. Finally, the seventh and eighth columns give the directions toward the apices of drifts I and II. The favored directions were determined by plotting on rectangular graph paper the actual numbers of stars moving against the directions, drawing free-hand curves, and reading off the maxima. In some cases where a blend occurred, the position of the secondary maximum—generally that due to drift II—was determined differentially, by assuming the principal maximum to be symmetrical. The actual numbers of stars found to be moving in different directions are given, for these 37 ΣΣ-regions, in Table 2.

TABLE 1

Serial No.	Center		No. of Regions		N	I	II
	α	δ					
1	.....	−90°	25	.....	1985	93°	264°
2	3h0	−68.7	36	.....	3100	44	197
3	9.0		36	.....	3825	311	139
4	15.0		36	.....	4675	229	62:
5	21.0		36	.....	5772	144	253:
6	1.5	−49.3	33	3	2700	98	188
7	4.5		33	.....	2619	58	183
8	7.5		33	.....	3213	311	147
9	10.5		33	.....	5350	278	132
10	13.5		33	.....	5286	246	154
11	16.5		33	.....	5434	204	.....
12	19.5		33	.....	4767	177	.....
13	22.5		33	.....	3449	114	170:
14	0.0	−30.0	24	.....	1975	106	192
15	2.0		24	1	1142	91	181
16	4.0		24	4	1001	.....	190
17	6.0		24	5	938	.....	171
18	8.0		24	.....	2407	292	163
19	10.0		24	.....	2880	282	150:
20	12.0		24	.....	2391	252	133
21	14.0		24	.....	2962	246	171:
22	16.0		24	.....	2580	241	197
23	18.0		24	.....	3071	197:	175:
24	20.0		24	.....	2185	148:	200:
25	22.0		24	.....	1971	131	193
26	0.0	−10.0	24	.....	1279	111	184
27	2.0		24	9	599	102	179
28	4.0		24	12	512	109	176
29	6.0		24	15	455	.....	173
30	8.0		24	9	1118	271	173
31	10.0		24	.....	1361	257	164
32	12.0		24	.....	1663	257	165
33	14.0		24	.....	2094	251	193
34	16.0		24	.....	1556	252	198
35	18.0		24	.....	1519	187	
36	20.0		24	.....	1666	121	184
37	22.0		24	.....	1336	118	170

TABLE 2

θ	ΣΣ																																		θ
	1	2	3	4	5	6	7	8	9	10	11	12	13	14	15	16	17	18	19	20	21	22	23	24	25	26	27	28	29	30	31	32	33	34	35	36	37	
0°	12	64	78	26	25	16	98	141	30	9	3	9	3	1	8	13	29	50	11	0	6	2	8	2	4	3	2	4	7	5	1	3	2	2	3	1	4	0°
15	14	194	54	45	13	35	129	102	20	14	4	6	10	5	14	38	26	27	6	1	4	2	12	1	5	4	1	4	6	3	4	3	1	1	3	7	5	15
30	25	360	34	41	21	47	123	42	17	7	14	3	9	10	17	25	6	9	2	1	2	3	4	5	5	0	3	0	3	1	0	1	4	4	1	1	3	30
45	85	408	45	62	21	90	167	26	13	15	12	5	13	26	25	33	11	10	4	2	3	4	6	5	8	5	2	3	2	2	1	0	2	0	2	2	9	45
60	105	363	34	63	35	203	176	41	15	30	25	7	41	70	67	47	4	11	9	5	6	3	8	10	23	20	23	15	7	3	4	5	6	2	4	17	30	60
75	207	297	38	64	91	274	163	39	39	41	25	25	92	124	103	63	22	20	7	11	12	8	13	29	63	86	54	26	12	1	2	17	9	1	6	27	39	75
90	313	205	72	58	205	310	128	46	99	44	24	38	268	205	149	56	19	17	27	25	20	8	15	27	70	135	87	22	12	4	10	19	17	8	10	35	107	90
105	245	134	126	37	478	316	112	76	153	84	53	100	482	300	115	67	25	59	75	60	50	13	21	72	197	195	108	49	22	36	39	46	25	6	21	59	146	105
120	212	90	166	54	611	263	150	200	275	110	70	232	513	212	103	74	52	145	147	109	88	35	47	139	243	183	67	42	35	63	66	65	69	32	25	106	180	120
135	138	70	191	57	880	201	161	254	314	122	115	448	404	190	92	93	90	232	203	148	97	78	117	205	267	102	34	34	28	77	72	81	82	42	46	68	131	135
150	67	85	164	61	862	131	178	234	212	116	169	572	308	103	55	88	91	241	177	95	119	110	150	219	195	77	26	40	43	103	95	95	87	77	84	125	114	150
165	47	101	87	71	739	146	218	224	192	117	266	850	316	152	84	94	148	251	224	103	137	176	407	377	219	101	39	67	95	197	175	136	144	135	225	290	137	165
180	30	114	73	167	465	151	258	204	152	148	517	917	262	137	60	103	141	242	124	88	133	274	601	375	135	91	60	100	90	218	107	97	138	146	337	382	129	180
195	30	164	62	319	287	162	200	130	95	194	1178	612	211	183	84	106	74	155	129	109	204	505	747	297	204	109	43	47	21	92	72	61	171	245	341	310	100	195
210	36	135	49	617	193	101	96	60	58	258	1197	397	134	80	53	33	31	55	62	94	203	378	392	153	89	62	17	20	11	38	47	64	140	183	190	111	58	210
225	38	100	44	913	146	103	57	35	108	657	884	166	124	64	35	22	14	48	82	138	327	300	230	109	79	25	7	9	2	9	40	78	151	88	62	30	34	225
240	58	64	47	836	116	71	35	35	227	1233	480	119	96	54	33	15	16	60	159	315	617	348	130	73	75	36	16	8	5	32	124	200	307	130	62	38	62	240
255	69	27	73	559	133	33	18	39	470	1143	207	85	85	30	13	8	14	59	285	479	511	190	86	39	51	19	8	7	3	61	184	312	343	129	43	20	24	255
270	85	12	185	310	126	7	19	74	1093	620	95	73	29	17	8	0	11	97	357	328	233	70	24	23	14	9	0	7	11	77	164	251	247	84	21	11	12	270
285	53	15	382	123	114	11	25	180	1114	237	55	54	20	4	2	7	31	220	427	214	133	48	24	15	15	7	0	1	7	62	99	94	112	27	11	12	4	285
300	43	12	578	81	71	7	18	297	427	65	23	25	13	4	5	4	20	208	201	38	35	13	9	2	4	6	1	1	8	17	30	24	22	8	9	7	2	300
315	33	15	648	36	69	4	20	352	136	12	12	8	7	3	10	6	28	116	75	20	14	8	12	3	4	2	0	3	4	5	12	6	9	2	2	3	2	315
330	22	22	432	40	46	7	29	236	53	4	6	11	8	0	5	3	20	39	22	4	7	4	2	4	2	2	0	2	5	4	8	4	2	2	7	2	2	330
345	18	49	163	35	25	11	41	146	38	5	0	5	1	1	2	3	15	36	5	4	1	0	6	1	0	0	1	1	16	8	5	1	4	2	4	2	2	345

5. Poles were then calculated for both favored directions, and these were plotted on a sphere. Those belonging to drift I arranged themselves so clearly along a great circle that no difficulty was encountered in deciding, for any particular region, which direction belonged to which drift. The apex of drift I was then found to lie at α 94°.8 ± 1°.0, δ −15°.1 ± 1°.0.

For drift II the "equator" of the apex was much less clearly defined by the poles calculated for the ΣΣ-regions; and the determination of the point to be considered as *the* apex presented peculiar difficulties. It became immediately evident that the apex differed much more from the position usually found than in the case of drift I. Since the stars under consideration have been selected because of their large proper motion, it is likely that among them will be found an unusually large percentage of high-velocity stars. Moreover, it seems probable that this percentage varies considerably, especially in the regions near the apices of the two drifts, and it is doubtful if one could really speak of an apex for these stars.

Using only the 16 ΣΣ-regions where the two drifts are most clearly separated, we find apex II to be at 225°, −68°, whereas a calculation using all poles determined and giving equal weights, regardless of how clearly or how badly the two drifts were separated, gave 232°, −74°. The position finally adopted for the apex of drift II is distant from the center of ΣΣ4 by less than 2°; yet the effect of the second drift is more pronounced here than in several other regions much more favorably situated. Similarly, the original ΣΣ-regions 28–33, none of which show drift II, are all farther distant from the apex than Σ1 = ΣΣ1, which does show it clearly but in direction 264°, or 36° different from what it should be according to the adopted position. Moreover, in this case we have stronger evidence, obtained from a discussion of the measured motions of 1434 stars south of −80°,[5] which gives 262° for the direction of apex II, agreeing almost exactly with the result from the approximate arrows and corresponding more nearly with the direction of the apex of drift II as usually obtained. On the other hand, a discussion of the motions of 500 stars which I measured in the foreground of the Large Magellanic Cloud gave 170° for the direction of apex II, markedly different from the expected value of about 195°.

It is clear that the uncertainty in the position of the apex of drift II is much greater than that for drift I; all we can determine is an average apex, and for this we may adopt the position $\alpha = 228° \pm 9°$, $\delta = -69° \pm 3°$.

In Figure 1 diagrams are given showing the distribution of the directions of motion in four cases. Following a suggestion of Professor Hertzsprung, the radius vector in these plots has been made proportional to the square root of the number of stars moving in that direction, thus insuring a truer equal-area representation of the motions and one which accentuates the two drifts less than usually. Furthermore, there is the practical advantage that now such regions as ΣΣ11, even though the numbers involved vary between 0 and 1200, can be represented on a reasonable scale, which is not possible when the radii vectores are proportional to the actual numbers themselves. Finally, the sampling error in each radius vector is now a constant and equal to one-half unit. In each figure the arrows indicate the directions from the center of the region to the finally adopted apices of the two drifts.

In the left part of Figure 1 two diagrams are given for the polar area ΣΣ1, the upper one made from the actually measured motions of 1434 stars, the lower one made from the estimated directions of 1985 motions as recorded in the observation book; and it is seen that the two are virtually identical. The upper right gives the diagram for ΣΣ9, centered at 10:30—49:20, where the two drifts are most clearly separated; the lower right, that for ΣΣ11, where the two drifts are indistinguishable, giving the impression of an overaccentuated single drift. Thus, whereas nearly 1200 stars are found to move in each of

[5] Arrows were marked in the blinkbook for 1985 stars south of −80°, but, owing to overlap, these were found to apply to only 1434 different stars.

the directions between 187° and 202° and between 202° and 218°, not a single star is found to move in a direction between 337° and 353°.

6. The foregoing analysis has been almost wholly empirical, and its solution graphical. Making use only of the observed fact that there appear to be two favored directions of motion among the stars, the apices of the two streams have been determined. At the opposite end of the various methods proposed for dealing with this problem stands that of Schwarzschild, which is almost automatic in its application. While it thus possesses a great practical advantage, difficulties may arise in the interpretation of the significance

FIG. 1.—Vector diagrams for the proper motions of stars in the southern hemisphere. The radii vectores are proportional to $\sqrt{N}$; arrows marked *I* and *II* indicate the directions toward the calculated apices of drifts I and II, respectively. *Upper left:* Measured motions of 1434 stars in the south polar area. *Lower left:* Estimated directions of motion for 1985 stars in the south polar area. *Upper right:* Estimated directions of motion for 5350 stars in ΣΣ9, centered at α 10^h30^m, δ $-49°20'$. *Lower right:* Estimated directions of motion for 5434 stars in ΣΣ11, centered at α 16^h30^m, δ $-49°20'$.

of the results, especially in the present case, where we are dealing with a restricted class of objects and with relative proper motions.

Applying the method as outlined by Knox Shaw in his Introduction to the Radcliffe catalogue, the directions toward the solar antapex, θ_A, and toward one of the vertices, θ_V, were determined, as well as the quantities h/β and β/α, giving the ratio between the projected velocity of the sun and the lesser ellipsoidal component and also that between the two ellipsoidal components themselves. The results of the calculation are given in Table 3, which is self-explanatory. All calculations were carried out to 0°.1, and thus, even when $\theta_A - \theta_V$ is small, h/β could be calculated; but, as it appears from the figures given, the results are not as reliable as one might wish.

When the directions thus found are plotted on a sphere, the θ_V define the vertex fairly clearly; and graphically a provisional position at α 269°, δ −20° may be determined. A least-squares solution was then made in the usual way, namely, from

$$-X \sin \alpha + Y \cos \alpha = \sqrt{\frac{\alpha^2}{\beta^2} - 1} \cdot \sin \theta_V ,$$

$$-X \cos \alpha \sin \delta - Y \sin \alpha \sin \delta + Z \cos \delta = \sqrt{\frac{\alpha^2}{\beta^2} - 1} \cdot \cos \theta_V ,$$

$$\tan A_V = \frac{Y}{X} ,$$

$$\tan D_V = \frac{Z}{\sqrt{X^2 + Y^2}} ,$$

$$\sqrt{\frac{A^2}{B^2} - 1} = X^2 + Y^2 + Z^2 .$$

Although the numbers of stars varied from 455 for ΣΣ29 to 5772 for ΣΣ5, equal weights were given to all regions, as an equitable system of weighting would also have to take into account the clearness with which θ_A and δ_V are separated, while the number of stars, even in the poorest region, is still so large that not much accuracy will be lost in this way. Moreover, giving equal weights to all regions results in the great practical advantage that all three normal equations become independent, and the coefficients (and hence also the weights) of all three, X, Y, and Z, become $74/3 = 24.67$. In this way we obtain

$$A_v = 264^\circ.1 ,$$

$$D_v = -17^\circ.5 ,$$

$$\frac{A}{B} = 2.24 .$$

Owing to the very large scatter of the quantities which should be proportional to sin λ_v (where λ_v is the angular distance from the center of the region to the vertex), another least-squares solution was made for which all values of $\sqrt{(\alpha^2/\beta^2) - 1}$ were replaced by sin λ_v as read from a sphere, using the provisional vertex at 260°, −20°. The position of the vertex is now determined from the θ_v alone, and the final value of A/B is given by

$$\sqrt{\frac{A^2}{B^2} - 1} = \frac{\sum \left(\sqrt{\frac{\alpha^2}{\beta^2} - 1} \cdot \sin \lambda \right)}{24.67} .$$

Performing the calculations, we find that

$$A = 261^\circ.8 ,$$

$$D = -17^\circ.5 ,$$

$$\frac{A}{B} = 2.26 ,$$

virtually coincident with that found before for the vertex; and we adopt as final values:

$$A = 263^\circ.0 \pm 1^\circ.2 ,$$

$$D = -17^\circ.5 \pm 1^\circ.1 ,$$

$$\frac{A}{B} = 2.25 \pm 0.15 ,$$

the mean errors having been determined from the individual discordances.

TABLE 3

SUMMARY OF ANALYSIS BY SCHWARZSCHILD'S METHOD

ΣΣ	θ_A	θ_V	h/β	β/α
1	106°	270°	0.61	0.80
2	68	213	0.72	.64
3	307	131	0.60	.66
4	239	54	1.21	.67
5	150	299	1.26	.47
6	115	235	0.91	.66
7	125	194	0.53	.56
8	283	142	0.21	.23
9	267	111	1.41	.30
10	242	87	1.85	.45
11	206	61	1.44	.80
12	174	301	1.28	.93
13	138	264	1.23	.58
14	130	246	1.06	.49
15	120	240	0.89	.68
16	140	198	0.79	.70
17	168	159	0.95	.56
18	183	134	0.65	.44
19	244	118	0.91	.26
20	243	99	1.48	.33
21	235	100	1.55	.46
22	205	98	1.35	.95
23	190	191	1.52	.83
24	173	260	1.21	.15:
25	150	258	1.08	.69
26	128	255	1.20	.44
27	116	244	1.35	.38
28	161	237	1.00	.61
29	164	342	1.2:	.54
30	177	123	1.08	.70
31	214	112	1.00	.24
32	240	102	1.36	.27
33	233	103	1.45	.38
34	201	108	1.30	.92
35	187	256	1.49	.80
36	176	240	1.25	.92
37	141	251	1.07	0.55

From the proper motions of the Boss stars Eddington found that $A = 274^\circ$, $D = -12^\circ$; and, in general, the vertex as determined from apparently bright stars, i.e., chiefly giants,

is found to lie in right ascension ranging from 271° to 289° and in declination ranging from −3° to −19°, or, converted into galactic co-ordinates, between longitudes 329° and 355° and latitudes −3° and +5°. On the other hand, analysis of large proper motions generally gives a smaller right ascension and a declination farther away from the equator, such as the result of Dyson, viz., $A = 268°, D = -21°$, or $l = 336°, b = 0°$. Using 25,000 proper motion stars between $9^{m}.0$ and $15^{m}.0$ (photographic), and with $\mu < 0''.1$, Knox Shaw and Barrett found that $A = 268° \pm 2°.0$, $D = -22° \pm 2°.0$, or $l = 335°$, $b = 0°$, almost coincident with that of Dyson.

From the absolute proper motions of 18,000 stars measured on parallax plates, Van de Kamp and Vyssotsky found the vertex to lie at $A = 269°.7 \pm 2°.4$, $D = -10°.5 \pm 2°.4$, or in $l = 345°.9$, $b = +4°.0$, while the 2000 stars among these with proper motions in excess of $0''.04$ annually gave $A = 267°.5 \pm 4°.2$, $D = -24°.8 \pm 4°.0$, or $l = 332°.4$, $b = -1°.4$. Similarly restricting the Radcliffe material to motions between $0''.03$ and $0''.10$ (2200 stars), the same investigators determined the vertex at $A = 266°.1 \pm 3°.3$, $D = -25°.0 \pm 3°.0$, or in $l = 331°.6$, b $= +0°.4$.

These last two determinations use a material similar to that of the present investigation, namely, stars with proper motions exceeding a given limit. It is questionable whether Schwarzschild's automatic method is really applicable to these three cases, since the method presupposes equal numbers of stars moving in the two drifts, whereas a restriction to size of proper motion increases the proportion of stars of drift I over those of drift II—but at any rate, one might expect the method to give similar results in all three cases. The lower limit of proper motion does not differ much, being $0''.040$ for the McCormick data, $0''.03$ (with an additional upper limit of $0''.10$) for the Radcliffe motions, and will not be far from $0''.04$ in the present case. The actual results give, for the galactic co-ordinates of the vertex:

2000 stars	$l = 332° \pm 4°$	$b = -1° \pm 4°$	Van de Kamp and Vyssotsky
2200 stars	$l = 332 \pm 3$	$b = 0 \pm 3$	Knox Shaw and Barrett
92,600 stars	$l = 336 \pm 1$	$b = +6 \pm 1$	Luyten

Considering the difference in apparent magnitude limits for the material (the lower limit for the present survey being from 1 to 3 units lower than that for the other two), the agreement may be considered satisfactory. If the difference should be significantly real, it may perhaps be due to the fact that the stars of the present material are quantitatively dwarfs, while those of the others contain an admixture of about 20 to 30 per cent giants.

7. The scatter of the directions θ_A in defining the solar antapex is not only considerably greater than that for the vertex but shows some systematic effects as well. Thus, the regions ΣΣ2, 5, 6, 10, 13, 14, 15, 21, 26, 27, 32, 33, and 37, all of which lie more than 45° distant from the antapex, and for which the two directions, toward antapex and vertex, are clearly separated, indicate an antapex at about $A = 100°$, $D = -34°$. The seven regions ΣΣ7, 16, 17, 18, 28, 30, and 31, all of which lie within 50° of the antapex, indicate an antapex at 112°, −60°. The explanation of this probably lies in the limitation of the material to proper motions exceeding a certain limit; the closer a region lies to the antapex the higher would be the percentage of high-velocity stars among those with $\mu > 0''.04$. The solar antapex is, thus, not uniquely defined, and any calculation based on all 37 regions will yield only an average compromise value which will probably be around 105°, −42°.

Employing the same method as for the vertex, i.e., calculating once with h/β and once

while replacing this quantity by sin λ_A as read off the sphere from the provisional antapex at 105°, −42°, and then determining h/β separately, we obtain:

	From h/β	Using sin λ_A
A	103°.2	104°.5
D	− 44°.2	− 41°.8
u/B	1.38	1.36

I am inclined to accord more weight to the second determination, and for the final values we adopt

$$A = 104°.1 \pm 2°.0,$$

$$D = -42°.6 \pm 1°.5,$$

$$\frac{u}{B} = 1.37 \pm 0.05.$$

The apex determined by Knox Shaw and Barrett from the 25,000 Radcliffe stars was found to depend largely upon the corrections applied to reduce the relative proper motions to absolute values and, in fact, was seen to reproduce faithfully the apex implied by those corrections.

In the present instance the motions were all relative, but the directions only were used. Since the average systematic motion of the comparison stars is probably no more than 0″.008, or about one-tenth of the average motion of the proper-motion stars, the systematic effect of such a correction would be extremely small. Only in so far as the mean parallactic motion of these comparison stars differs from that of the proper-motion stars would the correction play any role; and, apart from this, its principal effect would be to increase, by a small amount, the accidental error in the direction of the motion. It has, therefore, been neglected.

8. Even though the significance of the results derived thus far is not yet clear, we may at least see if they are consistent among themselves. Summarizing, we have Table 4. The fourth and fifth columns give the galactic co-ordinates of the five points referred to Pickering's pole at 12:40 + 28° (1900). When these cardinal points of the velocity distribution are plotted on a sphere, it is seen that they lie very close to a great circle whose pole lies at $l = 229°.0$, $b = +73°.4$, or at $\alpha = 178°.8$, $\delta = +15°.1$. The root-mean-square deviation from the circle amounts to only 1°.1, or less than the average mean error of the four points. If these points are corrected to lie exactly on this circle, we obtain the galactic longitude and latitude as given in the sixth and seventh columns, differing but slightly from the original values.

While it may have been surprising to find the vertices of star-streaming for these stars of large motion deviating from the galactic plane by as much as 5°, it is evident that this is not due to some anomalous region or to an improper system of weighting, since the final results for the four points appear to be far more consistent than we have any right to expect.

Using the mutual angular distances γ of the corrected points as given in the last column of Table 4, we may construct a diagram similar to that given by Eddington.[6] Expressed in the arithmetic mean velocity along the longest axis of the velocity ellipsoid as unit, we find for the different velocities the values given in the second column of Table 5.

[6] *Stellar Movements*, p. 101. London: Macmillan & Co., 1914.

From the calculation made for the apex and vertex separately we had $A/B = 2.25 \pm 0.15$, $u/B = 1.37 \pm 0.05$, or $u/A = 0.61 \pm 0.05$, which would give 1.22 for the solar velocity. Using the Boss stars, Eddington found the values given in the last column of Table 5. The agreement with those obtained here is excellent, though it may seem surprising at first that the present material, containing only large proper-motion stars and hence an unduly large proportion of drift-I stars, should give a ratio for the stars in the two drifts more nearly equal to unity than Eddington's material. However, the automatic method of Schwarzschild employed for the analysis presupposes equal numbers of stars moving in both directions. If we assume that the forcing-through of this method has resulted in the ratio found to be halfway between the "true" ratio and the 50:50 mark, we would determine the true ratio at 60:40, or identical with that of Eddington. If we further assume that the position of the vertex has not been affected by the limitations of the material, the above change in the ratio of stars implies a decrease of about 3° in the

TABLE 4

	α	δ	l	b	l'	b'	γ
Vertex II	83°.0±1°.2	+17°.5±1°.1	156°.5	− 6°.0	156°.8	− 5°.1	
							34°.4
Apex of drift I	94.8±1.0	−15.1±1.0	191.1	−11.5	190.7	−12.9	
							28.8
Solar antapex	104.1±2.0	−42.6±1.5	220.3	−15.7	220.3	−16.3	
							60.9
Apex of drift II	228 ±9	−69 ±3	283.0	−10.9	282.8	− 9.8	
							55.9
Vertex I	263.0±1.2	−17.5±1.1	336.5	+ 6.0	336.8	+ 5.1	

TABLE 5

	Luyten	Eddington
Speed of drift I relative to sun	1.66±0.06	1.62
Speed of drift II relative to sun	1.13± .07	0.93
Sun relative to centroid	1.05± .04	0.97
Ratio of numbers in two drifts	55:45±0.04	59.6:40.4

longitude of the solar antapex, corresponding to a change in its declination from −43° to −40°, and a very slight increase in u/B, to about 1.08.

The proportion of stars belonging to the two drifts might have been obtained directly by counting the stars moving in each favored direction. If this is done for each ΣΣ-region and the resulting numbers are added up, we obtain the following totals: drift I: 62,186 stars (mean sampling error 250, or 0.41 per cent); drift II: 30,470 (mean sampling error 175, or 0.57 per cent), which indicate a ratio 0.672:0.328, or practically 2:1.

However, the proportion thus obtained does not give a fair representation of the true state of affairs, since the richest regions (partly due to the greater frequency there of long-exposure plates) lie much closer to the apex of drift II than to that of drift I. Dividing the material into four zones, we obtain the data in Table 6, actually giving more second-stream than first-stream stars in the equatorial zone. Perhaps a closer approach to the true proportion may be obtained by determining the percentage of drift-II stars in each of the 37 regions and averaging for the entire hemisphere. In this way we obtain for the ratio, 0:59 to 0:41, with a sampling error not exceeding 0.003 in either number, again

virtually identical with the ratio previously found and with that determined by Eddington for the Boss stars.

The numerical constants of the ellipsoidal distribution itself are given in Table 7. The accidental error of measurement amounts to a sizable fraction of the total motion in the case of the first two sets of data, and its effect is to reduce the observed values of both u/B and A/B. The McCormick value for A/B has been corrected for this, but the other three numbers still require an increase by an unknown amount. Both the Radcliffe and the McCormick data were derived from all proper motions found on the plates; the present investigation deals only with stars whose proper motions exceed a given value—about 0".04 annually. A disproportionately large number of high-velocity stars has there-

TABLE 6

ΣΣ	Drift I	Drift II	Percentage of Drift II
1–5	15951	3406	17.6
6–13	24767	8051	24.6
14–25	14294	11209	44.0
26–37	7174	7804	52.3

TABLE 7

	Knox Shaw and Barrett	Van de Kamp and Vyssotsky	Luyten
u/B	0.42±0.01	0.61±0.03	1.37±0.05
A/B	1.31±0.05	1.59±0.04	2.25±0.15

fore been included, and both u and A have probably been increased at the expense of B. This would explain, at least qualitatively, the large difference between the two sets of data, but in the absence of any estimates on the numerical size of the quantities involved in the present work it does not seem possible to derive "true" values for the ellipsoidal constants. As a very rough estimate we might adopt $u/B = 0.9$, $A/B = 1.8$.

It is often, and perhaps generally, held that restriction of the proper motions to those larger than a given limit materially reduces the significance or the value of the results. Thus, in his rediscussion of my analysis of the motions of 500 stars in the foreground of the Large Magellanic Cloud, Smart[7] urged that in such investigations the motions of *all* stars on the plate be measured. In this particular case about 500,000 stars were shown on the plate, but about 90 per cent of these must belong to the Cloud itself. Measurement of the remaining 499,500 motions not only would thus have been a task of impossible magnitude but would have little bearing on the question of star-streaming in the Galaxy. Even in the general case, the material thus obtained would consist, at best, of a mixture of a large number of distant giants, a few near-by dwarfs, and some high-velocity stars, the proportions varying with galactic latitude; and it becomes a matter of personal opinion whether this is more representative of stars in general than the mixture as used in the present paper, even though here the apparent angular velocity has formed the basis of selection.

[7] *M.N.*, **90**, 120, 1929.

THE STARS OF LARGE PROPER MOTION

9. While it has not been possible to measure the proper motions of all stars found, this has been done for all stars with motions in excess of $0''.5$ annually and for all double stars. Discussion of the former indicates that the final list compiled is virtually complete down to $14^m.5$, but for the present the question of completeness is of no great importance so long as no selective effects in direction have entered. It was decided, therefore, to use all stars with motions in excess of $0''.5$ as measured, double stars being counted as one. The sky has again been divided into 37 ΣΣ-regions, and for each of these there were determined the arithmetic mean parallactic motion and the directions toward the apices of the two drifts.

In the determination of the solar antapex, Kapteyn's star was given half-weight in forming the mean for ΣΣ7, since its motion very nearly equaled the mean motion of the remaining 28 stars in this region; all other stars have been given full weight. The determination of the directions toward the drift apices presented some practical difficulties. Usually the position angles of the motions divided themselves into two distinct groups; arithmetic means of the position angles in these groups were then taken to represent the directions toward the apices and the number of stars in each group as that belonging to each drift. In some regions, however, the drifts were less clearly separated and the division made had to be somewhat arbitrary. In four regions, ΣΣ11, 12, 23, and 35, no separation of the drifts was possible, and the same direction was used for both.

Some stars, altogether 42 in number, were found to move in directions so different from those toward the apices that they could not properly be assigned to either drift; these were merely classed as "odd." A list of some of them follows in section 14.

Table 8 presents a summary of the data obtained. The first five columns show, respectively, the ΣΣ number, the right ascension and declination of the center of the region, the total number of stars, and the mean magnitude. The next two columns give the algebraic mean of $\mu_\alpha \cos\delta$ and of μ_δ; the four columns following give the directions toward the apices of the drifts and the number of stars belonging to each; the last column gives the number of "odd" stars.

10. Calculating the solar antapex from the data in the sixth and seventh columns of Table 8 yields

$$A = 113^\circ.6 \pm 3^\circ.5 \ (m.e.) ,$$

$$D = -37^\circ.5 \pm 2^\circ.5 ,$$

$$q = 0''.61 \pm 0''.03 .$$

The arithmetic mean magnitude and proper motion of the stars are found to be $\overline{m} = 12.1$ and $\overline{\mu} = 0''.83$, corresponding to $H = 16.7$. Using the measured parallaxes of 610 stars with $\mu > 0''.5$ (mostly northern), I previously derived[8] a regression curve for M on H which, with the present data, would give $p = 0''.050$. However, this is the geometric mean parallax; with a normal distribution in log p subject to a dispersion of 0.24 the arithmetic mean parallax $\overline{p} = 0''.0575 \pm 0''.002$. In conjunction with $q = 0''.61 \pm 0''.03$, we then derive for the speed of the sun relative to these stars of large proper motion,

$$V = 50 \pm 2 \text{ km/sec.}$$

This value appears perhaps a little on the high side when considered in conjunction with the declination of the antapex, $-37^\circ.5$, though one must remember that the stars involved all possess excessively large angular velocities and it should thus be not the solar

[8] *Pub. A. Obs. U. Minnesota*, **2**, 148, 1939.

velocity but, rather, the low value for the declination of the antapex which surprises us, a value of $-45°$ being perhaps more nearly that to be expected.

11. Inspection of the two favored directions derived for each region separately indicated that the position of the two apices would not differ greatly from those found before in this paper. In order to simplify the actual calculation of these apices, the lengths of

TABLE 8

ΣΣ	Center		N	$\bar{m}$	$\overline{\mu_\alpha \cos\delta}$	$\bar{\mu}_\delta$	θ_1	n_1	θ_2	n_2	Odd
	α	δ									
1	.....	$-90°$	12	12.0	+0".60	−0".20	101	11	216°	1	.....
2	3^h0		39	11.6	+ .44	+ .11	54	28	167	11	.....
3	9.0	−68.7	20	13.5	+ .19	+ .14	332	12	130	7	1
4	15.0		34	13.4	− .57	− .28	240	33	.....	0	1
5	21.0		49	12.8	+ .13	− .43	152	40	261	7	2
6	1.5		24	11.1	+ .39	− .16	84	14	186	8	2
7	4.5		29	12.1	+ .42	− .02	65	16	185	11	2
8	7.5		24	12.2	− .10	+ .40	351	19	158	4	1
9	10.5	−49.3	23	12.4	− .46	− .01	285	15	132	5	3
10	13.3		31	12.7	− .44	− .35	245	26	155	5	.....
11	16.5		28	12.8	− .41	− .69	.....	213	27	.....	1
12	19.5		28	13.3	+ .06	− .58	.....	264	24	.....	4
13	22.5		32	12.1	+ .45	− .53	136	26	220	5	1
14	0.0		34	12.3	+ .64	− .38	104	26	205	8	.....
15	2.0		29	12.7	+ .42	− .22	91	19	180	6	1
16	4.0		13	11.6	+ .31	− .09	59	7	186	6	.....
17	6.0		9	10.3	+ .02	− .18	317	3	166	5	1
18	8.0		14	12.2	+ .04	+ .01	328	5	156	8	1
19	10.0		9	13.4	− .28	+ .02	296	6	147	3	.....
20	12.0	−30.0	22	12.0	− .45	− .26	258	15	149	7	.....
21	14.0		30	11.1	− .44	− .29	248	24	135	4	.....
22	16.0		18	11.6	− .41	− .32	228	15	.....	0	3
23	18.0		16	12.3	− .02	− .53	.....	184	16	.....	.....
24	20.0		13	10.2	+ .20	− .55	150	7	195	4	2
25	22.0		17	12.1	+ .35	− .51	111	7	195	9	1
26	0.0		23	12.5	+ .24	− .45	105	12	195	11	.....
27	2.0		18	11.2	+ .44	− .09	98	15	187	2	1
28	4.0		15	10.4	+ .16	− .58	117	9	205	3	3
29	6.0		14	10.2	+ .03	− .61	99	3	187	10	1
30	8.0		15	10.9	+ .16	− .32	302	2	156	12	1
31	10.0	−10.0	27	12.4	− .33	− .31	267	15	164	12	.....
32	12.0		32	11.3	− .14	− .30	269	19	156	12	1
33	14.0		37	12.7	− .47	− .20	253	32	164	4	1
34	16.0		25	11.0	− .51	− .62	242	16	186	6	3
35	18.0		20	12.6	− .26	− .57	.....	197	20	.....	.....
36	20.0		18	12.2	− .05	− .59	134	6	212	12	.....
37	22.0		23	12.8	+0.52	−0.25	106	11	175	9	3

the drift vectors for each region were then assumed to be equal to sin λ, where λ is the angular distance from the center of the region to the assumed apex. The calculation of the apices then proceeds in the same way as for the solar antapex, and we find:

Drift I: $A = 99° \pm 1°.0$ Drift II: $A = 241° \pm 6°$

$D = -12° \pm 1°.0$ $D = -70° \pm 2°$

Owing to the simplifying assumptions made concerning the lengths of the vectors, the actual mean errors are probably somewhat larger than the values given here.

12. Plotting the three apices thus found on a sphere and drawing the great circle that best fits them, we obtain for the "corrected" positions:

Drift I: $A = 101°$	Solar antapex: $A = 109°$	Drift II: $A = 239°$
$D = -12°.5$	$D = -39°$	$D = -69°$

Making an equitable division between the two drifts in the four regions ΣΣ11, 12, 23, and 35, we find 575 stars belonging to drift I and 244 to drift II. Taking into account the fact that the procedure followed has naturally favored stars to be assigned to drift I at the expense of drift II, while, moreover, the most populous regions (those containing the long-exposure plates) lie close to the apex of drift II, the true proportion of stars in the two drifts may be placed at 2:1, corresponding to the actual numbers 546 and 273. Using this proportion, we then find the vertex to lie at 269°, −31°, and, with a solar velocity of 50 km/sec, the drift velocities relative to the sun become 70 km/sec for drift I and 71 km/sec for drift II.

At first it may seem surprising that the velocity of the second drift should be so high in a group of stars where selection strongly favors drift I over drift II. Inspection of the individual data, however, shows that stars here assigned to drift II contain a fair proportion of high-velocity stars. Thus, Kapteyn's star is counted among drift II in ΣΣ7, as is o_2 Eri in ΣΣ28, and the fast-moving pair BD −15°4041, with a tangential velocity of over 500 km/sec in ΣΣ34. The same is borne out by the fact that the apex here determined for drift II represents a compromise position between that usually found, at about 270°, −64°, and the solar antapex of the high-velocity stars, at about 135°, −72°.

13. The positions of the apices of the two drifts derived here differ but little from those found in section 8 from the estimated directions of all 92,656 stars, viz.,

Drift I: $A = 95°$	Drift II: $A = 228°$
$D = -15°$	$D = -68°$,

the great-circle distances amounting to but 6°.5 and 4°, respectively. The two determinations of the solar antapex agree, likewise, within the limits of error; but those for the vertices disagree, the angular distance being nearly 15°. The present vertex depends upon an extrapolation made by using the uncertain proportion of stars in the two drifts, while the former was derived by Schwarzschild's automatic method, which presupposes an ellipsoidal distribution with equal numbers of stars in both drifts. Assuming the previous vertex and the present drift, apices and solar antapex would result in a ratio of stars in the two drifts of 0.61 to 0.39, or nearly identical with that usually obtained. Furthermore, it was pointed out in section 8 that any increase in the fraction of stars belonging to drift I would shift the solar antapex closer to the apex of drift I and hence would bring the position of section 8 closer to that given here, at 109°, −39°. All in all, therefore, we conclude that the data on star-streaming, as obtained in sections 8 and 12, are in fair agreement.

14. Among the 42 "odd" stars listed in Table 8, there are several for which the direction of motion lies in the acute angle between those of drift I and drift II, and hence these stars probably represent members of one or the other of these drifts which have strayed far from the fold. There remain some 25 stars whose motions are so radically different in direction that it becomes difficult to assign these to any drift. Among these are the well-known stars γ Pavonis and δ and ε Eridani. For 16 among these, parallaxes have been measured; if we compare the absolute magnitudes obtained from these measured

parallaxes with those predicted from the formula quoted above,[9] we find that for *all* of them O − C is positive, having a mean value $\Delta M = +1.2$, with an individual dispersion of $\pm 0^m.84$. This was to be expected, of course; but the fact may be used to single out a few more of these stars, with as yet unmeasured parallaxes. Predicted (arithmetic-mean) parallaxes are given for nine of these in Table 9, which is self-explanatory. For the star L 789-6, I have published a provisional parallax of $0''.53 \pm 0''.3$ derived from plates taken with a very short-focus telescope. This determination is obviously not entitled to much weight, and the spectroscopic value derived by Joy should be more reliable. Joy finds $p = 0''.073$ disagreeing with the above suggestion of a parallax larger than average, but the small radial velocity (only +1 km/sec) would favor the larger parallax.

TABLE 9

Star	Position		Mag.	μ	θ	p
	α	δ				
L 511-7	$2^h01^m.4$	$-30°40'$	12.6	$0''.52$	286°	$0''.058$
L 763-66	13:48.4	19:46	14.5	0.58	59	.065
L 623-94	15:16.1	27:28	14.7	0.73	38	.070
L 482-30	16:13.5	37:19	12.0	1.22	325	.161
L 710-9	20:04.5	20:46	10.3	0.56	288	.068
L 211-59	20:55.7	57:21	13.7	0.51	317	.065
L 165-102	21:41.9	63:35	15.6	0.55	32	.044
L 789-6	22:33.0	15:52	14.3	3.27	46	.197
L 359-91	23:12.1	−48:51	15.2	0.79	21	0.074

DOUBLE STARS WITH COMMON PROPER MOTION

15. A statistical discussion of the double stars found was published as No. 5 of the "Bruce Proper-Motion Survey."[10] A pronounced and surprising irregularity in the distribution over the sky of these double stars was then found, and a further analysis of the stream-motions of these wide binaries may thus be of interest. The procedure followed has been the same as that for the stars with $\mu > 0''.5$ annually, as outlined in section 9, and the data obtained are given in Table 10, which is arranged similarly to Table 8 and needs no further explanation . In the present case, however, the proper motions used range in size from $0''.04$ to $3''.68$, and there would have been little point in averaging $\mu_\alpha \cos\delta$ and μ_δ for so heterogeneous a mixture; consequently, the determination of the solar apex has been omitted from the calculation, and only the directions toward the apices of the two drifts are given, together with the numbers of stars belonging to each drift.

Effecting the same calculations as before, we find for the apices of the two drifts:

Drift I: $A = 96° \pm 2°$ Drift II: $A = 250° \pm 12°$

$D = -9° \pm 2°$ $D = -71° \pm 4°$

The larger errors obtained this time need not surprise us, in view of the paucity of stars in some of the $\Sigma\Sigma$-regions, notably those nearest the equator, six of which contain fewer than 10 stars. Considering this, the agreement with the values for the apices derived before, for *all* stars (in sec. 5) and for the stars with $\mu > 0''.5$ annually (in sec. 11), appears satisfactory.

Using the actual numbers of stars belonging to each of the drifts, as given in Table 10,

[9] *Ibid.* [10] *Ibid.*, p. 183.

fifth and seventh columns, we find the totals 567 and 258, respectively, giving a ratio of 0.69:0.31. Again it would seem fairer to use percentages throughout; these yield the values 0.63:0.37, corresponding to a ratio of 6:3.5, which is intermediate between the ratio found for all stars (6:4) and that for the stars with $\mu > 0''.5$ (6:3).

TABLE 10

ΣΣ	Center		θ_1	n_1	θ_2	n_2	Odd
	α	δ					
1	.....	−90°	105	9	252	2	3
2	3.0		58	31	190	5	.....
3	9.0	−68.7	322	34	140	13	.....
4	15.0		235	53	52	8	.....
5	21.0		148	62	284	8	1
6	1.5		71	15	192	14	.....
7	4.5		36	12	170	5	.....
8	7.5		340	23	166	9	.....
9	10.5		288	30	135	10	.....
10	13.5	−49.3	261	32	159	10	.....
11	16.5		219	29	143	7	.....
12	19.5		153	24	222	7	.....
13	22.5		110	21	219	13	.....
14	0.0		111	14	220	3	.....
15	2.0		84	11	190	10	.....
16	4.0		36	6	190	10	.....
17	6.0		345	2	188	8	.....
18	8.0		308	10	177	15	.....
19	10.0		293	15	148	9	.....
20	12.0	−30.0	270	16	125	6	.....
21	14.0		262	9	174	11	1
22	16.0		239	7	175	3	3
23	18.0		.....	190° 18	.....	.....	.....
24	20.0		153	9	211	6	.....
25	22.0		106	8	192	2	.....
26	0.0		91	8	199	5	.....
27	2.0		97	5	.....	0	.....
28	4.0		.....	0	220	2	.....
29	6.0		319	2	163	3	.....
30	8.0		274	8	180	6	1
31	10.0	−10.0	256	5	160	6	1
32	12.0		274	11	143	8	.....
33	14.0		254	13	158	4	.....
34	16.0		255	4	172	4	.....
35	18.0		110	5	187	4	1
36	20.0		.....	172° 5	.....	.....	.....
37	22.0		122	7	233	5	.....

In conclusion it is a pleasure to record that the publication of this article has been made possible by a grant from the Society of Sigma Xi; the Proper Motion Survey from which the present material was taken has been generously supported by grants from the Gould Fund of the National Academy of Sciences, from the American Academy of Arts and Sciences, and from the Graduate School of the University of Minnesota.

Minneapolis, Minnesota
December 1939

ON THE THEORY OF THE ORIGIN OF THE PLANETS

R. A. LYTTLETON

ABSTRACT

Criticism of the double-star hypothesis as a basis of the theory of the origin of the planets is considered. The dynamical criticisms urged by Luyten are shown to have arisen as a result of wholly inaccurate dynamical arguments given by him and by Hill. The mass of the planetary filament initially set free need not greatly exceed the mass of the present planets. The primitive planets did not necessarily retain the atmosphere-forming materials; these could escape to form a medium round the sun and be picked up subsequently. The assumptions of the theory must not be confused with the essential dynamical constants, such as the masses of the stars involved and their initial velocities. It is improbable that the older difficulties concerning angular momentum of the planets could be overcome by changing the laws of mechanics without at the same time introducing comparable alternative difficulty with regard to certain of the satellite orbits.

INTRODUCTION

Early in 1936 the present writer put forward a new theory of the origin of the solar system.[1] The departure from previous ideas involved in this theory consisted in the notion that the angular momentum of the planets could be explained on the hypothesis that they had been formed from a companion star to the sun. A particular advantage of this suggestion was that it enabled many features of the already existing theory of Jeans and Jeffreys to be retained while at the same time resolving the angular-momentum difficulty drawn attention to by Russell. In my first paper examining this hypothesis the fact that considerable energy would be required to remove a mass equal to that of the planets from the surface of a star was overlooked. This omission, which was simply a survival from the former theories in which it had also been neglected, was pointed out by Luyten and Hill. Accordingly, it became necessary to rediscuss the hypothesis in the light of this new feature of the motion. This discussion was accordingly undertaken,[2] and it was shown that although the removal of the planets required about ten times the energy necessary to disrupt the binary suitable initial conditions could still be chosen. Moreover, such conditions are by no means limited to narrow ranges or to values that observation indicates as being in any way unsatisfactory.

But in spite of all this the theory has continued to be subjected to adverse criticism of a peculiarly inapplicable kind, and the object of the present paper is to discuss the arguments that have been made and directed against the theory. They are contained in a number of articles by W. J. Luyten and E. L. Hill together[3] and by Luyten separately.[4]

To begin with, the present writer desires to make due acknowledgment of the necessity to take into account the point raised by Hill and Luyten concerning the energy required to remove the planets from the parent stars. The writer does not, however, regard the discussion of this question given by Hill and Luyten[5] as in reality establishing to the smallest degree the conclusions that are claimed in the papers and letters of these authors. Owing to the severe nature of some of the criticism and the far-reaching claims made in advancing it, more particularly by Luyten, the writer has felt it desirable to undertake in detail an examination of these criticisms. The various questions may be discussed under several headings.

[1] *M.N.*, **96**, 559, 1936. [2] *M.N.*, **98**, 536, 1938.

[3] *Observatory*, **60**, 109, 1937; *Ap. J.*, **86**, 470, 1937.

[4] *Observatory*, **61**, 83, 1938; *M.N.*, **99**, 692, 1939; *Observatory*, **63**, 72, 1940.

[5] *Ap. J.*, **86**, 470, 1937; *M.N.*, **99**, 692, 1939.

DYNAMICAL CRITICISMS

1. The dynamical objection given greatest prominence by Luyten is to the effect that only 6 per cent of a filament linearly distributed between the parent-stars could escape from them and be available for capture by the sun. In answer to this contention (which happens to be false) it may be noticed that capture of the planets by the sun takes place only after the colliding stars have receded to a considerable distance so that the attraction of the sun becomes important. This would not happen until some ten years or more after the collision, and by then the planets would have condensed, while the 6 per cent of the region between the parent-stars would be several astronomical units. Thus, the 6 per cent can refer only to the region between these stars and not to the filament, and there would be no reason to suppose that the planets could not all lie in the 6 per cent; it would obviously be unnecessary to regard the remaining 94 per cent as equally filled with planets. This can most readily be seen in the case of equal stars receding from a single planet. The planet would remain at the center of mass of the system and occupy no more than a fraction of 1 per cent of the whole (linear) region between them.

The foregoing remarks appear in themselves sufficient answer to Luyten's claim, but in reality the assertion that only 6 per cent of the intermediate region can constitute a suitable location for capture of planets by the sun has arisen as a result of a fallacious dynamical argument.[6] Their discussion begins by supposing that the parent stars separate with parabolic velocity, but these stars must have had at least slightly hyperbolic velocity. It is clear that the smaller the relative velocity of the parent-stars after collision, the smaller will be the extent of the region in which the planets must move, and hence a hyperbolic velocity could be introduced in any case to extend the available region. But, even if the assumption of parabolic velocity is allowed, the subsequent treatment is erroneous in almost every way.

Briefly, Luyten and Hill consider B and C separating with parabolic velocity at a distance r apart and Q a particle of negligible mass at a distance αr from C in the line BC, the whole motion being confined to this line. The acceleration of Q is then $B/(1-\alpha)^2r^2$ toward B together with C/α^2r^2 toward C, or $C/\alpha^2r^2\{1-(B/C)\cdot[\alpha^2/(1-\alpha)^2]\}$ toward C. Luyten and Hill maintain that this acceleration can be used as an approximate criterion for the behavior of Q relative to C. But in addition to the procedure's being unsound, the above quantity is not even the acceleration of Q relative to C. Luyten and Hill have omitted the acceleration of C, which is B/r^2 toward Q. Thus, the acceleration of Q relative to C is really as if it were attracted by a mass

$$C\left\{1-\frac{B}{C}\cdot\frac{\alpha^3(2-\alpha)}{(1-\alpha)^2}\right\}$$

situated at C, and this differs greatly from the value used by Luyten and Hill. But this is not the only mistake, for these authors proceed to compute the motion of Q as if α were constant, whereas it has been shown by the writer that there is only one value of α that can remain constant throughout the (parabolic) motion.

On the other hand, in the case of hyperbolic motion the available region is not in reality subject to any such general limit as Luyten maintains. For consider B and C at the time when the action of the sun becomes important. Their distance apart, r, will be large, and they will be separating with (practically constant) hyperbolic velocity v, say. A particle Q at small distance d from B will have velocity dv/r relative to B, on the usual assumption of linearly distributed velocity and, being affected almost solely by B, can escape from this star if $(dv/r)^2 \geqslant 2B/d$. The critical value of d is, therefore, $(2Br^2/v^2)^{1/3}$, and although this distance tends to infinity with r it is seen that d/r tends

[6] *Ap. J.*, **86**, 479, 480, 1937.

to zero. Hence, the fraction of the linear region *BC* available as a suitable location for the planets may be regarded as tending to 100 per cent as the separation of *B* and *C* becomes large, provided only that v is not zero—the parabolic case. There is, accordingly, no basis whatever for the assertion by Hill and Luyten that only 6 per cent of the planets formed are available for capture.

It is exceedingly important to understand this point, for Hill and Luyten have argued further from it. On the express assumption that their view is correct they contend that since the present planets have a mass, say, $0.002\odot$, then the whole filament must have had a mass $0.002\odot \times (100 \text{ per cent} \div 6 \text{ per cent}) = 0.033\odot$. Indeed, Luyten has estimated the initial mass of the filament to be as high as $0.045\odot$.[7]

From the foregoing remarks it is evident that it is not necessary to regard the mass of the filament as exceeding $0.003\odot$ at most, whereas Luyten has maintained that fifteen times this amount is essential. Nevertheless, the writer showed that even were as much as $0.009\odot$ required, a suitable encounter could readily be devised.[8] Although it is unnecessary to investigate the matter in detail, it appears entirely possible that an encounter could be set up that would supply enough energy to remove even $0.045\odot$.

2. In a paper in the *Observatory*,[9] appearing shortly after the one in this *Journal*,[10] Luyten asserted that the crucial moment for capture of the planets by the sun would be when the filament first begins to condense, though no reason for this view was given.[11] As Luyten points out, this condensation would, of course, happen before the parent-stars had receded to any great distance, and it is evident that in reality the attraction of the sun at such time would be negligible. Luyten estimates the distance apart of the parent-stars as not more than 0.1 astronomical unit, while the distance of the sun at this time would be several astronomical units. It is obviously absurd to suppose that the sun could capture the material at this stage. In his more recent paper[7] Luyten has now recognized that capture could not take place until the stars had separated to great distance again, though he makes no explicit acknowledgment to my insistence on this point in the paper answering his earlier criticisms.[12]

3. It has been further maintained by Luyten[13] that the solar system presents a number of dynamical indications that the system has been built up from within. In support of this he cites the following points: (*a*) the small eccentricities of the orbits of the planets, (*b*) the near parallelism of the sun's axis to the angular momentum vector of the system, (*c*) the similarity between certain satellite systems and the planetary system, and (*d*) the gradual increase in the inclinations of the planes in which the satellites move, from Jupiter to Neptune. Let us consider, then, these points in turn.

a) It is known that for intervals in excess of 10^6 years the eccentricities of the planetary orbits may deviate considerably from the present small values. The planetary theory is incapable of determining the values of the eccentricities over periods comparable with 10^7 years. This is so short compared with the age of our system that the present eccentricities cannot possibly be used as a guide to the original values. Even if high eccentricities rendered the system unstable, it would not invalidate the present theory of the origin of the planets, for the system would move to a stable configuration, which we believe involves small eccentricities. These possibilities concerning the past history of the system had already been explained by E. W. Brown,[14] Jeffreys,[15] and H. N. Russell[16] before the appearance of Luyten's letter in the *Observatory* in 1938.

[7] *M.N.*, **99**, 694, 1939.

[8] *M.N.*, **98**, 538, 1938.

[9] **60**, 109, 1937.

[10] **86**, 470, 1937.

[11] *Observatory*, **61**, 83 (bottom), 1938.

[12] *M.N.*, **98**, 538 (top), 1938.

[13] *Observatory*, **61**, 85, 1938.

[14] U.S. National Research Council, **5**, 1931; and Brown and Shook, *Planetary Theory*, pp. 248, 249.

[15] *M.N.*, **92**, 887, 1932.

[16] *The Solar System and Its Origin* (1935), p. 29.

b) This feature of the solar system is capable of being explained on the present theory. For it is reasonable to suppose that any material that did not condense into planets and yet was retained by the sun would possess angular momentum closely parallel to the angular momentum of the planets. Accordingly, any of the material reabsorbed by the sun would bring angular momentum to the latter, and its axis of rotation would approach that of the angular momentum of the medium. This explanation of the sun's axis was given by Jeffreys.[17]

c) The remarks under (*a*) indicate that no inferences concerning the origin of the system can be made from the present dynamical features. Thus, it may well be that the planetary configuration of small eccentricities and inclinations represents the only stable motion for a number of small bodies moving near a single mass. In this event it is not surprising that the satellite orbits show features similar to the planetary orbits.

d) This suggestion is open to the same objection as those of (*a*) and (*c*). Owing to precession, the axis of rotation of a planet changes its direction in comparatively short periods. If the orbit of a planet were circular and undisturbed, the precession would take place in such a way that the axis of rotation of the planet would describe a circular cone about the perpendicular to the orbital plane. It is clear that changes in eccentricity and inclination taking place over very long intervals (10^7 years or more) would cause the direction of the rotation axis to undergo corresponding changes, and just as the present orbits cannot indicate the original ones, so the present axes of rotation of the planets can afford practically no indication of the original directions of the rotation axes.

It is therefore seen that the features that Luyten has advanced as evidence of gradual internal formation of the system cannot in reality be regarded as any guide to the original state of the system. Owing to the great age of the solar system, the present dynamical features appear more to be the result of gradual internal dynamical and dissipative effects in bringing the system to a stable configuration, independent of its original form.

OTHER CRITICISMS

In a more recent paper Luyten[7] has iterated his earlier attacks on the theory on the assumption that the dynamical arguments of his previous paper[5] are sound. Accordingly, it will not be necessary to consider these points again, but a number of other remarks in this later paper by Luyten require some comment.

Luyten has asserted categorically that the vector diagram of my first paper was incorrect, whereas in fact this was not the case, for the diagram dealt with the situation envisaged at the time. It is true that the energy required to liberate the planets was neglected in these first investigations, but Luyten has put this feature under a different heading in listing his objections.

Several arguments of Luyten's more recent paper[7] do not seem to the writer to be of a type that can carry any weight in a scientific discussion. For example, section 1 (pp. 692–93) contains a description of the motion that would enable the sun to capture the planets. The account itself is reasonable, apart from an invalid appeal to a probability argument, but Luyten simply concludes by stating that the motion "may be possible but it is evident that it is very *improbable in any event*." Now this is clearly a statement that would apply to the motion of any body in the universe and does not constitute an argument at all.

Continuing the discussion of the motion in section 2 (p. 694), Luyten points out that it is necessary for the sun and the planets to have roughly parallel motions for many years after the collision. This is correct, but it does not justify the statement that "this appears to be out of the question." In view of the fact that the sun and planets are being acted on by similar forces and have similar velocities, the capture appears to be reasonable enough. For it is clear that if the sun had much greater velocity than the

[17] *M.N.*, **89**, 637, 1929.

planets, though in the same direction, capture would not occur and the sun would always lie ahead of the planets and conversely if the planets had much greater velocity than the sun. Thus, somewhere between these two motions will be a range of motions in which the sun will be able to capture the planets.

In section 3 of this paper Luyten discusses the original mass of the filament and contends that the present planets can constitute at most only 50 per cent of the captured mass originally available, owing to the fact that lighter elements, such as hydrogen, could not be retained at the high initial temperature of the filament. It is easy to see, however, that this argument is not conclusive. For, although most of the hydrogen, etc., would in all probability escape from the filament, such gases would not necessarily all escape from the sun, and some, at least, would remain to form a medium moving around it. Thus, the primitive planets would probably contain only the heavy materials, such as silicates and metals; but there is no reason to suppose that these bodies could not afterward pick up atmosphere-forming gases. Indeed, it now seems that any gravitating body moving through a gas will gradually acquire material,[18] and this appears to be the most acceptable explanation of the huge atmospheric content of the great planets.

THE ASSUMPTIONS OF THE THEORY

A considerable amount of adverse criticism has recently centered round the so-called assumptions of the theory. The authors of these criticisms[19] appear to be confused as to what constitutes an assumption in science, for they refer to what are in reality essential dynamical concepts as *ad hoc* assumptions. If it were at the present time possible to see three stars moving in such a way that a system of planets was produced, there would be no question of the particular motion seen being regarded as "improbable" or the result of *ad hoc* assumptions, even though an infinite variety of different motions are equally possible. All such motions can be resumed by the Newtonian equations, and the various paths appear through the constants of integration. But neither the number of bodies involved nor the constants arising through integration are assumptions of the theory, any more than the eccentricities of the planetary orbits are assumptions in the dynamical theory of planetary motions. These latter are inevitably quantities to be derived from observation. In just the same way in the explanation of solar eclipses it would obviously be absurd to argue that the moon could not be responsible, as it is so improbable that the moon should be at exactly the right distance from the earth. Such an argument misunderstands what the laws of dynamics mean. Thus, the number of stars involved in the theory of the origin of the solar system and their initial positions and velocities are quantities that must be regarded as having definite values, even though it is not possible to fix them precisely. For example, for the purposes of dynamics, the moon's distance at any instant must be regarded as having a definite value, though it would still eclipse the sun even if this quantity had any value in a considerable permitted range. In the theory of the origin of the planets the idea of a collision can be introduced just because the equations of motion allow it to happen. Indeed, new ideas consist very largely of hitherto unnoticed combinations of the constants of integration.

The actual assumptions of the theory, in the correct sense of the word, concern the results of the collision and the subsequent condensation of the filament. They are not due to the present writer. They were introduced by Jeans and Jeffreys and, naturally enough, constitute the most reasonable suggestions that could be made for the discussion of such complex matters. It is obviously difficult to give any detailed treatment of the actual collision, and some assumption as to what takes place cannot be avoided if the problem is to be discussed at all. That material will be removed seems undeniable, as is also the suggestion that rotation would be developed in the filament by turbulent motion during the collision.

[18] *Proc. Cambridge Phil. Soc.*, **35** and **36**, 1940.

[19] *Observatory*, **63**, 72, 75, 1940.

From the nature of the formation of the planets it is evident that they are created at or near the neutral point of the field of force of the two parent stars. Now, it is well known that the motion of a body projected under circumstances such as these is extraordinarily sensitive to even the smallest changes in the initial conditions. Thus, a body projected from the surface of the sun with exactly the escape velocity will describe a parabola and escape, while a reduction or increase of the velocity by the slightest amount will result in two paths eventually differing from each other by an infinite amount. This feature of gravitational motion is, of course, very familiar to those acquainted with orbital questions. The difficulty is inherent in the motion and cannot be obviated by any mathematical device. It follows that no attempt to compute the orbit can be of much value, the whole range of motions being included in a comparatively small range of the values of the initial circumstances of projection of the planets. In the present problem the circumstances are even more unmanageable than this, for the two parent stars undergo a collision the actual effects of which cannot be accurately estimated, while, in addition, the stars would partake of strong tidal distortions and, moreover, the planets themselves would begin as a filament of gaseous material. Bearing all these features of the problem in mind, it becomes easy to see that any calculation would be so completely dependent on, and sensitive to, the initial conditions as to be utterly valueless.

It has, of course, been long since recognized that the problem can be satisfactorily dealt with only by reference to the broader dynamical requirements of energy and angular momentum, etc., and all previous investigators have adopted this plan. In spite of these unavoidable restrictions on the problem it is nevertheless clear that the conditions subsequent to the collision are such that the primitive planets can escape both parent-stars and be captured by the sun. For there will exist a triple infinity of possible orbits for a body through any point of space (corresponding to the velocity of projection at the point), and these paths range from orbits that imply capture by one parent-star to a series of similar orbits associated with the other parent-star. In between these two sets of paths there will exist trajectories passing through any point of space and having any desired velocity. In the present problem it is necessary that the primitive planets be captured by the sun. But there is no difficulty here, for it is evident that there must exist possible motions in which the planets are captured by the sun, even though such motions represent only a small fraction of the permitted motions, just as some of the filament may be captured by one of the parent-stars. To see that this is so we have only to consider the case of a hypothetical small body moving past a star like the sun, say. If the body divided into a very large number of independent fragments all moving with different velocities, some of the fragmentary particles obviously could be captured by the sun. This situation is similar to the problem of the initial planetary motion, except that in the latter case the question is complicated by the presence of two parent-stars in such a way that the initial distribution of velocities shortly after the collision is related in a complex and unascertainable way, as far as detail is concerned, with the velocities at the time when the sun's attraction again becomes important.

OTHER POINTS

In his most recent letter to *Observatory*,[19] Luyten claims that he has effectively demonstrated the dynamical untenability of the binary hypothesis, while in his paper in the *Monthly Notices*[7] he suggested that "at least one case should be calculated by quadratures." If the hypothesis had really been proved untenable, this latter procedure would clearly be unnecessary, as the result would be a foregone conclusion. The impression one gets from Luyten's writings is that the fact that a suitable encounter would be likely to occur only at very infrequent intervals represents a continual stumbling block to his acceptance of the theory. When one reflects on the number of stars in our galaxy and the

large number of galaxies available, there does not seem to be any serious objection to supposing that such an event as the one under discussion has occurred once.

It may further be noticed that the imposing of restrictions on the initial conditions can in no way be regarded as undesirable; indeed, it is only through the appearance of such restrictions (the more, the better, if we are to ascertain how the system formed) that knowledge of the primitive nature of the system is to be obtained. The main advance made since the Jeans-Jeffreys theory is in the recognition that the sun can no longer be regarded as the parent-star. Progress with the problem has been surprisingly slow and many "obvious" errors and "simple" possibilities have in the past remained unnoticed for many years. In the writer's opinion this has been largely due to the fact that the problem cannot be treated by detailed mathematical analysis, and, accordingly, it has been difficult to formulate simple yet adequate checks on the hypotheses that have been advanced.

Some reference may be made to the question of the initial condensation of the planets. It has been fairly generally felt that greatest uncertainty in the theory attaches to this point, and the recent work of Spitzer[20] raises considerable doubt as to whether the planets could condense from a filament initially at 10^6 degrees. Previous to this, however, the general situation with regard to this question represented vast improvement on the earlier form of the theory. In the first place, the parent-stars may well have been of lower average temperature than the sun, while, second, the smallest mass required to form would be of an order of that of Uranus as compared with that of Mercury in the older theory (a factor of 500); and, third, the present atmospheric materials may have been added subsequent to the formation of the primitive nuclei. Spitzer's calculations show that there is, nevertheless, considerable difficulty in the theory at this stage. The physical factors involved are, however, very complex, and it is yet early to judge whether the investigation is of sufficient generality to permit us to regard the question as finally settled. It may, however, turn out that none of the factors omitted from the analysis of Spitzer's paper will seriously alter the order of magnitude of the results arrived at, and it would then be necessary to modify the binary hypothesis in some way to overcome this difficulty. The present paper was written, however, mainly in order to dispose of the dynamical objections that had been made, and the preceding remarks are not intended as fully covering the issues arising from Spitzer's investigations.

It has already been seen that valid criticism of the theory cannot be made by arguments invoking the question of probability or improbability. The angular-momentum difficulty of the older theories, pointed out by Russell, represented, of course, a dynamical inconsistency and as such rendered these theories unacceptable. In principle this was itself a probability argument and, as some writers have suggested, could be overcome by a revision of the laws of mechanics. The appropriate revision would involve laws implying that the angular momentum of a system does not remain constant but increases with the time. In order to be of any interest in the problem of forming the planets from the sun the rate of increase of an angular-momentum vector would have to be very great and would, in addition, result in serious difficulty concerning the existence of near-satellites of some of the great planets. For the angular-momentum discrepancy noticed by Russell would require a factor of 10 to be supplied during the age of the system, and this implies a factor of 100 in the mean distance of a planet from the sun. The same laws applied to the satellite system of Jupiter, for example, would lead to the impossible requirement that some of these satellites moved originally at central distances less than the radius of the planet, for these satellites cannot be of recent origin.

Last, it may be worth while to notice that dynamically the binary hypothesis is really in a strong position, for the theory can be developed from general considerations of the requirements in the following way. The fact that 98 per cent of the angular mo-

[20] *Ap. J.*, **90**, 675, 1939.

mentum is possessed by the major planets leads to the abandonment of the view that the sun is the source of the planetary material. Since, however, the stars are the only known objects in which matter is collected in bulk (and, moreover, in the right form, with heavier elements present), we are driven to regard the source of the planets as having been some other star. This leads naturally to the idea of a collision of two stars in the neighborhood of the sun, and the binary hypothesis is the more feasible suggestion as compared with the idea of an encounter of two entirely independent stars taking place near the sun. It must be remembered, however, that this latter possibility is an equally tenable starting-point for the formulation of a theory.

CONCLUSION

We may conclude by summarizing the present position of the problem in the light of the disposal in the foregoing pages of the basis of the dynamical criticisms urged at various times. The hypothesis that the sun formerly possessed a companion moving at a distance comparable with that of the great planets clearly resolves the angular-momentum requirements. The removal of the companion and the formation of the primitive planets can be achieved by means of a collisional encounter with a third star. The whole amount of matter removed from the stars need not greatly exceed the present mass of the planets, for it can nearly all remain to be captured by the sun owing to the hyperbolic character of the motion of the parent-stars. The filamentary material would certainly be endowed with rapid internal rotation owing to the turbulent nature of the motion during the collision. The question of the condensation of the filament into the primitive planets is not yet settled beyond doubt, but the present form of the theory provides very considerable improvement on the situation that existed when the sun was thought to be the parent-star and all the planets were regarded as forming at the initial stages of development.

It may doubtless be supposed that further changes and improvements will become both necessary and possible as additional relevant astrophysical information comes to light. But in the meantime the present paper shows that the binary hypothesis may at least be regarded as sufficiently well established to serve as a basis for the consideration and formulation of future suggestions.

CAMBRIDGE, ENGLAND
May 1, 1940

INTERSTELLAR LINE INTENSITIES AND THE DISTANCES OF THE B STARS

JOHN W. EVANS

ABSTRACT

The relations between the intensities of the interstellar D and K lines and the distances of the O and B stars have been determined. Distances derived from the rotational-velocity displacements of the interstellar lines were used. The relations appear to be approximately linear and are represented by the formulae $r = 2.38D$ and $r = 3.00K$. The mean error of an individual distance derived from either of these formulae is about 20 per cent.

A separate study of the stars of large and small color excess confirmed previous conclusions by other investigators that there is no spatial relation between the interstellar atoms and the particles responsible for the photoelectric color excesses.

A comparison of color excess with Joy's coefficient of photographic absorption yielded a value of 7.9 for the ratio Δ_{ph}/E, in good agreement with the value 8.6 predicted by the λ^{-1} law of selective absorption.

The dispersion in the absolute magnitudes of the O and B stars of a given spectral subdivision and line quality was estimated to be $\pm 1^{M}3$, which corresponds to a mean error of a factor of nearly two in photometrically calculated distances.

The accurate determination of the distances of individual O and B stars for which we now have accurate color excesses[1] is an important problem in the study of stellar distribution. This paper presents the results of a purely empirical study of the usefulness of interstellar line intensities as a means for measuring distance. The theory of line absorption has not been considered. It differs from most previous investigations of this problem[2, 3, 4, 5, 6] in that accurate, photometrically measured line intensities are calibrated by means of geometrically determined distances, free from the errors arising from uncertainties in space absorption and absolute magnitudes which are inherent in photometric distance measurements.

For the sake of brevity and continuity in the discussion all definitions of symbols are collected below.

NOTATIONS

$D = 0.5\ (D_1 + D_2)$, the averaged intensity of the interstellar sodium lines, in equivalent angstroms,

K = intensity of the interstellar K line of calcium,

r = distance of star in kiloparsecs,

ρ = residual radial velocity (after removal of solar motion),

l = galactic longitude (Ohlsson's table),

b = galactic latitude,

E = photoelectric color excess,

$\epsilon = \dfrac{E}{r}$ = coefficient of color excess,

[1] Stebbins, Huffer, and Whitford, *Ap. J.*, **91**, 20, 1940.

[2] Struve, *Ap. J.*, **67**, 353, 1928.

[3] Plaskett and Pearce, *Pub. Dom. Ap. Obs.*, **5**, No. 3, 1933.

[4] Williams, *Ap. J.*, **83**, 305, 1936.

[5] Merrill, *Mt. W. Contr.*, No. 569, 1937; *Ap. J.*, **86**, 28, 1937.

[6] Sanford, *Mt. W. Contr.*, No. 573, 1937; *Ap. J.*, **86**, 136, 1937.

Δ = general absorption,

$a = \frac{\Delta}{r}$ = coefficient of general absorption,

λ = wave length of light.

Unless otherwise specified, mean errors given for the various relations will refer to individual stars.

The observational data consist in the intensities and velocity displacements of the interstellar sodium and calcium lines in the spectra of the O and B stars given in *Mount Wilson Contributions*, Nos. 576 and 613, and photoelectric color excesses given in the recent catalogue of Stebbins, Huffer, and Whitford.[1]

The distances used in calibrating the intensities have been derived from the radial component of the galactic rotation of the interstellar material by the formula

$$r = 0.125\rho \csc 2(l - 330^\circ) \text{ kpc} . \qquad (1)$$

Radial velocities of the stars themselves have not been used, because the peculiar motions are large (frequently leading to large negative values of r), and the systematic group motions are difficult to allow for.

EXPLANATION OF FIGURES

Many of the results of this investigation are evident in the accompanying figures. These figures will first be discussed individually, and, later on, collectively.

Figures 1 and 2 (128 and 87 stars, respectively).—Ordinates = r; abscissae = D and K, respectively. The stars were divided according to color excess as follows: small crosses stand for $E < 0^m.20$; large crosses stand for normal points; small open circles for $E > 0^m.19$; large open circles for normal points; triangles indicate that no color excess is available; filled circles represent normal points for all stars. All normal points represent regression of r on D and K. The mean (r, D) and (r, K) relations, represented by the straight lines, are

$$r = 2.38D \pm 0.84 \text{ (m.e.)} , \qquad (2d)$$

$$r = 3.00K \pm 0.84 \text{ (m.e.)} . \qquad (2k)$$

Stars for which $\csc 2\,(l - 330^\circ) > 2$ or $|b| > 22^\circ$ have been excluded. Williams[4] determined the (r, K) relation and found $r = 2.7K$. His distances depend upon proper motions and both stellar and interstellar rotational velocities. The agreement with equation $(2k)$ is satisfactory, in view of possible systematic differences in the intensity scales.

No evidence of blending of the stellar K line with the interstellar line in stars later than $B2$ was found. The algebraic mean residual of K for these stars is -0.014 e.a.

The dotted curves in the figures represent the (r, D) and (r, K) relations found by Merrill[5] and Sanford[6] from photometrically determined distances, uncorrected for space absorption. These distances depend upon mean absolute magnitudes which were derived without correction for absorption. The distances should, therefore, be generally correct except for the more remote stars. For these stars the computed distances will be too large because of the increasing absorption. The expected deviations are of the same type as those observed in the figures between Merrill's and Sanford's curves and the straight lines which depend upon rotational distances.

Stars of large and small color excesses were plotted separately in order to detect any tendency for the interstellar sodium and calcium atoms to coincide spatially with the

interstellar particles responsible for selective absorption. If they do coincide, D and K should be larger in stars of large color excess than in stars of small color excess, and the circles in the figures should be systematically displaced to the right of the crosses. The normal points exhibit no such displacement in either figure. As a further check, the means of the algebraic intensity residuals, $v = D - (r/2.38)$ and $v = K - (r/3.00)$, were computed separately for each E group. The mean residuals are given in Table 1.

We may conclude that the distributions of the interstellar atoms and absorbing particles are independent of each other and that the observed relations between line inten-

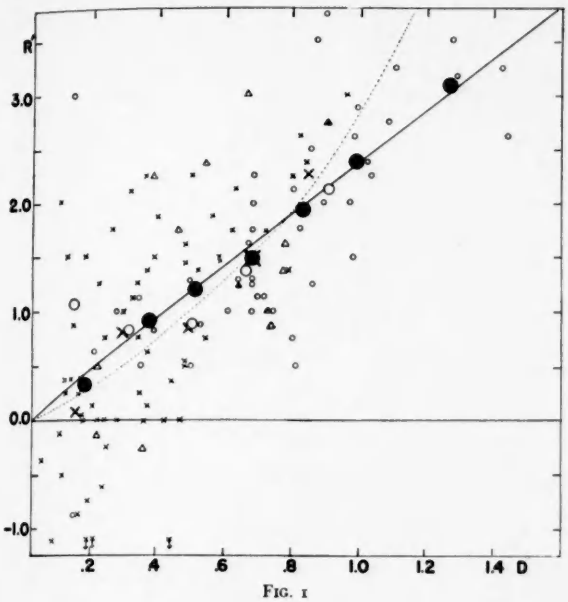

FIG. 1

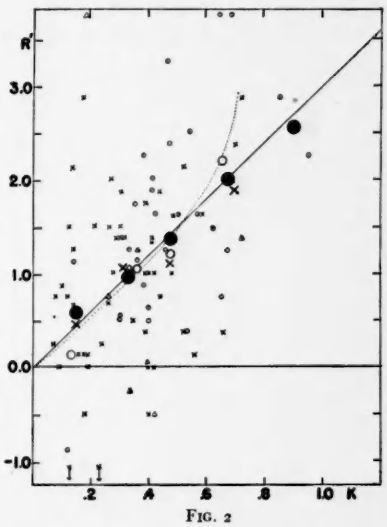

FIG. 2

FIG. 1.—The relation between distance (*ordinate*) and D-line intensity (*abscissa*). Small circles, crosses, and triangles represent individual stars of large, small, and unknown color excesses, respectively. Large solid circles are normal points for all stars combined. Large open circles and crosses are normal points for the stars represented by the small circles and crosses.

FIG. 2.—The relation between distance and the K-line intensity. The symbols are the same as those in Figure 1.

sity and color excess (Figs. 4 and 5) must be due solely to a tendency for both to increase with the distance. Williams[7] arrived at the same conclusion in his study of the K line.

Figure 3 (65 stars).—Ordinates = K; abscissae = D. (Both lines measured in the spectrum of the same star.) Filled circles represent normal points (regression of K on D).

The mean (K, D) relation represented by the straight line is

$$D = 1.36K \pm 0.14 \text{ (m.e.)} . \qquad (3)$$

The result of combining equations (2d) and (2k) is $D = 1.26K$, which is in fairly close agreement with equation (3). Figure 3 is introduced to obtain an estimate of the dispersion in the line intensities for stars at a given distance. If it be assumed that the dispersions in D and K contribute equally to the combined mean error, ± 0.14, we find

[7] *Ap. J.*, **79**, 280, 1934.

individual mean errors, $\sigma_D = \sigma_K = \pm 0.09$. Distances computed from line intensities should therefore have corresponding mean errors of ± 0.21 and ± 0.27 kpc, respectively.

Figures 4 and 5 (176 and 126 stars).—Ordinates = E; abscissae = D and K. Stars divided according to galactic latitude as follows: open circles stand for $|b| < 11°$; crosses for $|b| > 10°$; filled circles represent normal points (regression of E on D and K),

TABLE 1

	$E<0.20$	$E>0.19$
D	+0.014 e.a.	−0.004 e.a.
K	+0.013	−0.067

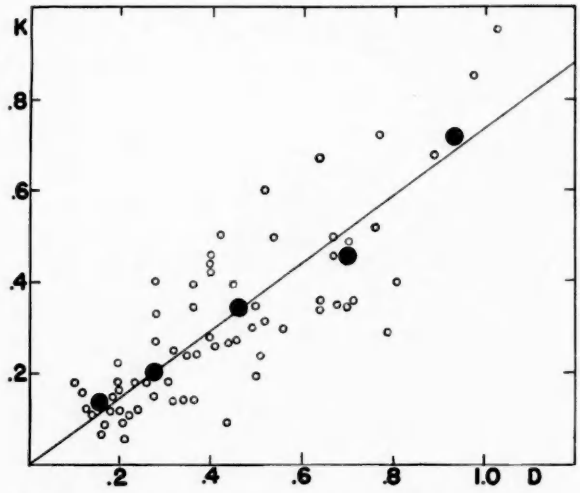

FIG. 3.—The relation between the intensities of the K line (*ordinate*) and the D-line (*abscissa*). The large circles are normal points.

depending only upon low-latitude stars. The mean (E, D) and (E, K) relations, represented by the straight lines are

$$E = 0.33D \pm 0^{m}10 \text{ (m.e.)}, \qquad (4d)$$

$$E = 0.42K \pm 0^{m}08 \text{ (m.e.)}. \qquad (4k)$$

Figures similar to these have been published by Williams,[7] Sanford,[6] Merrill and Wilson,[8] and Stebbins, Huffer, and Whitford.[9] The mean coefficient of photoelectric color excess ϵ is found at once by combining equations $(4d)$ and $(4k)$ with equations $(2d)$ and $(2k)$. The results for sodium and calcium are identical.

$$\epsilon = \frac{E}{r} = 0.14 \text{ mag/kpc}. \qquad (5)$$

[8] *Mt. W. Contr.*, No. 582, 1938; *Ap. J.*, **87**, 9, 1938.

[9] *Mt. W. Contr.*, No. 617, 1939; *Ap. J.*, **90**, 209, 1939.

Figure 6.—Ordinates = E; abscissae = r, the distance derived from rotational-velocity displacements of the interstellar lines. The straight line represents the relation $E = 0.14r$. The standard deviation from the line in units of color excess is $\pm 0^{m}.14$.

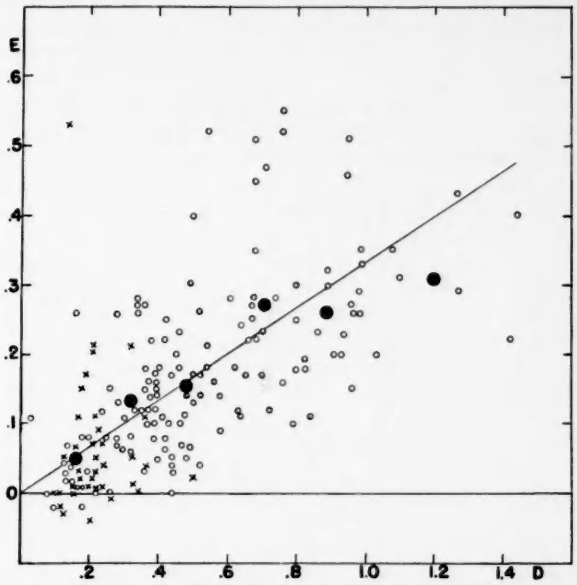

FIG. 4.—The relation between photoelectric color excess, E (*ordinate*), and D-line intensity (*abscissa*). Circles and crosses represent stars in low and high latitudes, respectively. The large circles are normal points for the low-latitude stars.

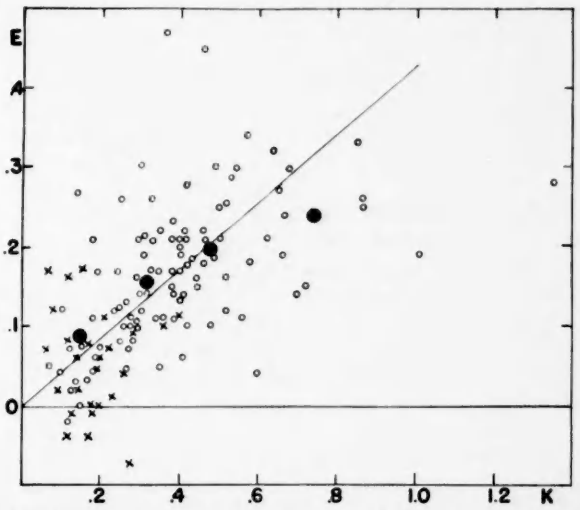

FIG. 5.—The relation between photoelectric color excess (*ordinate*) and K-line intensity (*abscissa*). The symbols are the same as those in Figure 4.

THE ACCURACY OF LINE INTENSITY AS A MEASURE OF DISTANCE

The large dispersion shown in Figures 1 and 2 and exemplified in the mean error ± 0.84 kpc for equations (2*d*) and (2*k*) is fully accounted for by the effect of the peculiar

motions of the interstellar material on r. The peculiar motions were estimated from the velocity displacements of the interstellar lines for 131 stars within 10° of the zeros of rotational velocity. The standard deviation from zero is ±5.4 km/sec, which should lead to a mean error of ±0.68 csc 2 (l − 330°) kpc in the computed distance r. The average value of csc 2 (l − 330°) for stars of Figures 1 and 2 is about 1.25. Hence, the expected mean error in r is ±0.85 kpc. The fact that the observed mean errors in equations (2d) and (2k) are almost exactly equal to this value indicates that the dispersion in D and K for stars at a given distance is small compared with the errors introduced into the computed distances by the random motions of the interstellar medium.

Confirmation is found in Figures 4, 5, and 6. The dispersion in the (E, r) relation (±0.14) is obviously greater than in the (E, D) and (E, K) relations (±0.10 and ±0.08). The greater deviations in (E, r) indicate that the dispersion in r must be much larger than

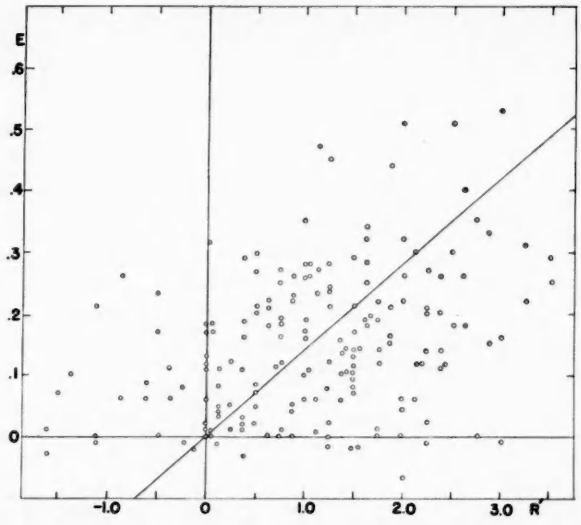

FIG. 6.—The relation between photoelectric color excess (*ordinate*) and distance (*abscissa*) derived from the rotational velocity displacements of the interstellar lines.

the dispersion in the line intensities, because any small difference between these dispersions would be completely swallowed up by the comparatively large spread in E for stars at a given distance and could not be detected.

The determination of the true dispersion in D and K for stars at a given distance is rather difficult. The mean error of ±0.09 e.a. derived from the comparison of D with K in the spectra of the same stars (Fig. 3) amounts roughly to 20 per cent of their average value and is probably a minimum estimate. The true value, however, cannot be much larger, for it would in that case contribute substantially to the observed scatter in the (r, D) and (r, K) relations, which is already fully accounted for by the random motions in the interstellar medium.

The dispersion in the line intensities was studied more directly from their spread within five groups of B stars, within each of which it is reasonable to assume that all members are at approximately equal distances. If so, differences in D and K within each group must be attributed to errors of measurement or to a real spread in the intensities. Three well-known groups in Cygnus, Perseus, and Orion were used, and the remaining two—in Auriga-Taurus and Sagittarius—were selected because their members exhibit very

uniform line intensities. The standard deviations from the group means, derived from a total of 74 stars, amount to about 17 per cent.

It is interesting to note that the color excesses of the stars of the Cygnus group are systematically smaller than those in immediately surrounding regions and that the spread in line intensity is conspicuously greater than in any other group. These facts support the suggestion of several previous investigations[10] that here we see a part of a populous stratum of B stars through a hole in the absorbing material.

The evidence presented thus far indicates that the standard deviation from the mean relation between the true distance and line intensity within a small group of stars is about 20 per cent. Large-scale deviations dependent on galactic latitude and longitude remain to be investigated.

A study of stars in different latitudes showed no dependence of the observed (r, D) and (r, K) relations on b. This does not mean, however, that there is no gradient perpendicular to the galactic plane in the density of the interstellar material. The intensities and rotational-velocity displacements of the interstellar lines would both be affected by a negative gradient in the same sense, so that their ratio would remain practically constant within the latitude zones occupied by the O and B stars.

A second attempt was made to evaluate the latitude effect by using stellar radial velocities, which are independent of interstellar density gradients. It failed, however, because of the large peculiar motions of the stars.

Until more data on high-latitude stars are available, the appropriate latitude correction for distances derived from equations (2*d*) and (2*k*) cannot be determined, but it is improbable that the uncorrected distances are seriously in error at latitudes of less than ten or fifteen degrees.

In order to study systematic longitude or regional variations in the distance-intensity relation, a large chart was made upon which the residuals $v = 2.38D - r$ or $v = 3.00K - r$ were plotted in galactic co-ordinates. Regions in which the residuals were systematically positive or negative could then be selected and investigated separately. The algebraic mean of the residuals was calculated for each such regional group and compared with the standard deviation σ for the mean of n stars.

Only five groups were found in which the mean residual exceeds σ. The residuals can be due either to abnormal interstellar velocities or to systematic deviations in the line intensities from the mean distance-intensity relations or to both. A comparison of the stellar velocities with the interstellar velocities gave the following facts:

Groups 1 and 2 (Aquila-Vulpecula and Canis Major). The systematic effect in the residuals disappears when stellar velocities are used in computing the distances. There is no evidence of abnormal line intensities.

Group 3 (Perseus). The stellar and interstellar velocities agree in giving a remarkably close distance-intensity relation, shown in Figure 7. (Open circles represent r computed from interstellar velocities; crosses are from stellar velocities.) Here ten of the thirty computed distances are negative. The systematic residuals are probably wholly attributable to the clearly abnormal velocities rather than to any abnormal intensities.

Group 4 (Cygnus). The stellar velocities are certainly anomalous, ranging from -45 to $+18$ km/sec and leading to three large negative distances. It is not improbable that the interstellar velocities share this anomaly. The mean residual is only 1.5σ. There is no definite evidence of abnormal intensities.

Group 5 (h and χ Persei). The stellar and interstellar velocities are in perfect agreement, giving $r = 2.46$ kpc, with a standard deviation of only 18 per cent. It appears probable that the systematic residuals are due to abnormally faint interstellar lines, which give a distance of 2.12 kpc. This is the only region where convincing evidence of systematic deviations from the mean distance-intensity relation was found.

[10] Bok, *The Distribution of the Stars in Space*, p. 118, University of Chicago Press, 1937.

Although the evidence favors the hypothesis of an approximately uniform distribution of the interstellar material, two other investigations which suggest exceptions should be mentioned.

1. Beals[11] has found three stars with double interstellar lines. These remarkable observations indicate distinct discontinuities in the interstellar velocities and suggest corresponding discontinuities in distribution.

2. Struve[12] has found the K line systematically weaker than average in Cygnus and Perseus, and stronger in Cepheus and Auriga. The present investigation confirms his results only in Perseus. Struve states, however, that he considers the reality of the deviations doubtful.

The regions near the zeros of rotational velocity, where the rotational distances are indeterminate, have necessarily been omitted from this study. Theoretical considerations suggest that the line intensities depend largely upon the rotational-velocity gradient along the line of sight. If so, the intensities at the rotational zeros would obviously be highly unreliable as indices of distance. Investigations by Beals,[13] Wilson and Merrill,[14] Sanford,[6] and Merrill[5] have shown, however, that galactic rotation plays, at most, a minor role in the formation of the interstellar lines and that there is no evidence of any noticeable change in the distance-intensity relation at the zeros. It appears probable that there are no great departures from uniformity, though definite positive evidence is lacking.

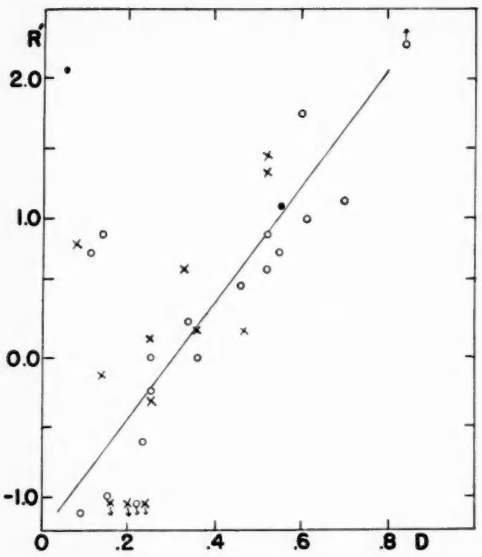

FIG. 7.—The (r', D) relation for group 3, at galactic longitudes between 105° and 135°. Circles represent distances derived from interstellar velocities; crosses, distances from stellar velocities.

The results of the foregoing sections indicate that the intensities of the interstellar D and K lines are probably the best available indices to the distances of individual O and B stars, with a mean error of about 20 per cent. Distant stars in high latitudes may, however, require some correction, undetermined as yet, for the negative density gradient of the interstellar material perpendicular to the galactic plane.

THE RATIO BETWEEN GENERAL AND SELECTIVE ABSORPTION

It is clear from the scatter of the points in Figures 4 and 5 that any mean relation between distance and space absorption is very unreliable in calculating the absorption for any single restricted region of the Milky Way. Equation (5), however, does enable us to estimate the ratio between general and selective absorption.

The most reliable value of the mean coefficient of photographic absorption, $\alpha = 0^m.85$/kpc, has been derived by Joy[15] from a study of the radial velocities of Cepheid variables. Van Rhijn[16] has applied a correction for a selection effect favoring Cepheids of

[11] *Ap. J.*, **87**, 568, 1938. [12] *Ap. J.*, **79**, 273, 1934. [13] *M.N.*, **96**, 661, 1936.

[14] *Mt. W. Contr.*, No. 570, 1937; *Ap. J.*, **86**, 44, 1937.

[15] *Mt. W. Contr.*, No. 607, 1939; *Ap. J.*, **89**, 356, 1939.

[16] *Groningen Pub.*, No. 47, 1936.

small absorption. He arrived at the value $\alpha = 1^{m}.1$/kpc, which is adopted in the following discussion.

The comparability of this value of α with $\epsilon = 0^{m}.14$/kpc depends upon the similarity in distribution of the B stars and the Cepheids used in the determinations. The numbers of Cepheids and B stars within four zones of distance are given in Table 2. It is evident that the two groups of stars occupy very nearly the same regions of space, and the mean absorption for both should be approximately the same.

TABLE 2

r(Kpc)	0–0.78	0.78–1.12	1.12–1.75	1.75–2.60
Cepheids	35	33	34	26
B stars	54	58	66	32

The coefficients of absorption and color excess give, then, $\alpha/\epsilon = \Delta_{ph}/E = 7.9$. The value of Δ_{ph}/E to be expected if we assume the absorption to be proportional to λ^{-1} is 8.6, provided there is no nonselective absorption (which would increase the figure). The agreement of the observed and calculated values is satisfactory and definitely favors the assumption of no nonselective absorption.

DISPERSION IN ABSOLUTE MAGNITUDES

Although distances derived from interstellar lines are not suitable data for the determination of mean absolute magnitudes because of a selection favoring the more luminous objects, they do permit an interesting estimate of the dispersion in the absolute magnitudes.

The stars were divided into groups according to spectral subdivision and line quality. The mean absolute magnitude was computed for each group, with distances determined from line intensities, and visual magnitudes from *Mount Wilson Contribution* No. 576, corrected for absorption by means of the relation $\Delta_{vis} = 7E$ (derived from the λ^{-1} law). Standard deviations were then computed from the residuals in absolute magnitude within each group and were combined into three groups of the different line qualities. The results are listed in Table 3.

TABLE 3

	c Stars	Normal	n Stars	All Stars
σ_M	$\pm 1^{M}.1$	$\pm 1^{M}.3$	$\pm 1^{M}.4$	$\pm 1^{M}.3$
n	59	111	68	238

There appears to be a tendency for the dispersion to increase as the lines become more nebulous, but no other systematic variation in the standard deviations was found.

Strictly speaking, the values tabulated above are standard deviations in the distance moduli of the O and B stars and include, in addition to the dispersion in absolute magnitudes, errors which may possibly arise from the assumption that Δ_{vis}/E is a constant for all stars. The variations in Δ_{vis}/E which would be required to affect the observed dispersions appreciably, however, are unreasonably large, and it is probably safe to assume that the effect of the existing variations is insignificant.

The mean error in the distances derived from distance moduli having a standard deviation of $\pm 1^{M}.3$ amounts to a factor of nearly two. Additional errors, however, may be introduced by uncertainties in absorption, if E is unknown, and by systematic errors in the assumed absolute magnitudes.

SUMMARY

1. The relations between the distance of a star and the intensity of its interstellar lines are $r = 2.38D$ and $r = 3.00K$. The mean error of an individual determination is probably about 20 per cent.

2. The (r, D) and (r, K) relations appear to be uniform in all longitudes, with the possible exception of longitudes of zero rotational velocities. Data were lacking for a study of deviations in high latitudes.

3. The space distributions of interstellar atoms and absorbing material were found to be quite unrelated.

4. The ratio of photographic absorption to photoelectric color excess is found to be 7.9, in good agreement with the value 8.6 predicted by the λ^{-1} law of absorption.

5. The dispersion in the absolute magnitudes of O and B stars of a given spectral subdivision and line quality is $\pm 1^{M}.3$. This corresponds to a mean error in distance of a factor of nearly two.

In conclusion, I wish to acknowledge the kindness of Drs. Stebbins, Huffer, and Whitford in permitting me to use their catalogue of photoelectric color excesses before its final publication. I am also indebted to Drs. B. J. Bok, P. W. Merrill, O. C. Wilson, J. L. Greenstein, and R. Trumpler for their helpful criticisms and comments during the course of this work.

MILLS COLLEGE
AND
CHABOT OBSERVATORY
OAKLAND, CALIFORNIA

THE TIME OF RELAXATION OF STELLAR SYSTEMS. I

S. CHANDRASEKHAR

ABSTRACT

In this paper the problem of the time of relaxation of a stellar system is formulated *de novo* and solved from the point of view of the energies exchanged between stars during encounters. The method consists in evaluating the sum $\Sigma\Delta E^2$ (where ΔE is the energy exchanged during a single encounter idealized as a two-body problem) for all possible encounters between an incident star having mass m_2 and a velocity v_2 during its motion through other field stars and determining its rate of increase with time. In forming the sum $\Sigma\Delta E^2$, particular attention has been given to determining the manner in which the various parameters (seen to be five in number) defining an encounter enter into the problem. For a Gaussian distribution of the velocities v_1 of the field stars the averaging over all the parameters defining an encounter can be effected. We find that

$$\Sigma\Delta E^2 = 8\pi NG^2m_1^2m_2^2v_2[G(x_0)\log_e(D_0v_2^2/Gm_1) + g(x_0, \mu)]dt\,, \tag{i}$$

where G is the constant of gravitation, m_1 the mass of a typical field star, D_0 the average distance between the stars in the system, $x_0 = hv_2$ (h being the "modulus of precision" occurring in the distribution of the velocities v_1), $\mu = m_1/m_2$, and where $G(x_0)$ and $g(x_0, \mu)$ are certain functions of x_0 and μ which are tabulated (Tables 2 and 4). The expression for the time of relaxation T_E is found to take the form

$$T_E = 4.21 \times 10^{12}\,\frac{v_2^3}{Nm_1^2\{G(x_0)\log_e[9.31 \times 10^4 D_0v_2^2/m_1] + g(x_0, \mu)\}}\ \text{years}\,, \tag{ii}$$

where m_1, D_0, v_2, and N are expressed in the units solar mass, parsec, 20 km/sec, and number per cubic parsec, respectively. This formula for T_E is applied for the conditions prevailing in (1) the galaxy and (2) the globular clusters. In the former case we obtain a justification of the fundamental principle of stellar dynamics, namely, that each star can be regarded as a conservative dynamical system. In the latter case the times of relaxation are found to be of the order of 5×10^9 years, suggesting that conditions toward a rough equipartition of the energy must be far advanced.

1. *Introduction.*—It is now generally agreed that the forces influencing the motions of the individual stars in a stellar system are essentially gravitational in character. In a general way it is clear that these forces arise, first, from the smoothed-out distribution of matter in the system and, secondly, from the effect of chance stellar encounters. The forces of the first kind are derivable from a gravitational potential $\mathfrak{V}$ representing the smoothed-out distribution of matter in the system. This gravitational potential is a function of the space and time co-ordinates only. On the other hand, the forces of the second kind arise from the accidental encounters with the other stars which happen to be in the neighborhood of the star we are considering. More explicitly, the manner in which these two types of forces influence the motion of any particular star can be described as follows: Consider a star which is at the point (x, y, z) at some specified instant of time, $t = 0$ (say). Without loss of generality we can suppose that at $t = 0$ the star is not experiencing appreciably the effects of a chance stellar encounter. The instantaneous force acting on the star at $t = 0$ will then be given in terms of the gravitational potential $\mathfrak{V}$ of the smoothed-out distribution only. We can therefore write

$$\frac{d^2\mathbf{r}}{dt^2} = -\text{grad}\,\mathfrak{V}\,. \tag{1}$$

The integration of the foregoing vector equation will uniquely determine a *theoretical orbit* for the star in terms of its position and velocity at time $t = 0$. Clearly, the star will follow this theoretical orbit only as long as stellar encounters have no appreciable influence. However, with the passage of time, stellar encounters will begin to have a cumulative effect and will tend to make the *actual orbit* of the star deviate more and more from the theoretical orbit. The question now arises: *How long will it take for the*

cumulative effect of stellar encounters to deviate the star so much from the orbit derived from (1) *that it can no longer be described even approximately by this theoretical orbit?* It is the estimation of this time that specifies *the time of relaxation* of a stellar system.

It will be noticed that the general ideas underlying the estimation of the time of relaxation of a stellar system are most conveniently expressed in terms of the deviation of the orbit actually described by any particular star from a theoretical orbit derived from the gravitational potential $\mathfrak{V}$. However, the notion itself has a wider scope. Thus, according to equation (1), we have the integral

$$\tfrac{1}{2}(\dot{x}^2 + \dot{y}^2 + \dot{z}^2) + \mathfrak{V}(x, y, z, t) = \int \frac{\partial \mathfrak{V}}{\partial t}\, dt + \text{constant} . \tag{2}$$

If $\mathfrak{V}$ is explicitly independent of the time, equation (2) reduces to the energy integral in its standard form. In any event, we can regard the existence of the integral (2) as equivalent to our being able to consider each star in the system as an independent conservative dynamical system. But this is true only as long as the effects of stellar encounters can be neglected. We can therefore ask: *How long will it take before the cumulative effect of stellar encounters prevents us from considering the stars as independent conservative dynamical systems?* Again, we can refer to this time as the time of relaxation of a stellar system.

It is thus seen that the fundamental ideas underlying the problem of the time of relaxation of a stellar system can be formulated in one of two ways. In this paper we shall consider the problem from the point of view of the energies exchanged during stellar encounters. In the paper which follows this one (referred to in the sequel as "II") the same problem is considered from the point of view of the deflections suffered by stars during such encounters.

2. *The formulation of the problem.*—We now consider in somewhat greater detail the problem of quantitatively evaluating the time of relaxation from the point of view of the energy exchanged during stellar encounters. Let us suppose that the different encounters can be treated independently of others and that they can be regarded individually as two-body encounters.[1] Under these circumstances each encounter will result in an exchange of energy of amount ΔE. The actual amount of this energy transfer, ΔE, will depend on the initial circumstances defining the encounter (see § 3). The method now consists in evaluating the sum

$$\Sigma \Delta E^2 \tag{3}$$

for all possible encounters and determining its rate of increase with time. It now appears that, when the root mean square of the energy exchanged in stellar encounters, $\sqrt{\Sigma \Delta E^2}$, becomes of the same order as the initial kinetic energy of the star, it will no longer be possible to assume even the approximate validity of the energy equation (2). It is clearly largely a matter of definition as to what we mean by the phrase "the same order as the initial kinetic energy of the star." However, we shall define the time of relaxation, T_E, as the time required for

$$\sqrt{\Sigma \Delta E^2} \tag{4}$$

to become equal to the initial kinetic energy of the star.[2]

[1] The limitations introduced by this assumption are considered in § 4 (see also II, § 10).

[2] The evaluation of the sum (4) as a means of estimating the time of relaxation is due to Karl Schwarzschild (*Seeliger Festschrift*, p. 94, Berlin, 1924), though the method is generally attributed to Rosseland (*M.N.*, **88**, 208, 1928). A comparison of the results of Schwarzschild and Rosseland indicate fundamental differences of a far-reaching character; and, while these differences are due to errors in both the investigations, the really serious ones occur in Rosseland's paper (see n. 5 below).

3. *The equations of the problem.*—As we have already stated in § 2, we shall idealize each stellar encounter as a two-body problem. In describing such an encounter, it is, however, important to remember that we should always refer the physically relevant quantities to some appropriately chosen *fixed* frame of reference.[3] Consider, then, the effect of encounters on a star of mass m_2 and having an initial velocity v_2 during its motion through other stars. Let m_1 and v_1 denote the mass and the velocity of a typical *field star*. The parameters defining such an encounter are five in number. These are (i) the magnitude v_1 of the vector v_1, (ii) the angle θ between the two vectors v_1 and v_2, (iii) the azimuthal angle φ referred to a system of co-ordinates the z-axis of which coincides with the direction of v_2, (iv) the impact parameter D, and finally (v) the angle Θ between the *orbital plane* and the *fundamental plane* containing the vectors v_1 and v_2. For the sake of brevity we shall denote such an encounter by the symbol $(v_1, \theta, \varphi, D, \Theta)$. Now, according to the elementary theory of the two-body problem,[4] the velocity of the center of gravity V_g remains constant during the encounter. Further, in the orbital plane each star describes a hyperbola about the other, and at the end of the encounter the direction of the relative velocity is deflected by an amount $\pi - 2\psi$ (in the orbital plane), where

$$\cos \psi = \frac{1}{\sqrt{1 + \dfrac{D^2 V^4}{G^2 (m_1 + m_2)^2}}} . \tag{5}$$

We shall now consider the exchange of energy ΔE which takes place between the two stars. By definition we have

$$V_g = \frac{1}{m_1 + m_2} (m_1 v_1 + m_2 v_2) ; \qquad V = v_2 - v_1 . \tag{6}$$

From the relations (6) we readily find that

$$v_2 = V_g + \frac{m_1}{m_1 + m_2} V . \tag{7}$$

According to equation (7), we have

$$v_2^2 = V_g^2 + 2 \frac{m_1}{m_1 + m_2} V_g V \cos \Phi + \left(\frac{m_1}{m_1 + m_2} \right)^2 V^2 , \tag{8}$$

where Φ is the angle between V_g and V (see II, Fig. 3 for the relations between the various angles). Similarly, at the end of the encounter we have

$$v_2'^2 = V_g^2 + 2 \frac{m_1}{m_1 + m_2} V_g V \cos \Phi' + \left(\frac{m_1}{m_1 + m_2} \right)^2 V^2 , \tag{9}$$

[3] The nonrecognition of this fact has led to several erroneous treatments of the problem (cf. II; also n. 5 below).

[4] See, e.g., W. M. Smart, *Stellar Dynamics*, pp. 315–317, Cambridge, England, 1938.

where Φ' is the angle between $\boldsymbol{V}_g$ and the relative velocity $\boldsymbol{V}'$ at the end of the encounter. Further, v_2' refers to the velocity of the star at the end of the encounter. Hence, the change in energy ΔE suffered by the star as a result of the encounter is given by

$$\left.\begin{aligned}\Delta E &= \tfrac{1}{2}m_2(v_2'^2 - v_2^2) \\ &= \frac{m_1 m_2}{m_1 + m_2} V_g V(\cos\Phi' - \cos\Phi)\,.\end{aligned}\right\} \tag{10}$$

Now, let i be the angle which the projection of $\boldsymbol{V}_g$ on the orbital plane makes with $\boldsymbol{V}_g$. Further, let ϕ and ϕ' be the angles which $\boldsymbol{V}$ and $\boldsymbol{V}'$ make with the projection of $\boldsymbol{V}_g$ on the orbital plane. We then have

$$\cos\Phi = \cos\phi\cos i\,; \qquad \cos\Phi' = \cos\phi'\cos i\,. \tag{11}$$

We can therefore re-write equation (10) in the form

$$\Delta E = \frac{m_1 m_2}{m_1 + m_2} V_g V(\cos\phi' - \cos\phi)\cos i\,, \tag{12}$$

or somewhat differently as

$$\Delta E = \frac{2m_1 m_2}{m_1 + m_2} V_g V \sin\frac{\phi + \phi'}{2}\sin\frac{\phi - \phi'}{2}\cos i\,. \tag{13}$$

On the other hand, we have (see II, Fig. 3)

$$\phi' - \phi = \pi - 2\psi\,, \tag{14}$$

whence

$$\tfrac{1}{2}(\phi + \phi') = \frac{\pi}{2} - \psi + \phi\,; \qquad \tfrac{1}{2}(\phi' - \phi) = \frac{\pi}{2} - \psi\,. \tag{15}$$

Combining equations (13) and (15), we have

$$\Delta E = -2\frac{m_1 m_2}{m_1 + m_2} V_g V\cos(\phi - \psi)\cos\psi\cos i\,, \tag{16}$$

where ψ is related to the impact parameter D and V according to equation (5).

We shall now obtain the expression for the number of $(v_1, \theta, \varphi, D, \Theta)$ encounters which take place in an interval of time dt. Let $N(v_1, \theta, \varphi)$ be the number of field stars per unit volume with velocities in the range $(v_1, v_1 + dv_1)$ and in directions confined by the element of solid angle $\sin\theta\, d\theta d\varphi$. For a spherical distribution of velocities we can write

$$N(v_1, \theta, \varphi)dv_1 d\theta d\varphi = 4\pi N f(v_1)v_1^2 dv_1 \frac{\sin\theta\, d\theta d\varphi}{4\pi}\,, \tag{17}$$

where N is the total number of field stars per unit volume. Further, in equation (17) $f(v_1)$ stands for the frequency function defining the distribution of the velocities v_1: thus for a Maxwellian distribution of velocities we have

$$f(v_1) = \frac{h^3}{\pi^{3/2}} e^{-h^2 v_1^2}, \tag{18}$$

where h is a constant defining the dispersion of the velocities. The number of $(v_1, \theta, \varphi, D, \Theta)$ encounters which occur in time dt is accordingly given by

$$N(v_1, \theta, \varphi) dv_1 d\theta d\varphi \cdot \frac{d\Theta}{2\pi} \cdot 2\pi D dD \cdot V dt . \tag{19}$$

Consequently, the contribution of these encounters to the sum can be written as

$$\Sigma \Delta E^2_{(v_1, \theta, \varphi, D, \Theta)} = 2\pi N(v_1, \theta, \varphi) \Delta E^2 V D dD \frac{d\Theta}{2\pi} dv_1 d\theta d\varphi dt ; \tag{20}$$

or, using (16), we have

$$\left.\begin{aligned} \Sigma \Delta E^2_{(v_1, \theta, \varphi, D, \Theta)} = {} & 8\pi N(v_1, \theta, \varphi) V_g^2 V^3 \left(\frac{m_1 m_2}{m_1 + m_2}\right)^2 \\ & \times \cos^2 i \cos^2 (\phi - \psi) \cos^2 \psi D dD \frac{d\Theta}{2\pi} dv_1 d\theta d\varphi dt . \end{aligned}\right\} \tag{21}$$

Our next problem is to integrate the foregoing expression over the relevant ranges of the various parameters D, Θ, φ, θ, and v_1. We shall now consider in turn the integration over each of these variables.

4. *The integration over the impact parameter*, D.—To integrate over D we shall introduce a change of variables. According to equation (5), we have

$$D dD = \frac{G^2 (m_1 + m_2)^2}{V^4} \frac{\sin \psi}{\cos^3 \psi} d\psi . \tag{22}$$

Hence, we can re-write (21) as

$$\left.\begin{aligned} \Sigma \Delta E^2_{(v_1, \theta, \varphi, \psi, \Theta)} = {} & 8\pi N(v_1, \theta, \varphi) G^2 m_1^2 m_2^2 \frac{V_g^2}{V} \\ & \times \cos^2 i \frac{\cos^2 (\phi - \psi) \sin \psi}{\cos \psi} d\psi \frac{d\Theta}{2\pi} dv_1 d\theta d\varphi dt . \end{aligned}\right\} \tag{23}$$

On integrating the foregoing expression over the relevant range of ψ we shall obtain the contribution to $\Sigma \Delta E^2$ by all those encounters which we can denote by the symbol $(v_1, \theta, \varphi, \Theta)$. We thus have

$$\left.\begin{aligned} \Sigma \Delta E^2_{(v_1, \theta, \varphi, \Theta)} = {} & 8\pi N(v_1, \theta, \varphi) G^2 m_1^2 m_2^2 \frac{V_g^2}{V} \\ & \times \cos^2 i \int \frac{\cos^2 (\phi - \psi) \sin \psi}{\cos \psi} d\psi \frac{d\Theta}{2\pi} dv_1 d\theta d\varphi dt . \end{aligned}\right\} \tag{24}$$

A consideration of the integral occurring in (24) introduces some new factors into the discussion. At first sight, it would appear that the appropriate limits for ψ are 0 and $\pi/2$ corresponding to the limits 0 and ∞ for D. But, and this is the crucial point, the integral in (24) does *not* converge at $\psi = \pi/2$ except in the trivial case $\phi = 0$.[5] Further, it is readily seen that (except when $\phi = 0$) the integral in (24) *diverges logarithmically* as $\psi \to \pi/2$. This divergence arises essentially from the improper use of the two-body approximation to describe distant encounters in a stellar system; for, the formula (16) for the energy exchanged between two stars involved in an encounter assumes them to be initially at an infinite distance from each other and to separate to an infinite distance after the encounter. Only then could we set for the deflection $(\pi - 2\psi)$ the angle between the two asymptotes of the relative orbit given according to equation (5). We should therefore conclude that, in practice, a "second" encounter begins to be effective before the "first" can be regarded as completed in the strict sense. Hence, the use of the expression (5) for the angle between the two asymptotes *overestimates* the actual deflection. This difference between the actual deflection and the full (theoretical) amount (5) is clearly of no importance for "close encounters," i.e., for encounters for which D is a fraction of the average distance D_0 between the stars in the system. However, for encounters for which D becomes of the same order as D_0, the errors introduced by using the expression (16) for ΔE become increasingly serious. Thus, the divergence of the integral occurring in (24) as $D \to \infty$ and $\psi \to \pi/2$ must be attributed, first, to the general overestimation of the energy exchange ΔE given by (16) (which is of particular importance for distant encounters) and, secondly, to the increasing difficulty of describing stellar encounters on a two-body idealization when the corresponding impact parameters become of the same order as the average distance D_0 between the stars. On the other hand, if we arbitrarily disregard all encounters with impact parameters greater than a certain amount, we shall be ignoring the small but finite contributions to $\Sigma\Delta E^2$ arising from these distant encounters. Consequently, by appropriately choosing *an upper limit* $D_{\max}$ for the impact parameter D, we can compensate for the errors introduced by overestimating ΔE for encounters with $D \leqslant D_{\max}$ and by ignoring ΔE for encounters with $D \geqslant D_{\max}$. In a general way it is clear that $D_{\max}$ should be equal to D_0 within a factor 2 or 3. It would be difficult to estimate $D_{\max}$ more closely than this without going into a considerable amount of detailed calculations. However, it is seen that an error of a factor 2 or 3 in the chosen value of $D_{\max}$ does not introduce any significant error in the final expression for the time of relaxation. This fortunate cir-

[5] It is readily verified that $\phi = 0$ corresponds to $v_2/v_1 = \infty$ (see II, Fig. 3). Consequently, the only case in which the integral (24) converges is, from physical considerations, quite unimportant. But it is precisely this case, $\phi = 0$, which has been considered by Rosseland (*loc. cit.*). Thus, Rosseland's claim that the evaluation of the sum $\Sigma\Delta E^2$ does not introduce any divergence when integrating over the *whole possible range* of the impact parameter ($0 \leqslant D \leqslant \infty$) is not substantiated. Rosseland's statement, that the "unattractive feature" associated with the divergence as D tends to infinity is eliminated when the squares of the contributions from independent encounters are compounded, appears therefore to be based on a misunderstanding of the true situation. On the other hand, Schwarzschild (like Rosseland) evaluated the sum $\Sigma\Delta E^2$, but he replaced $\cos^2(\phi - \psi)$ (which occurs under the integral sign in [24]) by a constant value $\frac{1}{2}$. Strictly speaking, Schwarzschild's procedure is erroneous, but, nevertheless, he retains the essential feature of the problem, namely, the divergence of the integral. It is to this difference that attention was directed in n. 2, above.

It should be emphasized here that the consideration of the convergence or the divergence of the integral in (24) is not a mere "academic" discussion; it is really the essence of the problem and has an important bearing on the validity or otherwise of the use of the two-body approximation to describe distant encounters (cf. II, § 10). Actually, as we shall see, the correct treatment of the integral in (24) affects even the order of magnitude of the time of relaxation as evaluated by Rosseland. It is important to stress this point, as Rosseland's results have been extensively used and quoted in the literature.

It is of interest to recall in the present connection that the question of the energy exchanged during stellar encounters was first considered by Eddington (*Stellar Movements*, pp. 248–252, London: Macmillan, 1914). However, Eddington evaluates the exchange of energy in the frame of reference in which the center of gravity of the two stars is at rest. In this frame of reference the energy exchanged is identically zero, and the fact that Eddington obtains a finite result is due to an erroneous limiting process.

cumstance arises from the fact that the integral occurring in (24) diverges only logarithmically as $\psi \to \pi/2$. We shall therefore assume that

$$D_{\max} \simeq D_0 . \tag{25}^{6}$$

Again, for the values of D_0 which come under discussion in the treatment of actual stellar systems the maximum value of ψ differs so slightly for $\pi/2$ that we can put $\psi = \pi/2$ in all terms except those which diverge at $\psi = \pi/2$.

According to our remarks in the preceding paragraph, we shall evaluate the integral in (24) between the limits $0 \leqslant \psi \leqslant \psi_0$ and put $\psi_0 = \pi/2$ in all terms except those which diverge at $\psi = \pi/2$. In this manner we readily find that

$$\left.\begin{aligned}\Sigma\Delta E^2_{(v_1,\,\theta,\,\varphi,\,\Theta)} &= 8\pi N(v_1,\,\theta,\,\varphi)G^2m_1^2m_2^2\,\frac{V_g^2}{V}\cos^2 i \\ &\times\left[\tfrac{1}{2}\cos^2\phi + \sin^2\phi(-\log\cos\psi_0 - \tfrac{1}{2}) + \frac{\pi}{4}\sin 2\phi\right]\frac{d\Theta}{2\pi}\,dv_1 d\theta d\varphi dt .\end{aligned}\right\} \tag{26}$$

Using the relations (see II, Fig. 2)

$$\cos\phi\cos i = \cos\Phi\,; \qquad \sin\phi\cos i = \sin\Phi\cos\Theta . \tag{27}$$

We can re-write equation (26) more conveniently as

$$\left.\begin{aligned}\Sigma\Delta E^2_{(v_1,\,\theta,\,\varphi,\,\Theta)} &= 8\pi N(v_1,\,\theta,\,\varphi)G^2m_1^2m_2^2\,\frac{V_g^2}{V} \\ &\times\left[\tfrac{1}{2}\cos^2\Phi + \frac{1}{2}\left\{\log\left(1 + \frac{D_0^2V^4}{G^2(m_1+m_2)^2}\right) - 1\right\}\sin^2\Phi\cos^2\Theta\right. \\ &\left.+\frac{\pi}{4}\sin 2\Phi\cos\Theta\right]\frac{d\Theta}{2\pi}\,dv_1 d\theta d\varphi dt .\end{aligned}\right\} \tag{28}$$

5. *The integration over the inclination of the orbital plane.*—The integration of (28) over the inclination of the orbital plane to the fundamental plane is simple. We readily find that

$$\left.\begin{aligned}\Sigma\Delta E^2_{(v_1,\,\theta,\,\varphi)} &= 8\pi N(v_1,\,\theta,\,\varphi)\,G^2m_1^2m_2^2\,\frac{V_g^2}{V} \\ &\times\left[\tfrac{1}{2}\cos^2\Phi + \frac{1}{4}\left\{\log\left(1 + \frac{D_0^2V^4}{G^2(m_1+m_2)^2}\right) - 1\right\}\sin^2\Phi\right]dv_1 d\theta d\varphi dt .\end{aligned}\right\} \tag{29}$$

6. *Some auxiliary formulae.*—The quantities V_g, V, and Φ which occur in equation (29) are all determined by v_1, v_2, and θ. We shall now obtain the explicit form of these relations.

From our definitions of the vectors $\boldsymbol{V}_g$ and $\boldsymbol{V}$ we directly obtain the formulae

$$V_g^2 = \frac{1}{(m_1+m_2)^2}\,(m_1^2v_1^2 + m_2^2v_2^2 + 2m_1m_2v_1v_2\cos\theta) \tag{30}$$

[6] This assumption is further discussed in II, § 10.

and

$$V^2 = v_1^2 + v_2^2 - 2v_1v_2 \cos\theta\,. \tag{31}$$

On the other hand, since (cf. eq. [7])

$$\boldsymbol{v}_1 = \boldsymbol{V}_g - \frac{m_2}{m_1 + m_2}\boldsymbol{V}\,, \tag{32}$$

we have

$$v_1^2 = V_g^2 - 2\frac{m_2}{m_1 + m_2}V_gV\cos\Phi + \left(\frac{m_2}{m_1 + m_2}\right)^2 V^2\,; \tag{33}$$

or, using equations (30) and (31), we readily obtain

$$2\frac{m_2}{m_1 + m_2}V_gV\cos\Phi = 2\frac{m_2}{(m_1 + m_2)^2}[m_2v_2^2 - m_1v_1^2 + v_1v_2(m_1 - m_2)\cos\theta]\,. \tag{34}$$

Hence,

$$\cos\Phi = \frac{m_2v_2^2 - m_1v_1^2 + v_1v_2(m_1 - m_2)\cos\theta}{\sqrt{(m_1^2v_1^2 + m_2^2v_2^2 + 2m_1m_2v_1v_2\cos\theta)(v_1^2 + v_2^2 - 2v_1v_2\cos\theta)}}\,. \tag{35}$$

From the foregoing relation we find

$$\sin\Phi = \frac{v_1v_2(m_1 + m_2)\sin\theta}{\sqrt{(m_1^2v_1^2 + m_2^2v_2^2 + 2m_1m_2v_1v_2\cos\theta)(v_1^2 + v_2^2 - 2v_1v_2\cos\theta)}}\,. \tag{36}$$

Combining equations (30), (31), (35), and (36), we obtain

$$\left.\begin{aligned}
\frac{V_g^2}{V}\cos^2\Phi &= \frac{1}{(m_1 + m_2)^2}\frac{[m_2v_2^2 - m_1v_1^2 + v_1v_2(m_1 - m_2)\cos\theta]^2}{(v_1^2 + v_2^2 - 2v_1v_2\cos\theta)^{3/2}}\,,\\
\frac{V_g^2}{V}\sin^2\Phi &= v_1^2v_2^2\frac{\sin^2\theta}{(v_1^2 + v_2^2 - 2v_1v_2\cos\theta)^{3/2}}\,,\\
\log\left(1 + \frac{D_0^2V^4}{G^2(m_1 + m_2)^2}\right) &= \log\left[1 + \frac{D_0^2(v_1^2 + v_2^2 - 2v_1v_2\cos\theta)^2}{G^2(m_1 + m_2)^2}\right]\,.
\end{aligned}\right\} \tag{37}$$

We can now re-write equation (29) in the form

$$\left.\begin{aligned}
\Sigma\Delta E^2_{(v_1,\,\theta,\,\varphi)} = 8\pi N(v_1, \theta, \varphi)G^2m_1^2m_2^2\Bigg[&\frac{1}{2(m_1 + m_2)^2}\\
\times\frac{[m_2v_2^2 - m_1v_1^2 + v_1v_2(m_1 - m_2)\cos\theta]^2}{(v_1^2 + v_2^2 - 2v_1v_2\cos\theta)^{3/2}} &+ \tfrac{1}{4}v_1^2v_2^2\frac{\sin^2\theta}{(v_1^2 + v_2^2 - 2v_1v_2\cos\theta)^{3/2}}\\
\times\left\{\log\left(1 + \frac{D_0^2(v_1^2 + v_2^2 - 2v_1v_2\cos\theta)^2}{G^2(m_1 + m_2)^2}\right) - 1\right\}\Bigg]\,&dv_1d\theta d\varphi dt\,.
\end{aligned}\right\} \tag{38}$$

7. *The integration over the angles θ and φ for a spherical distribution of the velocities of the field stars.*—To effect the integration of equation (38) over the angles θ and φ we need to know the explicit form of the function $N(v_1, \theta, \varphi)$. For a spherical distribution of the velocities we can write (cf. eq. [17])

$$N(v_1, \theta, \varphi)dv_1 d\theta d\varphi = 4\pi N f(v_1) v_1^2 dv_1 \frac{1}{4\pi} \sin\theta d\theta d\varphi . \tag{39}$$

For a Schwarzschild ellipsoidal distribution of the velocities the form of the function $N(v_1, \theta, \varphi)$ is somewhat more complicated and will depend on the directions of the principal axes of the velocity ellipsoid. It would be entirely feasible to write down the form of $N(v_1, \theta, \varphi)$ under these more general circumstances and thus take into account the phenomenon of star streaming in our analysis of stellar encounters. We shall not, however, do this but shall restrict ourselves in this paper to the simpler case of a spherical distribution of velocities. We can then write

$$N(v_1, \theta, \varphi) = \frac{1}{4\pi} N(v_1) \sin\theta , \tag{40}$$

where we have used $N(v_1)$ to denote

$$N(v_1) = 4\pi N f(v_1) v_1^2 . \tag{41}$$

With the foregoing form for $N(v_1, \theta, \varphi)$ the integration of (38) over φ is immediate. We find

$$\left.\begin{aligned} \Sigma\Delta E^2_{(v_1,\theta)} = 8\pi N(v_1) G^2 m_1^2 m_2^2 \Bigg[& \frac{1}{4(m_1+m_2)^2} \\ \times & \frac{[m_2 v_2^2 - m_1 v_1^2 + v_1 v_2 (m_1 - m_2)\cos\theta]^2 \sin\theta}{(v_1^2 + v_2^2 - 2v_1 v_2 \cos\theta)^{3/2}} + \tfrac{1}{8} v_1^2 v_2^2 \frac{\sin^3\theta}{(v_1^2 + v_2^2 - 2v_1 v_2 \cos\theta)^{3/2}} \\ & \times \left\{ \log\left(1 + \frac{D_0^2 (v_1^2 + v_2^2 - 2v_1 v_2 \cos\theta)^2}{G^2 (m_1+m_2)^2}\right) - 1 \right\} \Bigg] dv_1 d\theta dt . \end{aligned}\right\} \tag{42}$$

The integration over θ can now be effected. We have

$$\Sigma\Delta E^2_{v_1} = 8\pi N(v_1) G^2 m_1^2 m_2^2 (J_1 - J_2 + J_3) dv_1 dt , \tag{43}$$

where

$$\left.\begin{aligned} J_1 &= \frac{1}{4(m_1+m_2)^2} \int_0^\pi \frac{[m_2 v_2^2 - m_1 v_1^2 + v_1 v_2 (m_1 - m_2)\cos\theta]^2}{(v_1^2 + v_2^2 - 2v_1 v_2 \cos\theta)^{3/2}} \sin\theta d\theta , \\ J_2 &= \tfrac{1}{8} v_1^2 v_2^2 \int_0^\pi \frac{\sin^3\theta d\theta}{(v_1^2 + v_2^2 - 2v_1 v_2 \cos\theta)^{3/2}} , \\ J_3 &= \tfrac{1}{8} v_1^2 v_2^2 \int_0^\pi \frac{\sin^3\theta}{(v_1^2 + v_2^2 - 2v_1 v_2 \cos\theta)^{3/2}} \log\left(1 + \frac{D_0^2 (v_1^2 + v_2^2 - 2v_1 v_2 \cos\theta)^2}{G^2 (m_1+m_2)^2}\right) d\theta . \end{aligned}\right\} \tag{44}$$

The evaluation of the integrals J_1 and J_2 is elementary but somewhat tedious. We find that

$$\left.\begin{aligned} J_1 &= \frac{1}{6(m_1+m_2)^2 v_2}\left[3m_2^2 v_2^2 - (2m_2^2 + 2m_1 m_2 - m_1^2)v_1^2\right] \qquad (v_2 \geqslant v_1)\,, \\ &= \frac{1}{6(m_1+m_2)^2 v_1}\left[3m_1^2 v_1^2 - (2m_1^2 + 2m_1 m_2 - m_2^2)v_2^2\right] \qquad (v_2 \leqslant v_1)\,, \end{aligned}\right\} \tag{45}$$

and

$$\left.\begin{aligned} J_2 &= \frac{1}{6}\frac{v_1^2}{v_2} \qquad (v_2 \geqslant v_1)\,, \\ &= \frac{1}{6}\frac{v_2^2}{v_1} \qquad (v_2 \leqslant v_1)\,. \end{aligned}\right\} \tag{46}$$

The evaluation of the integral J_3 is somewhat more difficult. Since integrals of this form are found to be of frequent occurrence in problems of stellar encounters, we shall briefly outline the method of evaluating such integrals. Introducing the new variable y defined by

$$y^2 = v_1^2 + v_2^2 - 2v_1 v_2 \cos\theta\,, \tag{47}$$

we find that J_3 reduces to

$$J_3 = \frac{1}{32 v_1 v_2}\int_{\sqrt{b}}^{\sqrt{a}} \frac{(a-y^2)(y^2-b)}{y^2}\log(1+q^2y^4)dy\,, \tag{48}$$

where

$$q = \frac{D_0}{G(m_1+m_2)}\,, \tag{49}$$

and

$$a = (v_2+v_1)^2\,; \qquad b = (v_2-v_1)^2\,. \tag{50}$$

We verify that equation (48) is equivalent to

$$J_3 = \frac{1}{32 v_1 v_2}\int_{\sqrt{b}}^{\sqrt{a}} \frac{d}{dy}\left[\frac{ab}{y} + (a+b)y - \tfrac{1}{3}y^3\right]\log(1+q^2y^4)dy \tag{51}$$

or, after an integration by parts, to

$$\left.\begin{aligned} J_3 = \frac{1}{32 v_1 v_2}&\left[\frac{ab}{y} + (a+b)y - \tfrac{1}{3}y^3\right]\log(1+q^2y^4)\Big|_{\sqrt{b}}^{\sqrt{a}} \\ &- \frac{q^2}{8 v_1 v_2}\int_{\sqrt{b}}^{\sqrt{a}}\left[aby^2 + (a+b)y^4 - \tfrac{1}{3}y^6\right]\frac{1}{1+q^2y^4}\,dy\,. \end{aligned}\right\} \tag{52}$$

After some further reductions we have

$$\left.\begin{aligned} J_3 = {} & \frac{1}{16 v_1 v_2}\left[a^{1/2}(b+\tfrac{1}{3}a)\log(1+q^2a^2) - b^{1/2}(a+\tfrac{1}{3}b)\log(1+q^2b^2)\right] \\ & + \frac{1}{8 v_1 v_2}\left[\tfrac{8}{9}(b^{3/2}-a^{3/2}) + a^{1/2}b^{1/2}(a^{1/2}-b^{1/2})\right] \\ & - \frac{1}{8 v_1 v_2}\int_{\sqrt{b}}^{\sqrt{a}} \frac{(abq^2+\tfrac{1}{3})y^2 - (a+b)}{1+q^2y^4}\,dy\,. \end{aligned}\right\} \tag{53}$$

On the other hand, we have the elementary integrals

$$\left.\begin{aligned} \int \frac{y^2 dy}{1+q^2y^4} &= \frac{1}{4\sqrt{2}\,q^{3/2}}\left[\log\frac{qy^2-\sqrt{2q}\,y+1}{qy^2+\sqrt{2q}\,y+1} + 2\tan^{-1}\frac{\sqrt{2q}\,y}{1-qy^2}\right], \\ \int \frac{dy}{1+q^2y^4} &= \frac{1}{4\sqrt{2}\,q^{1/2}}\left[\log\frac{qy^2+\sqrt{2q}\,y+1}{qy^2-\sqrt{2q}\,y+1} + 2\tan^{-1}\frac{\sqrt{2q}\,y}{1-qy^2}\right]. \end{aligned}\right\} \tag{54}$$

Hence, our expression for J_3 becomes

$$\left.\begin{aligned} J_3 = {} & \frac{1}{16 v_1 v_2}\left[a^{1/2}(b+\tfrac{1}{3}a)\log(1+q^2a^2) - b^{1/2}(a+\tfrac{1}{3}b)\log(1+q^2b^2)\right] \\ & + \frac{1}{8 v_1 v_2}\left[\tfrac{8}{9}(b^{3/2}-a^{3/2}) + a^{1/2}b^{1/2}(a^{1/2}-b^{1/2})\right] - \frac{1}{32\sqrt{2}\,q^{3/2}v_1v_2} \\ & \times\left[\{(aq+1)(bq+1) - \tfrac{2}{3}\}\log\frac{(qa-\sqrt{2qa}+1)(qb+\sqrt{2qb}+1)}{(qa+\sqrt{2qa}+1)(qb-\sqrt{2qb}+1)}\right. \\ & \left. + 2\{(aq-1)(bq-1) - \tfrac{2}{3}\}\left\{\tan^{-1}\frac{\sqrt{2qa}}{1-qa} - \tan^{-1}\frac{\sqrt{2qb}}{1-qb}\right\}\right]. \end{aligned}\right\} \tag{55}$$

The foregoing expression for J_3 is much too complicated to be of any practical value. However, a circumstance which we have so far ignored introduces an essential simplification: Now q is of the dimensions (velocity)$^{-2}$, and we find that

$$q = \frac{D_0}{G(m_1+m_2)} = 2.33\times 10^4\,\frac{(D_0/\text{parsec})}{[(m_1+m_2)/\odot]}\,\frac{1}{[10\ \text{km/sec}]^2}\,. \tag{56}$$

Consequently, qa and qb are both generally of the order $10^4 - 10^5$. An exception, however, arises when $v_2 = v_1$, in which case $b = 0$ and $qb \equiv 0$. On the other hand, for qb to become of the order unity, v_1 and v_2 must differ from each other by an extremely small amount. Thus, according to (56),

$$qb \simeq 1 \qquad \text{when} \qquad v_2 - v_1 \simeq 0.1\ \text{km/sec}\,. \tag{57}$$

In other words, at $v_2 = v_1$ we have a phenomenon analogous to a *sharp resonance*. But as v_2 begins to differ appreciably from v_1, qb rapidly increases and becomes of the order

of 100 or more already when $v_2 - v_1 \sim 1$ km/sec. Thus, in general, we can expand the quantities in the last of the three square brackets in (55) in powers of $(\sqrt{qa})^{-1}$ or $(\sqrt{qb})^{-1}$ and neglect all terms of order higher than the first. We then find that

$$-\frac{1}{32\sqrt{2}\,q^{3/2}v_1v_2}\left[\quad\right] = -\frac{1}{8v_1v_2}\,a^{1/2}b^{1/2}(a^{1/2}-b^{1/2})\,, \tag{58}$$

and this cancels the term $a^{1/2}b^{1/2}(a^{1/2}-b^{1/2})$ in the second square bracket in (55). When, however, $v_2 = v_1$ and $qb = 0$, the last square bracket in (55) becomes

$$-\frac{1}{32\sqrt{2}\,q^{3/2}v_1v_2}\left[(aq+\tfrac{1}{3})\log\frac{qa-\sqrt{2qa}+1}{qa+\sqrt{2qa}+1} - 2(aq-\tfrac{1}{3})\tan^{-1}\frac{\sqrt{2qa}}{1-qa}\right], \tag{59}$$

and this vanishes to the first order. But when $b = 0$, the term $a^{1/2}b^{1/2}(a^{1/2}-b^{1/2})$ also vanishes. Hence, to a sufficient degree of accuracy we can write quite generally that

$$\left.\begin{aligned} J_3 = \frac{1}{16v_1v_2}\,[a^{1/2}(b+\tfrac{1}{3}a)\log(1+q^2a^2) - b^{1/2}(a+\tfrac{1}{3}b)\log(1+q^2b^2)] \\ + \frac{1}{9v_1v_2}\,(b^{3/2}-a^{3/2})\,. \end{aligned}\right\} \tag{60}$$

We can simplify the foregoing expression still further. Since qa and qb are both generally very large compared to unity, we can write

$$\left.\begin{aligned} \log(1+q^2a^2) &\simeq 2\log qa\,, \\ \log(1+q^2b^2) &\simeq 2\log qb\,. \end{aligned}\right\} \tag{61}$$

But the term $\log qb$ diverges logarithmically to $-\infty$ as $v_2 \to v_1$. However, in view of (57) we need not distinguish between $b^{1/2}\log(1+q^2b^2)$ and $b^{1/2}\log q^2b^2$, particularly as both these expressions predict the correct limiting values. The errors introduced by this procedure are entirely negligible under all circumstances which are likely to be of any interest. We thus have

$$J_3 = \frac{1}{8v_1v_2}\,[a^{1/2}(b+\tfrac{1}{3}a)\log qa - b^{1/2}(a+\tfrac{1}{3}b)\log qb] + \frac{1}{9v_1v_2}\,(b^{3/2}-a^{3/2})\,. \tag{62}$$

Substituting now for a and b according to (49), we obtain

$$\left.\begin{aligned} J_3 = \frac{1}{6v_1v_2}\,[(v_2^3+v_1^3)\log q(v_1+v_2)^2 - (v_2^3-v_1^3)\log q(v_2-v_1)^2] \\ + \frac{1}{9v_1v_2}\,[(v_2-v_1)^3 - (v_2+v_1)^3] \qquad (v_2 \geqslant v_1) \end{aligned}\right\} \tag{63}$$

and

$$J_3 = \frac{1}{6v_1v_2}\left[(v_2^3 + v_1^3)\log q(v_1 + v_2)^2 - (v_1^3 - v_2^3)\log q(v_1 - v_2)^2\right] + \frac{1}{9v_1v_2}\left[(v_1 - v_2)^3 - (v_1 + v_2)^3\right] \qquad (v_2 \leqslant v_1)\ ; \tag{64}$$

or after some further rearrangements of the terms we finally have

$$J_3 = \frac{v_1^2}{3v_2}\log q(v_2^2 - v_1^2) + \frac{v_2^2}{3v_1}\log\frac{v_2 + v_1}{v_2 - v_1} - \tfrac{2}{3}v_2 - \frac{2v_1^2}{9v_2} \qquad (v_2 \geqslant v_1) \tag{65}$$

and

$$J_3 = \frac{v_2^2}{3v_1}\log q(v_1^2 - v_2^2) + \frac{v_1^2}{3v_2}\log\frac{v_1 + v_2}{v_1 - v_2} - \tfrac{2}{3}v_1 - \frac{2v_2^2}{9v_1} \qquad (v_2 \leqslant v_1)\ . \tag{66}$$

Again, combining equations (46), (65), and (66), we have

$$\text{or} \quad \begin{aligned} J_3 - J_2 &= \frac{v_1^2}{3v_2}\log q(v_2^2 - v_1^2) + \frac{v_2^2}{3v_1}\log\frac{v_2 + v_1}{v_2 - v_1} - \tfrac{2}{3}v_2 - \frac{7v_1^2}{18v_2}\ , \\ J_3 - J_2 &= \frac{v_2^2}{3v_1}\log q(v_1^2 - v_2^2) + \frac{v_1^2}{3v_2}\log\frac{v_1 + v_2}{v_1 - v_2} - \tfrac{2}{3}v_1 - \frac{7v_2^2}{18v_1}\ , \end{aligned} \tag{67}$$

according as $v_2 \geqslant v_1$ or $v_2 \leqslant v_1$. In order to write our final expression for $\Sigma\Delta E_{v_1}^2$ in the most convenient form, we shall introduce two further quantities. Let

$$\alpha = \frac{v_1}{v_2}\ ; \qquad \mu = \frac{m_1}{m_2}\ . \tag{68}$$

Equation (45) for J_1 can now be written in the form

$$\begin{aligned} J_1 &= (C_1 - C_2\alpha^2)v_2 \qquad (\alpha \leqslant 1)\ , \\ &= (C_1'\alpha - C_2'\alpha^{-1})v_2 \qquad (\alpha \geqslant 1)\ , \end{aligned} \tag{69}$$

where

$$\begin{aligned} C_1 &= \frac{1}{2(1+\mu)^2}\ ; \qquad C_2 = \frac{2 + 2\mu - \mu^2}{6(1+\mu)^2}\ , \\ C_1' &= \frac{\mu^2}{2(1+\mu)^2}\ ; \qquad C_2' = \frac{2\mu^2 + 2\mu - 1}{6(1+\mu)^2}\ . \end{aligned} \tag{70}$$

Again, equation (67) for $J_3 - J_2$ becomes

$$\begin{aligned} J_3 - J_2 &= \left\{\tfrac{1}{3}\alpha^2\log\frac{\mu}{1+\mu}\,q_1v_2^2 + Q(\alpha)\right\}v_2 \qquad (\alpha \leqslant 1)\ , \\ &= \left\{\frac{1}{3\alpha}\log\frac{\mu}{1+\mu}\,q_1v_2^2 + Q(\alpha)\right\}v_2 \qquad (\alpha \geqslant 1)\ , \end{aligned} \tag{71}$$

where

$$q_1 = \frac{D_0}{Gm_1}\,; \qquad q = q_1\,\frac{\mu}{1+\mu}\,, \tag{72}$$

and

$$\left.\begin{aligned} Q(a) &= \tfrac{1}{3}a^2 \log (1-a^2) + \frac{1}{3a}\log\frac{1+a}{1-a} - \tfrac{7}{18}a^2 - \tfrac{2}{3} && (a \leqslant 1)\,, \\ &= \frac{1}{3a}\log (a^2-1) + \tfrac{1}{3}a^2 \log\frac{a+1}{a-1} - \frac{7}{18a} - \tfrac{2}{3}a && (a \geqslant 1)\,. \end{aligned}\right\} \tag{73}$$

Hence, according to equations (43), (69), and (71), we finally have

$$\Sigma\Delta E_{v_1}^2 = 8\pi N(v_1)G^2m_1^2m_2^2v_2\,dv_1\,dt \times \left\{\begin{aligned} &[\tfrac{1}{3}a^2 \log q_1v_2^2 + S(a,\mu)] && (a \leqslant 1)\,, \\ &\left[\frac{1}{3a}\log q_1v_2^2 + S(a,\mu)\right] && (a \geqslant 1)\,, \end{aligned}\right\} \tag{74}$$

where

$$S(a,\mu) = Q(a) + \left\{\begin{aligned} &C_1 - \left[C_2 + \tfrac{1}{3}\log\left(1+\frac{1}{\mu}\right)\right]a^2 && (a \leqslant 1)\,, \\ &C_1'a - \left[C_2' + \tfrac{1}{3}\log\left(1+\frac{1}{\mu}\right)\right]a^{-1} && (a \geqslant 1)\,. \end{aligned}\right\} \tag{75}$$

We may note that when $a = 1$ we have

$$S(1,\mu) = \frac{1}{6}\left(\frac{1-\mu}{1+\mu}\right)^2 + \tfrac{1}{3}\log\frac{4\mu}{1+\mu} - \frac{19}{18}\,. \tag{76}$$

Also, at $a = 0$ we have

$$S(0,\mu) = C_1 = \frac{1}{2(1+\mu)^2}\,. \tag{77}$$

The function $S(a, \mu)$ for different values of a and μ are tabulated in Table 1. It is seen that this function has a sharp minimum at $a = 1$.[7]

8. *The integration over the velocities* v_1.—In § 7 we have evaluated the contribution to $\Sigma\Delta E^2$ by all encounters in which the field stars have some prescribed value of v_1. However, in carrying out the integrations over θ and φ it was further assumed that the distribution of the velocities of the field stars is a spherical one. In order now to average over the velocities of the field stars we need to know the form of the function $N(v_1)$. Here we meet certain difficulties of principle. Strictly speaking, the problem of the time of relaxation of a stellar system is also the problem of determining the rate of approach of the system toward some kind of "thermal" equilibrium. Consequently, there exist no a priori considerations (apart from the present ones) which would suggest a particular form for $N(v_1)$. Indeed, we should rather expect that a correct statistical theory of stellar encounters would itself lead to a definite form for $N(v_1)$. There is, however, no formal difficulty in our present connection, since for any prescribed form for $N(v_1)$ the necessary integration of equation (74) can be carried out by using the table of the func-

[7] Actually the function has a discontinuous derivative at this point.

tion $S(a, \mu)$. In a general way we are now primarily interested to find the effect of a distribution of velocities v_1 on $\Sigma\Delta E_{v_1}^2$ and to remove the arbitrariness of using a particular value of v_1. For this purpose a Gaussian distribution of the velocities of the field stars is likely to be adequate. We shall therefore assume that (cf. eq. [18])

$$N(v_1)dv_1 = \frac{4h^3}{\sqrt{\pi}} Ne^{-h^2v_1^2}v_1^2dv_1 , \qquad (78)$$

TABLE 1

$S(a, \mu)$

a	μ							
	0.125	0.25	0.5	1	2	4	8	∞
0.0	+0.3951	+0.320	+0.2222	+0.125	+0.0556	+0.020	+0.0062	0.0
0.1	+0.3831	+0.3103	+0.2148	+0.1198	+0.0521	+0.0180	+0.0050	0.0
0.125	+0.3764	+0.3049	+0.2107	+0.1168	+0.0502	+0.0168	+0.0044	−0.0001
0.15	+0.3681	+0.2982	+0.2055	+0.1131	+0.0478	+0.0154	+0.0036	−0.0001
0.20	+0.3470	+0.2811	+0.1924	+0.1038	+0.0417	+0.0116	+0.0014	−0.0003
0.25	+0.3197	+0.2590	+0.1754	+0.0915	+0.0336	+0.0066	−0.0016	−0.0008
0.30	+0.2860	+0.2316	+0.1543	+0.0763	+0.0234	+0.0002	−0.0055	−0.0017
0.35	+0.2457	+0.1989	+0.1289	+0.0578	+0.0109	−0.0078	−0.0106	−0.0031
0.40	+0.1987	+0.1605	+0.0989	+0.0359	−0.0041	−0.0176	−0.0171	−0.0054
0.45	+0.1446	+0.1161	+0.0642	+0.0103	−0.0219	−0.0296	−0.0252	−0.0089
0.50	+0.0829	+0.0654	+0.0243	−0.0195	−0.0429	−0.0441	−0.0354	−0.0138
0.55	+0.0134	+0.0080	−0.0213	−0.0538	−0.0676	−0.0615	−0.0482	−0.0207
0.60	−0.0646	−0.0568	−0.0730	−0.0932	−0.0965	−0.0824	−0.0639	−0.0301
0.65	−0.1518	−0.1296	−0.1317	−0.1386	−0.1303	−0.1076	−0.0835	−0.0427
0.70	−0.2492	−0.2115	−0.1982	−0.1907	−0.1700	−0.1380	−0.1079	−0.0595
0.75	−0.3580	−0.3036	−0.2739	−0.2508	−0.2169	−0.1749	−0.1382	−0.0818
0.80	−0.4800	−0.4077	−0.3605	−0.3209	−0.2726	−0.2200	−0.1764	−0.1113
0.85	−0.6178	−0.5266	−0.4607	−0.4034	−0.3400	−0.2760	−0.2250	−0.1507
0.90	−0.7761	−0.6647	−0.5789	−0.5029	−0.4235	−0.3474	−0.2885	−0.2045
0.95	−0.9640	−0.8313	−0.7246	−0.6288	−0.5323	−0.4435	−0.3763	−0.2821
0.975	−1.0767	−0.9329	−0.8153	−0.7093	−0.6039	−0.5085	−0.4370	−0.3373
1.00	−1.2251	−1.0699	−0.9412	−0.8245	−0.7101	−0.6078	−0.5319	−0.4268
1.05	−1.0297	−0.8806	−0.7545	−0.6366	−0.5182	−0.4112	−0.3316	−0.2212
1.10	−0.9048	−0.7612	−0.6373	−0.5180	−0.3954	−0.2838	−0.2005	−0.0849
1.15	−0.8066	−0.6678	−0.5458	−0.4249	−0.2982	−0.1819	−0.0948	+0.0261
1.20	−0.7252	−0.5909	−0.4705	−0.3478	−0.2169	−0.0958	−0.0050	+0.1211
1.25	−0.6560	−0.5257	−0.4066	−0.2821	−0.1468	−0.0210	+0.0735	+0.2048
1.30	−0.5961	−0.4694	−0.3515	−0.2249	−0.0853	+0.0453	+0.1435	+0.2801
1.40	−0.4971	−0.3768	−0.2605	−0.1295	+0.0189	+0.1589	+0.2647	+0.4117
1.50	−0.4185	−0.3036	−0.1881	−0.0525	+0.1048	+0.2545	+0.3677	+0.5252
1.60	−0.3545	−0.2441	−0.1289	+0.0117	+0.1780	+0.3372	+0.4579	+0.6259
1.70	−0.3015	−0.1949	−0.0796	+0.0662	+0.2416	+0.4105	+0.5386	+0.7171
1.80	−0.2569	−0.1535	−0.0377	+0.1135	+0.2980	+0.4765	+0.6121	+0.8011
1.90	−0.2190	−0.1184	−0.0017	+0.1551	+0.3488	+0.5370	+0.6800	+0.8795
2.00	−0.1864	−0.0881	+0.0296	+0.1921	+0.3952	+0.5930	+0.7435	+0.9535
2.25	−0.1223	−0.0284	+0.0930	+0.2703	+0.4967	+0.7186	+0.8879	+1.1241
2.50	−0.0756	+0.0155	+0.1417	+0.3342	+0.5841	+0.8303	+1.0183	+1.2807
2.75	−0.0404	+0.0490	+0.1807	+0.3888	+0.6624	+0.9329	+1.1397	+1.4283
3.00	−0.0132	+0.0754	+0.2131	+0.4372	+0.7346	+1.0294	+1.2549	+1.5698
4.00	+0.0514	+0.1421	+0.3076	+0.5972	+0.9904	+1.3826	+1.6831	+2.1029
5.00	+0.0829	+0.1803	+0.3768	+0.7334	+1.2230	+1.7128	+2.0882	+2.6130
6.00	+0.1011	+0.2076	+0.4365	+0.8610	+1.4472	+2.0346	+2.4852	+3.1148
8.00	+0.1217	+0.2500	+0.5461	+1.1076	+1.8875	+2.6703	+3.2709	+4.1104
10.00	+0.1346	+0.2870	+0.6519	+1.3510	+2.3250	+3.3032	+4.0539	+5.1033

where N is the number of stars per unit volume. In terms of α we have

$$N(v_1)dv_1 = \frac{4x_0^3}{\sqrt{\pi}} Ne^{-(x_0\alpha)^2}\alpha^2 d\alpha \,, \tag{79}$$

where we have used x_0

$$x_0 = hv_2 \,. \tag{80}$$

Thus, x_0 is a measure of the velocity of the incident star in units of the mean velocity of the field stars.

According to equations (74) and (79), we now have

$$\Sigma\Delta E^2 = 8\pi NG^2m_1^2m_2^2v_2\left[G(x_0)\log\frac{q_1}{h^2}x_0^2 + g(x_0,\mu)\right]dt \,, \tag{81}$$

where

$$G(x_0) = \frac{4x_0^3}{3\sqrt{\pi}}\left[\int_0^1 \alpha^4 e^{-(x_0\alpha)^2}d\alpha + \int_1^\infty \alpha e^{-(x_0\alpha)^2}d\alpha\right] \tag{82}$$

and

$$g(x_0,\mu) = \frac{4x_0^3}{\sqrt{\pi}}\int_0^\infty S(\alpha,\mu)\alpha^2 e^{-(x_0\alpha)^2}d\alpha \,. \tag{83}$$

An explicit form for $G(x_0)$ is readily found. We have

$$G(x_0) = \frac{1}{2x_0^2}[\Phi(x_0) - x_0\Phi'(x_0)] \,, \tag{84}$$

where we have used $\Phi(x_0)$ to denote the error function

$$\Phi(x_0) = \frac{2}{\sqrt{\pi}}\int_0^{x_0} e^{-y^2}dy \,; \qquad \Phi'(x_0) = \frac{2}{\sqrt{\pi}}e^{-x_0^2} \,. \tag{85}$$

Again, according to equations (75) and (83), we can write

$$g(x_0,\mu) = R_1(x_0) + R_2(x_0,\mu) \,, \tag{86}$$

where

$$R_1(x_0) = \frac{4x_0^3}{\sqrt{\pi}}\int_0^\infty Q(\alpha)\alpha^2 e^{-(x_0\alpha)^2}d\alpha \tag{87}$$

and

$$\left.\begin{aligned} R_2(x_0,\mu) = \frac{4x_0^3}{\sqrt{\pi}}\Bigg[\int_0^1 \left\{C_1 - \left(C_2 - \tfrac{1}{3}\log\frac{\mu}{1+\mu}\right)\alpha^2\right\}\alpha^2 e^{-(x_0\alpha)^2}d\alpha \\ + \int_1^\infty \left\{C_1'\alpha - \left(C_2' - \tfrac{1}{3}\log\frac{\mu}{1+\mu}\right)\alpha^{-1}\right\}\alpha^2 e^{-(x_0\alpha)^2}d\alpha\Bigg] \,. \end{aligned}\right\} \tag{88}$$

It is seen that $R_2(x_0, \mu)$ can be expressed in terms of the error function. We find

$$\left.\begin{aligned} R_2(x_0, \mu) = \left[C_1 - \frac{1}{2x_0^2}\left\{3C_2 - \log\frac{\mu}{1+\mu}\right\}\right]\Phi(x_0) \\ + \frac{1}{x_0}\left[C_1' + \frac{1}{2}\left\{3C_2 - \log\frac{\mu}{1+\mu}\right\}\right]\Phi'(x_0)\,. \end{aligned}\right\} \quad (89)$$

However, $R_1(x_0)$ cannot be so easily expressed in terms of elementary or known functions. But the integral defining $R_1(x_0)$ has been evaluated by numerical methods for some values of x_0. Finally, the functions $G(x_0)$, $R_1(x_0)$, $R_2(x_0, \mu)$, and $g(x_0, \mu)$ are tabulated in Tables 2, 3, and 4.

9. *The time of relaxation* T_E *of a stellar system.*—According to our definition of the time of relaxation T_E, we have

$$\int_0^{T_E} \Sigma \Delta E^2 = \tfrac{1}{4} m_2^2 v_2^4\,. \quad (90)$$

Strictly speaking, the velocity of the incident star changes with the passage of time, and equation (81) provides us only the *instantaneous* rate of increase of $\Sigma\Delta E^2$. In other words, equation (81) will enable us to follow the star *statistically* during its motion. However, in a first approximation we can write as our definition of T_E the equation

$$\tfrac{1}{4} m_2^2 v_2^4 = 8\pi N G^2 m_1^2 m_2^2 v_2 [G(x_0) \log q_1 v_2^2 + g(x_0, \mu)] T_E\,. \quad (91)$$

Hence,

$$T_E = \frac{v_2^3}{32\pi N G^2 m_1^2\left[G(x_0)\log\dfrac{D_0 v_2^2}{G m_1} + g(x_0, \mu)\right]}\,. \quad (92)$$

A limiting case of our formula for T_E may be noted. We readily verify that, as $x_0 \to \infty$, we have (cf. eqs. [84], [87], and [89])

$$G(x_0) \to 0\,; \qquad R_1(x_0) \to 0\,; \qquad R_2(x_0, \mu) \to C_1 = \tfrac{1}{2}(1+\mu)^{-2}\,. \quad (93)$$

Hence, for this limiting case equation (92) becomes

$$T_E = \frac{(1+\mu)^2 v_2^3}{16\pi N G^2 m_1^2} \qquad (x_0 \to \infty)\,, \quad (94)$$

which agrees with a formula originally given by Rosseland.[8] However, as we shall see in § 10, this limiting case ($x_0 \to \infty$) of equation (92) is entirely misleading both as regards the order of magnitude of the time of relaxation predicted and as regards its dependence on μ.

Returning to equation (92), we find that on expressing m_1, D_0, v_2, and N in the units solar mass, parsec, 20 km/sec, and number per cubic parsec, respectively, it becomes

$$T_E = 4.21 \times 10^{12} \frac{v_2^3}{N m_1^2\{G(x_0)\log_e [9.31 \times 10^4 D_0 v_2^2/m_1] + g(x_0, \mu)\}} \text{ years}\,. \quad (95)$$

[8] *Op. cit.*, Eq. (12).

TABLE 2

$G(x_0)$; $R_1(x_0)$

x_0	$G(x_0)$	$R_1(x_0)$	x_0	$G(x_0)$	$R_1(x_0)$	x_0	$G(x_0)$	$R_1(x_0)$
0.0.....	0.0	.....	1.0.....	+0.2138	−0.143	2.0.....	+0.1192	−0.112
.2.....	+ .0734	.....	1.2.....	+ .2047	− .175	3.0.....	+ .0555	− .0388
.4.....	+ .1368	.....	1.4.....	+ .1862	− .178	4.0.....	+ .0313	− .0188
.6.....	+ .1827	+0.016	1.6.....	+ .1634	− .162	5.0.....	+ .0200	− .0113
0.8.....	+0.2079	−0.077	1.8.....	+0.1404	−0.137	∞.....	0.0	0.0

TABLE 3

$R_2(x_0, \mu)$

x_0	μ							
	0.125	0.25	0.5	1	2	4	8	∞
0.0...	.....	.....	.....	.....	.....	.....	.....	.....
0.2...	−0.1048	+0.0042	+0.2251	+0.6270	+1.1790	+1.7315	+2.1551	+2.7471
0.4...	− .2373	− .1417	− .0051	+ .2079	+0.4873	+0.7637	+0.9751	+1.2703
0.6...	− .3159	− .2170	− .1052	+ .0444	+0.2308	+0.4131	+0.5524	+0.7474
0.8...	− .3426	− .2444	− .1492	− .0363	+0.0991	+0.2314	+0.3330	+0.4758
1.0...	− .3230	− .2329	− .1552	− .0711	+0.0286	+0.1276	+0.2047	+0.3145
1.2...	− .2694	− .1933	− .1353	− .0770	−0.0057	+0.0684	+0.1276	+0.2137
1.4...	− .1965	− .1378	− .1004	− .0656	−0.0180	+0.0362	+0.0817	+0.1498
1.6...	− .1173	− .0770	− .0594	− .0457	−0.0181	+0.0201	+0.0547	+0.1090
1.8...	− .0414	− .0184	− .0188	− .0232	−0.0121	+0.0132	+0.0391	+0.0825
2.0...	+ .0260	+ .0338	+ .0179	− .0017	−0.0040	+0.0109	+0.0300	+0.0648
3.0...	+ .2240	+ .1873	+ .1273	+ .0657	+0.0269	+0.0143	+0.0154	+0.0278
4.0...	+ .2988	+ .2453	+ .1688	+ .0916	+0.0394	+0.0168	+0.0114	+0.0156
5.0...	+ .3335	+ .2722	+ .1880	+ .1037	+0.0452	+0.0179	+0.0095	+0.0100
∞....	+0.3951	+0.3200	+0.2222	+0.1250	+0.0556	+0.0200	+0.0062	0.0

TABLE 4

$g(x_0, \mu)$

x_0	μ							
	0.125	0.25	0.5	1	2	4	8	∞
0.6.....	−0.299	−0.201	−0.089	+0.061	+0.247	+0.430	+0.569	+0.764
0.8.....	− .419	− .321	− .226	− .113	+ .022	+ .155	+ .256	+ .399
1.0.....	− .466	− .376	− .299	− .214	− .115	− .016	+ .061	+ .171
1.2.....	− .445	− .368	− .310	− .252	− .181	− .107	− .048	+ .0386
1.4.....	− .374	− .316	− .278	− .243	− .196	− .142	− .096	− .0279
1.6.....	− .279	− .239	− .221	− .207	− .180	− .142	− .107	− .0527
1.8.....	− .178	− .155	− .156	− .160	− .149	− .124	− .098	− .0543
2.0.....	− .086	− .078	− .094	− .114	− .116	− .101	− .0819	− .0471
3.0.....	+ .185	+ .149	+ .089	+ .027	− .0119	− .0245	− .0234	− .0110
4.0.....	+ .280	+ .227	+ .150	+ .073	+ .0206	− .0020	− .0074	− .0032
5.0.....	+ .322	+ .261	+ .177	+ .092	+ .0339	+ .0066	− .0018	− .0013
∞.....	+0.395	+0.320	+0.222	+0.125	+0.0556	+0.0200	+0.0062	0.0

In this equation D_0 and N are not independent, since, according to our fundamental assumption (eq. [25]), D_0 is to be taken as the average distance between the stars. Consequently, D_0 is determined in terms of N by the relation

$$D_0 \simeq \left(\frac{6}{\pi N}\right)^{1/3} . \tag{96}$$

Equation (95) and the Tables 2 and 4 of the functions $G(x_0)$ and $g(x_0, \mu)$ will enable us to determine T_E in terms of the physical data giving N and m_1 and certain assumed values for x_0 and μ.[9]

10. *Numerical applications.*—We shall first apply our formula for the time of relaxation to the galactic system. For this purpose we shall adopt the following numerical values:

$$N = 0.1 \text{ parsec}^{-3} ; \quad D_0 = 2.7 \text{ parsecs} ; \quad m_1 = 0.5\ \odot ; \quad v_2 = 20 \text{ km/sec} . \tag{97}$$

These values have been chosen to resemble the conditions in the Galaxy in the general neighborhood of the sun, though no special emphasis is laid on the particular values

TABLE 5

THE TIME OF RELAXATION OF THE GALAXY

$N = 0.1/\text{parsec}^3$; $D_0 = 2.7$ parsecs; $m_1 = 0.5$; $v_2 = 20$ km/sec

Unit of Time, 10^{13} Years

x_0	μ							
	0.125	0.25	0.5	1	2	4	8	∞
0.6	8.0	7.7	7.3	6.9	6.4	6.0	5.7	5.3
0.8	7.3	7.0	6.7	6.4	6.1	5.8	5.6	5.4
1.0	7.2	6.9	6.7	6.5	6.3	6.0	5.9	5.7
1.2	7.5	7.3	7.1	6.9	6.7	6.5	6.4	6.2
1.4	8.1	7.9	7.8	7.7	7.5	7.3	7.2	7.0
1.6	9.0	8.8	8.8	8.7	8.6	8.4	8.3	8.1
1.8	10	10	10	10	9.9	9.8	9.7	9.4
2.0	11	11	11	12	12	12	11	11
3.0	18	19	21	22	24	24	24	24
4.0	24	26	30	35	39	41	42	41
5.0	29	32	38	48	57	62	65	64
∞	43	53	76	135	300	840	2800	∞

adopted. The resulting values of T_E for various values of x_0 and μ are tabulated in Table 5. The most striking feature of this table is that, for values of x_0 in the range $0.6 \leqslant x_0 \leqslant 2.5$, the dependence of T_E on μ is very slight. However, the dependence of T_E on μ becomes quite pronounced for extreme values of x_0 (cf., e.g., the last two lines of Table 5 with the lines for $x_0 = 1.6$, 1.8, or 2.0). Again, the order of magnitude of T_E computed for values of x_0 in the range $0.6 \leqslant x_0 \leqslant 1.6$ is different from that predicted for values of $x_0 > 5$. Thus, for $\mu = 1$, $T_E \simeq 7 \times 10^{13}$ years for $0.6 \leqslant x_0 \leqslant 1.6$, while for this same value of μ, $T_E = 135 \times 10^{13}$ years for $x_0 \to \infty$; i.e., it increases by a factor of about 20.

[9] Strictly speaking, to determine the time of relaxation of a stellar *system*, we should appropriately average eq. (95) over m_1, v_2, x_0, and μ. But these refinements are postponed to a future occasion.

The slight dependence of T_E on μ for values of x_0 which are not very extreme arises from the fact that the term $G(x_0) \log_e (D_0 v_2^2/Gm_1)$ in equation (92) is generally ten to twenty times larger than the mass dependent terms included in $g(x_0, \mu)$. Indeed, to within an accuracy of 10 per cent we can re-write equation (92) as

$$T_E \simeq \frac{v_2^3}{32\pi N G^2 m_1^2 G(x_0) \log_e \dfrac{Dv_2^2}{G(m_1 + m_2)}} \qquad (0.5 \leqslant x_0 \leqslant 2.5)\,, \quad (98)$$

in which form, it is seen, the dependence on μ is, in fact, very slight.

The main conclusion to which the calculations summarized in Table 5 leads us, is, of course, the well-known one that in considering the dynamics of the Galaxy (and possibly also the extragalactic systems) we can regard each star as an independent conservative dynamical system.

As a further illustration of the use of our formula for the time of relaxation, we shall apply it to conditions which may be expected to prevail in globular clusters: We now assume that

$$N = 75 \text{ parsec}^{-3}; \qquad D = 0.3 \text{ parsec}; \qquad m_1/\odot = 1; \qquad v_2 = 10 \text{ km/sec}\,. \quad (99)$$

The resulting values of T_E for $x_0 = 1$ and $x_0 = \infty$ for different values of μ are given in Table 6. An examination of this table shows in a particularly striking manner the importance of using the correct formula (92) for T_E and moderate values of x_0. For, it is now seen that under the conditions which may be expected in globular clusters the time of relaxation is of the same order of magnitude as the life of the objects themselves. Consequently, the state of motions now obtaining in globular clusters must be the result of numerous stellar encounters. We can therefore expect that equipartition of energy must have approximately set in, particularly in the central dense regions of the system. There appears to be other indirect evidence which lends support to this view. But we shall not go into these matters here.

TABLE 6

THE TIME OF RELAXATION OF A GLOBULAR CLUSTER

$N = 75/\text{parsec}^3$; $D_0 = 0.3$ parsec; $m_1 = 1$; $v_2 = 10$ km/sec

Unit of Time, 10^9 Years

x_0	μ							
	0.125	0.25	0.5	1.0	2.0	4.0	8.0	∞
1.0	4.9	4.6	4.4	4.2	4.0	3.7	3.6	3.4
∞	18	22	32	55	125	350	1140	∞

In conclusion, I wish to record my indebtedness to Mrs. T. Belland, who carried out the entire numerical work connected with the preparation of the Tables 1–6; but for Mrs. Belland's assistance the present paper would not have achieved the degree of completeness which it now has.

YERKES OBSERVATORY
September 17, 1940

THE TIME OF RELAXATION OF STELLAR SYSTEMS. II

RALPH E. WILLIAMSON AND S. CHANDRASEKHAR

ABSTRACT

In this paper the problem of the time of relaxation of a stellar system is considered from the point of view of the deflections suffered by stars during encounters. The method consists in evaluating the sum $\Sigma \sin^2 2\Psi$ (where $\pi - 2\Psi$ is the true deflection experienced by a star in a fixed frame of reference as a result of a single encounter idealized as a two-body problem) for all possible encounters between an incident star having mass m_2 and velocity v_2 during its motion through other field stars, and determining its rate of increase with time. As in the preceding paper, particular attention is given to determining the manner in which the various parameters defining an encounter enter the problem. For a Gaussian distribution of the velocities v_1 of the field stars the dominant term in $\Sigma \sin^2 2\Psi$ can be averaged over all the parameters defining an encounter. We find that

$$\Sigma \sin^2 2\Psi = \frac{8\pi N G^2 m_1^2}{v_2^3} H(x_0) \log \left[\frac{D_0 v_2^2}{G(m_1 + m_2)} \right] dt , \qquad \text{(i)}$$

where G is the constant of gravitation, m_1 the mass of a typical field star, D_0 the average distance between the stars in the system, $x_0 = hv_2$ (h being the modulus of precision occurring in the distribution of velocities v_1), and $H(x_0)$ is a certain function of x_0 which is tabulated. In obtaining equation (i) certain other nondominant terms have been neglected. The expression for the time of relaxation T_D is found to take the form

$$T_D = 1.68 \times 10^{13} \frac{v_2^3}{N m_1^2 H(x_0) \log_e [9.31 \times 10^4 D_0 v_2^2/(m_1 + m_2)]} \text{ years} , \qquad \text{(ii)}$$

where m_1, D_0, v_2, and N are expressed in the units solar mass, parsec, 20 km/sec, and number per cubic parsec, respectively. Comparing T_D with the time of relaxation T_E obtained from a consideration of the energies exchanged during encounters, it is found that T_D/T_E varies from 1.7 to 0.34 as x_0 varies from 0.6 to 2.5.

1. *Introduction.*—As has been explained in the preceding paper,[1] the most straightforward way of formulating the problem of the time of relaxation of a stellar system leads us directly to consider the gradual deviation of the actual orbit described by a star from the "theoretical" orbit derived in terms of the general gravitational potential. Although somewhat less directly, the problem is also connected with the extent of the accuracy to which we can regard each star as an independent conservative dynamical system. The time of relaxation of a stellar system from this latter point of view has already been examined in Part I.

In this present paper we shall re-examine the same problem according to the more direct formulation of the fundamental ideas. Some remarks of a general character reviewing the whole position are also made toward the end of the paper.

2. *The formulation of the problem.*—Let m_2 and v_2 denote the mass and the velocity of a star whose motion among the other "field" stars we are to follow. As in Part I we shall assume that each encounter can be idealized individually as a two-body problem. Consider, then, an encounter with another field star of mass m_1. Let the parameters describing the encounter be v_1, θ, φ, D, and Θ.[2] Then in the orbital plane (see Fig. 3 and also Fig. 1) the orbit of each star with respect to the common center of gravity is a hyper-

[1] Referred to as "I."

[2] See I, p. 287. In this paper we shall use the same notation as in I.

bola. Furthermore, in this plane the direction of the relative velocity is deflected by an amount $\pi - 2\psi$, where

$$\cos \psi = \frac{1}{\sqrt{1 + \frac{D^2 V^4}{G^2(m_1 + m_2)^2}}}. \tag{1}$$

This equation does not, however, define the true deflection of the star with respect to our fixed frame of reference.[3] The actual deflection $\pi - 2\Psi$ of the star can, however, be de-

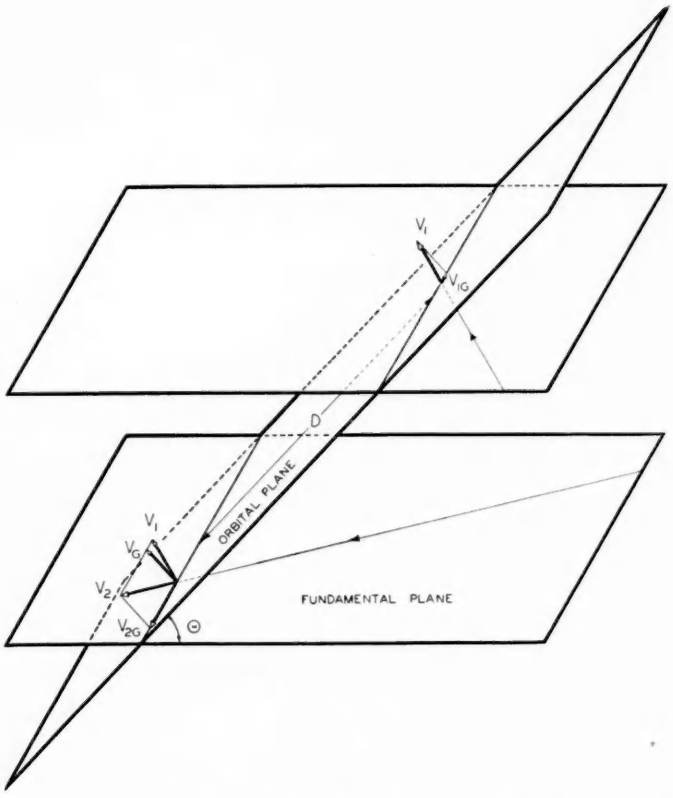

FIG. 1.—Space diagram for stellar encounters. Illustrates how the initial space motions of the two stars define the various parameters specifying the encounter and in particular the inclination Θ of the orbital plane to the fundamental plane.

termined as follows: Let $\boldsymbol{v}_2'$ denote the velocity of the star at the end of the encounter. Then

$$\cos (\pi - 2\Psi) = \frac{\boldsymbol{v}_2 \cdot \boldsymbol{v}_2'}{v_2 v_2'} \tag{2}$$

[3] It is precisely the nonrecognition of this circumstance which vitiates all earlier treatments of this problem by Jeans and others (see n. 6).

(see also Fig. 3, where the situation is made apparent). The explicit formula for the deflection $\pi - 2\Psi$ defined according to equation (2) is obtained in § 3, but meantime we shall outline the general method.

Analogous to the procedure adopted in the problem of energy exchanges during encounters, we shall form the sum

$$\sum \sin^2 2\Psi \tag{3}$$

for all possible encounters and determine its rate of increase with time. When $\Sigma \sin^2 2\Psi$ becomes of the order of unity, we can conclude that the star would most probably have deviated quite considerably from its original direction of motion. More particularly, if T_D is the time required for $\Sigma \sin^2 2\Psi$ to become equal to unity, we may say that by then the star will, on the average, have deviated by an angle $\pi/2$ from its original direction. From our present point of view T_D can therefore be taken to define the time of relaxation.

3. *The true deflection of a star resulting from a stellar encounter.*—In order to determine the true deflection of the star according to equation (2), we first need to specify the vector $\boldsymbol{v}_2'$. To do this, we proceed as follows:

Let $\boldsymbol{v}_{2g}$ and $\boldsymbol{v}_{2g}'$ denote the velocity of the star before and after the encounter in the frame of reference in which the center of gravity of the two stars is at rest. Then

$$\boldsymbol{v}_{2g} = \boldsymbol{v}_2 - \boldsymbol{V}_g\,; \qquad \boldsymbol{v}_{2g}' = \boldsymbol{v}_2' - \boldsymbol{V}_g\,, \tag{4}$$

where, by definition,

$$(m_1 + m_2)\boldsymbol{V}_g = m_1\boldsymbol{v}_1 + m_2\boldsymbol{v}_2 = m_1\boldsymbol{v}_1' + m_2\boldsymbol{v}_2'\,. \tag{5}$$[4]

From equations (4) and (5) we readily obtain

$$\boldsymbol{v}_{2g} = \frac{m_1}{m_1 + m_2}\boldsymbol{V}\,; \qquad \boldsymbol{v}_{2g}' = \frac{m_1}{m_1 + m_2}\boldsymbol{V}'\,; \tag{6}$$

in other words, the vectors $\boldsymbol{v}_{2g}$ and $\boldsymbol{v}_{2g}'$ are numerical multiples of $\boldsymbol{V}$ and $\boldsymbol{V}'$, respectively. Hence, the angle between the vectors $\boldsymbol{v}_{2g}$ and $\boldsymbol{v}_{2g}'$ is the same as that between $\boldsymbol{V}$ and $\boldsymbol{V}'$, i.e., $\pi - 2\psi$ where ψ is given by equation (1).[5] Further, it is also clear that $|\boldsymbol{V}| = |\boldsymbol{V}'|$ and $|\boldsymbol{v}_{2g}| = |\boldsymbol{v}_{2g}'|$.

Now, according to equation (4), we have

$$\boldsymbol{v}_2 \cdot \boldsymbol{v}_2' = \boldsymbol{v}_2 \cdot (\boldsymbol{v}_{2g}' + \boldsymbol{V}_g)\,, \tag{7}$$

[4] Since, according to the elementary theory of the two-body problem, $\boldsymbol{V}_g$ remains constant during the encounter.

[5] When considering the motion of a star relative to the center of gravity, the deflection is generally written as $\pi - 2\psi_g$ where

$$\cos\psi_g = \frac{1}{\sqrt{1 + \dfrac{D_2^2 v_{2g}^4 (m_1 + m_2)^4}{G^2 m_1^6}}}\,. \tag{1'}$$

Here D_2 is the impact parameter defined with respect to the center of gravity. Since, however,

$$D_2 = \frac{m_1}{m_1 + m_2}D \quad \text{and} \quad v_{2g} = \frac{m_1}{m_1 + m_2}V\,,$$

we verify that ψ_g as defined by (1′) is identically the same as ψ defined according to (1).

or

$$v_2 v_2' \cos(\pi - 2\Psi) = \boldsymbol{v}_2 \cdot \boldsymbol{v}_{2g}' + \boldsymbol{v}_2 \cdot \boldsymbol{V}_g . \tag{8}$$

The direction cosines of $\boldsymbol{v}_2$ with respect to $\boldsymbol{V}$, a direction in the orbital plane and at right angles to $\boldsymbol{V}$, and a direction perpendicular to the orbital plane are seen to be (see Fig. 3)

$$\cos(\Phi - \vartheta), \qquad -\sin(\Phi - \vartheta)\cos\Theta, \qquad \sin(\Phi - \vartheta)\sin\Theta, \tag{9}$$

where ϑ is the angle between $\boldsymbol{v}_2$ and $\boldsymbol{V}_g$. Again, since $\boldsymbol{v}_{2g}'$ is in the same direction as $\boldsymbol{V}'$, the direction cosines of $\boldsymbol{v}_{2g}'$ with respect to the same three directions are

$$\cos(\phi' - \phi), \qquad \sin(\phi' - \phi), \qquad 0 . \tag{10}$$

Hence,

$$\boldsymbol{v}_2 \cdot \boldsymbol{v}_{2g}' = v_2 v_{2g}' \{\cos(\phi' - \phi)\cos(\Phi - \vartheta) - \sin(\phi' - \phi)\sin(\Phi - \vartheta)\cos\Theta\} . \tag{11}$$

Combining equations (8) and (11), we now obtain

$$\left.\begin{aligned} &v_2' \cos(\pi - 2\Psi) \\ &\quad = v_{2g}' \{\cos(\phi' - \phi)\cos(\Phi - \vartheta) - \sin(\phi' - \phi)\sin(\Phi - \vartheta)\cos\Theta\} \\ &\qquad\qquad + V_g \cos\vartheta . \end{aligned}\right\} \tag{12}$$

Since

$$\phi' - \phi = \pi - 2\psi , \tag{13}$$

equation (12) can be re-written as

$$\left.\begin{aligned} &\cos 2\Psi \\ &\quad = \frac{1}{v_2'} \{v_{2g}[\cos 2\psi \cos(\Phi - \vartheta) + \sin 2\psi \sin(\Phi - \vartheta)\cos\Theta] - V_g \cos\vartheta\} . \end{aligned}\right\} \tag{14}$$

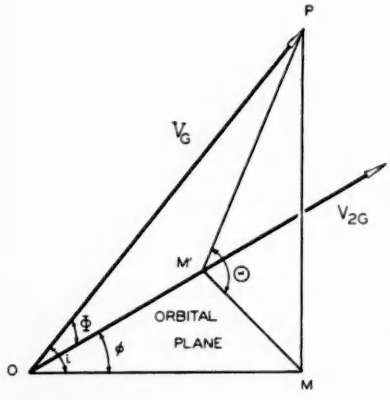

FIG. 2.—Illustrating the relationships between the various angles ϕ, Φ, i, and Θ. OM is the projection of $\boldsymbol{V}_g$ on the orbital plane. The angles $OM'P$, $OM'M$, OMP, and $M'MP$ are all right angles. We thus have the relations $\cos\Phi = \cos i \cos\phi$ and $\sin\Phi\cos\Theta = \cos i \sin\phi$.

We shall now express v_2', v_{2g}, Φ, and ϑ explicitly in terms of the known quantities v_1, v_2, and θ.

Since

$$\boldsymbol{v}_2' = \boldsymbol{v}_{2g}' + \boldsymbol{V}_g , \tag{15}$$

we have, on squaring this equation,

$$v_2'^2 = v_{2g}^2 + 2 v_{2g} V_g \cos\Phi' + V_g^2 . \tag{16}$$

On the other hand (see Fig. 3 and also Fig. 2),

$$\cos\Phi' = \cos\phi' \cos i , \tag{17}$$

or somewhat differently as (cf. eq. [13])

$$\cos\Phi' = \cos(\pi + \phi - 2\psi)\cos i . \tag{18}$$

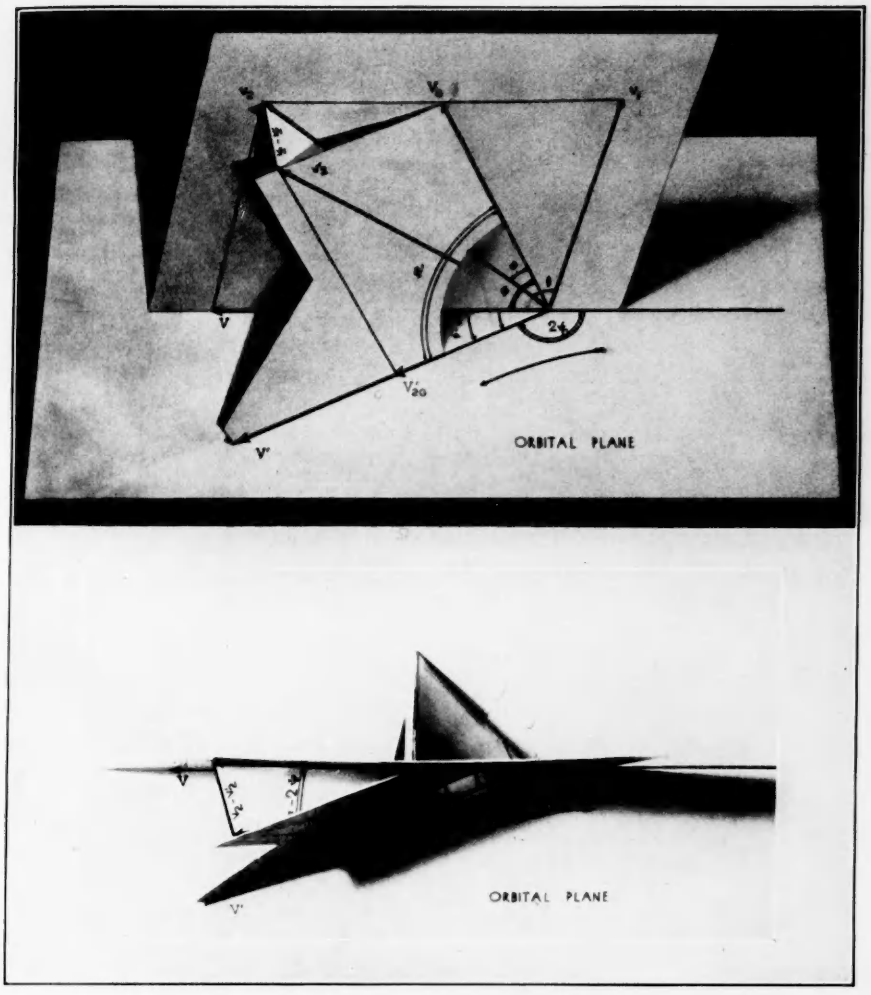

FIG. 3.—Vector model for stellar encounters. The fundamental plane is defined by the vectors v_1 and v_2 representing the velocities of the two stars before the encounter. The velocity of the center of gravity, denoted by V_g, remains constant during the encounter. In a frame of reference in which the center of gravity is at rest, the two stars describe hyperbolae in the orbital plane, which is, in general, inclined at some definite angle to the fundamental plane (see Fig. 1). The vectors V and v_{2g}, representing respectively the initial relative velocity and the initial velocity of one of the stars with respect to the center of gravity, lie in the orbital plane and are in the same direction. As a result of the encounter, these vectors are deflected by the same angle $\pi - 2\psi_g$ and become respectively V' and v'_{2g}. Finally, $v'_2 = v'_{2g} + V_g$ defines the velocity of the star at the end of the encounter. The angle $\pi - 2\Psi$ between the vectors v_2 and v'_2 measures the true deflection suffered by the star as a result of the encounter.

Hence, we can re-write equation (16) in the form

$$v_2'^2 = v_{2g}^2 + V_g^2 - 2v_{2g}V_g(\cos 2\psi \cos\phi \cos i + \sin 2\psi \sin\phi \cos i)\,. \tag{19}$$

Using the relations (see Fig. 2)

$$\sin\phi \cos i = \sin\Phi \cos\Theta\,; \qquad \cos\phi \cos i = \cos\Phi\,, \tag{20}$$

equation (19) reduces to

$$v_2'^2 = v_{2g}^2 + V_g^2 - 2v_{2g}V_g(\cos 2\psi \cos\Phi + \sin 2\psi \sin\Phi \cos\Theta)\,. \tag{21}$$

From equations (5) and (6) we directly obtain

$$\left.\begin{aligned} v_{2g}^2 &= \frac{m_1^2}{(m_1+m_2)^2}\,(v_1^2 + v_2^2 - 2v_1v_2\cos\theta)\,,\\ V_g^2 &= \frac{1}{(m_1+m_2)^2}\,(m_1^2v_1^2 + m_2^2v_2^2 + 2m_1m_2v_1v_2\cos\theta)\,. \end{aligned}\right\} \tag{22}$$

Further, we have (cf. I, eqs. [35] and [36])

$$\left.\begin{aligned} v_{2g}V_g\cos\Phi &= \frac{m_1}{(m_1+m_2)^2}\,[m_2v_2^2 - m_1v_1^2 + v_1v_2(m_1-m_2)\cos\theta]\,,\\ v_{2g}V_g\sin\Phi &= \frac{m_1}{m_1+m_2}\,v_1v_2\sin\theta\,. \end{aligned}\right\} \tag{23}$$

Substituting for v_{2g}, V_g, $\cos\Phi$, and $\sin\Phi$ from the foregoing equations in (21), we finally have

$$\left.\begin{aligned} v_2'^2 = \frac{1}{(m_1+m_2)^2}\,\{&(m_1+m_2)^2v_2^2 - 4m_1[(m_2v_2^2 - m_1v_1^2)\\ &+ (m_1-m_2)v_1v_2\cos\theta]\cos^2\psi\\ &- 4m_1(m_1+m_2)v_1v_2\sin\theta\cos\Theta\sin\psi\cos\psi\}\,. \end{aligned}\right\} \tag{24}$$

Multiplying the equation defining $\boldsymbol{V}_g$ scalarly by $\boldsymbol{v}_2$, we obtain

$$V_g\cos\vartheta = \frac{1}{m_1+m_2}\,(m_1v_1\cos\theta + m_2v_2)\,. \tag{25}$$

Again, multiplying the equation defining $\boldsymbol{v}_{2g}$ scalarly by $\boldsymbol{v}_2$, we find

$$v_{2g}\cos(\Phi - \vartheta) = \frac{m_1}{m_1+m_2}\,(v_2 - v_1\cos\theta)\,. \tag{26}$$

Or, using equation (22), we have

$$\cos(\Phi - \vartheta) = \frac{v_2 - v_1\cos\theta}{\sqrt{v_1^2 + v_2^2 - 2v_1v_2\cos\theta}}\,. \tag{27}$$

From equation (27) we derive that

$$\sin(\Phi - \vartheta) = \frac{v_1 \sin\theta}{\sqrt{v_1^2 + v_2^2 - 2v_1v_2\cos\theta}}. \tag{28}$$

Substituting for $V_g \cos\vartheta$, $\cos(\Phi - \vartheta)$, and $\sin(\Phi - \vartheta)$ from equations (25), (27), and (28) in equation (14) for $\cos 2\Psi$, we find

$$\left.\begin{aligned}\cos 2\Psi = \frac{1}{(m_1 + m_2)v_2'}\,[&2m_1(v_2 - v_1\cos\theta)\cos^2\psi \\ &+ 2m_1v_1\sin\theta\cos\Theta\sin\psi\cos\psi - (m_1 + m_2)v_2]\,.\end{aligned}\right\} \tag{29}$$

Finally, substituting for v_2' its value (24), we have

$$\cos 2\Psi = \frac{2m_1(v_2 - v_1\cos\theta)\cos^2\psi + 2m_1v_1\sin\theta\cos\Theta\sin\psi\cos\psi - (m_1+m_2)v_2}{\sqrt{(m_1+m_2)^2v_2^2 - 4m_1[(m_2v_2^2 - m_1v_1^2) + (m_1 - m_2)v_1v_2\cos\theta]\cos^2\psi - 4m_1(m_1+m_2)v_1v_2\sin\theta\cos\Theta\sin\psi\cos\psi}}. \tag{30}$$

From the foregoing equation we find

$$\left.\begin{aligned}\sin^2 2\Psi &= 4m_1^2\cos^2\psi \\ &\quad \frac{v_1^2 + v_2^2 - 2v_1v_2\cos\theta - [(v_2 - v_1\cos\theta)\cos\psi + v_1\sin\theta\cos\Theta\sin\psi]^2}{(m_1+m_2)^2v_2^2 - 4m_1[(m_2v_2^2 - m_1v_1^2) + (m_1 - m_2)v_1v_2\cos\theta]\cos^2\psi - 4m_1(m_1+m_2)v_1v_2\sin\theta\cos\Theta\sin\psi\cos\psi}.\end{aligned}\right\} \tag{31}$$

It is of interest to see the limiting form which the foregoing expression for the true deflection takes for distant encounters. Under these circumstances $\psi \to \pi/2$ and $D \to \infty$, and equation (31) becomes

$$\sin^2 2\Psi \simeq \frac{4m_1^2}{(m_1 + m_2)^2v_2^2}\,[v_1^2 + v_2^2 - 2v_1v_2\cos\theta - v_1^2\sin^2\theta\cos^2\Theta]\cos^2\psi\,; \tag{32}$$

or, using equation (1) and after a slight rearrangement of the terms, we obtain

$$\sin^2 2\Psi \simeq \frac{4m_1^2G^2}{D^2v_2^2V^4}\,[(v_2 - v_1\cos\theta)^2 + v_1^2\sin^2\theta\sin^2\Theta] \qquad (D \to \infty)\,. \tag{33}$$

On the other hand, for the deflection $(\pi - 2\psi)$ in the relative orbit we have

$$\sin^2 2\psi \simeq \frac{4G^2(m_1 + m_2)^2}{D^2V^4} \qquad (D \to \infty)\,. \tag{34}$$

Thus, for distant encounters the ratio of the true deflection $(\pi - 2\Psi)$ to the deflection $(\pi - 2\psi)$ in the relative orbit becomes

$$\frac{\sin 2\Psi}{\sin 2\psi} = \frac{m_1}{(m_1 + m_2)v_2}\sqrt{(v_2 - v_1\cos\theta)^2 + v_1^2\sin^2\theta\sin^2\Theta}\,, \tag{35}$$

which is seen to depend on v_1, θ, and Θ, i.e., three of the five parameters defining the encounter. The ratio (35) reduces to a simple numerical factor (namely, $m_1/(m_1 + m_2)$) only in the physically unimportant case of $v_2/v_1 \to \infty$. The principal misconception

in the current treatments[6] of the problem of the deflection of stars arising from stellar encounters now becomes apparent. In these studies the deflection $(\pi - 2\psi)$ which takes place in the orbital plane with respect to the relative orbit is treated as though it were the true deflection in a fixed frame of reference. This is clearly not true; and, except in the trivial case $v_2/v_1 \to \infty$, the true deflection $(\pi - 2\Psi)$ is not even a numerical multiple of the relative deflection $(\pi - 2\psi)$.[7]

4. *The fundamental equation.*—In Part I we have already obtained the number of $(v_1, \theta, \varphi, D, \Theta)$ encounters which take place in an interval of time dt; we have (cf. I, eq. [19])

$$2\pi N(v_1, \theta, \varphi) DV dD dt \frac{d\Theta}{2\pi} dv_1 d\theta d\varphi . \tag{36}$$

Hence, the contribution of these encounters to the sum $\Sigma \sin^2 2\Psi$ can be written as

$$\sum \sin^2 2\Psi_{(v_1,\theta,\varphi,D,\Theta)} = 2\pi N(v_1, \theta, \varphi) \sin^2 2\Psi V dD d \frac{d\Theta}{2\pi} dv_1 d\theta d\varphi dt ; \tag{37}$$

or, using (31), we have

$$\left.\begin{aligned}\Sigma \sin^2 2\Psi_{(v_1,\theta,\varphi,D,\Theta)} &\\ = 4m_1^2 \cos^2\psi \frac{v_1^2+v_2^2-2v_1v_2\cos\theta-[(v_2-v_1\cos\theta)\cos\psi+v_1\cos\Theta\sin\theta\sin\psi]^2}{(m_1+m_2)^2v_2^2-4m_1[(m_2v_2^2-m_1v_1^2)+(m_1-m_2)v_1v_2\cos\theta]\cos^2\psi-4m_1(m_1+m_2)v_1v_2\sin\theta\cos\Theta\sin\psi\cos\psi}& \\ \times 2\pi N(v_1,\theta,\varphi) V dD d\frac{d\Theta}{2\pi} dv_1 d\theta d\varphi dt .&\end{aligned}\right\} \tag{37'}$$

Our next problem is to integrate the foregoing expression over the various parameters defining the encounter, namely, D, Θ, φ, θ, and v_1.

5. *The integration over the impact parameter.*—Instead of D, we shall use ψ as the variable of integration. According to (1),

$$dD = \frac{G^2(m_1 + m_2)^2}{V^4} \frac{\sin\psi}{\cos^3\psi} d\psi . \tag{38}$$

Introducing equation (38) in (37′), we obtain the total contribution to the sum $\Sigma \sin^2 2\Psi$ by all the $(v_1, \theta, \varphi, \Theta)$ encounters by integrating over ψ. We thus have,

$$\left.\begin{aligned}\Sigma \sin^2 2\Psi_{(v_1,\theta,\varphi,\Theta)} = 8\pi N(v_1,\theta,\varphi)\frac{G^2(m_1+m_2)^2m_1^2}{V^3}\frac{d\Theta}{2\pi}dv_1d\theta d\varphi dt& \\ \times\int\frac{v_1^2+v_2^2-2v_1v_2\cos\theta-[(v_2-v_1\cos\theta)\cos\psi+v_1\cos\Theta\sin\theta\sin\psi]^2}{(m_1+m_2)^2v_2^2-4m_1[(m_2v_2^2-m_1v_1^2)+(m_1-m_2)v_1v_2\cos\theta]\cos^2\psi-4m_1(m_1+m_2)v_1v_2\sin\theta\cos\Theta\sin\psi\cos\psi}& \\ \times\frac{\sin\psi}{\cos\psi}d\psi .&\end{aligned}\right\} \tag{39}$$

In equation (39) the integration is to be extended over the relevant range of ψ.

[6] J. H. Jeans, *M.N.*, **74**, 109, 1913; *ibid.*, **76**, 554, 1916; also Jeans, *Problems of Cosmogony and Stellar Dynamics*, pp. 224–229, Cambridge, England, 1919, and *Astronomy and Cosmogony*, pp. 317–320, Cambridge, 1929; A. S. Eddington, *Stellar Movements*, pp. 249–252, Macmillan, 1914; H. Kienle in *Encyklopädie der Mathematischen Wissenschaften*, p. 1051, Leipzig, 1934; von der Pahlen, *Stellarstatistik*, pp. 802–807, Leipzig, 1937; W. M. Smart, *Stellar Dynamics*, pp. 315–321, Cambridge, 1938.

[7] Apart from the principal error we have referred to, there are other less serious ones which vitiate the current treatments. Thus, a common feature is the occurrence of the logarithmic divergence not only as $D \to \infty$ but also when $D \to 0$. This spurious divergence as $D \to 0$ arises from extending the range of integration over D from zero to infinity of quantities which are "valid" only for distant encounters.

We notice that the integral in (39) diverges logarithmically as $\psi \to \pi/2$. This divergence which we now encounter arises for essentially the same reasons as those which caused a similar divergence in our discussion of the time of relaxation from the point of view of the energies exchanged during stellar encounters. Briefly, it is due to the impossibility of idealizing stellar encounters, with impact parameters D of the same order as the average distance D_0 between stars, as two-body problems. We shall later return to this question (§ 10), but meantime we shall adopt the procedure which has been followed in Part I, namely, of extending the range of integration over values of D less than a certain maximum value $D_{\max} \simeq D_0$. Further, for the values of D_0 which come under consideration in the treatment of actual stellar systems the maximum value ψ_0 of ψ differs so slightly from $\pi/2$ that we can put $\psi_0 = \pi/2$ in all terms except those which diverge at $\psi = \pi/2$.

In order to evaluate the integral in (39), we shall first remove from the integrand the part of it which diverges at $\psi = \pi/2$. This is seen to be

$$\frac{(v_2 - v_1 \cos\theta)^2 + v_1^2 \sin^2\theta \sin^2\Theta}{(m_1 + m_2)^2 v_2^2} \frac{\sin\psi}{\cos\psi}; \tag{40}$$

and, subtracting this term from the integrand of (39), we find, after some rather lengthy reductions, that we are left with

(37′)
$$\frac{1}{(m_1 + m_2)^2 v_2^2} \frac{A\cos\psi + B\sin\psi}{X\sin^2\psi + Y\sin\psi\cos\psi + Z\cos^2\psi} \sin\psi\,, \tag{41}$$

where

$$\left.\begin{aligned} A &= v_2^2(m_1 + m_2)^2[v_1^2 \sin^2\theta\cos^2\Theta - (v_2 - v_1\cos\theta)^2] \\ &\quad + 4m_1[v_2^2 - 2v_1v_2\cos\theta + v_1^2(1 - \sin^2\theta\cos^2\Theta)] \\ &\quad\quad \times [m_2v_2^2 - m_1v_1^2 + (m_1 - m_2)v_1v_2\cos\theta]\,, \\ B &= 2(m_1 + m_2)v_1v_2\sin\theta\cos\Theta[2m_1v_1^2(\sin^2\Theta + \cos^2\Theta\cos^2\theta) \\ &\quad + (m_1 - m_2)v_2^2 - (3m_1 - m_2)v_1v_2\cos\theta]\,, \end{aligned}\right\} \tag{42}$$

and where

(39)
$$\left.\begin{aligned} X &= (m_1 + m_2)^2 v_2^2\,, \\ Y &= -4m_1(m_1 + m_2)v_1v_2\sin\theta\cos\Theta\,, \\ Z &= 4m_1^2v_1^2 + (m_1 - m_2)^2v_2^2 - 4m_1(m_1 - m_2)v_1v_2\cos\theta\,. \end{aligned}\right\} \tag{43}$$

Thus we can re-write equation (39) as

$$\sum \sin^2 2\Psi_{(v_1,\theta,\varphi,\Theta)} = 8\pi N(v_1, \theta, \varphi) \frac{G^2m_1^2}{V^3v_2^2} (K_1 + K_2) \frac{d\Theta}{2\pi} dv_1 d\theta d\varphi dt\,, \tag{44}$$

where

$$K_1 = [(v_2 - v_1\cos\theta)^2 + v_1^2\sin^2\theta\sin^2\Theta]\int_0^{\psi_0} \frac{\sin\psi}{\cos\psi}\, d\psi \tag{45}$$

and

$$K_2 = \int_0^{\pi/2} \frac{A\cos\psi + B\sin\psi}{X\sin^2\psi + Y\sin\psi\cos\psi + Z\cos^2\psi} \sin\psi\, d\psi\,. \tag{46}$$

The evaluation of the integral K_1 is immediate. We find

$$K_1 = \tfrac{1}{2}[(v_2 - v_1 \cos\theta)^2 + v_1^2 \sin^2\theta \sin^2\Theta] \log\left(1 + \frac{D_0^2 V^4}{G^2(m_1 + m_2)^2}\right). \tag{47}$$

To evaluate the integral K_2, we put

$$\cot\psi = z\,, \tag{48}$$

whereupon (46) becomes

$$K_2 = \int_0^\infty \frac{Az + B}{(X + Yz + Zz^2)(1 + z^2)}\, dz\,, \tag{49}$$

which is an elementary integral. We find that we can express the result of the integration in the form

$$\left.\begin{aligned} K_2 = {} & K_{21} \log\left(\frac{Z}{X}\right) \\ & + K_{22} \frac{1}{v_1 v_2 \sqrt{1 - \sin^2\theta\cos^2\Theta}} \left\{\frac{\pi}{2} + \tan^{-1}\frac{\sin\theta\cos\Theta}{\sqrt{1 - \sin^2\theta\cos^2\Theta}}\right\} + \pi K_{23}\,, \end{aligned}\right\} \tag{50}$$

where

$$\left.\begin{aligned} K_{21} &= \frac{YB - (X - Z)A}{2[(X - Z)^2 + Y^2]}\,, \\ K_{22} &= \frac{(Y^2 + 2Z^2 - 2XZ)B - Y(X + Z)A}{2[(X - Z)^2 + Y^2]}\,, \\ K_{23} &= \frac{YA + (X - Z)B}{2[(X - Z)^2 + Y^2]}\,. \end{aligned}\right\} \tag{51}$$

The quantities K_{21}, K_{22}, and K_{23} can be evaluated on substituting for A, B, X, Y, and Z from equations (42) and (43). However, these expressions are found to be rather involved, and we shall therefore give their explicit forms only for the case $m_1 = m_2$:

$$\left.\begin{aligned} K_{21} = {} & \frac{v_1^2}{2[(v_1^2 - v_2^2)^2 + 4v_1^2 v_2^2 \sin^2\theta\cos^2\Theta]} \{\cos^2\theta\,[v_2^4 - v_1^4 - 4v_1^2 v_2^2 \sin^2\theta\cos^2\Theta] \\ & + 2v_1 v_2 \cos\theta\,[v_1^2 + v_2^2(2\cos^2\Theta - 1) - 2v_2^2\cos^2\theta\cos^2\Theta] \\ & + v_1^2[v_2^2 - v_1^2 - 4v_2^2\sin^2\theta\cos^2\Theta]\sin^2\Theta\sin^2\theta\}\,, \\ K_{22} = {} & \frac{v_1^3 v_2 \sin\theta\cos\Theta}{(v_1^2 - v_2^2)^2 + 4v_1^2 v_2^2 \sin^2\theta\cos^2\Theta} \{\cos^2\theta\,[v_1^4 - v_2^4 \\ & - 4v_1^2 v_2^2(1 - \sin^2\theta\cos^2\Theta)] + 4v_1 v_2^3 \cos\theta(1 - \sin^2\theta\cos^2\Theta) \\ & + v_1^2\sin^2\theta\sin^2\Theta(v_1^2 - 3v_2^2 + 4v_2^2\sin^2\theta\cos^2\Theta)\}\,, \\ K_{23} = {} & \frac{v_1^2 v_2^2 \sin\theta\cos\Theta}{(v_1^2 - v_2^2)^2 + 4v_1^2 v_2^2 \sin^2\theta\cos^2\Theta} \{2v_1 v_2\cos^2\theta \\ & - \cos\theta\,(v_1^2 + v_2^2) + v_1 v_2 \sin^2\theta\sin^2\Theta\}\,. \end{aligned}\right\} \tag{52}$$

6. *The integration over the inclination of the orbital plane.*—According to equation (44), the contribution to the sum $\Sigma \sin^2 2\Psi$ by the (v_1, θ, φ) encounters is

$$\sum \sin^2 2\Psi_{(v_1,\theta,\varphi)} = 8\pi N(v_1, \theta, \varphi) \frac{G^2 m_1^2}{V^3 v_2^2} \int_0^{2\pi} (K_1 + K_2) \frac{d\Theta}{2\pi} dv_1 d\theta d\varphi dt . \quad (53)$$

The integration of K_1 over Θ is immediate. We have (cf. eq. [47])

$$\int_0^{2\pi} K_1 \frac{d\Theta}{2\pi} = \tfrac{1}{2}[(v_2 - v_1 \cos\theta)^2 + \tfrac{1}{2} v_1^2 \sin^2\theta] \log\left(1 + \frac{D_0^2 V^4}{G^2(m_1 + m_2)^2}\right). \quad (54)$$

On the other hand, the integration of K_2 over Θ is seen to lead, in general, to rather lengthy and involved expressions. However, for the case $m_1 = m_2$ the situation is somewhat simpler. For $m_1 = m_2$, K_{21} is an even function of Θ, while K_{22} and K_{23} are both odd. Hence,

$$\left.\begin{aligned} \int_0^{2\pi} K_2 \frac{d\Theta}{2\pi} &= \frac{2}{\pi} \log\frac{v_1}{v_2} \int_0^{\pi} K_{21} d\Theta \\ &+ \frac{1}{\pi v_1 v_2} \int_0^{\pi} \frac{K_{22}}{\sqrt{1 - \sin^2\theta\cos^2\Theta}} \tan^{-1} \frac{\sin\theta\cos\Theta}{\sqrt{1 - \sin^2\theta\cos^2\Theta}} d\Theta . \end{aligned}\right\} \quad (55)$$

The expressions resulting from the foregoing can be handled without undue difficulty. But we shall not carry these terms any farther, for they are generally small, compared to the "dominant term" arising from the divergent part (40) of the integrand of equation (39). We may recall in this connection that in our discussion of the problem of the exchange of energies during stellar encounters the total contribution to $\Sigma \Delta E^2$ arose from two types of terms: a dominant term similar to (54), and certain other terms which were relatively unimportant. Thus, for not too extreme values of $x_0 (0.5 \leqslant x_0 \leqslant 2.5)$, the non-dominant terms contributed less than 10 per cent of the entire amount (cf. the remarks made in I, § 10). In a general way it is clear that a similar situation must obtain in our present case.[8] Consequently, in a first analysis of the problem of the true deflections arising from stellar encounters it would not seem necessary to go into the minor refinements arising from the terms K_{21} and K_{22}.

7. *The integration of the dominant term over the angles φ and θ.*—Retaining only the dominant term, we have

$$\left.\begin{aligned} \sum \sin^2 2\Psi_{(v_1,\theta,\varphi)} &= 4\pi N(v_1, \theta, \varphi) G^2 m_1^2 \frac{1}{V^3 v_2^2} \\ &\times [(v_2 - v_1\cos\theta)^2 + \tfrac{1}{2} v_1^2 \sin^2\theta] \log\left(1 + \frac{D_0^2 V^4}{G^2(m_1 + m_2)^2}\right) dv_1 d\theta d\varphi dt . \end{aligned}\right\} \quad (56)$$

To integrate the foregoing equation over the angles φ and θ, we need to know the form of the function $N(v_1, \theta, \varphi)$. As in Part I, we shall effect these integrations only for the case of a spherical distribution of the velocities v_1. Under these circumstances we can write (cf. I, eqs. [39])

$$N(v_1, \theta, \varphi) dv_1 d\theta d\varphi = N(v_1) \frac{\sin\theta d\theta d\varphi}{4\pi} dv_1 , \quad (57)$$

[8] We have examined the magnitude of terms arising from the integration of K_{21} and K_{22} in certain special cases (e.g., $\Theta = 0$ and $\theta = \pi/4$) and find that these are, in fact, small compared to the dominant term.

where

$$N(v_1) = 4\pi N f(v_1) v_1^2 . \tag{58}$$

For this form of $N(v_1, \theta, \varphi)$ the integration over φ is simple, and we obtain (cf. eq. [56])

$$\left.\begin{aligned}\sum \sin^2 2\Psi_{(v_1,\theta)} = {} & 2\pi N(v_1) G^2 m_1^2 \frac{1}{v_2^2} \\ & \times \frac{\sin\theta}{(v_1^2 + v_2^2 - 2v_1 v_2 \cos\theta)^{3/2}} [(v_2 - v_1 \cos\theta)^2 + \tfrac{1}{2} v_1^2 \sin^2\theta] \\ & \times \log\left(1 + \frac{D_0^2 (v_1^2 + v_2^2 - 2v_1 v_2 \cos\theta)^2}{G^2 (m_1 + m_2)^2}\right) dv_1 d\theta dt .\end{aligned}\right\} \tag{59}$$

To integrate equation (59) over θ, we shall introduce a new variable y defined by the relation

$$y^2 = v_1^2 + v_2^2 - 2v_1 v_2 \cos\theta . \tag{60}$$

Using this variable in equation (59), we find, after some elementary transformations, that

$$\sum \sin^2 2\Psi_{v_1} = \frac{\pi G^2 m_1^2}{4 v_1 v_2^5} N(v_1) J \, dv_1 dt , \tag{61}$$

where we have used J to stand for the integral

$$J = \int_{\sqrt{b}}^{\sqrt{a}} [ab + 2y^2(3v_2^2 - v_1^2) + y^4] \log(1 + q^2 y^4) \frac{dy}{y^2} . \tag{62}$$

In equation (62) we have used the further abbreviations

$$a = (v_2 + v_1)^2 ; \qquad b = (v_2 - v_1)^2 ; \tag{63}$$

and

$$q = \frac{D_0}{G(m_1 + m_2)} . \tag{64}$$

The integral (62) is similar to one we have encountered in Part I and can be evaluated by similar methods: We can re-write equation (62) in the form

$$J = \int_{\sqrt{b}}^{\sqrt{a}} \frac{d}{dy} \left[-\frac{ab}{y} + 2(3v_2^2 - v_1^2) y + \tfrac{1}{3} y^3 \right] \log(1 + q^2 y^4) dy ; \tag{65}$$

or, after an integration by parts, we have

$$\left.\begin{aligned} J = {} & \frac{1}{y} [\tfrac{1}{3} y^4 + 2(3v_2^2 - v_1^2) y^2 - ab] \log(1 + q^2 y^4) \Big|_{\sqrt{b}}^{\sqrt{a}} \\ & - 4q^2 \int_{\sqrt{b}}^{\sqrt{a}} [-aby^2 + 2(3v_2^2 - v_1^2) y^4 + \tfrac{1}{3} y^6] \frac{1}{1 + q^2 y^4} dy .\end{aligned}\right\} \tag{66}$$

After some further reductions we find

$$\left.\begin{aligned} J = {} & \tfrac{8}{3}\{(v_1+v_2)^2(2v_2-v_1)\log(1+q^2[v_1+v_2]^4) \\ & \mp (v_2-v_1)^2(2v_2+v_1)\log(1+q^2[v_2-v_1]^4)\} \\ & + \int_{\sqrt{b}}^{\sqrt{a}} \left[-\tfrac{4}{3}y^2 - 8(3v_2^2-v_1^2) + \frac{4(abq^2+\tfrac{1}{3})y^2 + 8(3v_2^2-v_1^2)}{1+q^2y^4}\right] dy\,, \end{aligned}\right\} \tag{67}$$

where the minus or the plus sign in the braces ($\{\ \}$) should be taken according as v_2 is greater than or less than v_1. The integral in (67) is seen to become

$$\left.\begin{aligned} & \int_{\sqrt{b}}^{\sqrt{a}} \frac{4(abq^2+\tfrac{1}{3})y^2 + 8(3v_2^2-v_1^2)}{1+q^2y^4}\,dy \\ & \qquad - \begin{cases} \tfrac{8}{9}v_1(55v_2^2-17v_1^2) + \tfrac{16}{9}v_1v_2^2 & (v_2 \geqslant v_1)\,, \\ \tfrac{8}{9}v_2(55v_2^2-17v_1^2) + \tfrac{16}{9}v_1^2v_2 & (v_2 \leqslant v_1)\,. \end{cases} \end{aligned}\right\} \tag{68}$$

Again, the integral in equation (68) can be evaluated using the elementary integrals quoted in Part I (eq. [54]). However, the expressions are found to simplify considerably for the cases which are of practical interest, namely, when $qa \gg 1$. If $qb \neq 0$, the main contribution to the integral arises from

$$4abq^2 \int_{\sqrt{b}}^{\sqrt{a}} \frac{y^2}{1+q^2y^4}\,dy\,, \tag{69}$$

which, to the first order in $(\sqrt{qa})^{-1}$ and $(\sqrt{qb})^{-1}$, is found to be

$$4a^{1/2}b^{1/2}(a^{1/2}-b^{1/2})\,. \tag{70}$$

On the other hand, when $b = 0$ the integral in (68) vanishes to the first order in $(\sqrt{qa})^{-1}$. But when $b = 0$, the term (70) also vanishes. Hence, to the first order in $(\sqrt{qa})^{-1}$ we can write quite generally that

$$\int_{\sqrt{b}}^{\sqrt{a}} \frac{4(abq^2+\tfrac{1}{3})y^2 + 8(3v_2^2-v_1^2)}{1+q^2y^4}\,dy = 4a^{1/2}b^{1/2}(a^{1/2}-b^{1/2})\,. \tag{71}$$

Combining equations (67), (68), and (71), we find that

$$\left.\begin{aligned} J = {} & \tfrac{8}{3}\{(v_1+v_2)^2(2v_2-v_1)\log(1+q^2[v_1+v_2]^4) - (v_2-v_1)^2 \\ & \times (2v_2+v_1)\log(1+q^2[v_2-v_1]^4) + \tfrac{8}{3}v_1(v_1^2-6v_2^2)\} \qquad (v_2 \geqslant v_1) \end{aligned}\right\} \tag{72}$$

and

$$\left.\begin{aligned} J = {} & \tfrac{8}{3}\{(v_1+v_2)^2(2v_2-v_1)\log(1+q^2[v_1+v_2]^4) + (v_2-v_1)^2 \\ & \times (2v_2+v_1)\log(1+q^2[v_2-v_1]^4) + \tfrac{8}{3}v_2(3v_1^2-8v_2^2)\} \qquad (v_2 \leqslant v_1)\,. \end{aligned}\right\} \tag{73}$$

In the foregoing expressions we can further neglect the unity compared to $q^2(v_1+v_2)^4$ and $q^2(v_2-v_1)^4$ occurring in the logarithmic terms. When $v_2 = v_1$, although log

$q^2(v_2 - v_1)^4$ diverges to $-\infty$, we need not distinguish[9] between $(v_2 - v_1)^2 \log q^2(v_2 - v_1)^4$ and $(v_2 - v_1)^2 \log (1 + q^2[v_2 - v_1]^4)$. Hence, we finally have

$$\sum \sin^2 2\Psi_{v_1} = \frac{8\pi G^2 m_1^2 N(v_1)}{3 v_1 v_2^5}\, dv_1 dt \times \begin{cases} \left[(3v_1v_2^2 - v_1^3) \log q(v_2^2 - v_1^2) + 2v_2^3 \log \frac{v_2 + v_1}{v_2 - v_1} + \frac{2}{3} v_1 (v_1^2 - 6v_2^2) \right] & (v_2 \geqslant v_1), \\ \left[2v_2^3 \log q(v_1^2 - v_2^2) + (3v_1v_2^2 - v_1^3) \log \frac{v_2 + v_1}{v_1 - v_2} + \frac{2}{3} v_2 (3v_1^2 - 8v_2^2) \right] & (v_2 \leqslant v_1), \end{cases} \tag{74}$$

or, if we introduce, as in Part I, the quantity α, defined by

$$\alpha = \frac{v_1}{v_2}, \tag{75}$$

we can re-write equations (74) in the form

$$\sum \sin^2 2\Psi_{v_1} = \frac{8\pi G^2 m_1^2 N(v_1)}{3 v_2^3}\, dv_1 dt \times \begin{cases} \left[(3 - \alpha^2) \log q v_2^2 + (3 - \alpha^2) \log (1 - \alpha^2) + \frac{2}{\alpha} \log \frac{1 + \alpha}{1 - \alpha} + \frac{2}{3}(\alpha^2 - 6) \right] & (\alpha \leqslant 1), \\ \left[\frac{2}{\alpha} \log q v_2^2 + \frac{2}{\alpha} \log (\alpha^2 - 1) + (3 - \alpha^2) \log \frac{\alpha + 1}{\alpha - 1} + \frac{2}{3\alpha} (3\alpha^2 - 8) \right] & (\alpha \geqslant 1). \end{cases} \tag{76}$$

In equation (76) the term $(3 - \alpha^2) \log q v_2^2$ (or $2\alpha^{-1} \log q v_2^2$) is, for all cases of practical interest, ten to twenty times as large as the remaining terms; actually these other terms are of the same order of magnitude as those which we have already neglected in ignoring the K_2-term in equation (53). We can therefore write

$$\sum \sin^2 2\Psi_{v_1} = \frac{8\pi G^2 m_1^2 N(v_1)}{3 v_2^3}\, dv_1 dt \begin{cases} (3 - \alpha^2) \log q v_2^2 & (\alpha \leqslant 1), \\ \frac{2}{\alpha} \log q v_2^2 & (\alpha \geqslant 1). \end{cases} \tag{77}$$

8. *The integration of the dominant term over the velocities* v_1.—In § 7 we have evaluated the contribution to $\Sigma \sin^2 2\Psi$ (arising from the dominant term) by all encounters in which the field stars have some prescribed value of the velocity, v_1. However, in carrying

[9] For a more explicit statement of the arguments which are made here see I, p. 295.

out the integration over θ and φ a spherical distribution of the velocities was assumed. To average now over the velocities of the field stars, we need to know the form of $N(v_1)$. For the reasons already given in Part I, § 8, we shall assume a Gaussian distribution of the velocities v_1. This implies that (see I, eq. [79])

$$N(v_1)dv_1 = \frac{4x_0^3}{\sqrt{\pi}} e^{-(x_0\alpha)^2}\alpha^2 d\alpha\,, \tag{78}$$

where

$$x_0 = hv_2\,. \tag{79}$$

For this form of $N(v_1)$ we have

$$\sum \sin^2 2\Psi = \frac{8\pi NG^2m_1^2}{3v_2^3}\left[\frac{4x_0^3}{\sqrt{\pi}}\left\{\int_0^1 (3-\alpha^2)\alpha^2 e^{-(x_0\alpha)^2}d\alpha + 2\int_1^\infty \alpha e^{-(x_0\alpha)^2}d\alpha\right\}\right]\log qv_2^2 dt\,. \tag{80}$$

The integrals occurring in the foregoing equation can be evaluated in terms of the error function $\Phi(x_0)$. We find that

$$\sum \sin^2 2\Psi = \frac{8\pi NG^2m_1^2}{v_2^3} H(x_0)\log qv_2^2 dt\,, \tag{81}$$

where

$$H(x_0) = \frac{1}{2x_0^2}\left[x_0\Phi'(x_0) + (2x_0^2 - 1)\Phi(x_0)\right]. \tag{82}$$

The function $H(x_0)$ is tabulated in Table 1.

TABLE 1

x_0	$H(x_0)$	T_D/T_E	x_0	$H(x_0)$	T_D/T_E
0.6	0.421	1.74	1.8	0.849	0.66
0.8	.534	1.56	2.0	.876	.55
1.0	.629	1.36	2.5	.920	0.35
1.2	.706	1.16	3.0	.944	.....
1.4	.766	0.97	4.0	0.969	.....
1.6	0.813	0.80			

9. *The time of relaxation* T_D *of a stellar system.*—According to our definition of the time of relaxation T_D, we have

$$\int_0^{T_D} \sum \sin^2 2\Psi = 1\,. \tag{83}$$

Strictly speaking, the direction of motion of a star changes during its motion through the other stars, and equation (81) provides us with a measure of only the instantaneous

rate of deflection of the star. However, in a first approximation we can write as our definition of T_D the equation

$$\frac{8\pi NG^2m_1^2}{v_2^3} H(x_0)\, T_D \log qv_2^2 = 1 . \tag{84}$$

Hence,

$$T_D = \frac{v_2^3}{8\pi NG^2m_1^2H(x_0) \log_e \left[\frac{D_0v_2^2}{G(m_1 + m_2)}\right]} . \tag{85}$$

It is of interest to compare this formula for the time of relaxation with a similar one which was obtained from consideration of the energies exchanged during encounters (cf. I, eq. [98]):

$$T_E = \frac{v_2^3}{32\pi NG^2m_1^2G(x_0) \log_e \left[\frac{D_0v_2^2}{G(m_1 + m_2)}\right]} \qquad (0.5 \leqslant x_0 \leqslant 2.5) . \tag{86}$$

These expressions for T_D and T_E are seen to be of identical forms. Further, the ratio between the times of relaxation determined from the two different points of view is given by

$$\frac{T_D}{T_E} = \frac{4G(x_0)}{H(x_0)} \qquad (0.5 \leqslant x_0 \leqslant 2.5) . \tag{87}$$

This ratio is tabulated in Table 1. It is of interest to draw particular attention in this connection to the fact that the dependence of T_D on m_2 is quite unpronounced. In this respect, the deflection of a star from the theoretical orbit derived from the general gravitational potential behaves in a manner quite analogous to the deviation from constancy of the energy integral. There is, however, one important difference between the two problems. According to equation (82),

$$H(x_0) \to 1 \quad \text{as} \quad x_0 \to \infty . \tag{88}$$

Consequently,

$$T_D = \frac{v_2^3}{8\pi NG^2m_1^2 \log_e \left[\frac{D_0v_2^2}{G(m_1 + m_2)}\right]} \qquad (x_0 = \infty) . \tag{89}$$

On the other hand, as we have seen in Part I, § 10, as $x_0 \to \infty$, $G(x_0) \to 0$ and the contribution to $\Sigma\Delta E^2$ now arises from the nondominant terms. Thus, in the limit $x_0 \to \infty$ we had a formula for T_E (I, eq. [94]) whose dependence on m_2 was very pronounced. However, in our present problem, since $H(x_0) \to 1$, it appears that the range of validity of equation (85) is probably greater than that of equation (86) for larger values of x_0. However, in the latter case the nondominant terms have been explicitly evaluated so that the circumstance that $G(x_0) \to 0$ as $x_0 \to \infty$ does not introduce any difficulty.

Finally, we may notice that if we express m_1 and m_2, D_0, v_2, and N in units of solar

mass, parsecs, 20 km/sec, and number per cubic parsec, respectively, equation (85) becomes

$$T_D = 1.68 \times 10^{13} \frac{v_2^3}{N m_1^2 H(x_0) \log_e [9.31 \times 10^4 D_0 v_2^2/(m_1 + m_2)]} \text{ years} . \quad (90)$$

In this form the equation can be conveniently used for determining T_D. We shall not, however, give any explicit numerical applications of our present formula, since from our knowledge of the ratio T_D/T_E (cf. Table 1) we can directly evaluate the times T_D for the cases considered in Part I (cf. Tables 5 and 6).

10. *General remarks.*—We have now considered the two associated problems of the deflections suffered and the energies exchanged by stars during stellar encounters. Our discussion of these two problems has been based on two principal assumptions: the first is the idealization of stellar encounters as two-body problems; and the second is the assumption that all encounters with impact parameters D, greater than the average distance D_0 between the stars, can be ignored. In view of the fundamental nature of these two assumptions, we shall now re-examine them in somewhat greater detail.

As we have already explained in Part I, § 4, the need for disregarding all encounters with $D > D_0$ arises primarily from the increasing difficulty of adequately describing such encounters on the two-body idealization. For, in considering either the energy ΔE exchanged or the true deflection $(\pi - 2\Psi)$ suffered as the result of an encounter thus idealized, we have assumed that the deflection $(\pi - 2\psi)$ in the relative orbit in the orbital plane is given by the formula

$$\cos \psi = \frac{1}{\sqrt{1 + \frac{D^2 V^4}{G^2 (m_1 + m_2)^2}}} . \quad (91)$$

Strictly speaking, the use of equation (91) implies that the two stars involved in an encounter are initially at an infinite distance apart and separate to an infinite distance after the encounter. We should therefore conclude that, in practice, a second encounter begins to be effective before the first can be regarded as completed in the strict sense. Consequently, the use of equation (91) for the angle between the asymptotes of the relative orbit overestimates both ΔE and $(\pi - 2\Psi)$. We shall now try to estimate the magnitude of the errors thus introduced. For this purpose we shall find the distance between two stars involved in an encounter at a point in the relative orbit where the direction of motion makes an angle $\psi + \Delta\psi$ with the transverse axis. Let

$$\Delta\psi = \kappa\left(\frac{\pi}{2} - \psi\right) \qquad (\kappa < 1) , \quad (92)$$

and denote by $r(\kappa)$ the corresponding distance between the two stars. We readily find that

$$\frac{r(\kappa)}{D} = \frac{1}{\sqrt{2\kappa - \kappa^2}} \quad (93)$$

for large eccentricities of the orbit. Table 2 gives $r(\kappa)$ for certain values of κ.

Consider now an encounter with $D = 0.5 D_0$. Then, according to equation (93) (also see Table 2),

$$r(0.1) = 1.15 D_0 \qquad (D = 0.5 D_0) . \quad (94)$$

In other words, we may say that about 90 per cent of the relative orbit has been completed before the two stars have separated to a distance of the order of D_0. It would thus appear that for stellar encounters with $D = 0.5D_0$ the use of equation (91) is unlikely to lead to an overestimation of ψ by more than 10 per cent; on the average, the overestimation will probably be less than this amount.

Consider next an encounter with $D = D_0$. Again, according to equation (93) and Table 2,

$$r(0.3) = 1.4D_0 \qquad (D = D_0) . \quad (95)$$

This indicates that for encounters with $D = D_0$ the overestimation of the actual deflection in the relative orbit resulting from the use of (91) will be of the order of 20–30 per

TABLE 2

κ	$r(\kappa)/D$	κ	$r(\kappa)/D$
0.05	3.20	0.30	1.40
.10	2.29	.40	1.25
0.20	1.67	0.50	1.16

cent. This further shows that encounters with $D > D_0$ must contribute, to some extent, to $\Sigma\Delta E^2$ or $\Sigma \sin^2 2\Psi$. Consequently, by ignoring all encounters with $D > D_0$ and using equation (91) for all encounters with $D \leqslant D_0$, the two sources of error will probably compensate. In any case, an examination of Table 2 suggests that the method which has been adopted to avoid the divergence of the integrals which occur in the evaluation of $\Sigma\Delta E^2$ and $\Sigma \sin^2 2\Psi$ is not likely to lead to errors of more than a few per cent, since D_0 enters in the various expressions only through a logarithmic term.

YERKES OBSERVATORY
September 18, 1940

THE TIME OF RELAXATION OF STELLAR SYSTEMS. III

S. CHANDRASEKHAR

ABSTRACT

Certain difficulties of principle which confront a rigorous and satisfactory analysis of stellar encounters within the framework of a theory which idealizes them, individually, as two-body problems are pointed out.

1. *Introduction.*—In the two preceding papers[1] the time of relaxation of a stellar system has been considered from two distinct points of view. In both cases the problem has a twofold character: first, to determine the effectiveness of stellar encounters in influencing the motions of the individual stars in a stellar system and, second, to estimate the rate at which a stellar system may be expected to approach the final state of "thermodynamic" equilibrium. The clearest formulation of this latter aspect of the ideas underlying the problem of the time of relaxation of a stellar system is due to Rosseland,[2] who has pointed out that after a sufficient length of time (long enough for a star to have suffered a large number of encounters) successive values of ΔE may be expected to be independent. Consequently, we can expect the ΔE's to combine according to the Gaussian error law. Thus, the probability that, after a time t, ΔE may have a value in the range $\{\Delta E, \Delta E + d(\Delta E)\}$ will be given by an expression of the form (cf. Rosseland, *op. cit.*, eq. [1])

$$W_t(\Delta E)d(\Delta E) = \frac{1}{\sqrt{2\pi \sum_0^t \Delta E^2}} e^{-\left(\Delta E - \sum_0^t \Delta E\right)^2 \Big/ 2\sum_0^t \Delta E^2} d(\Delta E)\,. \qquad (1)$$

In other words, $\sum_0^t \Delta E^2$ is a measure of the *dispersion* in ΔE to be expected after a given length of time. It is primarily for this reason that the quantity $\Sigma \Delta E^2$ was evaluated in Part I. (Similar arguments apply to the consideration of the sum $\Sigma \sin^2 2\Psi$ where $(\pi - 2\Psi)$ is the true deflection of a star with respect to fixed frame of reference.) Thus, at first sight, it would appear that, by combining the methods of Parts I and II with a law of the form (1) we should be able to make some progress toward a *statistical theory* of stellar encounters. Such a theory would clearly be of the greatest importance, particularly in an analysis of the problem of clusters. However, and it is the object of this note to point out, that a description of stellar encounters from a very much more fundamental standpoint than has been adopted in Parts I and II is necessary before a really satisfactory start can be made toward a statistical theory of stellar encounters.

2. *The evaluation of the sum* $\Sigma\Delta$E.—It is clear that in order that we may be able to use equation (1) it is necessary to evaluate not only the sum $\Sigma \Delta E^2$ but also the sum $\Sigma \Delta E$, and it is in this connection that we encounter certain fundamental difficulties.

Let us suppose that, as in Parts I and II, we can idealize stellar encounters, individually, as two-body problems. As we have seen in Part I, § 3, the parameters defining

[1] Referred to as "I" and "II."

[2] *M.N.*, **88**, 208, 1928.

such an encounter are v_1, θ, φ, D, and Θ.[3] Consider, then, a (v_1, θ, φ, D, Θ) encounter. The exchange of energy ΔE resulting from such an encounter is (cf. I, eq. [16])

$$\Delta E = -\frac{2m_1m_2}{m_1 + m_2} V_g V \cos(\phi - \psi) \cos\psi \cos i . \tag{2}$$

The contribution to $\Sigma\Delta E$ by all the (v_1, θ, φ, D, Θ) encounters can therefore be written as (cf. I, eq. [19])

$$\Sigma\Delta E_{(v_1, \theta, \varphi, D, \Theta)} = 2\pi N(v_1, \theta, \varphi)\Delta E V D dD \frac{d\Theta}{2\pi} dv_1 d\theta d\varphi dt , \tag{3}$$

or, using equation (2), as

$$\left.\begin{aligned}\Sigma\Delta E_{(v_1, \theta, \varphi, D, \Theta)} = &-4\pi N(v_1, \theta, \varphi) \\ &\times \frac{m_1m_2}{m_1 + m_2} V_g V^2 \cos i \cos(\phi - \psi) \cos\psi \, DdD \frac{d\Theta}{2\pi} dv_1 d\theta d\varphi dt .\end{aligned}\right\} \tag{4}$$

If we used ψ as the variable instead of D, then equation (4) becomes (cf. I, eq. [22])

$$\left.\begin{aligned}\Sigma\Delta E_{(v_1, \theta, \varphi, \psi, \Theta)} = &-4\pi N(v_1, \theta, \varphi) G^2 m_1 m_2 (m_1 + m_2) \frac{V_g}{V^2} \cos i \\ &\times \frac{\cos(\phi - \psi) \sin\psi}{\cos^2\psi} d\psi \frac{d\Theta}{2\pi} dv_1 d\theta d\varphi dt .\end{aligned}\right\} \tag{5}$$

On integrating the foregoing equation over ψ, we obtain

$$\left.\begin{aligned}\Sigma\Delta E_{(v_1, \theta, \varphi, \Theta)} = &-4\pi N(v_1, \theta, \varphi) G^2 m_1 m_2 (m_1 + m_2) \frac{V_g}{V^2} \cos i \\ &\times \int \frac{\cos(\phi - \psi) \sin\psi}{\cos^2\psi} d\psi \frac{d\Theta}{2\pi} dv_1 d\theta d\varphi dt .\end{aligned}\right\} \tag{6}$$

In equation (6) the integration will have to be extended over the relevant range in ψ. Now, the integral occurring in equation (6) diverges at $\psi = \pi/2$. This, in itself, is not surprising. Actually, the corresponding integrals which occur in the evaluation of either of the sums $\Sigma\Delta E^2$ or $\Sigma \sin^2 2\Psi$ (cf. I, eq. [24], and II, eq. [39]) also diverge at $\psi = \pi/2$. But there is one important difference: the integral in equation (6) diverges to a higher order in D than in either of the two previous cases. To examine explicitly the nature of this higher order of divergence, let us extend the range of integration to $0 \leqslant \psi \leqslant \psi_0$ and put $\psi_0 = \pi/2$ in all terms except those which diverge at $\psi = \pi/2$. Using this method, we readily find that

$$\int \frac{\cos(\phi - \psi) \sin\psi}{\cos^2\psi} d\psi = (-\log\cos\psi_0) \cos\phi + \left(\tan\psi_0 - \frac{\pi}{2}\right) \sin\phi . \tag{7}$$

[3] The notation is the same as in I and II.

Combining equations (6) and (7), we find that

$$\left.\begin{aligned}\Sigma\Delta E_{(v_1,\,\theta,\,\varphi,\,\Theta)} &= -4\pi N(v_1,\,\theta,\,\varphi)G^2m_1m_2(m_1+m_2)\,\frac{V_g}{V^2}\cos i\,\frac{d\Theta}{2\pi}\,dv_1d\theta d\varphi dt\\ &\times\left[\frac{1}{2}\left\{\log\left(1+\frac{D_0^2V^4}{G^2(m_1+m_2)^2}\right)\right\}\cos\phi+\left\{\frac{D_0V^2}{G(m_1+m_2)}-\frac{\pi}{2}\right\}\sin\phi\right].\end{aligned}\right\}\quad(8)$$

Using the relations (27) of Part I, we can re-write the foregoing equation more conveniently in the form

$$\left.\begin{aligned}\Sigma\Delta E_{(v_1,\,\theta,\,\varphi,\,\Theta)} &= -4\pi N(v_1,\,\theta,\,\varphi)G^2m_1m_2(m_1+m_2)\,\frac{V_g}{V^2}\cdot\frac{d\Theta}{2\pi}\,dv_1d\theta d\varphi dt\\ &\times\left[\frac{1}{2}\left\{\log\left(1+\frac{D_0^2V^4}{G^2(m_1+m_2)^2}\right)\right\}\cos\Phi+\left\{\frac{D_0V^2}{G(m_1+m_2)}-\frac{\pi}{2}\right\}\sin\Phi\cos\Theta\right].\end{aligned}\right\}\quad(9)$$

Now, the dominant term in the foregoing expression is the one which involves $[D_0V^2/G(m_1+m_2)]$, and this is seen to be very much more important than the non-dominant terms, for (cf. I, eq. [56])

$$\frac{D_0V^2}{G(m_1+m_2)}=9.31\times10^4\,\frac{[D_0/\text{parsec}]}{[(m_1+m_2)/\odot]}\,[V/20\ \text{km/sec}^{-1}]^2\,.\qquad(10)$$

Consequently, the term $[D_0V^2/G(m_1+m_2)]$ is generally $10^{3.5}$ to $10^{4.5}$ times as large as the logarithmic term, $\log[D_0V^2/G(m_1+m_2)]$. However, the dominant term occurs with $\cos\Theta$ as a factor, and it would appear that the averaging over Θ would eliminate the dominant term from equation (9) and retain only the logarithmically diverging term. But it is now clear that the $[D_0V^2/G(m_1+m_2)]$ term can be ignored only if the average value of $\cos\Theta$ for $0\leqslant\Theta\leqslant2\pi$ under the conditions of the *physical problem* is less than 10^{-4}. This is hardly likely to be the case, since any fluctuation giving even the slightest preference to a particular value of Θ will make the $[D_0V^2/G(m_1+m_2)]$ term far more important than any of the other terms which would normally be retained. We cannot thus ignore the dominant term in equation (9), for the *formal* reason that the average value of $\cos\Theta$ in the range $0\leqslant\Theta\leqslant2\pi$ vanishes.[4] At the same time it would be difficult

[4] A recent paper by L. Spitzer (*M.N.*, **100**, 387, 1940) contains an evaluation of the sum $\Sigma\Delta E$. It will be noted that Spitzer retains only the logarithmic term in his expressions. For reasons which are stated in the text the evaluation of $\Sigma\Delta E$ which ignores the dominant term $[D_0V^2/G(m_1+m_2)]$ is likely to underestimate it by a factor of the order of 100 or more when any particular star is being followed during its motion. However, as Dr. Spitzer has pointed out to the writer, if one averages over a large number of "incident" stars, a more complete cancelation of the $[D_0V^2/G(m_1+m_2)]$ term may be expected. If this be assumed, the averaging of equation (9) over Θ will give

$$\left.\begin{aligned}\Sigma\Delta E_{(v_1,\theta,\varphi)} &= -\,2\pi N(v_1,\,\theta,\,\varphi)\,G^2m_1m_2(m_1+m_2)\,\frac{V_g}{V^2}\cos\Phi\\ &\times\log\left(1+\frac{D_0^2\,V^4}{G^2(m_1+m_2)^2}\right)\,dv_1d\theta d\varphi dt\,.\end{aligned}\right\}\qquad(11)$$

If we adopt a spherical distribution of the velocities v_1 for purposes of averaging, equation (11) becomes (cf. I, eqs. [40] and [41])

$$\left.\begin{aligned}\Sigma\Delta E_{(v_1,\theta,\varphi)} &= -\,\tfrac{1}{2}N(v_1)\,G^2m_1\,m_2\,(m_1+m_2)\,\frac{V_g}{V^2}\cos\Phi\sin\theta\\ &\times\log\left(1+\frac{D_0^2\,V^4}{G^2(m_1+m_2)^2}\right)\,dv_1d\theta d\varphi dt\,.\end{aligned}\right\}\qquad(12)$$

The averaging of the foregoing equation over φ is immediate. To average over θ, we should first express

to incorporate in a satisfactory manner the $[D_0V^2/G(m_1 + m_2)]$ term within the framework of a theory which idealizes stellar encounters as two-body problems. The problems which we have to face in the present connection are several. First, if we retain the two-body approximation, the main contribution to $\Sigma\Delta E$ would arise, as we have already pointed out, from the random fluctuations which would give preference to certain values of Θ. Second, any error in estimating the "cut-off" distance D_0 will directly influence the results, and this, we may note, is contrary to our earlier experience in Parts I and II, where an uncertainty of a factor of 2 or 3 in D_0 introduced errors of less than 10 per cent. Third, the extreme importance of the dominant term in the present problem indicates that very great care should be exercised in including the distant encounters. And finally, if the distant encounters are as important as they appear to be, it would appear more profitable to abandon the two-body approximation of stellar encounters altogether and devise a more satisfactory statistical method. It is not the object of this note to go into these matters here. We wish only to draw attention to the fundamental difficulties which a proper discussion of stellar encounters must necessarily confront.

YERKES OBSERVATORY
September 18, 1940

V_θ, V, and $\cos\Phi$ in terms of θ. Using the relations (30), (31), and (35), and after some further reductions, we find

$$\left.\begin{aligned}\Sigma\Delta E_{v_1} = &-N(v_1)\,\frac{\pi G^2 m_1 m_2 (m_1 + m_2)}{2v_1 v_2}\,dv_1 dt \\ \times &\int_{|v_1 - v_2|}^{|v_1 + v_2|} \left[\frac{v_2^2 - v_1^2}{V^2} - \frac{m_1 - m_2}{m_1 + m_2}\right] \log\,(1 + q^2V^4)dV\,,\end{aligned}\right\} \tag{13}$$

where

$$q = \frac{D_0}{G(m_1 + m_2)}\,. \tag{14}$$

The integral occurring in equation (13) can be evaluated by the methods described in I and II (cf. pp. 294 and 295). We find

$$\Sigma\Delta E_{v_1} = -\,N(v_1)\,\frac{4\pi G^2 m_1 m_2}{v_1 v_2}\,dv_1 dt$$

$$\times \left\{\begin{array}{ll} \left[m_2 v_1 \log q\,(v_2^2 - v_1^2) - m_1 v_2 \log\dfrac{v_2 + v_1}{v_2 - v_1} + 2m_1 v_1\right] & (v_2 > v_1)\,, \\ \tfrac{1}{2}(m_2 - m_1)\,(\log 4qv^2 - 2)v & (v_2 = v_1)\,, \\ \left[-\,m_1 v_2 \log q(v_1^2 - v_2^2) + m_2 v_1 \log\dfrac{v_1 + v_2}{v_1 - v_2} - 2m_2 v_2\right] & (v_2 < v_1)\,. \end{array}\right\}, \tag{15}$$

THE RATIO OF INTERSTELLAR ABSORPTION TO REDDENING

J. L. GREENSTEIN AND L. G. HENYEY

ABSTRACT

Spectrophotometric investigations of reddened B stars have determined the law of variation of the interstellar absorption with wave length, except for an additive constant. The uncertainty as to the order of magnitude of any possible non-selective absorption appears in the ratio of absorption to reddening, a quantity of great practical importance. It is shown that the ratio of the intensities, at two wave lengths, of the total light from stars of a given type depends on the intrinsic color of the stars and on the ratio of the interstellar absorption coefficients at those two wave lengths. The ratio of the interstellar absorption coefficients at the two effective wave lengths of the photoelectric color indices determined by Stebbins, Huffer, and Whitford is evaluated in Table 1. The non-selective absorption is found to be small or zero. The ratio of photographic absorption to photoelectric color excess is found to be 8.1 ± 0.4.

I

In recent years several observational investigations have been carried out with the purpose of determining the law of selective absorption by interstellar matter. In these investigations spectrophotometric methods have been used to compare, at various wave lengths, the light of reddened B stars with that of normal stars. Such comparisons are capable of determining total absorption to within an additive constant; that is, they determine a function, $f(\lambda)$, such that the absorption, $A(\lambda)$, is given by an expression of the form

$$A(\lambda) = f(\lambda) + A_0 , \tag{1}$$

where A_0 is an unknown constant. These observations have, in fact, shown that $f(\lambda)$ is very nearly proportional to $1/\lambda$ in the observable region,[1, 2, 3] so that

$$A(\lambda) \propto \left(\frac{1}{\lambda} + \frac{a}{\lambda_0}\right) . \tag{2}$$

The last term in (2) contains the unknown constant, where for convenience we have written λ_0 as the photographic effective wave length.

The evaluation of the additive constant, or the constant a in (2), may be accomplished in principle through the determination of the total absorption in the line of sight at some wave length for such objects as have been examined spectrophotometrically. An equivalent method involves a determination of the ratio of the absorptions at two wave lengths. If we know the value of the ratio, say X, defined as

$$X = \frac{f(\lambda_2) + A_0}{f(\lambda_1) + A_0} , \tag{3}$$

we can determine A_0, since we know $f(\lambda)$. In the present investigation such a ratio is estimated from a suitably defined mean color excess of groups of stars.

[1] Stebbins, Huffer, and Whitford, *Ap. J.*, **90**, 209, 1939.

[2] Greenstein, *Ap. J.*, **87**, 151, 1938.

[3] Oort, *B.A.N.*, **8**, 248, 1938.

The problem of the determination of the additive constant is equivalent to the important problem of the determination of the ratio, R, of photographic absorption to color excess. If the colors are based on the effective wave lengths, λ_1 and λ_2, with $\lambda_1 > \lambda_2$, the ratio, R, is

$$R = \frac{A(\lambda_0)}{A(\lambda_2) - A(\lambda_1)} = \frac{f(\lambda_0) + A_0}{f(\lambda_2) - f(\lambda_1)} . \tag{4}$$

According to the observed law (2),

$$R = (1 + a) \frac{\frac{1}{\lambda_0}}{\frac{1}{\lambda_2} - \frac{1}{\lambda_1}} . \tag{5}$$

Evidently, R depends directly on the value of a.

II

The ratio of the absorptions at two wave lengths may be estimated from the ratio of the intensities, at the two wave lengths, of the total light reaching the earth from all stars of a given group. If $\epsilon(\lambda)$ is the volume coefficient of emission at wave length λ by the stars of the given group at distance r and if $k(\lambda)$ is the coefficient of absorption, the total intensity, $I(\lambda)$, of light arriving from the stars along some line of sight is

$$I(\lambda) = \int_0^\infty \epsilon(\lambda) e^{-\int_0^r k(\lambda) dr} dr .$$

Suppose that $\epsilon(\lambda)/k(\lambda)$ is constant along the line of sight. After introducing the optical depth $\tau(\lambda)$, we find

$$I(\lambda) = \frac{\epsilon(\lambda)}{k(\lambda)} \int_0^\infty e^{-\tau(\lambda)} d\tau(\lambda) = \frac{\epsilon(\lambda)}{k(\lambda)} = a(\lambda) . \tag{6}$$

It follows that for two wave lengths,

$$\frac{k(\lambda_2)}{k(\lambda_1)} = \frac{I(\lambda_1)}{I(\lambda_2)} \frac{\epsilon(\lambda_2)}{\epsilon(\lambda_1)} . \tag{7}$$

In practice, it is difficult to find any group of stars for which $a(\lambda)$ is constant over large distances. Certainly, for very large distances the emission must terminate. In or near the galactic plane, however, the assumption of constant $a(\lambda)$ is a useful first approximation. It must be remembered that variations of $a(\lambda)$ do not enter in full force into equation (7). Any variation will be partly canceled in the ratio of the two effective mean values of $a(\lambda)$. Later we shall estimate the errors involved in the assumption of constant $a(\lambda)$.

The ratio of intensities may be most accurately determined by the use of a table of color excesses for stars of the same intrinsic color. In such cases the ratio $\epsilon(\lambda_2)/\epsilon(\lambda_1)$ is given in terms of the intrinsic color index, C, by

$$\frac{\epsilon(\lambda_2)}{\epsilon(\lambda_1)} = 10^{-0.4C} ,$$

provided stars of magnitude zero are taken as the units of intensity at both wave lengths. The total intensity at any wave length is the sum of contributions, for each star, of the form

$$10^{-0.4m(\lambda)} . \tag{8a}$$

When $m(\lambda_2)$ is the blue magnitude and $m(\lambda_1)$ is the red magnitude,

$$m(\lambda_2) = m(\lambda_1) + C + E ,$$

where E is the color excess. The total intensity of light from stars of the group is obtained by a summation, over all the stars, of terms of the form of (8*a*), as

$$\frac{I(\lambda_1)}{I(\lambda_2)} = 10^{0.4C} \frac{\sum 10^{-0.4m(\lambda_1)}}{\sum 10^{-0.4m(\lambda_1)} \times 10^{-0.4E}} . \tag{8b}$$

Hence, from equation (7),

$$\frac{k(\lambda_2)}{k(\lambda_1)} = \frac{\sum 10^{-0.4m(\lambda_1)}}{\sum 10^{-0.4m(\lambda_1)} \times 10^{-0.4E}} . \tag{9a}$$

In other words, $k(\lambda_1)/k(\lambda_2)$ is the mean value of $10^{-0.4E}$, weighted according to the brightnesses of the stars:

$$\frac{k(\lambda_2)}{k(\lambda_1)} = (\overline{10^{-0.4E}})^{-1} = X . \tag{9b}$$

We can define a type of mean color excess of the total light of the stars of the group. It is given by

$$\overline{E} = -\tfrac{5}{2} \log_{10} (\overline{10^{-0.4E}}) . \tag{10}$$

The major assumption involved in this method of determining the ratio of two absorption coefficients is obviously the constancy of $a(\lambda)$ along the line of sight. Let us examine several typical variations of $a(\lambda)$ and estimate the error introduced by our assumption of constant $a(\lambda)$. From the equation for the intensity,

$$I = \int_0^\infty a e^{-\tau} d\tau ,$$

it is apparent that the effect of the variation of a depends strongly on the optical depth at which the variation occurs. Let us consider a model in which a decreases exponentially outward, i.e., a relative increase of absorption over emission, according to the relation

$$a = a_0 e^{-(\tau/t)} .$$

Then we find that the true intensity, I', is

$$I' = a_0 \int_0^\infty e^{-\tau} e^{-(\tau/t)} d\tau = a_0 \frac{t}{1 + t} . \tag{11}$$

In case t is unity, a drops to 0.37 of its local value, a_0, within an optical distance of 1 mag. In that case equations (6) and (11) show that $I' = 0.5I$. The variations of a in the galactic plane are probably smaller; and if we average over a wide range of galactic longitudes and distances, regions with high a (star clouds and clusters) and low a (dark nebulae) will partly balance. The error introduced into the value of $k(\lambda_2)/k(\lambda_1)$, by neglecting the variation of a, will be only 6 per cent even for $t = 1$ and 4 per cent for $t = 2$.

In order to study the effect of fluctuations in a, let us investigate another model in which the variation of a is a periodic function of optical depth from the sun. Such a model will probably represent the fluctuating conditions in the Milky Way, when we average over a wide range of longitudes. We assume that

$$a = a_0 \left(1 + b \sin \frac{\tau}{t} + c \cos \frac{\tau}{t}\right).$$

Then we find that

$$I' = a_0 \left(1 + \frac{bt + ct^2}{1 + t^2}\right). \tag{12}$$

The ratio of the intensities at two wave lengths will deviate by small amounts from that obtained with constant a. For example, if b or $c = \pm 0.5$, the maximum value of a will be three times the minimum value. Yet for $t = 0.2$, 0.5, and 1.0 the percentage errors in $k(\lambda_2)/k(\lambda_1)$ when $b = 0.5$ are only 1, 1, and 0 per cent; for $b = -0.5$ the errors are 0, 2, and 1 per cent, respectively. For $c = 0.5$ the errors are 2, 1, and 0 per cent; for $c = -0.5$ they are 4, 2, and 0 per cent. Since fluctuations corresponding to values of b or c greater than 0.5 are unlikely, we may safely conclude that the uncertainties arising from fluctuations of a are small.

III

The mean color excess, or the ratio of absorption coefficients, according to equations (9) and (10), may be evaluated only for those groups of stars for which the total absorption approaches a value effectively infinite within the magnitude range for which complete catalogues of color excesses are available. This limits our data very strongly, at present, to those stars which are intrinsically very luminous. If the integration in equation (6) is carried to a limiting optical thickness, τ', rather than to infinity, we find that

$$I' = a(1 - e^{-\tau'}).$$

In order to avoid an error greater than 4 per cent in the ratio of intensities at two wave lengths, τ' must exceed 2. In other words, we require completeness to a distance of the order of 2000 parsecs, or a modulus (including absorption) of 13.5 mag. Since spectral classifications become incomplete around magnitude 8.5, the incompleteness sets in for stars fainter than absolute magnitude -5. It follows that the method must necessarily be limited to supergiants and early B stars. While the limit of incompleteness for the supergiants is less than 8.5, these are, at the same time, considerably brighter[4] intrinsically. As is well known, the number of apparently faint B stars is small, and their contribution to the total light of the B stars is found to be negligible. The high galactic concentration of the B stars also helps to insure that the total absorption in the line of sight is very large. With the conventionally adopted value of the thickness of the absorbing layer in the Galaxy, the line of sight to B stars within 5° of the galactic plane lies wholly within the absorbing medium.

[4] Greenstein, *Proc. Nat. Acad. Sci.*, **26**, 259, 1940.

The catalogue of 1332 photoelectric color excesses of B stars by Stebbins, Huffer, and Whitford[5] affords a homogeneous set of color excesses for early-type B stars in the accessible regions of the Milky Way, i.e., all O–B2 stars north of $-40°$ in the *Henry Draper Catalogue*. The color excesses of the stars in the catalogue have been determined with reference to the colors of bright and presumably unreddened standard stars. The stars were treated in several groups of spectral type and galactic longitude, as listed in Table 1. The stars were grouped and counted according to apparent visual magnitude, within intervals of 1 mag., and according to color excess within intervals of 0.1 mag. A numerical summation was performed to obtain the total light-intensity for each group, as well as the summation of the intensity multiplied by $10^{-0.4E}$, according to equation (9*a*). Only stars within galactic latitudes $\pm 5°$ were used. The total intensity was found to be well determined by the available stars for the supergiants and O–Bo stars and fairly well determined for the O–B2 stars. For B1–B3 the incompleteness of the catalogues for stars fainter than the eighth magnitude results in an underestimation of the total intensity and of the mean reddening.

TABLE 1

MEAN REDDENING OF THE LIGHT OF THE B STARS

Type	Galactic Longitude	$\frac{k(\lambda_2)}{k(\lambda_1)}$	$\overline{E}$	n
cB–cA	310°–230°	1.154	+0^m.16	54
O–Bo	310 – 60	1.181	.18	101
O–Bo	60 –230	1.100	.10	86
O–Bo	310 –230	1.134	.14	187
Bo–B2	310 –230	1.124	.13	340
B1–B3	310 –230	1.067:	+0.07:	300

The last column of Table 1 contains the number of stars involved in each determination. Two stars, α Cyg and γ Cas, have been excluded because of their great apparent brightness and correspondingly excessive weight in the solution. The effect of the incompleteness of the catalogue for B1–B3 should be noted. To a given limiting magnitude those stars will be observed which have suffered less than average absorption and therefore less reddening. The resultant mean color will be too blue. The adopted mean value of the ratio of the absorptions, X, has been obtained from the data of Table 1 by giving the results for the cB–cA stars weight 3, the O–Bo stars weight 2, and the Bo–B2 stars weight 1. We obtain the value

$$X = \frac{k(\lambda_2)}{k(\lambda_1)} = 1.142 \pm 0.009 .$$

If the normal color indices adopted in the system of photoelectric color excesses should require correction by a quantity δE, the mean color $\overline{E}$ should be decreased by δE. It seems improbable that δE can exceed 0.03 mag. for our groups of stars. Any absolute magnitude effects in the intrinsic color indices of the stars will affect the color excesses and therefore our results. It is thought that such absolute magnitude effects are also small.[2, 3]

In order to interpret our results, we shall require the effective wave lengths of the photoelectric color indices. They are given as $\lambda_1 = 4710$ A, $\lambda_2 = 4170$ A, for stars of color temperature 20,000° and as $\lambda_1 = 4770$ A, $\lambda_2 = 4260$ A, for color temperature 6000°.

[5] *Ap. J.*, **91**, 20, 1940.

The B stars which have most weight in our solutions possess an intermediate color temperature, and we shall adopt the values $\lambda_1 = 4740$ A and $\lambda_2 = 4215$ A. We also require the photographic effective wave length, a quantity which depends strongly on the telescope and plate used. On the international scale it is often given as $\lambda_0 = 4250$ A; for convenience in the analysis we shall take $\lambda_0 = \lambda_2 = 4215$ A. If the interstellar absorption coefficient were strictly proportional to $1/\lambda$ and if there were no additive constant in (2), we would expect $k(\lambda_2)/k(\lambda_1)$ to be equal to 1.125. We will show that the close agreement of this value with the observed ratio indicates that the non-selective absorption is small.

Let us assume that the interstellar absorption coefficient varies according to (2) and determine the additive constant a from our observed value of the ratio, X, Then

$$X = \frac{\frac{1}{\lambda_2} + \frac{a}{\lambda_0}}{\frac{1}{\lambda_1} + \frac{a}{\lambda_0}} .$$

Since we have taken $\lambda_0 = \lambda_2$, we find that

$$\frac{X}{X - 1}\left(1 - \frac{\lambda_0}{\lambda_1}\right) = 1 + a . \tag{13}$$

The value of a is found to be -0.13 ± 0.05. The mean error is probably an underestimate, since we have not included the effect of errors of interpretation such as arise from variations of a. In any case we may safely assert that a is a small quantity and that the non-selective absorption is small. The negative sign of a requires that the absorption become zero at 32,000 A. No physical reality need be ascribed to such behavior, since we have no evidence as to how far into the infrared the $1/\lambda$ variation continues.

We may evaluate directly from our observed ratio of absorption coefficients the ratio, R, of photographic absorption to color excess. We require no information concerning the form of the dependence of the absorption coefficient on wave length. From equation (4) we can show that

$$\frac{f(\lambda_0) + A_0}{f(\lambda_0) - f(\lambda_1)} = R = \frac{X}{X - 1} . \tag{14}$$

We obtain, finally,

$$R = 8.1 \pm 0.4 .$$

Again, the uncertainty of R is larger than the mean error. We estimate that the total uncertainty in R is of the order of ± 0.8.

The new method presented here for the determination of the ratio of absorption to reddening has several advantages in principle over other methods. For example, spectrophotometric results alone can only establish[3] that $5.5 < R < \infty$. Spectrophotometric results, combined with estimates of the total absorption,[2] require some knowledge of the absolute value of the general interstellar absorption coefficient. If other complete catalogues of the colors of highly luminous stars can be obtained, it should be possible to evaluate more accurately the ratio of absorption to reddening.

YERKES OBSERVATORY
August 1940

THE RECENT SHELL SPECTRUM OF γ CASSIOPEIAE

RALPH B. BALDWIN

ABSTRACT

Spectrograms of γ Cassiopeiae taken since the early part of 1939 give evidence of an extensive outer shell of gas. Strong absorption lines of *H*, *He* I, and *Fe* III are produced in the shell. Weaker lines of other elements are also found. The lines show that there is an appreciable dilution of the photospheric radiation. An analysis of the shell spectrum is given.

The star, γ Cassiopeiae, is one of the most interesting objects, since it continually undergoes new and unexpected changes which may affect the appearance of the entire spectrum, continuous, emission, and absorption. An example of the changes is the development of the third shell spectrum starting early in 1939.

An analysis of this sharp and strong absorption spectrum revealed that it was similar to, but much more intense than, the shell spectrum of 1936.[1] In the second shell hydrogen and helium were the only elements to appear strongly. In the spectrum of the third shell the lines of the light gasses were again present but were supplemented by a host of weaker lines, among which those of *Fe* III were prominent.[2] *O* III, *Ni* II, *Al* III, and *N* II may have contributed weak lines. The H and K lines of *Ca* II were present and were probably blends of the stellar and interstellar lines. Interstellar sodium and ionized titanium were not found.

Neither *Si* II nor *Mg* II were found; hence the dilution of radiation was considerable, and the shell absorption occurred at an appreciable height above the effective photosphere.

An application of the method of Struve and Wurm[3] to the helium lines of the 1936 shell gave 3 radii as the lowest value which could be assigned to the height of the shell.[1] This value was a lower limit and not an exact figure because the emission in the $2^1P^0 - 1^1S$ transition could not be taken into account. An intercomparison of the metastable and the nonmetastable singlet levels of helium shows that the dilution of radiation was not as great in the latest shell stage as it was in 1936. However, the visible helium emission lines were very much weaker than in 1936. Consequently, the shell was nearer to the minimum height which could be derived by such an intercomparison. A preliminary estimate places the shell at 2 to 3 radii from the photosphere.

The conditions of excitation which are shown in the shell spectrum are higher than are compatible with the appearance of the *Mg* I lines, λ 3829 and λ 3838. However, two weak lines were measured near those wave lengths, while none was measured near λ 3832, the third member of the *Mg* I triplet. This is to be expected under conditions of dilute radiation, as the lower level of λ 3832 may be depopulated by direct transitions to the ground level of the atom, while the lower levels of the other two lines of the triplet will act as though they were metastable.

Numerous absorption lines were found in γ Cassiopeiae having wave lengths similar to those of unidentified lines in the 1914 shell spectrum of ζ Tauri. In an unpublished study of the latter star the author found about five hundred absorption lines in the photographic region. Most of them were very sharp and arose in the shell. They consisted of *H*, *Fe* II, *Ni* II, *Ti* II and other elements requiring similar excitation. Other lines in the spectrum were not as sharp. They were classified on a scale of 1–5, the former

[1] Baldwin, *Ap. J.*, **92**, 97, 1940.

[2] Struve, Elvey, *Pub. A.S.P.*, **52**, 140, 1940.

[3] *Ap. J.*, **88**, 84, 1938.

Table 1

Shell Absorption Lines in the Ultraviolet Region

December 8, 1939. Corrected for velocity of +17 km/sec

Measured λ (I.A.)	Int	Identification	Measured λ (I.A.)	Int	Identification	Measured λ (I.A.)	Int	Identification
3065.06	2		3333.42	1	OIII 3.00 (4)c	3515.82	0	
86.31	2	FeIII 6.31 (6)	35.28	3		24.72	1	
3106.86	2		38.37	3		28.86	0	
36.24	1	FeIII 6.43(10)	39.33	4	FeIII 9.36(10)	30.58	2	HeI 0.49 (-)
44.61	0		47.79	1	FeIII 7.70 (8)	54.38	5	HeI 4.44 (1)
73.78	2	FeIII 4.09(10)	54.45	5	HeI 4.52 (1)			4.57 (1)
75.92	2	FeIII 6.00(10)	96.65	0	FeIII 6.71 (7)	56.96	2	τ Scorpii
78.13	1	FeIII 8.03(10)	3400.69	1		70.55	2	
87.64	13	HeI 7.74 (8)	03.82	1		86.00	2	FeIII 6.12 (9)
90.53	0	FeIII 0.81 (8)	15.50	0?		87.40	3	HeI 7.28 (2)
94.43	1		18.39	0				7.42 (1)
96.78	0	HeI 6.68 (1)	20.02	1	10 Lacertae	99.26	1	HeI 9.32 (1)
3204.72	1	FeIII 4.76 (6)	42.30	0?				9.46 (1)
11.94	4	HeI 1.50 (1)b	47.50	7	HeI 7.59 (2)	3600.24	0	FeIII 9.49 (3)c
26.43	0		49.82	1	HeI 0.22 (-)	00.89	2	FeIII 0.93(10)
31.48	1	HeI 1.20 (1)	52.01	0	HeI 3.21 (-)			AlIII 1.62 (6)b
48.01	1		54.25	2		03.18	0?	
58.01	1	HeI 8.30 (1)	56.78	0	HeI 6.79 (-)	03.80	3	FeIII 3.88 (9)
60.54	1	OIII 0.98 (8)	60.75	1	HeI 0.94 (-)	12.00	1	AlIII 2.35 (4)
63.58	0?	FeIII 2.44 (6)c	65.80	2	HeI 5.91 (-)	12.76	0	
65.56	2	OIII 5.46(10)	69.99	1	FeIII 0.26 (4)	13.59	7	HeI 3.64 (3)
66.58	4	FeIII 6.88(20)	72.00	2	HeI 1.80 (-)	18.02	3	
		OIII 7.31 (5)b	75.66	2	τ Scorpii	21.51	1	
71.76	0		79.12	1	HeI 8.97 (-)	26.32	0	
75.99	6	FeIII 6.08(15)	82.07	2	FeIII 2.36 (4)	29.71	0	
79.79	1	FeIII 0.58 (6)	87.52	1	HeI 7.72 (-)	30.54	0	
85.14	0		90.18	2		31.79	2	
88.39	6	FeIII 8.81(15)	91.78	1		33.29	2	γ Pegasi
92.62	2	FeIII 2.04(8-)	98.94	1	HeI 8.64 (-)	34.19	7	HeI 4.24 (2)
94.55	0	FeIII 4.50 (4)	3500.18	1	FeIII 9.57 (7)			4.37 (1)
96.95	2	HeI 6.76 (1)			0.29 (7)	36.75	0?	
3304.01	0	FeIII 4.31 (9)	02.48	2	FeIII 1.75 (8)	46.52	1	
05.27	2	FeIII 5.22(10)	05.10	1		48.78	2	
09.80	0	FeIII 9.40 (6)	06.82	0	FeIII 6.93 (5)	49.76	2	γ Pegasi
25.51	1	FeIII 4.72 (3)c	08.78	0		52.05	1	HeI 2.00 (1)a
29.72	0	FeIII 9.89 (7)	12.77	3	HeI 2.51 (-)			2.12 (1)
								FeIII 2.65 (6)b

Table 3

Shell Absorption Lines in the Visual Region

October 17, 1939. Corrected for velocity of +4 km/sec

Measured λ (I.A.)	Int	Identification	Measured λ (I.A.)	Int	Identification	Measured λ (I.A.)	Int	Identification
4879.75	0		5198.02	1		5901.10	0?	
99.17	3	ζ Tauri	5213.19	1		32.47	0	NII 1.79 (7)c
4906.40	1	ξ Tauri?	19.90	0		42.34	0?	NII 1.67 (8)c
21.70	5	HeI 1.93 (4)	5326.38	0		93.31	1	
5015.47	4	HeI 5.68 (6)	32.31	1		6026.98	1	
48.21	2	HeI 7.74 (2)	45.27	2		6140.04	0	
63.73	0	FeIII 3.4 (2)	76.22	0		52.10	0?	
73.50	0	FeIII 3.78 (3)	5434.11	1		6207.67	2	
86.80	0	FeIII 6.7 (3)	44.40	0		26.45	0	
5114.24	0?	FeIII (pred.)	5551.71	2		6410.65	2	
26.16	2	FeIII 7.3 (6)	5652.96	1		6514.97	2	
56.81	1	FeIII 5.97 (4)	5777.66	0		62.49	0	Hδ 2.82 Hα
		7.85 (4)	5846.56	0				
93.82	0	FeIII 3.90 (4)	76.47	5	HeI 5.62(10)			
		4.43 (4)			5.96 (1)			

Table 2

Shell Absorption Lines in the Photographic Region

February 2, 1940. Corrected for velocity of -2 km/sec

Measured λ (I.A.)	Int	Identification	Measured λ (I.A.)	Int	Identification	Measured λ (I.A.)	Int	Identification
3658.81	0	H34 8.64	3837.88	2	HeI 8.09 (1)	4141.41	0	ζ Tauri
59.57	0	H33 9.42			MgI 8.50(100)d	43.78	7	HeI 3.77 (2)
60.32	0	H32 0.28	45.62	2	ζ Tauri	55.87	1	
61.22	0	H31 1.22	49.47	0	NiII 9.54 (2)	68.39	0	HeI 8.97 (1)
62.32	0	H30 2.26	59.47	0	ζ Tauri	72.36	0	
63.41	1	H29 3.40	67.47	3	HeI 7.46 (2)	86.62	0	ζ Tauri
64.63	1	H28 4.68			7.62 (1)	4222.45	0	FeIII 2.39 (8)
66.00	1	H27 6.10	68.91	1		25.55	0	
67.54	2	H26 7.68 Hω	70.16	1		29.76	0	
68.39	1		71.84	3	HeI 1.80 (1)	40.78	0	
69.39	3	H25 9.47 Hψ	78.20	0	HeI 8.18 (1)	44.39	1	NiII 4.81 (1)
71.28	4	H24 1.48 Hχ	80.40	1		48.41	1	ζ Tauri
73.70	5	H23 3.76 HΦ	88.80	25	HeI 8.65(10)	56.02	1	
76.47	6	H22 6.36 Hυ			H8 9.05 Hζ	66.24	2	CII 7.02 (8)c
79.40	7	H21 9.36 Hτ	3901.72	2	ζ Tauri?			7.27(10)c
82.80	7	H20 2.81 Hσ	04.68	1	ζ Tauri	69.37	1	
84.75	1		14.03	0		74.48	1	
85.62	0		26.60	5	HeI 6.53 (1)	4340.57	18	H5 0.48 Hγ
86.83	8	H19 6.83 Hρ	27.73	2	ζ Tauri	52.45	3	FeIII 2.70 (4)
88.84	1	ζ Tauri	28.84	1		66.18	1	
91.54	8	H18 1.56 Hτ	29.68	2		72.03	2	FeIII 2.41(20)
97.12	8	H17 7.15 Ho	31.16	3	ζ Tauri?	80.76	0	
3703.92	9	H16 3.86 Hι	32.48	2	ζ Tauri	82.27	0	FeIII 2.5(comp)
05.07	11	HeI 5.00 (3)	33.65	3	CaII 3.68(400)	88.03	9	HeI 7.93 (3)
		5.14 (1)	35.86	1	HeI 5.91 (1)	91.54	0	
11.98	10	H15 1.97 Hυ	39.79	0		95.91	2	FeIII 5.78 (6)
21.98	12	H14 1.94 Hμ	54.42	1	ζ Tauri?	97.70	1	ζ Tauri
24.24	2	ζ Tauri?	60.08	0		99.95	1	ζ Tauri?
33.11	0	HeI 2.85 (1)	64.71	12	HeI 4.73 (4)	4402.05	0	ζ Tauri
		2.99 (1)	68.48	1	CaII 8.49(350)	08.09	0	
34.43	13	H13 4.37 Hλ	70.08	19	H7 0.08 Hι	12.13	1	χ Tauri
41.22	0		97.39	0		15.72	1	
47.55	0		4000.76	0		19.58	4	FeIII 9.59(10)
50.21	14	H12 0.15 Hκ	04.98	2		27.46	2	ζ Tauri
56.02	2	HeI 6.09 (1)b	09.52	5	HeI 9.27 (1)	30.96	3	FeIII 0.95 (7)
57.96	3		23.90	2	HeI 3.99 (1)	34.79	1	χ Tauri
59.83	0	OIII 9.87 (9)	26.21	13	HeI 6.19 (5)	37.87	2	HeI 7.55 (1)
63.93	1				6.36 (1)	56.52	0	χ Tauri
68.03	0	HeI 8.80 (1)	47.44	0		71.65	15	HeI 1.48 (6)
70.71	15	H11 0.63 Hι	52.14	0				1.69 (1)
75.36	0		54.29	0	ζ Tauri?	76.80	1	
84.83	2	HeI 4.88 (1)	55.38	0		80.19	0	
92.57	1	χ Tauri	66.92	1	NiII 7.04 (3)	90.50	1	
97.97	17	H10 7.90 Hθ	70.15	1	ζ Tauri?	4502.96	0	ζ Tauri
3805.73	0	HeI 5.75 (1)	71.66	0	ζ Tauri	09.70	1	
06.35	2		78.92	2	ζ Tauri	15.55	2	
20.04	14	HeI 9.61 (4)	86.85	0	ζ Tauri	20.80	0	
		9.75 (1)	92.61	0	ζ Tauri	40.70	0	
22.42	3		4101.72	19	Hδ 1.75 Hδ	55.27	1	
28.91	1	MgI 9.37(40)d	20.84	5	HeI 0.81 (3)	67.60	0	
30.67	0	ζ Tauri			0.98 (1)	4697.27	3	ζ Tauri
33.53	3	HeI 3.56 (1)	25.01	0		4713.27	7	HeI 3.14 (3)
35.41	18	H9 5.39 Hη	27.07	0				3.37 (1)
						51.80	3	
						4861.36	12	H4 1.34 Hβ

Table 4

Hydrogen and Helium Series

Hydrogen	λ6562.82, $2^2S - 3^2P^o$, to λ3658.64, $2^2S - 34^2P^o$
Helium	λ5015.68, $2^1S - 3^1P^o$, to λ3196.68, $2^1S - 12^1P^o$
	λ3888.65, $2^3S - 3^3P^o$, to λ3187.74, $2^3S - 4^3P^o$
	λ5047.74, $2^1P^o - 4^1S$, to λ3838.09, $2^1P^o - 10^1S$
	λ4713.20, $2^3P^o - 4^3S$, to λ3599.39, $2^3P^o - 9^3S$
	λ4921.93, $2^1P^o - 4^1D$, to λ3756.09, $2^1P^o - 14^1D$
	λ5875.65, $2^3P^o - 3^3D$, to λ3450.22, $2^3P^o - 21^3D$

being the sharp shell lines and the latter being the rotationally broadened hydrogen and helium lines. On the rotational model the broader the absorption line the lower in the atmosphere it is produced and, presumably, the higher the state of excitation.

Of the unidentified lines present in both γ Cassiopeiae and ζ Tauri, a majority were estimated to be of width 2 in the latter. Hence they were produced lower in the atmosphere, under conditions of higher excitation than the sharp shell lines.

The γ Cassiopeiae shell lines indicate a higher state of excitation than do the ζ Tauri shell lines, i.e., there is strong *Fe* III and no *Fe* II in the former and strong *Fe* II with weak *Fe* III in the latter. Therefore the identification of many of the broader lines in ζ Tauri with shell lines in γ Cassiopeiae is probable.

The spectra of the doubly ionized metals such as *Ti* III, *Ni* III, and *Cr* III are practically unknown. It is entirely possible that many of the unidentified absorption lines arise from metastable levels in these atoms and others of similar ionization potentials.

In the table of lines *a* designates a major contributor, *b*, a minor contributor, *c*, an identification which is inadequate or doubtful; *d* shows that the excitation energy required is much less than that indicated by remainder of shell spectrum. The lines in 10 Lacertae, τ Scorpii, and γ Pegasi are from "The Ultraviolet Spectra of A and B Stars" by Struve (*Ap. J.*, **90**, 699, 1939). The lines in ζ Tauri are from the author's unpublished study of that star's shell spectrum.

From an inspection of the tables of lines in the shell spectrum of γ Cassiopeiae, Dr. P. Swings compiled a list of suggested identifications of *Fe* III lines additional to those already given in Tables 1, 2, and 3. Most of these identifications are given in the following table.

Measured λ (I.A.)	Int.	Identification	Notes*	Measured λ (I.A.)	Int.	Identification	Notes*
3065.06	2	*Fe* III 5.60 (4)	.....	4000.76	0	*Fe* III 0.83 (4)	.....
3211.94	4	*He* I 1.50 (1)	*b, e*	4070.15	1	*Fe* III 0.53 (3)	.....
		Fe III 2.05 (10)	*a*	4092.61	0	*Fe* III 2.43 (3)	.....
3279.79	1	*Fe* III 9.67 (6)	*a*	4141.41	0	*Fe* III 1.63 (2)	.....
		0.58 (6)	*a, e*	4186.62	0	*Fe* III 6.50 (4)	.....
3325.51	1	*Fe* III 4.72 (3)	*a*	4240.78	0	*Fe* III 0.71 (4)	.....
		4.93 (3)	*a*	4244.39	1	*Fe* III 3.85 (8)	.....
		5.41 (2bl)	*b*	4248.41	1	*Fe* III 8.58 (4)	.....
3333.42	1	*O* III 3.00 (4)	*c, e*	4266.24	2	*Fe* III 6.88 (5)	.....
		Fe III 3.27 (3)	*a*	4366.18	1	*Fe* III 5.56 (3)	.....
3338.37	3	*Fe* III 8.72 (7)	.....	4408.09	0	*Fe* III 7.94 (2)	.....
3454.25	2	*Fe* III 4.35 (3)	.....	4480.19	0	*Fe* III 9.60 (2)	*a*
3515.82	0	*Fe* III 5.57 (5)	.....			0.57 (2)	*a*
2524.72	1	*Fe* III 4.15 (3)	*a*	4567.60	0	*Fe* III 7.41 (4)	*a*
		5.17 (3)	*a*			7.83 (4)	*a*
3612.00	1	*Fe* III 1.72 (3)	*a*	5198.02	1	*Fe* III 8.95 (4)	.....
		Al III 2.35 (4)	*c, e*	5376.22	0	*Fe* III 5.68 (5)	.....

* Notes *a*, *b*, and *c* have same meanings as for Tables 1–3. Note *e*, previously identified.

The spectrograms were loaned by the Observatory of the University of Michigan. They were taken with the one-prism spectrograph and the new ultraviolet spectrograph recently constructed in the observatory machine shop. The author wishes to express his appreciation to that observatory and to Dr. Struve, director of the Yerkes Observatory, for sending reproductions of ultraviolet spectra of γ Cassiopeiae, taken at the McDonald Observatory during the shell stage.

DEARBORN OBSERVATORY
NORTHWESTERN UNIVERSITY
October 14, 1940

THE SPECTRUM OF THE NIGHT SKY*

C. T. ELVEY, P. SWINGS, AND WALTER LINKE

ABSTRACT

A conservative list of lines in the spectrum of the night sky is given, using spectrograms obtained at the McDonald Observatory with the nebular spectrograph. The identifications are discussed, and the attention of the laboratory spectroscopists is called to the various experimental problems connected with this question. The main features of the spectrum of the night sky are represented by the atomic lines of *Na* I and [*O* I] and the band spectrum of N_2, particularly the Vegard-Kaplan and the First Positive systems.

Estimates of the relative intensities of some of the lines in the spectrum of the night sky show that the sodium line is weak during the summer. Also, it was found that the sodium line was enhanced in a luminous area of the night sky. The estimates of intensities of the forbidden oxygen lines show that the red line, λ 6300, is very strong at the end of twilight and decreases to a more or less constant value around midnight, while the green auroral line shows the tendency to reach a maximum shortly after midnight, as many others have observed.

Many descriptions of the spectrum of the night sky have been published in recent years and also, many lists of lines and identifications. Some of these lists contain a large proportion of uncertain lines, and a careful examination of our material has convinced us that many of the announced lines do not actually exist on our spectrograms. This may be due to the fact that the spectrum of the night sky may be accidentally richer at certain locations and at certain times; or, it is possible that techniques in observing, measuring, and reducing the material have given erroneous results. Because of this uncertainty in part of the collected materials, tentative identifications and discussions have appeared which are without sound bases.

It has seemed to us that it would be useful to publish a conservative list of lines in the spectrum of the night sky (table 5) which could be a basis for future discussion of the fundamental features. The table is preceded by a discussion of the identifications. The main purpose of this attempt is to call the attention of the spectroscopists to the various experimental problems connected with this question. Our identifications will be based exclusively on our list and on one by H. W. Babcock[1] for the wave lengths greater than 5000 A. No attempt will be made to give a critical discussion of the previous publications or to give a complete bibliography,[2] as this would require too much space.

We will also give some preliminary results of intensity variations in the spectrum of the night sky obtained from spectrograms taken with the nebular spectrograph in the survey for emission nebulosities in the Milky Way.

The spectrograms under discussion were obtained with the nebular spectrograph of the McDonald Observatory, a description of which has been given by Struve, Van Biesbroeck, and Elvey.[3] The light from the sky is picked up by the narrow mirror which acts as the slit of the spectrograph and which is on an equatorial mounting and is reflected to a stationary mirror located 75 feet along the polar axis, which, in turn, sends the beam of light back to an objective-prism camera mounted on the polar axis with the slit. The long distance of the slit, 150 feet, makes a collimating lens unnecessary. Two quartz prisms and an f/1 Schmidt camera are used, thus making an instrument especial-

* *Contributions from the McDonald Observatory, University of Texas*, No. 29.

[1] *Pub. A.S.P.*, **51**, 47, 1939.

[2] For references earlier than 1935 see G. Dejardin, *Rev. Mod. Phys.*, **8**, 1, 1936. For more recent work see J. Gauzit, *Ann. d'Ap.*, **1**, 334, 1938, and M. Nicolet, *Mémoires de l'Institut royal météorologique de Belgique*, Vol. **9**, 1939, and *Bull. Acad. R. Belgique*, **25**, 81, 1939.

[3] *Ap. J.*, **87**, 559, 1938.

ly useful in the near ultraviolet. The correcting plate of the Schmidt camera is of ultraviolet glass which begins to lose transparency around λ 3200; thus the far ultraviolet regions are rather weak on our spectrograms.

The linear dispersion varies from 115 A per millimeter at λ 3200 to 500 A per millimeter at λ 5000. The slit as imaged on the spectrogram has a width of 0.04 mm, and thus, considering the dispersion, the effective width of the slit is about 5 A at λ 3200 to 20 A at λ 5000. Band structure or close lines cannot be resolved, and consequently the identification of some of the lines cannot be made with very great certainty.

Five spectrograms of the night sky with exposures ranging up to 9 hours have been used for the determinations of wave lengths. A comparison spectrum of mercury was impressed on the spectrograms by placing a mercury tube in the center of the slit of the nebular spectrograph.

The spectrograms were measured on a Gaertner measuring-machine, and the wave lengths were determined by a graphical method, inasmuch as the diffuse character of the lines did not warrant a more refined method. To help construct a standard dispersion curve, we used spectra of the iron arc, the Balmer lines of hydrogen in stellar spectra, and the ozone spectrum found on spectrograms of stars exposed for the far ultraviolet region. One of the spectrograms of the night sky is shown in Plate XIV. Two prints of the same spectrogram are placed side by side in order to help separate the faint detail from defects of the plate. In the reproduction processes two or three of the faint lines at the violet end of the spectrum have been lost. We have measured only details which we feel reasonably certain to represent lines. No attempt has been made to measure the lines from microphotometric tracing, for it has been our experience that a line cannot be detected with any certainty on a tracing unless it can be seen by a visual inspection of the spectrogram.

The measured wave lengths of the lines observed on our spectrograms are in the first column of Table 5, along with the mean errors of the wave length whenever a line has been measured on two or more plates. In case it has been measured on only one spectrogram, a mean error is not shown; and in those cases where the wave length is quite uncertain, owing to the faintness of a line being measured on only one spectrogram, it is inclosed in parentheses.

Two good spectrograms were obtained with the nebular spectrograph, using glass prisms, thus resulting in a linear dispersion about twice that of the quartz prisms. These were measured from λ 3900 to the red end of the spectrum and are included in Table 5.

The wave lengths of the three principal lines in the red-green region of the spectrum—λλ 6300, 5893, and 5577—have been assumed, since so much more accurate values exist.

In the second column of Table 5 are listed the estimated intensities of the lines and a brief description of their character. The remainder of the table is devoted to the identifications, which are being discussed in the following sections.

ATOMIC LINES

Besides the forbidden transitions of [*O* I], λλ 5577, 6300, and 6364, and the D lines of *Na* I, there is also some evidence, though not quite conclusive, in favor of the second line of the principal series of *Na* I, λ 3303, $3s^2S - 4p^2P^o$.

The line measured by H. W. Babcock[1] near λ 6401 is certainly not the component $^3P_0 - {}^1D_2$ of the nebular transition of [*O* I] at λ 6392, which should be extremely weak compared with λ 6364 of the same transition.

Many discussions have been published recently concerning the presence in the spectrum of the night sky of the forbidden line[4] $^4S_{3/2} - {}^2P_{3/2,\,1/2}$ of [*N* I] at λ 3466.5. That

[4] This is actually a doublet, but the separation of the two components of ^2P is only of the order of 0.5 cm^{-1}. A search for the transition, of auroral type λ 10,407, in the spectrum of the night sky would be interesting.

PLATE XIV

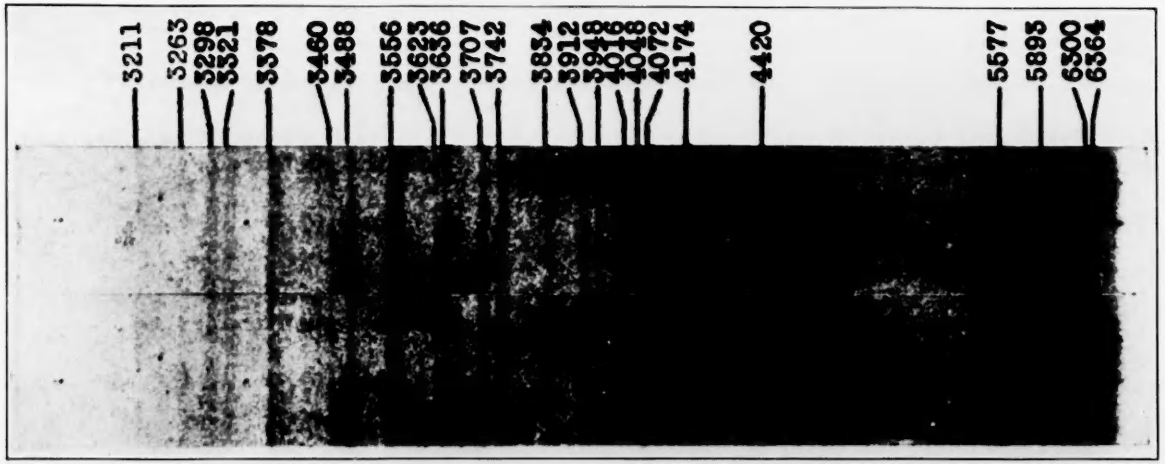

THE SPECTRUM OF THE NIGHT SKY

UNIV. OF MICH.

there is no line of appreciable intensity at that wave length is certain, as our line λ 3460 ± 1 A is narrow, and an error of measurement of 6 A is excluded in that region.

A systematic discussion of all forbidden and permitted atomic transitions has revealed no other reliable identification.[5] This is similar to the results of M. Nicolet[6] concerning the spectrum of the aurora borealis.

MOLECULAR BANDS

The main role in the spectrum of the night sky is played by the molecules, and especially by N_2; however, the identifications are in many cases still very uncertain. The first reason is observational, owing to the low dispersion and the low resolving-power available; however, in this regard we feel that our material is among the best collected so far. A second reason is our ignorance concerning the mechanism of excitation; even if we suppose that we know the general type of excitation, it does not seem safe to assume a priori any distribution on the rotational and vibrational levels. It seems that the rotational distribution corresponds to a low temperature, from 200° to 300° K; but different systems may be excited by different mechanisms or at various altitudes, and the distribution on the excited levels may differ widely from the thermodynamic equilibrium at the low kinetic temperature of the emitting regions. We also know that the excitation process may give rise to a strong selectivity among the vibrational transitions.

It would be interesting to compute systematically all the intensity distributions in the bands, assuming a low temperature—say 250° K. This could be done according to the general procedure followed by Swings and Nicolet,[7] or by Dufay,[8] for the spectra of comets. For the following discussion these complete calculations have not been made, and the effect has only been roughly estimated.

N_2 molecules.—All of the band systems of N_2 have been examined in order of increasing electronic excitation.

The Vegard-Kaplan system, $A^3\Sigma \rightarrow X^1\Sigma$, is similar to the atmospheric absorption bands of O_2, the upper level being metastable in both cases. The Vegard-Kaplan bands are degraded to the red in the laboratory, but in our present knowledge of the excitation processes in the high atmosphere it would be dangerous to assume that those in the spectrum of the night sky should show a sharp violet head. According to reliable identifications, the Vegard-Kaplan bands do not show any conspicuous structure on our spectrograms. This may be expected on a very low dispersion spectrogram of a low temperature emission.

The presence of the Vegard-Kaplan bands in the spectrum of the night sky seems quite certain, but some of the identifications still remain doubtful, owing partly to the fact that we had to use mostly calculated wave lengths. It is very desirable to obtain more laboratory information concerning these bands, particularly the relative intensities of those transitions observed in the spectrum of the night sky.

A first attempt in that direction has been made recently by R. Bernard,[9] who was able to excite the Vegard-Kaplan bands by electronic collisions. The bands are especially strong in the presence of a great excess of argon, and the sequences $v'' - v' = 10, 11, 12, 13$, are then as prominent as they are in the spectrum of the night sky. Bernard has given preliminary intensity estimates of the various vibrational transitions. Considering

[5] Our spectrograms exclude emissions such as *He* I, *Fe* II, etc., in interstellar space as well.

[6] *Ann. d'Ap.*, **1**, 381, 1938.

[7] *Ap. J.*, **88**, 173, 1938. [8] *Ap. J.*, **91**, 91, 1940.

[9] *Ann. d. Phys.*, **13**, 1, 1940. O. R. Wulf and E. H. Melvin (*Phys. Rev.*, **55**, 687, 1939) have recently succeeded in exciting the Vegard-Kaplan bands in N_2 at atmospheric pressure and at a temperature which is practically that of the walls. The (0-5), (0-6), (1-4), and (1-5) transitions show a rotational structure which has been measured.

the laboratory and the observational techniques, the agreement with our observations is rather satisfactory.

If we introduce our identifications in a vibrational diagram, we obtain Figure 1. The Condon parabola is quite displaced, as compared with the theoretical curve computed by J. Gauzit;[10] but on the other hand, it agrees with Gauzit's observations. The shift is due to the fact that we are already dealing with fairly high vibrational levels, v.

The First Positive system, $B^3\Pi \rightarrow A^3\Sigma$, is especially difficult to detect with certainty, owing to the fact that the intensity distribution depends so very much on the type of excitation among the vibrational transitions. The probable identifications in the list of the McDonald Observatory are indicated in Table 5. Among them, λ 5442 (10, 5) and λ 5755 (12, 8) are present in active nitrogen. For the identifications the wave lengths

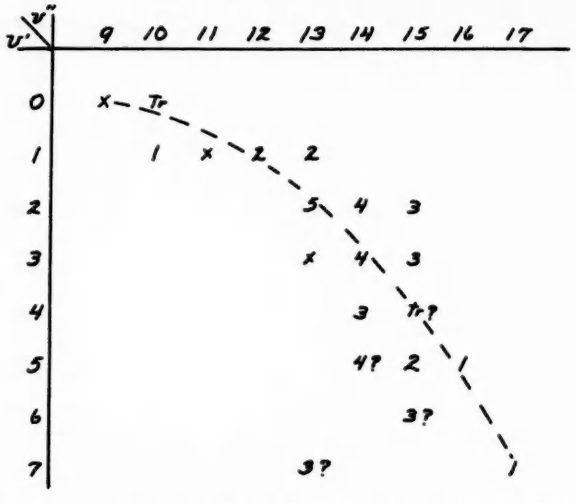

FIG. 1.—Vibrational diagram of Vegard-Kaplan bands of N_2 in the night sky. Crosses indicate bands which have not with certainty been observed in the night sky but which may be present.

of the heads have been considered, which seems plausible on low-dispersion spectrograms, owing to the prominence of the Q branch. Eleven bands observed by H. W. Babcock[1] are in good agreement with the wave lengths of the bands of this system. They are collected together in Table 1; however, some of these attributions are obviously uncertain. It is seen that the observed bands (except λ 5060) belong to the three sequences $\Delta v = 3$, 4, and 5.

The largest excitation potential observed is a little higher than 10 volts. The system is very weak, compared to the Vegard-Kaplan system, which requires only about 7 volts. It seems to us that, although there may still be some doubt concerning the identifications, the presence of the First Positive system may be accepted.

The Lyman-Birge-Hopfield system, $a\,^1\Pi \rightleftharpoons X\,^1\Sigma$, has been observed only in the region 1200–2500 A; but as the excitation energy is close to the higher level of the First Positive system, its extension toward the longer wave lengths should be considered, just as has been the case for the Vegard-Kaplan system. As far as we know, its possible presence in the night-sky spectrum has not been discussed previously. For identification purposes we shall use the wave lengths of the band heads, which again seems to be safe; the Lyman-Birge-Hopfield bands are degraded toward the red. We have computed the

[10] *Op. cit.*, p. 334.

wave lengths of the band heads of the series, $v' = 0, 1, \ldots, 10$,[11] but actually we should start the present discussion by examining the series of lowest excitation, $v' = 0$ (Table 2).

Many other suggestions have been introduced in Table 5. As in most of the identifications, we again cannot be certain with regard to the presence of the Lyman-Birge-Hopfield system; but at least there seems to be a fairly strong probability in favor of it, especially since two strong bands observed in the spectrum of the night sky, 3378 A and 3834 A, are degraded toward the red, as would be expected.

The main purpose of the present suggestion is to call the attention of the laboratory spectroscopists to this system of N_2, which should be reinvestigated and whose extension toward longer wave lengths should be attempted experimentally.

TABLE 1

N_2 BANDS OF THE $B^3\Pi \rightarrow A^3\Sigma$ SYSTEM IN BABCOCK'S LIST

λ (Obs.)	Transition	λ (Obs.)	Transition
5060 (1)	(11–5)+(10–4)*	6166 (1)	(4–0)
5242 (1)	(16–11)	6258 (3)	(11–8)*
5317 (1)	(14–9)	6401 (1)	(9–6)
5374 (0)	(12–7)*	6464 (2)	(8–5)
5709 (1)	(13–9)	6560 (3bb)	(7–4)
5965 (0)	(8–4)		

* Observed in active nitrogen.

TABLE 2

$v'=0$ SERIES OF THE LYMAN-BIRGE-HOPFIELD SYSTEM

Transition	λ (Calc.)	λ (Sky)	Intensity (Sky)
0–19	3375.2	3378 ± 2	5; wide, violet edge sharp
0–20	3591.3	Absent	
0–21	3832.6	3834 ± 1	4; wide, violet edge sharp
0–22	4103.7	(4107)	Weak, uncertain
0–23	4410.8	4420 ± 3	5; wide (blended with other bands)

The excitation potential of the excited level $v' = 0$ is 8.5 volts.

The Second Positive system, $C^3\Pi \rightarrow B^3\Pi$, if present, must be of extreme weakness. The (0, 0) transition, which is the strongest in the system, has its head at λ 3371 and is degraded toward the violet. It seems very improbable that even this band plays any role as a blend in the strong band λ 3378, which has a sharp violet edge.

N_2^+ molecule.—The Negative system, $B^2\Sigma \rightarrow X^2\Sigma$, of the N_2^+ molecule has its strongest band at λ 3914.4, and it gives a partial identification of the narrow band observed at 3912 ± 2 A.

NO molecule.—The spectrum of the *NO* molecules has usually been considered to be absent from the night sky.

The β bands, $B^2\Pi \rightleftarrows X^2\Pi$, have double heads with an interval $\Delta\nu = 91.5$ cm^{-1}, and the bands are degraded toward the violet. Each band consists of a *P*, an *R*, and a weak *Q* branch. In this case it seems safe to use the origins for the identifications, but with the understanding that a systematic $\Delta\nu$ may appear. The origins of the three strongest

[11] The extension has been limited at $v' = 10$, owing to the hypothetic character of the identification; evidently it could be extended to higher vibrational levels.

double bands of the observable region are transition (0, 9), 3386.38 and 3376.43; transition (0, 10), 3583.48 and 3572.39; transition (0, 11), 3800.91 and 3788.48, each group having laboratory intensity 10.

It may be noticed that the (0–9) bands fall in the region of the strong, wide observed line λ 3378 ± 2, intensity 5. The absence of the (0–10) transitions may be due to their proximity to the very strong band at λ 3556. Finally, the (0–11) transition may play some role in the wide band λ 3789, whose measured wave length is too great to assume a pure identification with a Vegard-Kaplan band, (2–12), λ 3769.

The presence of the β bands of *NO* is not ascertained, nor has it been excluded. The excitation potential required is 5.6 volts.

The γ bands, $A^2\Sigma \rightleftarrows X^2\Pi$, the Third Positive group of Deslandres, give coincidences as listed in Table 3. These identifications do not fit too well in the Condon parabola,[12] and we should not give too much weight to the coincidences indicated here. The excitation potential required is 5.5 volts.

TABLE 3

COINCIDENCES OF NIGHT-SKY LINES WITH γ BANDS OF NO

λ Laboratory	λ Night Sky
(1–8), 3112	(3110)
(3–12), 3303	3298 ± 3, (3) wide, diffuse
(0–8), 3375	3378 ± 2, (5) wide, violet edge sharp
(1–10), 3458	3460 ± 1, (2) narrow

NH molecules.—The remarkable structure of the β bands, $B^3\Pi \rightarrow A^3\Sigma$, λ 3360 (0–0) and λ 3371 (1–1), is well known. On low-dispersion spectrograms with short exposures they appear like lines, although λ 3360 is wider than λ 3371. These bands may quite possibly play some role in the wide band observed at λ 3378, but the fact that the measured wave length is so different from 3360–3371 indicates that at least the contribution from *NH* must be small.

Other nitrogen compounds.—The molecules NO_2, N_2O_4, N_2O, N_2O_3, ... , seem to be absent from the spectrum of the night sky.

CH molecules.—J. Cabannes, J. Dufay, and J. Gauzit[13] have observed that the Vegard-Kaplan bands vary from the zenith to the horizon, whereas a group of lines near λ 4300 does not vary and would thus seem to be of interplanetary or interstellar origin.[14] They assume that these lines of constant intensity are due to the $A^2\Delta \rightarrow X^2\Pi$ system of *CH*.

If we assume a terrestrial (or near interplanetary) origin of the bands, the discussion of the *CH* violet system is easy, when using the theoretical intensity distribution in the spectra of comets, as indicated by P. Swings and M. Nicolet[7] and as actually used by M. Nicolet[15] to identify *CH* in comets, or when using the similar but more elaborate procedure of J. Dufay.[8] These theoretical diagrams show that the *Q* branch near λ 4313 may play a role in the observed line at 4316 A, together with a Vegard-Kaplan band.

On the other hand, the $B^2\Sigma \rightarrow X^2\Pi$ system near λ 3900 seems to be absent on our spectrograms.

The system $C^2\Sigma \rightarrow X^2\Pi$ is characterized by two bands: (0, 0) at λ 3143 and (1, 1) at λ 3157. It seems probable that these two bands are identical with our observed lines at λ 3145 ± 2 (intensity 1) and λ 3157.

[12] Schmidt, *Z. f. Phys.*, **64**, 119, 1930. [13] *Nature*, **142**, 718, 1938.

[14] If the origin is interstellar, we should expect only the first rotational lines to appear, namely, λ 4300.2 and λ 4303.9, and these are not seen on our spectrograms. As far as our observations indicate, an interstellar emission is thus excluded. This does not apply to interplanetary origin.

[15] *Z. f. Ap.*, **15**, 154, 1938.

CN molecules.—According to Cabannes, Dufay, and Gauzit,[16] the *CN* bands are present in the spectrum of the night sky, and they belong to a group similar to the *CH* bands which do not vary from the zenith to the horizon, whereas the Vegard-Kaplan bands weaken at the zenith.

In the violet system, $B^2\Sigma \rightarrow X^2\Sigma$, the $\Delta v = 0$ group near λ 3883 should be considered essentially, but this band is absent from our spectra. Similarly, the $\Delta v = -1$ group near λ 4216 and the $\Delta v = +1$ group near λ 3590 are absent.

The agreement of some observed wave lengths with the tail bands (corresponding to $v' = 9, 10, \ldots, 15$) are pure chance coincidences.

Other carbon compounds.—The molecular bands of C_2, CO, CO^+, CO_2, are all absent from our spectrograms.

TABLE 4

SERIES $v'=0$ AND 1 OF THE SCHUMANN-RUNGE SYSTEM OF O_2

v''	Series $v'=0$		Series $v'=1$	
	λ Lab.	λ Sky	λ Lab.	λ Sky
12	3104.3	(3110)	.....	.....
13	3232.9	3233	3162.5	(3157)
14	3370.0	3378±2	3293.7	3298±3
15	3516.5	.....	3433.4	3425±3
16	3673.3	.....	3583.0	.....
17	3841.1	3834±1	3742.1	3742±1
18	4021.1	4016±2	3912.8	3912±2

O_2 molecules.—The Schumann-Runge system, $B^3\Sigma \rightleftarrows X^3\Sigma$, of O_2 for transitions from $v' = 0$ and 1, corresponding to the lowest excitation, has been observed in the laboratory up to the visible region. The origins of the Schumann-Runge bands of the $v' = 0$ and 1 series are given in Table 4, along with lines observed in the spectrum of the night sky. Owing to the rotational structure of these bands, the observed centers of gravity should lie to the red of the origins by, say, about 5 A. Obviously, the coincidences do not all give reliable identifications, but there is some suspicion in favor of the presence of the Schumann-Runge bands. As Table 5 shows, they are the most probable blends of the observed lines listed in Table 4.

There is very little evidence for the presence of the atmospheric bands of O_2, $A^1\Sigma \rightarrow X^3\Sigma$, in the spectrum of the night sky measured by Babcock,[1] except possibly the α' band ($v' = 3$, $v'' = 0$), which could possibly explain λ 5775 and λ 5816.

OH molecule.—There is no definite evidence showing the presence of the *OH* system, $B^2\Sigma \rightleftarrows A^2\Pi$, in the night sky except for some possible blending of the (1, 1) transition at λ 3122 to form a very weak and uncertain line measured at λ 3110.

H_2O molecule.—The so-called "*C* band" (transition from 1, 3, 1 to 0, 0, 0) may play some role in the broad band observed by Babcock at λ 6560 (3bb?). The weak ζ band (3, 2, 0) coincides practically with λ 5453 (2), observed by Babcock, but this may be merely a chance effect. The whole problem of the emission of bands of H_2O should be considered still unsettled.

INTENSITY VARIATIONS

The intensity variations in the spectrum, and of the integrated light, of the night sky have been the subject of many investigations, and again we will not attempt to give a bibliography of the work. G. Dejardin[2] has summarized much of the work prior to

[16] *Op. cit.*, p. 755.

TABLE 5

SPECTRUM OF THE NIGHT SKY

Wave Length and Mean Error	Intensity	Identification				
		Atom or Molecule	System*		Transition	Wave Length
(3110)		O_2	SR	0–12	$B^3\Sigma \rightarrow X^3\Sigma$	3104
		N_2	LBH	7–24	$a^1\Pi \rightarrow X^1\Sigma$	3116
		NO	γ	1–8	$A^2\Sigma \rightarrow X^2\Pi$	3112
		OH		1–1	$B^2\Sigma \rightarrow A^2\Pi$	3122
3145 ± 2	1	CH		0–0	$C^2\Sigma \rightarrow X^2\Pi$	3143
		N_2	LBH	9–26	$a^1\Pi \rightarrow X^1\Sigma$	3148
(3157)		CH		1–1	$C^2\Sigma \rightarrow X^2\Pi$	3157
		N_2	LBH	10–27	$a^1\Pi \rightarrow X^1\Sigma$	3164
		O_2	SR	1–13	$B^3\Sigma \rightarrow X^3\Sigma$	3162
		N_2	2d Pos.	1–0	$C^3\Pi \rightarrow B^3\Pi$	3159
3211 ± 1	3, narrow	N_2	LBH	2–20	$a^1\Pi \rightarrow X^1\Sigma$	3210
		N_2	VK	7–13	$a^3\Sigma \rightarrow X^1\Sigma$	3209
3233		O_2	SR	0–13	$B^3\Sigma \rightarrow X^3\Sigma$	3233
3263 ± ½	1, narrow					
3298 ± 3	3, wide, diffuse	N_2	LBH	8–26	$a^1\Pi \rightarrow X^1\Sigma$	3298
		Na			$3s^2S \rightarrow 4p^2P^o$	3303
3321 ± 2	2, wide, diffuse					
3378 ± 2	5, wide, violet edge sharp, red edge diffuse	N_2	LBH	0–19	$a^1\Pi \rightarrow X^1\Sigma$	3375
		N_2	LBH	1–20	$a^1\Pi \rightarrow X^1\Sigma$	3388
		O_2	SR	0–14	$B^3\Sigma \rightarrow X^3\Sigma$	3370
		NO	β	0–9	$B^2\Pi \rightarrow X^2\Pi$	3386–3376
		NH	β	0–0	$B^3\Pi \rightarrow A^3\Sigma$	3360
		NH	β	1–1	$B^3\Pi \rightarrow A^3\Sigma$	3371
		N_2	VK	0–9	$a^3\Sigma \rightarrow X^1\Sigma$	3353
		N_2	2d Pos.	0–0	$C^3\Pi \rightarrow B^3\Pi$	3371
3425 ± 3	1, diffuse	N_2	VK	1–10	$a^3\Sigma \rightarrow X^1\Sigma$	3425
		N_2	VK	4–12	$a^3\Sigma \rightarrow X^1\Sigma$	3417
		N_2	VK	7–14	$a^3\Sigma \rightarrow X^1\Sigma$	3424
		N_2	LBH	4–23	$a^1\Pi \rightarrow X^1\Sigma$	3428
3460 ± 1	2, narrow	NO	γ	1–10	$A^2\Sigma \rightleftarrows X^2\Pi$	3458
3488 ± 1	3, narrow	N_2	LBH	9–28	$a^1\Pi \rightarrow X^1\Sigma$	3492
3556	10†					
(3598)		N_2	VK	0–10	$a^3\Sigma \rightarrow X^1\Sigma$	3603
		N_2	LBH	1–21	$a^1\Pi \rightarrow X^1\Sigma$	3602
3623	1, very narrow	N_2	LBH	3–23	$a^1\Pi \rightarrow X^1\Sigma$	3625

*The abbreviations for the names of the systems are: SR, Schumann-Runge; LBH, Lyman-Birge-Hopfield; VK, Vegard-Kaplan.

†This is a very wide line and it is the strongest in the ultraviolet region. Its violet edge is sharper than the red edge. On one plate the wide line appeared to be separated into two lines with the wave lengths 3549 A and 3558 A.

TABLE 5—*Continued*

Wave Length and Mean Error	Intensity	Identification				
		Atom or Molecule	System*		Transition	Wave Length
3636	2, narrow	N_2	LBH	4–24	$a^1\Pi \rightarrow X^1\Sigma$	3635
3664 ± 1	1, narrow	N_2	VK	4–13	$a^3\Sigma \rightarrow X^1\Sigma$	3666
		N_2	LBH	7–27	$a^1\Pi \rightarrow X^1\Sigma$	3667
3707 ± 3	3, wide	N_2	VK	1–11	$a^3\Sigma \rightarrow X^1\Sigma$	3685
3742 ± 1	4, wide	N_2	VK	5–14	$a^3\Sigma \rightarrow X^1\Sigma$	3753
		O_2	SR	1–17	$B^3\Sigma \rightarrow X^3\Sigma$	3742
3787	1, wide	N_2	VK	2–12	$a^3\Sigma \rightarrow X^1\Sigma$	3769
3817	1, very narrow	.....	.....	.....	.....	.....
3834 ± 1	4, wide, violet edge sharp, red edge diffuse	N_2	VK	6–15	$a^3\Sigma \rightarrow X^1\Sigma$	3845
		N_2	LBH	0–21	$a^1\Pi \rightarrow X^1\Sigma$	3833
		O_2	SR	0–17	$B^3\Sigma \rightarrow X^3\Sigma$	3841
3912 ± 2	5, narrow	N_2^+	Neg.	0–0	$B^2\Sigma \rightarrow X^2\Sigma$	3914
		N_2	LBH	10–31	$a^1\Pi \rightarrow X^1\Sigma$	3910
		O_2	SR	1–18	$B^3\Sigma \rightarrow X^3\Sigma$	3913
3948 ± 3	3, narrow	N_2	VK	4–14	$a^3\Sigma \rightarrow X^1\Sigma$	3949
3984 ± 2	2	N_2	VK	1–12	$a^3\Sigma \rightarrow X^1\Sigma$	3979
4016 ± 2	2, wide	O_2	SR	0–18	$B^3\Sigma \rightarrow X^3\Sigma$	4021
4048 ± 1	2	N_2	VK	5–15	$a^3\Sigma \rightarrow X^1\Sigma$	4046
4072 ± 2	5, wide	N_2	VK	2–13	$a^3\Sigma \rightarrow X^1\Sigma$	4073
(4107)	.....	N_2	LBH	0–22	$a^1\Pi \rightarrow X^1\Sigma$	4104
4134 ± 2	3, narrow	N_2	LBH	7–29	$a^1\Pi \rightarrow X^1\Sigma$	4133
4174 ± 2	5, wide	N_2	VK	3–14	$a^3\Sigma \rightarrow X^1\Sigma$	4171
4259	1, wide	N_2	VK	7–17	$a^3\Sigma \rightarrow X^1\Sigma$	4254
(4268)	.....	N_2	VK	4–15	$a^3\Sigma \rightarrow X^1\Sigma$	4270
4316	2	N_2	VK	1–13	$a^3\Sigma \rightarrow X^1\Sigma$	4321
		CH		0–0	$A^2\Delta \rightarrow X^2\Pi$	4313
4379	1, narrow	N_2	VK	5–16	$a^3\Sigma \rightarrow X^1\Sigma$	4383
4420 ± 3	5, wide	N_2	VK	2–14	$a^3\Sigma \rightarrow X^1\Sigma$	4425
		N_2	LBH	0–23	$a^1\Pi \rightarrow X^1\Sigma$	4411
4543 ± 1	3, wide	N_2	VK	3–15	$a^3\Sigma \rightarrow X^1\Sigma$	4536
4587 ± 3	1, narrow	.....	.....	.....	.....	.....
4669 ± 1	1, wide	.....	.....	.....	.....	.....

TABLE 5—*Continued*

Wave Length and Mean Error	Intensity	Identification			
		Atom or Molecule	System*	Transition	Wave Length
4827±3	3	N_2	VK 2–15	$a^3\Sigma \rightarrow X^1\Sigma$	4838
4878±1	1, narrow				
(4994)					
5213		N_2	1st Pos. 17–12	$B^3\Pi \rightarrow A^3\Sigma$	
(5352)		N_2	1st Pos. 13–8	$B^3\Pi \rightarrow A^3\Sigma$	5339
		O_2	Atm. 4–0	$A^1\Sigma \rightarrow X^3\Sigma$	5360
(5441)		N_2	1st Pos. 10–5	$B^3\Pi \rightarrow A^3\Sigma$	5442
5577	500, narrow	[O I]		$[2p^1D - 2p^1S]$	5577
(5750)		N_2	1st Pos. 12–8	$B^3\Pi \rightarrow A^3\Sigma$	5755
5893	25, narrow	Na I		$3s^2S - 3p^2P^o$	5893
6235	5, narrow	N_2	1st Pos.	Blend	
6300	25, narrow	[O I]		$[2p^3P_2 - 2p^1D_2]$	6300
6364	3, narrow	[O I]		$[2p^3P_1 - 2p^1D_2]$	6364
6580	1, wide	N_2	1st Pos.	Blend	

1936, while some of the more recent investigations have been reported by Dufay.[17] We will give only some preliminary observations of the variations in the intensities of some of the lines we have observed in the spectrum of the night sky.

Many exposures were made with the nebular spectrograph of the McDonald Observatory in the survey by Struve and Elvey[18] for emission nebulosities in the Milky Way. These exposures are all long enough to show a fairly intense spectrum of the night sky, and although many of them are not calibrated for photometric purposes they are satisfactory for making estimates of the relative intensities of the spectral lines. We have 280 spectrograms well distributed over the sky and taken throughout the year, and we believe that the estimated intensities will suffice to bring out the macroscopic character of the changes and will point the way for more detailed photometric investigations.

All the spectrograms were examined indiscriminately, and the estimates of the relative intensities of the green auroral line to that of the sodium line and the oxygen line at λ 6300 were recorded. The estimates are on an arbitrary scale and have not been calibrated. In order to smooth over the diurnal and the irregular variations, the estimated ratios for a given lunation were grouped together, and average values were obtained. These are plotted in Figure 2. The upper curve gives the relative intensities for λ 5577/λ 5892, and the lower curve those for λ 5577/λ 6300. It is seen from the curves that the relative intensities of the two oxygen lines (lower curve) are reasonably constant throughout the year. On the other hand, the relative intensities of oxygen to sodium (upper curve) show a definite maximum in the summer. The point marked with an arrow

[17] *Trans. I.A.U.*, **6**, 164, 1938.

[18] *Ap. J.*, **89**, 119 and 517, 1939; **90**, 301, 1939.

is indeterminate because the sodium line was so weak that an estimate could not be made. The curves, being plots of a ratio, do not indicate which of the two lines involved is variable. However, an inspection of the plates shows that the sodium lines are weak, relative to the rest of the spectrum. This is confirmed by observations by H. W. Babcock[1], in which he found that spectrograms taken during the same summer showed very weak sodium lines, while those taken during the following October showed sodium lines approximately fivefold stronger.

Unfortunately, our observations were not carried through the summer of 1939. A few observations were obtained in August and September and are shown on the diagram. Those for September are rather discordant, but this seems definitely to be due to an enhancement of the green auroral line relative to the remainder of the spectrum at that time.

An explanation of the observed phenomenon would be rather hazardous at present, since we have no sound theory to explain the origin of the sodium atoms in the atmosphere, and it would be rather difficult to tell whether the variation is a matter of abundance or of excitation. The increase in the intensity of the sodium line does correspond with the time of the year when the meteors are most abundant (one of the suggested origins for the sodium atoms), but this meager evidence cannot be taken to confirm the meteoric origin of the sodium atoms.

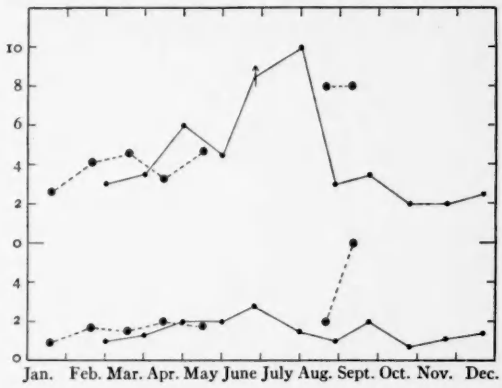

FIG. 2.—Estimated relative intensities of λ 5577/λ 5892 (*upper curves*) and λ 5577/λ 6300 (*lower curves*). The dots are observations for 1938, and the dot with circle for 1939.

Another phenomenon exhibited by the sodium atoms is the great enhancement of the sodium D lines in the spectrum of dawn and of twilight. This is, no doubt, a direct resonance phenomenon which is caused by the illumination of sunlight and which must be quite different from the nocturnal excitation of the sodium atoms. S. Chapman[19] has discussed the excitation of sodium in the upper atmosphere and has suggested that it is a result of a collisional process whereby excited oxygen atoms give up energy to the sodium atoms.

These two mechanisms of excitation of the sodium atoms in the upper atmosphere should help to throw some light upon the question of the variability of the sodium observed, for if both the night-sky spectra and the dawn or twilight spectra had weak sodium lines at the same time, we could reasonably well interpret the decreased intensity of the sodium lines as an abundance phenomenon rather than one of excitation. Unfortunately, we have only two spectra of dawn at the time of the observed minimum of the sodium lines in the night sky, and although they do not show a trace of the sodium lines, we cannot draw any conclusions, for the spectrograms were taken when the illuminated atmosphere at the end of the exposure was 85 km above the surface of the earth. To obtain the best dawn spectra of the sodium lines, the illuminated atmosphere should be as low as 60 km.

With respect to the sodium line, we have one lone observation which is of interest. During the night of February 11/12, 1939, while we were making an exposure with the nebular spectrograph of a region of BD − 3°1643, we observed in the eastern part of

[19] *Ap. J.*, **90**, 309, 1939.

the sky a diffuse luminous area extending from the southeast to the northeast along the horizon and reaching an altitude of about 10° in the east. We completed the exposure and then made a similar one on the luminous area, the area having decreased somewhat in luminosity before the end of the exposure. A reproduction of the green-red region of the two spectrograms is shown in Plate XV. The sodium line, λ 5893, is distinctly enhanced in the luminous area, showing either an excess of sodium atoms in that region or a condition of excitation more favorable to the production of the sodium line. There was no ionospheric storm, and the magnetic character figure at the time was 0.0.

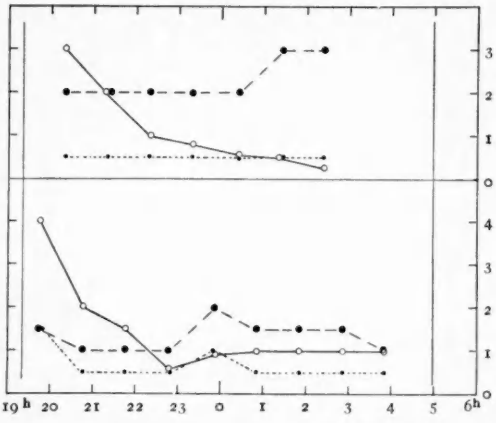

FIG. 3.—Diurnal variations of λλ 5577 (large dots), 5892 (small dots), and 6300 (circles) for the nights of November 16/17 (*upper curve*) and 19/20, 1938. The abscissae are Central Standard Times, and the ordinates are estimates of intensities on an arbitrary scale.

On several nights during November, 1938, the nebular spectrograph was used to obtain a series of exposures of one-hour duration, each to show the diurnal variations of the principal radiations in the visual region of the spectrum of the night sky. Since the slit of the spectrograph is quite long, it was possible, with the aid of a specially constructed set of apertures, to make a series of five exposures on each film. When more than one film was taken on a night, all were developed together. For the purposes of the present investigation, estimates of intensities have been made for the lines λλ 5577, 5892, and 6300 A on two nights: November 16/17 and 19/20, 1938. The results are plotted in Figure 3, the abscissae being the hours of the night in Central Standard Time, and the ordinates the estimated intensities in arbitrary units.

The data for the two nights show similar results, with the exception that the line λ 5577 is consistently stronger on November 16/17. The striking feature of the curves is the high intensity of λ 6300 at the beginning of the night and its gradual decrease to a more or less steady value around midnight.[20] The tendency of λ 5577 to reach a maximum after midnight, as noted by many observers, is indicated but is not very pronounced. Apparently, the sodium line is quite constant throughout the nights in question.

The oxygen line λ 5577 originates from the metastable state ^1S and terminates in the ^1D state, which is metastable and is at the same time the origin of λ 6300. Our observations show that the oxygen atoms can reach the ^1D state independently of the transition from the ^1S state. The processes of excitation must be considered in order to explain the differences in the behavior of the two lines of oxygen throughout the night, but we shall postpone such considerations until our spectrophotometric observations are complete.

This work was in part supported by a grant from the American Association for the Advancement of Science, for which grateful acknowledgment is made.

McDONALD OBSERVATORY
August 1940

[20] This phenomenon has been observed by H. Garrigue, *C.R.*, **202**, 1807, 1936; **205**, 491, 1937.

PLATE XV

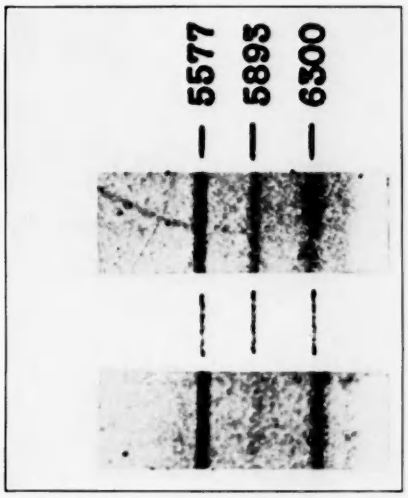

a) Spectrum of Luminous Area of Night Sky Observed on Feb. 11/12, 1939 5^h20^m to 8^h25^m U.T.

b) Normal Spectrum of Night Sky Observed during the Same Night 2^h10^m—5^h10^m U.T.

UNIV. OF MICH.

THE SPECTRA OF TWO PECULIAR STARS MWC 17 AND CD−27°11944*

P. SWINGS AND O. STRUVE

ABSTRACT

Wave lengths and radial velocities of emission lines in the peculiar stars MWC 17 and CD−27°11944 have been tabulated. The former is interesting because it contains forbidden [*Fe* III] and [*Fe* II], which places it between RY Scuti and η Carinae. The spectrum also shows *H*, *He* I, *N* II, *N* III, *O* II, *Si* II, [*N* II], [*O* I], [*S* II], etc. CD−27°11944 is a P Cygni type star showing *H*, *He* I, *Fe* II, *Ca* II, *Na* I, *N* II, and very weak [*Fe* II]. The dilution effect is small for *He* I, while the presence of forbidden [*Fe* II] suggests great distance from the photosphere. It is probable that this apparent discrepancy is caused by stratification. There is some suspicion that both stars may possess red companions.

THE SPECTRUM OF MWC 17

The bright-line spectrum of MWC 17[1] has been observed by Merrill, Humason, and Burwell,[2] who describe it as follows: "The bright *H* lines are very intense and numerous. Other bright lines are outstanding even with low dispersion. Chief among these are *Fe* II lines (with the forbidden lines relatively strong as in η Car) and the nebular line of unknown origin λ 4658 with its companion line λ 4701."

Recent work by Edlén and Swings[3] has shown that λ 4658 and λ 4701 are forbidden lines of [*Fe* III], and the brief description by Merrill, Humason, and Burwell suggests that MWC 17 shows simultaneously strong [*Fe* II] and [*Fe* III], thus combining the essential features of η Carinae ([*Fe* II] only) and RY Scuti ([*Fe* III] only).

Four spectrograms were secured at the McDonald Observatory on August 16, 20, 23, and 24, 1940; two were taken with the quartz prisms (dispersion, 100 A/mm at λ 3933) and two with the glass prisms (dispersion, 50 A/mm at λ 3933). The spectrum has not appreciably changed since the Mount Wilson observations. The continuous spectrum is very weak except in the red, where it is strong and where it gives rise to the suspicion that a late-type component may be associated with an early-type spectrum whose maximum of intensity lies in the violet region. The presence of several strong emission lines in the red region makes it impossible to identify the hypothetical red component. The radial velocities are collected in Table 1.

Since these radial velocities are practically equal, we have adopted $V_{rad} = -35$ km/sec and have corrected the measured wave lengths accordingly. These are given in Table 2.

The Balmer lines are very strong and may be followed to H_{18}. Several *He* I lines are present. Among the permitted lines we find, in addition to strong *Fe* II, the following elements: *C* III is possibly present (λ 5696, as in RY Scuti and 9 Sagittae) but is very weak; *N* II, *N* III, and *O* II are weak; *O* III is very doubtful; *Al* II is weakly present; *Si* II: λλ 3856–3863 are present, while λλ 4128–4131 and 5041–5056 are absent, this being the same selectivity which we have previously discussed for Z Andromedae, BD+11°4673, and P Cygni;[4] *Ti* II is doubtful. The permitted lines of the following elements are absent: *Fe* III, *He* II, *C* II, *Mg* I and II, *Al* I and III, *Ca* II, and *Si* I and III.

The forbidden lines of the following elements are observed: [*N* II], [*O* I], [*S* II], [*Fe* II], and [*Fe* III], whereas [*O* II], [*O* III], and [*Ne* III] are absent.

* *Contributions from the McDonald Observatory, University of Texas*, No. 30.

[1] α (1900) 1^h41^m; δ (1900) +60°12′; 40ˢ following and 2′N of BD+59°318; $m_{phot} = 12.2$; No. 101 of Mount Wilson discovery lists of Be stars.

[2] *Ap. J.*, **76**, 156, 1932. [3] *Observatory*, **62**, 234, 1939. [4] *Ap. J.* in press.

The transition of auroral type of [*N* II], λ 5755, is strong. Because of the great intensity of *Hα*, it is difficult to ascertain whether the nebular transitions of [*N* II] are present, but they cannot be very strong. The simultaneous appearance of [*N* II] and [*Fe* II or III] is known in other stars, such as RY Scuti, BD+11°4673, etc.

In [*O* I] the transitions of nebular type are very strong, whereas there is only a trace of the auroral line. [*O* I] and [*Fe* II] appear also simultaneously in other stars, for example, HD 45677.

In [*S* II] the transauroral transitions are present. These behave like auroral lines with regard to electron density, and their presence, together with [*N* II] 5755, is not surprising. [*Fe* II] and [*S* II] have also been observed simultaneously in other stars, for example, *η* Carinae, VV Cephei, BD+11°4673, etc.

TABLE 1

RADIAL VELOCITIES OF THE EMISSION LINES IN MWC 17

Element	Lines Used	V_{rad}
		km/sec
H	All lines from H_{18} to $H\gamma$, with the exception of H_8	−28
	$H\gamma$ and $H\delta$	37
He I	λ 4471 and λ 5876	29
[*S* II]	λλ 4068–4076	43
Fe II	Ten unblended lines of laboratory intensity ≥ 8	37
[*Fe* II]	Four unblended lines	−37

The [*Fe* II] lines are strong, and, as in *η* Carinae and BD+11°4673, they belong to the following transitions: $a^6D - a^6S$, b^4F, b^4P; $a^4F - a^4G$, b^4F, b^4P, and possibly also $a^2P - c^2D$.

The [*Fe* III] lines belong to two multiplets $^5D - {}^3F$ and $^5D - {}^3P$. The relative intensities of the seven lines observed in MWC 17 are quite similar to those in RY Scuti.[5] Table 3 gives the more important ionization and excitation potentials.

The presence of [*Fe* III] shows that an appreciable part of the iron atoms are doubly ionized and that the mean ionization must be around 16.5 v. (Table 3) or less, because [*Fe* II] is stronger than [*Fe* III] despite the greater number of lines. The absence of permitted *Fe* III lines shows that the mean ionization is much lower than 30 v. and, consequently, is too low to give rise to [*O* III] and [*Ne* III]; this also explains the relative weakness of *He* I, which is a recombination spectrum. The presence of [*N* II] and [*S* II] is quite natural, and the absence of [*O* II] (transition of nebular type) must be attributed to the high electron density prevailing in those regions where oxygen is ionized. On the other hand, the presence of nebular [*O* I] suggests that these lines are emitted in the outer regions where the ionization and the electron density are lower. Such a stratification effect is well known. For example, in IC 4997, [*O* III] shows a strong transition of auroral type, whereas [*O* I] shows only the nebular type.[4]

The ratio in intensity of the permitted and forbidden lines of *Fe* II is quite similar in *η* Carinae and in MWC 17. But it should be remembered that the *Fe* II lines may be due both to recombinations and to electron collisions ([N II] 5755 requires an electron energy of 4.0 v. and is strong; hence, an appreciable fraction of the electrons must have kinetic energies of around 5.6 v., which is required for *Fe* II). In any case, the intensity ratio *Fe* II/[*Fe* II] is not indicative of the excitation temperature. In *Fe* II the excited levels of metastable character are only about 2 v. lower than the ordinary excited levels

[5] *Ap. J.*, **91**, 584, 1940.

giving rise to the observed *Fe* II lines. If collisional excitation is important, the intensity ratio *Fe* II/[*Fe* II] will depend to a considerable extent upon the electron density. A

TABLE 2

EMISSION LINES IN MWC 17

λ	Int.	Identification			λ	Int.	Identification		
		Elem.	λ	Int.			Elem.	λ	Int.
3691.58	0	H_{18}	3691.56	2	4452.4‡	0–1	[*Fe* II]	4452.11	.....
3696.90	0	H_{17}	3697.15	3			*Fe* II	4451.54	4
3703.56	0	H_{16}	3703.85	4	4457.4‡	1	[*Fe* II]	4457.95	.....
3712.81	1	H_{15}	3711.98	5	4471.56	1–2	*He* I	4471.48	100
3722.03	1	H_{14}	3721.95	6	4487.9‡	1	[*Fe* II]	4488.75	.....
3734.35	1	H_{13}	3734.37	8			*Fe* II	4489.18	4
3749.91	1	H_{12}	3750.15	10					
3761.22	0	*Ti* II	3761.22	300	4492.2‡	1	[*Fe* II]	4492.64	.....
		Ti II	3759.30	400			*Fe* II	4491.40	5
		Fe II	3759.46	6	4516.33	1	*Fe* II	4515.34	7
		(*O* III	3759.87	9)*	4521.52	1	*Fe* II	4522.63	9
3770.75	1	H_{11}	3770.63	15			*Fe* II	4520.22	7
3798.79	1–2	H_{10}	3797.90	20					
3835.13	2	H_9	3835.39	40	4549.62	1	*Fe* II	4549.47	10
3856.38	1	*Si* II	3856.09	8			*Ti* II	4549.63	200
3861.98	0	*Si* II	3862.51	7	4555.24	1	*Fe* II	4555.89	8
3888.72	3	H_8	3889.05	60	4583.37	2	*Fe* II	4583.84	11
		He I	3888.65	1000	4629.03	2	*Fe* II	4629.34	7
3960.25	1	(*O* III	3961.59	8)			*N* II	4630.55	300
3970.41	3	$H\epsilon$	3970.07	80					
4068.50	3	[*S* II]	4068.62	.....	4634.74	1	*N* III	4634.16	9
		(*C* III	4067.87	9)			(*Fe* II	4635.33	5)
		(*C* III	4068.97	10)					
		(*C* III	4070.30	10)	4641.43	1–2	*N* III	4640.64	10
							([*Fe* II]	4639.68	.....)
4076.14	1	[*S* II]	4076.22	.....	4657.36‡	2	[*Fe* III]	4658.18	.....
		O II	4075.87	800	4663.0‡	1	*Al* II	4663.05	11
4101.71	4	$H\delta$	4101.73	100	4701.8	1–2	[*Fe* III]	4701.54	.....
4173.7	2	*Fe* II	4173.45	8	4732.1	1	[*Fe* III]	4733.82	.....
4178.8	2	*Fe* II	4178.85	8			[*Fe* II]	4728.07	.....
		[*Fe* II]	4177.21	.....	4755.4	1	[*Fe* III]	4754.87	.....
					4769.0	0	[*Fe* III]	4769.34	.....
4186.3	0	*C* III	4187.05	10	4813.9	1	[*Fe* II]	4814.55	.....
		O II	4185.45	150	4861.6	8	$H\beta$	4861.33	500
4191.5	0	*O* II	4189.79	500	4923.4	1	*Fe* II	4923.93	12
4201.2†	1	(*N* III	4200.02	9)	4958.3	0–1	[*Fe* II]	4958.22	.....
4232.8	1–2	*Fe* II	4233.17	11	5010.1	1	[*Fe* III]	5010.86	.....
4243.5	2	[*Fe* II]	4243.98	.....	5018.8	1–2	*Fe* II	5018.43	12
4277.5	1	[*Fe* II]	4276.84	.....	5050	1n	(*He* I	5047.74	15)
4287.25	3	[*Fe* II]	4287.41	.....			[*Fe* II]	5048.2§	.....
4295.7	0	*Fe* II	4296.57	6	5157.9	1	[*Fe* II]	5158.02	.....
		(*Ti* II	4294.12	80)	5169.4	1–2	*Fe* II	5169.05	12
4303.1	1	*Fe* II	4303.17	8	5197	0	*Fe* II	5197.57	6
4340.42	6	$H\gamma$	4340.46	200	5235	1	*Fe* II	5234.62	7
4352.1	1	*Fe* II	4351.77	9	5270.3	2	[*Fe* III]	5270.30	.....
4359.19	3	[*Fe* II]	4359.34	.....	5275.0	1	*Fe* II	5275.99	7
4372.7	1	[*Fe* II]	4372.44	.....			[*Fe* II]	5273.39	.....
		(*Fe* III	4372.40	20)	5316.8	1	*Fe* II	5316.61	8
					5337	1	.....	.....	.....
4385.3	1n	*Fe* II	4385.38	7	5363	0	*Fe* II	5362.86	5
		He I	4387.93	30	5434	1	[*Fe* II]	5433.15	.....
		[*Fe* II]	4382.76	.....	5577‖	0	[*O* I]	5577.3	.....
					5698‖	0	(*C* III	5695.8	5)
4413.36	2	[*Fe* II]	4413.78	.....	5754.4	4	[*N* II]	5755.0	.....
		(*O* II	4414.89	300)	5875.8	3	*He* I	5875.62	1000
4416.58	3	[*Fe* II]	4416.28	.....	6299.1	6	[*O* I]	6300.2	.....
		Fe II	4416.82	7	6314	3	([*S* III]	6310.2	.....
					6346‖	2	*Si* II	6347.01	50
					6364.1	3	[*O* I]	6363.9	.....
4433.4	1–2	[*Fe* II]	4432.45	.....	6385	2	.....	.....	.....
		N II	4432.71	30	6503	25	*Hα*	6562.82	2000
4448.2‡	1–2	*N* II	4447.03	300					

* Identifications in parentheses are uncertain or constitute minor contributors.

† Also present in η Carinae. ‡ Separation difficult. § Transition $a^2P_{1\frac{1}{2}} - c^2D_{2\frac{1}{2}}$. ‖ Line uncertain.

more reliable criterion of excitation is the intensity ratio [*Fe* II]/[*Fe* III], although even here the electron density may play a role if the collisional processes have very different probabilities for Fe^+ and Fe^{++}, but this is probably not the case. In order of decreasing

excitation, we then have[6] RY Scuti ([*Fe* III] strong, [*Fe* II] absent); MWC 17 (both [*Fe* III] and [*Fe* II] present); η Carinae ([*Fe* II] strong, [*Fe* III] absent).

This agrees with the other observed features. In RY Scuti, *He* II is fairly strong, whereas in MWC 17 it is absent and *He* I is present, while in η Carinae *He* I is absent. Other evidence is provided by the presence of weak [*O* III] and *C* III and the absence of [*O* I] in RY Scuti and the weakness of [*S* II] in η Carinae.

THE SPECTRUM OF CD $-27^{\circ}11944$

The object CD $-27^{\circ}11944$[7] was included in our program of peculiar bright-line stars because of its well-marked P Cygni characteristics, its broad lines, and its decidedly red color. A description of the spectrum has been published by Merrill,[8] who has identified

TABLE 3

IONIZATION AND EXCITATION POTENTIALS OF ABUNDANT ATOMS

Element	Ionization Potential			Element	Excitation Potential
	I	II	III		
H	13.53			*H*	12 −13.5
He	24.46	54.14		*He* I	23 −24
N	14.48	29.47		[*N* II]	4.0
O	13.55	34.93		[*S* II]	3.0
Ne	21.47	40.9		[*Fe* II]	$\leqslant$ 3.2
S	10.3	23.3		[*Fe* III]	$\leqslant$ 2.7
Fe	7.83	16.5	30.48	*Fe* II	5.2− 5.6
				Fe III	>11

the bright and dark lines of *H*, *He* I, and *Fe* II. He had noticed the P Cygni characteristics and had found that the emission lines have a small, positive displacement, whereas the absorption components give large, negative velocities. No actual radial velocities were given. The continuous spectrum, although strong at $H\beta$, did not extend beyond $H\gamma$ on Merrill's spectrograms, and the drop in the spectral intensity-curve was found to be much more rapid than for a normal B-type star.

Four spectrograms were secured at the McDonald Observatory in July and August, 1940, with dispersions from 40 A/mm to 100 A/mm at λ 3933. On our low-dispersion ultraviolet spectrogram the continuous spectrum may be observed as far as λ 3700, and the Balmer series extends to H_{15}. The red region of the continuous spectrum is unusually strong. Except for a strong, bright $H\alpha$ line, the region above λ 5900 shows only absorption features which certainly do not belong to an early-type star.

The strongest feature is a fairly broad band at about λ 6280. This wave length is suspiciously close to that of the strong telluric line O_2 6278.101 of Rowland intensity 4, which on our plates is probably blended with several other telluric lines of intensity 2 or 3. The same feature is present in many of our spectrograms, and it is clear that the low altitude of the star resulted in an unusually long path through the earth's atmosphere. It is probable that several other absorption features are also of telluric origin. There may be left a few faint absorption lines or bands, such as $\lambda\lambda$ 6310, 6330, and 6345, for which no satisfactory identification has been found.

A comparison with typical M-type stars such as β Pegasi and *o* Ceti shows that the

[6] In this sequence the spectrum of DO Aquilae 1925 discussed by Vorontsov-Velyaminov (*Ap. J.*, **92**, 283, 1940) would be placed between RY Scu and MWC 17.

[7] α (1900) $17^{h}41^{m}9$, δ (1900) $-27^{\circ}59'$; mag. 9.0.

[8] *Ap. J.*, **61**, 418, 1925.

strong *TiO* bands are certainly absent. Neither is there any similarity with the N stars 19 Piscium, BD+34°4500, and S Cephei, or with the S star HD 172804. There is some similarity, however, with the Ro star BD−10°5057. This may be purely fortuitous, but the features at λλ 6310, 6330, and 6345 agree reasonably well. There are, however, several features which are present in only one of the two objects.

TABLE 4

LINES IN THE P CYGNI TYPE COMPONENT OF CD−27°11944

λ	Int.	Identification			λ	Int.	Identification		
		Elem.	λ	Int.			Elem.	λ	Int.
3708.04	1A	H_{13}	3711.98	5	4453.52	0Enn	[Fe II]	4452.11	.....
3717.40	1A	H_{14}	3721.95	6			[Fe II]	4457.95	.....
3728.68	1A	H_{15}	3734.37	8	4466.42	2A	He I	4471.48	100
3745.01	2A	H_{12}	3750.15	10	4471.59	3E			
3750.77	1E				4517.12	1A	Fe II	4522.63	9
3765.68	2A	H_{11}	3770.63	15	4523.11	2E			
3770.55	2E				4554.44	2En	Fe II	4549.47	10
3794.33	2A	H_{10}	3797.90	20			Fe II	4555.89	8
3797.79	2E				4583.87	2E	Si III	4552.65	9
3831.33	2A	H_9	3835.39	40			Fe II	4583.84	11
3835.86	2–3E				4632.64	2En	Fe II	4629.34	7
3885.27	2–3A	H_8	3889.05	60	4707.27	1A	Fe II	4635.33	5
3889.36	4E	He I	3888.65	1000	4714.02	2E	He I	4713.14	40
3929.15	1A	Ca II	3933.67	600	4816.68	1En	[Fe II]	4814.55	.....
3934.37	0E				4855.48	5A†	Hβ	4861.33	500
3965.42	4A	$H\epsilon$	3970.07	80	4861.58	7E‡			
3970.23	4E				4918.30	2A	He I	4921.93	50
3991.74	0A	N II	3995.00	300	4924.67	3E	Fe II	4923.93	12
3995.53	0E				5011.19	3A	Fe II	5018.43	12
4021.12	1A	He I	4026.19	70	5018.59	3E	He I	5015.67	100
4026.44	2E				5161.55	2A	Fe II	5169.05	12
4096.84	5A	$H\delta$	4101.73	100	5169.36	2E			
4101.52	5E				5197.58	0E	Fe II	5197.57	6
4171.6	0A	Fe II	4178.85	8	5235.8	0E	Fe II	5234.62	7
4177.66	2E				5275.4	1E	Fe II	5275.99	7
4228.19	0A	Fe II	4233.17	11			[Fe II]	5273.39	.....
4232.70	2E				5307.91	1A	Fe II	5316.61	8
4243.67	0E	[Fe II]	4243.98	.....	5316.87	2E			
		N II	4241.80	100	5335.6	1E	[Fe II]	5333.66	.....
4287.49	0E	[Fe II]	4287.4	.....	5660.15	2A	N II	5666.64	300
4336.30	5A	$H\gamma$	4340.46	200	5666.59	1E			
4341.05	5E*				5672.57	2A	N II	5679.56	500
4355.29	2En	Fe II	4351.77	9	5680.2	1E			
		[Fe II]	4359.34	.....	5867.41	2As	He I	5875.62	1000
4391.86	1–2En	He I	4387.93	30	5876.05	6E§			
		Ti II	4395.04	150	5886.01	4A‖	Na I	5889.95	9000
4416.01	1–2En	[Fe II]	4416.28	.....	5896.62	3E¶	Na I	5895.92	5000
		Fe II	4416.82	7	6563	10E	Hα	6562.82	2000
					6666	3A	He I	6678.15	100
					6678	3E			

* Extends from λ 4337.58 to λ 4344.56.
† Extends from λ 4853.25 to λ 4857.91.
‡ Extends from λ 4857.91 to λ 4866.40.
§ Extends from λ 5871.20 to λ 5879.56.
‖ Extends from λ 5879.56 to λ 5889.99.
¶ Extends from λ 5889.99 to λ 5904.31.

The question whether there is a red companion and whether CD−27°11944 belongs to the same group of binaries as RW Hya, Z And, T CrB, R Aqr, AX Per, CI Cyg, etc., which we have recently discussed,[9] must remain open for the present.

[9] *Ap. J.*, **91**, 546, 1940; *Proc. Nat. Acad. Sci.*, **26**, 458, 1940; also Swings, Elvey, and Struve, *Pub. A.S.P.*, **52**, 199, 1940.

Table 4 gives the wave lengths corrected to the sun. Besides the elements observed by Merrill, lines of the P Cygni type are also observed for *Ca* II, *Na* I, and *N* II; weak [*Fe* II] lines are present. The mean radial velocities are shown in Table 5.

The ejection velocity is about 350 km/sec. This may be compared with the values obtained for other stars: about 120 km/sec in P Cygni; 125 km/sec in BD+11°4673; 180 km/sec in BD+47°3487; 250 km/sec in 9 Sagittae, and 300 km/sec in BD+35°3930 N. In other words, the ejection is more violent than in P Cygni but is comparable to that in some Oe stars and in novae. Z CMa is also similar as far as the velocity of ejection is concerned. It is often assumed that the lines in P Cygni stars are narrower than in novae and in Wolf-Rayet stars; but CD−27°11944 shows that P Cygni emission lines may sometimes extend over 600 or 700 km/sec. We know, on the other hand, that there are Wolf-

TABLE 5

RADIAL VELOCITIES IN CD−27°11944

Element	Absorption Component	Emission Component	Lines Used
	km/sec	km/sec	
H	−337	+23	From H_{15} to $H\beta$; weight 5 to $H\gamma$ and 3 to $H\beta$
He I	−373	+20	λλ 4026, 4471 (weight 3), 4713, 5876 (weight 2)
N II	−320	+22	λλ 3995, 5666, 5680
Ca II	−346	+52	K
Fe II		+17	λλ 4522, 4584, 5169, 5316

Rayet stars whose lines are not broader than this. For example, in BD+30°3639 (Campbell's object) the lines of *Si* IV, *C* III, and *O* III have widths smaller than 700 km/sec;[10] in the nucleus of HD 167362 the typical Wolf-Rayet lines due to *He* II, *C* III, C IV, and *O* III are still narrower, the ejection velocity of *C* III being only 186 km/sec.[11] This applies also to certain slow novae or nova-like objects. The nucleus of IC 4997 has also comparatively sharp lines, although the identified atoms are exactly the same as those ordinarily found in Wolf-Rayet stars.[12]

The presence of *Ca* II and *Na* I in emission is interesting. For *Ca* II the velocity of ejection may be determined, and, within the errors of measurement, it is practically the same as the value obtained from hydrogen or from other abundant elements. Thus, *Ca* II is presumably ejected and excited together with hydrogen and helium and does not originate in a region of the late-type atmosphere excited by the hot companion. In the P Cygni star Z CMa, *Ca* II is also present in emission and absorption, but *Na* I is only an absorption line.

CD−27°11944 belongs to that group of P Cygni type stars in which only the expanding shell is observed and not the exciting star. If we assume that the width of the absorption components of the Balmer lines is mainly due to the range in the radial component of the ejection velocity, it is found immediately that the hydrogen absorbing layer of CD−27°11944 lies very close to the effective photosphere. Other stars like 17 Leporis, BD+47°3487, HD 190073, 9 Sagittae, and BD+35°3930 N show conspicuously the spectrum of the stellar reversing layer (especially the Balmer lines broadened by rotation and Stark effect). In these cases the continuous absorption in the expanding shell is too small to produce an effective photosphere in the ejected layers.

[10] *Proc. Nat. Acad. Sci.*, **26**, 548, 1940.

[11] *Ibid.*, **26**, 454, 1940.

[12] Except that carbon and nitrogen are both present (in press).

The faintness of [*Fe* II] indicates that the main part of the ejected matter is close to the photosphere; the [*Fe* II] lines must be excited principally in the outer regions. That the dilution of the photospheric radiation must be small is also apparent from the intensity of the *He* I absorption lines starting from ordinary excited levels (for example, λ 4471 and λ 4026); the *He* I lines starting from metastable levels are not appreciably favored.

Whereas the *He* I lines of $-27°11944$ suffer practically no dilution effect, showing that the absorbing *He* I atoms are close to the photosphere, the weak [*Fe* II] lines must be excited in the outer regions. This kind of stratification is similar to that observed in other P Cygni or Wolf-Rayet stars. For example, in the P Cygni star BD+11°4673, we observe bright lines of silicon in four successive stages of ionization—*Si* I to *Si* IV. In Wolf-Rayet stars bands due to atoms of different ionization potentials have different ejection velocities and widths and the same star may show *He* I (I.P. 24 v.) and *N* V (97 v.).[13]

In the family of P Cygni objects, CD$-27°11944$ should be placed among the stars of average excitation. In P Cygni, permitted *Fe* III is very conspicuous, whereas permitted *Fe* II is absent. In others, such as RY Scuti or novae at a certain stage (for example, DO Aquilae 1925, in August, 1926[14]), forbidden [*Fe* III] is the conspicuous feature. In some stars, such as Z CMa, $-27°11944$, and in novae at a certain stage, *Fe* II is conspicuous, while [*Fe* II] is very weak and *He* I is still strong. In still others, like η Carinae, [*Fe* II] is strong, and *He* I is absent.

McDonald Observatory
October 5, 1940

[13] C. S. Beals, *J.R.A.S. Canada*, **34**, 169, 1940.

[14] Vorontsov-Velyaminov, *loc. cit.*

THE EVOLUTION OF A PECULIAR STELLAR SPECTRUM Z ANDROMEDAE

(With a Note on the Spectrum of IC 4997)*

P. SWINGS AND O. STRUVE

ABSTRACT

The spectral lines of Z Andromedae have been measured on plates taken between May 12 and August 25, 1940, when the brightness had decreased to magnitude 9.7 after the outburst in 1939. The spectrum shows emission lines of a thin and dilute nebula and resembles the spectrum observed by H. H. Plaskett in 1923–1926. There is some evidence of a late-type companion, in addition to a hot nucleus, which resembles some of the slow novae, and a fairly pronounced P Cygni type spectrum of an expanding shell. The latter is a remnant of the shell which was formed in the outburst of 1939.

The nebular spectrum shows strong forbidden lines, but there are relatively few stages of ionization, which shows that the nebula consists of a fairly thin layer. The intensity of the auroral transition of [*O* III], λ 4363, is relatively strong—a phenomenon which is characteristic of other binaries of similar type, and of novae. Among the nebulae the stellar planetary IC 4997 shows the same feature. A list of lines of this object is given in Table 4.

I. INTRODUCTION

Z Andromedae is an exceptionally interesting object whose spectrum was first described in detail by H. H. Plaskett[1] on the basis of spectrograms taken during the period 1923–1926. At that time the spectrum showed no absorption lines but contained numerous bright lines, especially those of *H*, *He* I, *Mg* II, *Fe* II, *Ti* II, *He* II, *C* III, *N* III, *O* III, and the forbidden lines of [*O* III], [*Ne* III], [*Ne* V], [*Fe* III?] and [*S* II]. H. H. Plaskett divided the lines into two groups which he designated as the "stellar part" (lines of low excitation: *H*, *He* I, *Mg* II, *Fe* II, etc.) and the "nebular part" (lines of high excitation: *He* II, *N* III, [*O* III], [*Ne* III], etc.). The continuous spectrum was very strong in the red region, and on Plaskett's spectrograms Hogg[2] was able to see weak absorption band heads of *TiO;* these increased in intensity in the years following, when the star was fading in light. Mrs. Greenstein[3] determined the light-curve for the object until 1936; during the interval 1922–1936 the star slowly decreased in brightness with some irregular fluctuations. The light-curve has been extended by L. Campbell,[4] who recorded an increase in light from visual magnitude 10.7 in April, 1939, to 8.6 on August 21 and to 7.9 shortly afterward. Since the fall of 1939 the star has declined in brightness, reaching magnitude 9.7 on August 15, 1940.

It is tempting to consider Z Andromedae as a binary system consisting of a nova-like object, subject to moderate outbursts at somewhat irregular intervals of about fifteen years, and of a variable late-type companion whose period is probably not identical with the 650-day period suggested by Prager,[4] because the amplitude of the latter appears to be least when the nova-like object is faint.

This picture receives strong confirmation from a study of spectrograms taken at the McDonald Observatory during the past year. Spectrograms taken from September 14 to December 5, 1939, revealed a spectrum completely different from that described by

* *Contributions from the McDonald Observatory, University of Texas*, No. 31.

[1] *Pub. Dom. Ap. Obs., Victoria*, **4**, 119, 1928.

[2] *Pub. A.S.P.*, **44**, 328, 1932; *Pub. A.A.S.*, **8**, 14, 1934.

[3] *Harvard Bull.*, No. 906, 1937.

[4] L. Campbell, *Pop. Astr.*, **47**, 335, 447, 571, 1939; K. Himpel, *Die Sterne*, **19**, 210, 1939, and **20**, 14, 1940.

PLATE XVI

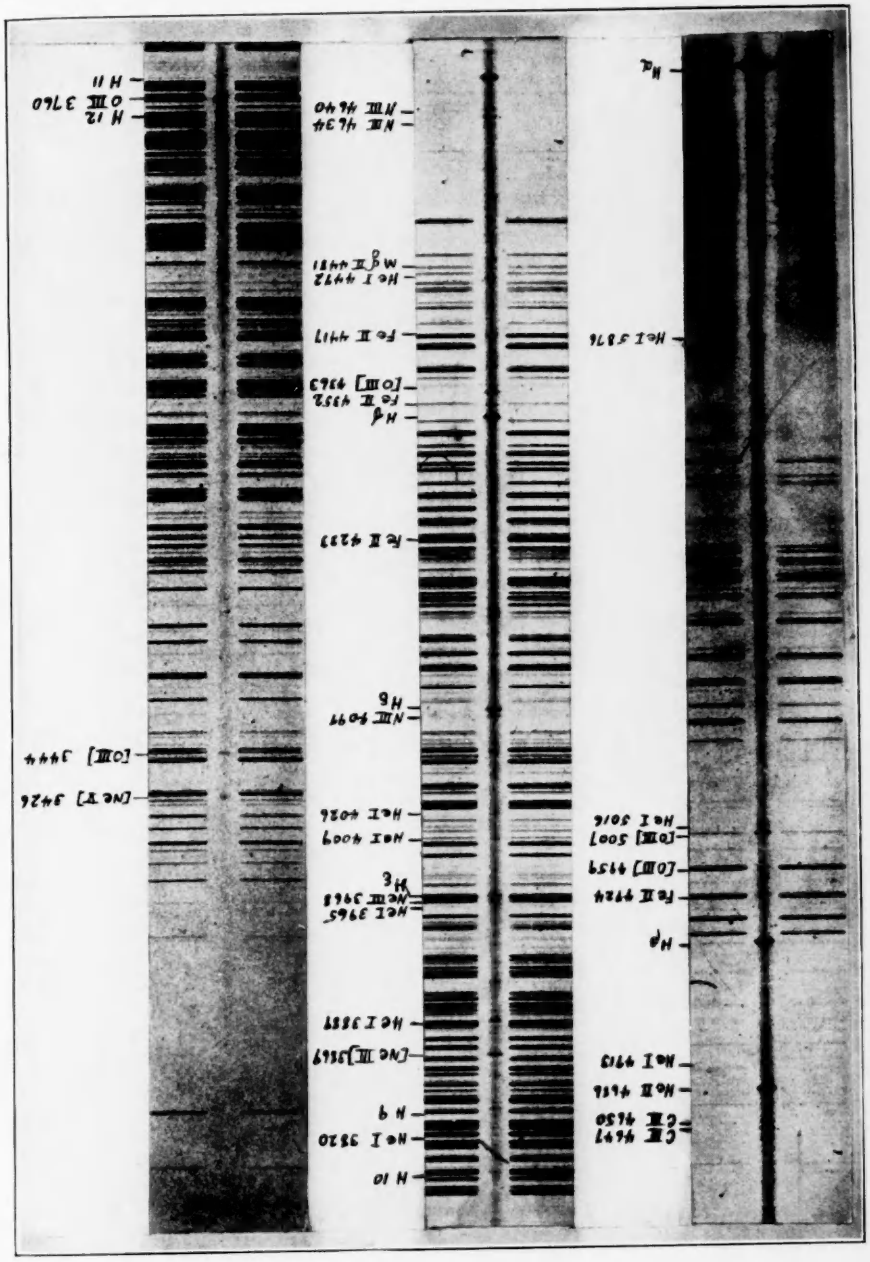

THE SPECTRUM OF Z ANDROMEDAE, AUGUST 15, 1940

UNIV. OF MICH.

Plaskett.[5] It was then of the P Cygni type with the "nebular part" of Plaskett's description completely missing. The spectrum showed many permitted lines of low excitation and was very similar to certain early stages of slow novae.

The transition from the high-excitation spectrum to one of P Cygni type must have occurred mainly between July 30 and September 14, 1939. On July 30, when the visual magnitude was about 8.9, the object was observed in Berlin-Babelsberg by P. Wellmann,[6] and the spectrum showed the lines of *He* II and *N* III; but there already seemed to appear weak absorption lines on the violet side of certain emissions, and traces of the *TiO* bands were still present at that time.[7]

The spectroscopic survey was resumed in the spring of 1940, when the star again became observable in the east; our first plate was taken on May 12. The entire aspect of the spectrum had changed. Again it resembled that described by Plaskett, although there were important differences. Strong nebular lines were again present; but, contrary to Plaskett's description, our spectrograms show many absorption lines. The development of the spectrum bears a strong resemblance to that of a slow nova.

This type of combination of a late-type star and an early-type companion—which, in this case, is nova-like—is by no means exceptional. Several other objects of the same type have recently been investigated, namely, T Coronae Borealis[8] (nova + M star), AX Persei and CI Cygni[9] (very high-excitation nebulosity + M star), RW Hydrae[10] (nebulosity of medium excitation + late K or early M), R Aquarii[11] (nebulosity + M7e + high-excitation companion), α Scorpii[12] (B4ne + M), o Ceti[13] (B8e + M), WY Geminorum[9] (B3e + M3e), W Cephei[9] (O? + Me), VV Cephei[14] (B9e + M2), etc.

The dynamical and physical processes involved in such binaries are not yet fully understood. It is probable that the emission lines are excited by the radiation of the early-type star outside its own reversing layer. There may be a departure from spherical symmetry in the excited layers, owing to the presence of the late-type companion. It is also probable that in some cases the radiation of the early-type component may excite the outer regions of the cool companion.

II. GENERAL DESCRIPTION OF THE SPECTRUM

The following description of the spectrum of Z Andromedae is based upon several spectrograms taken at the Cassegrain focus of the 82-inch reflector between May 12 and August 15, 1940, the best plate having been taken on August 15 with the quartz prisms and the 500-mm camera (dispersion 40 A/mm at λ 3933). The star was of about visual magnitude 9.7.

The visual region is quite strong, and a search for the *TiO* band heads found by Hogg ($\lambda\lambda$ 6159, 5448, 5167, and 4955) makes it appear probable that the red companion again begins to play an appreciable role in the visual region of the spectrum.

The results of the measurement of the spectrogram of August 15 are collected in Table 1, in which the late-type absorption features have not been included. The wave lengths have been corrected for the motion of the earth, but because of the complexity of the spectrum no attempt has been made to correct for the motion of the star.

Table 1 shows that the spectrum of Z Andromedae is very complex. We recognize at once the existence of the "nebula" whose spectrum was described by Plaskett. This

[5] Struve and Elvey, *Pub. A.S.P.*, **51**, 297, 1939; Swings and Struve, *Ap. J.*, **91**, 601, 1940.

[6] *Beobachtungs-Zirkular d. A.G.*, **21**, 105, 1939.

[7] *Vierteljahrsschrift d. A.G.*, **75**, 53, 1940.

[8] *Pub. A.S.P.*, **52**, 199, 1940.

[9] *Ap. J.*, **91**, 546, 1940.

[10] *Proc. Nat. Acad.*, **7**, 458, 1940.

[11] *Ap. J.*, **91**, 616, 1940; P. W. Merrill, *Spectra of Long-Period Variable Stars*, p. 82, 1940.

[12] *Ap. J.*, **92**, 316, 1940.

[13] P. W. Merrill, *op. cit.*, p. 75, 1940.

[14] C. and S. Gaposchkin, *Variable Stars*, 1938.

TABLE 1

LIST OF LINES IN Z ANDROMEDAE

λ	Int.	Identification*		
		Elem.	λ	Int.
3121.5†	1E	O III	3121.71	5
3132.7†	6E	O III	3132.86	6
3202.9†	6E	He II	3203.16	.....
3277.0†	1E	.....	.....	.....
3281.1†	1E	.....	.....	.....
3312.3†	4E	O III	3312.30	5
3323.6†	1E	.....	.....	.....
3340.5†	5E	O III	3340.74	6
3345.8†	4E	[Ne V]	3345.8	.....
3425.85	6E	[Ne V]	3425.8	.....
3443.60	6E	O III	3444.10	5
3455.27	0E	O III	3455.12	5
3662.08	1A	H_{10}	3662.26	.....
3663.03	1A	H_{29}	3663.40	.....
3664.25	1A	H_{28}	3664.68	.....
3664.92	0E			
3665.70	1A	H_{27}	3666.10	.....
3666.53	0E			
3667.47	1A	H_{26}	3667.68	.....
3668.26	0E			
3669.12	1A	H_{25}	3669.47	.....
3669.94	1E			
3671.21	1+A	H_{24}	3671.48	.....
3672.00	1E			
3673.24	1+A	H_{23}	3673.76	.....
3674.42	1E			
3676.07	2A	H_{22}	3676.36	.....
3676.94	1E			
3679.10	2A	H_{21}	3679.35	.....
3679.75	1E			
3682.37	2A	H_{20}	3682.81	.....
3683.27	1E			
3686.19	1+A	H_{19}	3686.83	.....
3687.35	1E			
3689.24	1+A	.....	.....	.....
3690.37	0E			
3691.30	1+A	H_{18}	3691.56	2
3692.21	1+E			
3696.88	1+A	H_{17}	3697.15	3
3697.79	1E			
3704.18	1+A	H_{16}	3703.85	4
		He I	3705.00	30
3705.62	1+Enn	Fe I	3705.57	700
		Ti II	3706.23	125
		Ca II	3706.03	40
3711.56	1+A	H_{15}	3711.98	5
3712.72	2E			
3718.76	0A	Fe I	3719.93	1000R
3719.91	0E			
3721.40	1+A	H_{14}	3721.95	6
3722.53	2E			
3733.43	1A	H_{13}	3734.37	8
3734.94	2E			
3737.10	1E‡	Fe I	3737.13	1000r
		Ca II	3736.90	50
3741.39	0E	Ti II	3741.64	200
3748.34	1E	Fe II	3748.49	8
		O II	3749.47	125
		Fe I	3748.26	500
		Fe I	3749.49	1000r
3749.57	1+A	H_{12}	3750.15	10
3750.86	2E			
3755.00	2E	N III	3754.62	6
		O III	3754.67	7
		Fe II	3755.56	4
		He I	3756.09	1
3757.81	1E	Ti II	3757.69	100
		Fe I	3758.23	700
		O III	3757.21	5
3760.08	2En	O III	3759.87	9
		Ti II	3759.30	400
		Fe II	3759.46	6
3762.35	0E	Fe II	3762.89	5
		Ti II	3761.32	300r
		O II	3762.51	120
3770.52	1A	H_{11}	3770.63	15
3771.25	2E	N III	3771.08	7
3795.27	1E	Fe I	3795.00	500
3797.30	1A	H_{10}	3797.90	20
3798.69	3E			
3819.35	1A	He I	3819.61	50
3819.93	2E	Fe I	3820.43	800
3824.47	0E	Fe II	3824.91	4
3834.48	1A	H_9	3835.40	40
3835.63	3E			
3847.06	1E	.....	.....	.....
3853.94	1E	Si II	3853.67	3
3855.92	3E	Si II	3856.09	8
3862.60	2E	Si II	3862.51	7
3868.75	7E	[Ne III]	3868.74	.....
3880.69	0A	O II	3882.19	35
3882.22	0E			
3887.84	5A	He I	3888.65	1000
3889.28	5E§	H_8	3889.05	60
3899.58	1E	Fe I	3899.71	500
3902.91	1E	Fe I	3902.95	500
3905.62	1Es	Si I	3905.53	20
3914.19	1En	Fe II	3906.04	5
		Ti II	3913.46	70
3919.22	1En	C II	3918.98	80
		C II	3920.68	200
		N II	3919.00	35
		O II	3919.28	35
3923.24	1E	Fe I	3922.91	600
3926.55	1E	He II	3923.51	.....
3930.47	1E	He I	3926.53	7
3934.95	1E	Fe I	3930.30	600
		Ca II	3933.67	600R
		He I	3935.91	4
		Fe II	3935.94	6
		N III	3934.41	3
3938.39	1+E	Fe II	3938.97	4
		N III	3938.52	4
3945.35	1E	O II	3945.04	20
3961.77	1+E	O III	3961.59	8
		Al I	3961.53	3000

* All the laboratory wave lengths and intensities have been taken from the M.I.T. wave-length table, except for *Fe* II (J. C. Dobbie, *Annals of the Solar Physics Observatory, Cambridge*, Vol. V, Part I) and the doubly or trebly ionized atoms (C. E. Moore, *Multiplet Table of Astrophysical Interest*). In the M.I.T. table the intensities in the arc or in the spark have been taken for the neutral or ionized elements. The lines of stellar intensity zero are uncertain.

† These lines were measured on a plate taken January 5, 1941.

‡ Probably absorption of P Cygni type.

§ Violet wing weaker.

TABLE 1—*Continued*

λ	Int.	Identification*			λ	Int.	Identification*		
		Elem.	λ	Int.			Elem.	λ	Int.
3964.84	2E	*He* I	3964.73	50	4451.23	oE	*Fe* II	4451.54	4
3967.33	2E	[*Ne* III]	3967.51	.....	4457.57	1E	?[*Fe* II]	4457.97	.....
3970.34	4E	*He*	3970.07	80	4470.08	1A	*He* I	4471.48	100
3973.83	1E	*O* II	3973.27	125	4472.08	3E			
4009.24	1E	*He* I	4009.27	10	4480.96	2E	*Mg* II	4481.33	100
4013.95	2A	.....	.....	.....	4488.98	1E	*Fe* II	4489.19	4
4014.85	1E				4491.32	1E	*Fe* II	4491.41	5
					4501.07	1E	*Ti* II	4501.27	100
4016.62	1+A	.....	.....	.....	4506.84	1A	*Fe* II	4508.28	8
4017.56	oE				4508.26	1+E			
4025.56	2A	*He* I	4026.19	70	4514.10	1A	*Fe* II	4515.34	7
4026.43	2E				4515.29	2E	*N* III	4514.89	7
		C III	4068.94	10	4521.06	1E‖	*Fe* II	4520.22	7
		C III	4070.30	8	4522.89	1+E‖	*Fe* II	4522.64	9
4070.30	2En	*O* II	4069.90	125	4528.75	1E	*Fe* I	4528.62	600
		O II	4072.16	300			?*Al* III	4529.18	6
		[*S* II]	4068.50	.....					
4073.89	2A	*O* II	4075.87	800	4534.64	1E	*N* III	4534.57	3
4075.82	2E						*Ti* II	4533.97	150
4097.35	4Es	*N* III	4097.31	10					
4101.97	6E‖	*Hδ*	4101.73	100	4540.92	1+E	*He* II	4541.61	5
4103.54	2E	*N* III	4103.37	9			*Fe* II	4541.52	4
4121.31	1E	*He* I	4120.81	25					
4123.65	oE	*Fe* II	4122.64	4	4549.04	1E‡	*Fe* II	4549.47	10
4144.25	1En	*He* I	4143.76	15			*Ti* II	4549.63	200
4162.35	1E	*C* III	4162.80	4	4556.30	1E	*Fe* II	4555.89	8
4173.12	2En	*Fe* II	4173.45	8	4576.51	oE	*Fe* II	4576.33	4
4175.78	2A	*Fe* II	4178.87	8	4583.11	2E	*Fe* II	4583.83	11
4178.17	2En				4629.86	3E	*Fe* II	4629.34	7
							N II	4630.55	300
4225.15	oA	?*Ca* I	4226.73	500*R*	4631.69	1A?	*N* III	4634.16	8
4226.21	oE	?*Al* II	4226.81	35	4634.70	3En	*Fe* II	4635.33	5
4230.95	1A	*Fe* II	4233.17	11	4637.66	3A	*N* III	4640.64	10
4233.13	3E				4640.30	4En			
4244.83	oEn	[*Fe* II]	4243.97	.....	4645.74	3A	*C* III	4647.40	10
4264.55	1A	*C* II	4267.02	350	4648.10	3En‖			
4267.17	1E	*C* II	4267.27	500	4651.05	2En‖	*C* III	4650.16	9
4277.23	oE	[*Fe* II]	4276.87	.....			*C* III	4651.35	8
4288.70	oE	[*Fe* II]	4287.40	.....					
4340.67	8E	*Hγ*	4340.46	200	4653.87	1A?	*C* IV	4658.64	5
4351.83	3E	*Fe* II	4351.77	9	4657.92	1+E	[*Fe* III]	4658.18	.....
4363.46	6E	[*O* III]	4363.20	.....	4685.46	10E	*He* II	4685.75	300
4366.92	oE	*O* II	4366.91	100	4713.82	1+E	*He* I	4713.14	40
4369.24	1+E	?*O* II	4369.28	50	4861.59	10E	*Hβ*	4861.33	500
4379.66	oE	*N* III	4379.09	10	4920.08	2A	*He* I	4921.93	50
		Fe I	4383.55	1000	4922.59	2+En	*Fe* II	4923.92	12
4384.16	1E	*Fe* II	4385.38	7	4958.86	3E	[*O* III]	4958.91	.....
4387.63	2E	*He* I	4387.93	30	5007.23	5Es	[*O* III]	5006.84	.....
4395.19	1E	*Ti* II	4395.03	150	5012.21	2A	*He* I	5015.67	100
		O II	4395.95	80	5015.74	3E‖			
4399.92	1E	*Ti* II	4399.77	100	5018.93	2E‖	*Fe* II	5018.43	12
4404.65	1E	*Fe* I	4404.75	1000	5169	1E	*Fe* II	5169.03	12
4413.86	oE	[*Fe* II]	4413.78	.....	5235	1E	*Fe* II	5234.62	7
		Fe II	4416.82	7	5317	2E	*Fe* II	5316.61	8
4416.78	2En	[*Fe* II]	4416.28	.....	5412	2E	*He* II	5411.55	50
		Ti II	4417.72	80	5876	5Es	*He* I	5875.62	1000
		O II	4416.97	150	6503	20E	*Hα*	6562.82	2000
4437.67	oE	*He* I	4437.55	10					
4444.97	oE	?*Ti* II	4443.80	125					
4447.41	oE	*N* II	4447.03	300					
		O II	4448.20	70					

‖ Separation difficult, but the line seems definitely double.

spectrum consists of two groups of lines: the first includes forbidden and permitted lines usually associated with planetary nebulae; the other includes permitted lines, principally in the region λλ 4632–4658, of *N* III, *C* III, and *C* IV, bordered by absorption on the violet side. This second group—which exhibits some of the characteristics of lines in Wolf-Rayet stars, except that in Z Andromedae they are fairly sharp—we shall attribute somewhat arbitrarily to the hot nucleus. We do not wish to imply that this nucleus is a normal Wolf-Rayet star, and it is possible that what we have designated as the nuclear lines are really lines produced in the innermost layer of the nebular shell.

In addition to the "nebula" and the "nucleus" there is a spectrum of the P Cygni type. It consists of *H*, *He* I, and *Fe* II; and we are inclined to attribute to it also the bright lines of low excitation: *Mg* II, *Si* I, *Si* II, *Ti* II, *Fe* I, and extremely weak [*Fe* II]. This spectrum is the remnant of the P Cygni type spectrum which predominated in the fall of 1939, when the star was near maximum light. It has undergone large changes since December, 1939, having developed strong lines of *He* I and having lost most of its violet-absorption features. But it has not yet returned to the character of spectrum designated by Plaskett as "Z Andromedae-Star."

The strong continuous spectrum of Z Andromeda in the photographic region must come from the hot nucleus. It is too blue to be associated with the M star.

III. THE SPECTRUM OF THE NUCLEUS

Carbon is represented by very weak *C* II (λ 4267), strong *C* III (λλ 4648–4651), and *C* IV (λ 4658); all these bright lines are flanked by absorption components on the violet side. The carbon lines have the usual intensities of Wolf-Rayet stars and of pure re-

TABLE 2

VELOCITIES OF EJECTION

Element	V_{ej} in km/sec
Balmer lines of P Cygni type	83
λ 3889 *He* I	111
Other lines of *He* I	81
C III	174
N III	182
C II	186

combination spectra; in an O star of the 9 Sagittae type, λ 5696 *C* III would be an emission line instead of λλ 4648–4651, according to previous investigations by the authors.[9]

Nitrogen is characterized by the strong bright lines of *N* III at λ 4634 and λ 4641, with P Cygni absorption components. It is difficult to decide whether broader lines are superposed on the strong, sharp nebular *N* III lines measured at λλ 4097–4103.

Several weak *O* III lines which cannot be excited in the nebulosity by Bowen's fluorescence mechanism probably belong to the nucleus. The question arises whether the lines of *H* and *He* I also belong to the nucleus. Strong evidence against such an assumption is found in the measured differences between the radial velocities of the emission and absorption components of the lines. These are collected in Table 2.

The spectrum of the nucleus contains both nitrogen and carbon. Like the nucleus of NGC 6543,[15] it is an object intermediate between the usual carbon and nitrogen sequences. It would, indeed, be difficult to apply to it the usual classification criteria for Wolf-Rayet stars.[16] For example, we are not allowed to use the intensities of the *He* I lines which belong mainly to the P Cygni layer or those of the *He* II lines which belong to the nebula. This difficulty presents itself in all cases where a Wolf-Rayet star having relatively narrow lines is surrounded by an emission nebulosity. The absence of *N* V and the intensity ratio of the *C* IV and *C* III lines suggest that the nucleus may have a temperature of the order of 70,000°.

This would be in agreement with the lines observed in the nebula, where [*Ne* III] is stronger than [*Ne* V]. It should be remembered that the lines of the nucleus of Z Andromedae are much sharper than those of Wolf-Rayet stars. But the nucleus of HD 167362, which is an object resembling Campbell's hydrogen-envelope star, has also fairly narrow lines of Wolf-Rayet type. It is possible that the nucleus of Z Andromedae is of the same character.

[15] *Ap. J.*, **92**, 289, 1940.

[16] *Trans. I.A.U.*, **6**, 248, 1938.

IV. THE NEBULAR SPECTRUM

The following observed lines belong to a dilute nebulosity: (*a*) the transitions of nebular type of [*O* III] (int. 3–5), [*Ne* III] (int. 7–3), and [*Ne* V] (int. 6–4); (*b*) the transition of auroral type of [*O* III] (int. 6); and (*c*) the lines of *He* II (at least in part) and the fluorescence lines of *O* III and *N* III excited by the resonance line of *He* II. The emission lines of *H* and *He* I may also belong in part to the nebulosity. The excitation of this nebular spectrum may be attributed to the hot nucleus described in section III. The mean radial velocities of the pure emission lines are: forbidden lines, +5.8 km/sec; *N* III 4097–4103, +7.6 km/sec; Balmer lines (*Hε*–*Hβ*), +16.0 km/sec.

Since the nucleus continuously ejects nitrogen and since λλ 4097–4103 are fairly strong in the nebula, we should have expected to observe [*N* II] or [*N* I] in the nebulosity.

TABLE 3

COMPARISON OF INTENSITIES OF EMISSION LINES IN PLASKETT'S "NEBULAR PART"

λ	Elem.	Intensity		Notes	λ	Elem.	Intensity		Notes
		Plaskett	Swings-Struve				Plaskett	Swings-Struve	
3425.8	[*Ne* V]	4	6		4634.2	*N* III	3	3	
3444.1	*O* III	4	2		4640.6	*N* III	6	4	
3759.9	*O* III	3	2	1	4647.4	*C* III	2	3	
3868.7	[*Ne* III]	2	6	2	4650.2	*C* III	4	2	
3967.5	[*Ne* III]	2	2		4685.7	*He* II	9	10	
4068.9	*C* III	<1	2		4958.9	[*O* III]	2	3	
4097.3	*N* III	2	4		5006.8	[*O* III]	5	5	
4199.9	*He* II	<1	0		5411.6	*He* II	2	2	
4363.2	[*O* III]	6	6		5801.4	*C* IV	2	0	
4541.6	*He* II	3	1						

1. Blend.
2. Plaskett estimates intensity 6 on ultraviolet spectra.

In reality, neither their nebular nor their auroral transitions are observed.[17] This is certainly an effect of ionization, as [*O* II] and [*O* I] are also absent despite the high intensity of [*O* III]. This is quite different from what we normally observe in planetary nebulae and in the nebulosities of slow post-novae. For example, in Nova Herculis, 1934, we observe at the present time [*O* I], [*O* II], [*N* II], [*S* II], [*Fe* VII], and other elements,[18] in addition to strong [*O* III], [*Ne* III], and [*Ne* V]. Essentially similar elements are also present in the extremely slow nova RT Serpentis, 1909. The absence of other stages of ionization in the nebulosity of Z Andromedae suggests that this nebulosity consists of a rather thin layer.

The intensities of the nebular and nuclear lines, which we observed in the summer of 1940, closely resemble those observed by Plaskett[1] in 1923–1926. Table 3 contains those lines which Plaskett attributed to the "nebular part" and which are not seriously blended with lines of the P Cygni spectrum. There are only minor differences in the intensities. We conclude that the nucleus and the nebula have not been appreciably altered by the outburst.

It is of great interest to compare Z Andromedae with the binaries of similar excitation. T Coronae Borealis, which, like Z Andromedae, consists of an M-type star and of a nova-like companion, has shown an irregular increase in brightness since 1936. The forbidden

[17] [*O* I], [*O* II], and [*N* II] were also absent on Plaskett's spectrograms.

[18] *Ap. J.*, **92**, 295, 1940.

lines now present in its spectrum belong to [*O* III], [*O* II], and [*Ne* III].[8] Hachenberg and Wellmann[19] have shown that the nebulosity of T Coronae was optically too thin to permit the application of the theory of Zanstra, which requires complete absorption of all the nuclear radiation beyond the Lyman limit. In RW Hydrae [*O* II] is extremely weak, whereas [*O* III] and [*Ne* III] have similar intensities.[10]

The striking intensity of the transition of auroral type, λ 4363, compared with the transitions of nebular type, N_1 and N_2, is well known in the novae at the beginning of their nebular stages. It is also a characteristic feature of all similar binaries, such as T Coronae, AX Persei, CI Cygni, RW Hydrae, etc. On the other hand, in only one planetary nebula observable in our latitude, IC 4997, is the auroral transition λ 4363 very strong compared with N_1 and N_2. In almost all other nebulae, N_1 and N_2 are much stronger than λ 4363.[20] Actually, IC 4997 is often considered as an object intermediate between nebulae and stars. The following section contains a description of its spectrum.

V. THE SPECTRUM OF IC 4997

Except for the high intensity of λ 4363, the spectrum of IC 4997 has the usual appearance of a planetary nebula, according to W. H. Wright[21] and R. H. Stoy.[22] It is certainly not a nebula of very high excitation,[23] because [*Ne* V] is absent. On the other hand, there is no reason to suspect an abnormally low abundance of oxygen, nitrogen, etc. Hence, the cooling effect[24] of the elements other than *H* upon the electrons, resulting from the photoionization of hydrogen, must be of the usual type. According to the work of Menzel and his collaborators,[25] the presence of a strong λ 4363 implies that the electron density of IC 4997 is much higher than in the other nebulae thus far investigated—say between 10^5 and 10^6 electrons per cubic centimeter, instead of 10^4. The following questions arise in connection with this stellar planetary: (*a*) Of what type is the exciting nucleus (which has not been observed previously)? (*b*) How do the elements other than [*O* III] behave? (*c*) Is there any way to observe "stratification-effects" in stellar planetaries of higher electron density and in which slitless spectra cannot reveal appreciable differences among the monochromatic images?

We secured in June and August, 1940, four spectrograms of IC 4997 with the 82-inch McDonald reflector. Three were taken with the quartz prisms and the F/2 Schmidt camera (exposures, 1^h20^m, 1^h57^m, 8^h44^m). The fourth was obtained with the glass prisms and the same camera (exposure, 8^h40^m). On the two long-exposure spectrograms the continuous spectrum is relatively strong and the Balmer continuum is very strong, extending at least to λ 3300. Superimposed on the strong Balmer continuum are eight lines of *He* I which we could measure only with difficulty;[26] these have not been included in Table 4, which contains all the other lines. The radial velocities given by the different lines are entirely consistent, and Table 4 gives the wave lengths corrected for the motion of the object.

[19] *Zs. f. Ap.*, **17**, 246, 1939.

[20] The majority of the brighter Magellanic nebulae are similar to IC 4997 (C. and S. Gaposchkin, *op. cit.*, p. 316, 1938).

[21] *Lick Obs. Pub.*, **13**, 193, 1918.

[22] *Lick Obs. Bull.*, **17**, 179, 1935.

[23] Even if the excitation were high, this would not have a great influence upon the electron temperature. Menzel and his collaborators have shown that the electron temperatures, which range from 6,000° to 10,000°, seem to be independent of the temperature of the central star.

[24] Because of the loss of energy by the electrons in the collisional excitation of the metastable levels of *O* III, *Ne* III, etc. (Menzel).

[25] Series of papers in *Ap. J.*, 1938–1940.

[26] Wave lengths: λλ 3634 (2), 3614 (2), 3599 (1), 3587 (1), 3554 (1), 3537 (1), 3530 (1), 3517 (1).

a) THE SPECTRUM OF THE NUCLEUS

The main characteristic of the nucleus is the group from λ 4637 to λ 4690. There is probably also a trace of *N* III 4634. Some *He* I lines seem to have weak P Cygni absorption components, which would indicate that *He* I plays some role in the nuclear spectrum. There is also a trace of *N* IV 4058 and of *C* III 4070, which belong to the nucleus.

It is immediately seen that the group of *N* III, *C* III, and *C* IV lines near λ 4650 is similar to that observed in the nucleus of Z Andromedae. *C* III and *C* IV are of the regular Wolf-Rayet type; *N* III is more nearly of the 9 Sagittae type. The nucleus must

TABLE 4

LIST OF LINES IN IC 4997

λ	Int.	Identification			Note	λ	Int.	Identification			Note
		Elem.	λ	Int.				Elem.	λ	Int.	
3676.7	1	H_{22}	3676.36	.....		4143.56	2	*He* I	4143.77	15	
3679.5	1	H_{21}	3679.35	.....		4340.63	12	*Hγ*	4340.46	200	W
3683.0	1	H_{20}	3682.81	.....		4363.25	15	[*O* III]	4363.2	.....	W
3687.0	2	H_{19}	3686.83	.....		4387.79	3	*He* I	4387.93	30	
3691.69	3	H_{18}	3691.56	2		4471.41	6	*He* I	4471.48	100	W
3696.98	3	H_{17}	3697.15	3		4637.06	2A	*N* III	4640.64	10	
3703.87	3	H_{16}	3703.85	4	W	4640.64	2En				
3711.91	4	H_{15}	3711.97	5	W						
3721.92	4	H_{14}	3721.94	6	W	4645.22	2A	*C* III	4647.40	10	
3726.1	7	[*O* II]	3726.12	.....	W1	4649.11	2⁺En	*C* III	4650.16	9	
3728.7	5	[*O* II]	3728.91	.....				*C* III	4651.35	8	
3734.25	4	H_{13}	3734.37	8	W						
3744.37	1	.....	.....	.....		4653.33	1⁺A	*C* IV	4658.64	5	
3750.03	5	H_{12}	3750.15	10	W	4658.86	2En				
3770.87	5	H_{11}	3770.63	15	W	4685.5	1⁺n	*He* II	4685.81	300	
3797.93	6	H_{10}	3797.90	20	W	4702.2	2n	.....	.....	.....	1
3819.59	3	*He* I	3819.61	50	W	4712.8	3	*He* I	4713.14	40	
3835.53	6	H_9	3835.39	40	W			[*A* IV]	4711.4	.....	
3868.82	15	[*Ne* III]	3868.74	.....	W	4740.6	1–2	[*A* IV]	4740.3	.....	
		He I	3867.5	15		4861.5	18	*Hβ*	4861.34	500	W
3888.48*	7	*He* I	3888.65	1000	W1	4921.8	2⁺s	*He* I	4921.93	50	
3888.99*	8	H_8	3889.05	60		4958.8	20	[*O* III]	4958.91	.....	W
						5006.4	25	[*O* III]	5006.84	.....	W
3964.71	3	*He* I	3964.73	50		5016	4	*He* I	5015.67	100	
3967.40	10	[*Ne* III]	3967.51	.....	W1	5048	1	*He* I	5047.74	15	
3970.14	8	*He*	3970.07	80		5755	3	[*N* II]	5755.0	.....	S
4009.11	2	*He* I	4009.27	10		5876	8	*He* I	5875.62	1000	S
4026.30	4	*He* I	4026.19	70	W	6300	6	[*O* I]	6300.2	.....	S
4058.2	on	*N* IV	4057.8	2		6310	4	[*S* III]	6310.2	.....	S
4068.70	3	[*S* II]	4068.62	.....	W	6364	3	[*O* I]	6363.9	.....	S
4071.0†	1	*C* III	4070.43	8		6548	5	[*N* II]	6548.4	.....	S
4076.37	2	[*S* II]	4076.22	.....	W	6563	25	*Hα*	6562.82	2000	S
4098.0†	0	*N* III	4097.31	10		6584	7	[*N* II]	6583.9	.....	S
4101.70	10	*Hδ*	4101.75	100	W	6678	3	*He* I	6678.15	100	S
4120.67	2	*He* I	4120.81	25							

* Separation difficult.

† Doubtful line.

W. Observed by W. H. Wright.

W. 1. Observed by Wright as a blend.

S. Observed by R. H. Stoy.

1. Also present in BD+30°3639.

be a Wolf-Rayet star containing both *N* III and *C* III and *C* IV. NGC 6543 is another planetary whose Wolf-Rayet nucleus also contains both nitrogen and carbon with similar intensities, but it is of earlier type than in IC 4997. We should classify the nucleus of IC 4997 as W7 or W8. The bright lines are abnormally narrow, but they are appreciably broader than the lines of the nebula.

The simultaneous presence of nitrogen and carbon in several planetary nuclei of Wolf-Rayet type is of great importance for the classification of the Wolf-Rayet stars. Other nuclei are typical members of the usual sequences; for example, the nuclei of Campbell's envelope star[27] and of HD 167362[28] are pure carbon stars containing no nitrogen, despite the high abundance of nitrogen in the surrounding nebulosities.

[27] *Proc. Nat. Acad.*, **26**, 548, 1940.

[28] *Ibid.*, p. 454.

b) THE SPECTRUM OF THE NEBULA

The nebula is responsible for the continuous spectra[29] at the *H* limits, for the Balmer series up to H_{22}, for a rich spectrum of *He* I, and for a large number of forbidden lines. The latter are collected in Table 5.

There is no trace of the auroral transition of [*O* I] at λ 5577, although the transition probabilities are practically the same for [*O* I] and [*O* III].[30] This suggests stratification. We should expect the collisional cross-sections to be of the same order of magnitude for the corresponding metastable levels ^1S of *O* I (4.2 v.) and *O* III (5.3 v.). The different behavior of [*O* I] and [*O* III] may be due to the fact that the O^{++} ions are excited near the nucleus, whereas neutral oxygen occurs mostly at the outskirts of the nebula where the density is considerably reduced. [*S* III] also shows a strong line of the auroral type. It

TABLE 5

FORBIDDEN LINES IN IC 4997

NEBULAR TYPE		AURORAL TYPE		TRANSAURORAL TYPE	
Element	Intensity	Element	Intensity	Element	Intensity
O I	6–3	*O* III	15	*S* II	3–2
O II	7–5	*N* II	3		
O III	25–20	*S* III	4		
N II	5–7				
Ne III	15–9				
A IV	3–2				

would be interesting to search for the auroral transitions of [*O* II] at λλ 7319.0–7330.3 and for the nebular transitions of [*S* II] at λλ 6717.3–6731.5. This region is not covered by our spectrograms. [*Ne* III] is very strong: λ 3869 is certainly as strong as $H\gamma$. On our spectrograms we do not find the auroral transition of [*Ne* III] at λ 3342.8; it must be much weaker than the transitions of nebular type. [*Ne* III] is probably excited in the denser regions near the nucleus, together with [*O* III], [*A* IV], and, to a lesser extent, [*S* III]. The absence or weakness of the auroral transition of [*Ne* III] may be due either to the higher excitation potential required (6.9 v.) or to specific atomic properties affecting the collisional cross-section. The ionization potentials of Ne^+ and A^{++} being 40.9 v. and 40.7 v., respectively, we should expect the presence of [*A* IV] because we know that [*Ne* III] is very strong. The auroral transition of [*Ne* III] is also absent in Z Andromedae.

The ratio of intensity of the auroral to the nebular transition is much smaller for [*N* II] than for [*O* III]. This can also be understood if we assume that the collisional cross-sections for [*O* III] and [*N* II] are the same, because N^+ must extend much farther from the nucleus than O^{++}, but not as far as neutral oxygen.

VI. THE SPECTRUM OF THE P CYGNI TYPE OF Z ANDROMEDAE

In the Balmer lines the ratio of intensity of the emission components and the absorption components decreases steadily toward the higher members. From $H\epsilon$ to $H\alpha$ the

[29] A part of the continuous spectrum is probably due to the nucleus.

[30] The transition probabilities are shown in the accompanying table.

	Nebular	($^3P-{}^1D$)	Auroral ($^1D-{}^1S$)
[*O* III]	0.016	0.0055	2.7
[*O* I]	0.013	0.0040	2.8

lines appear purely in emission. The Balmer continuum is still weakly present in absorption,[31] but it has decreased much since last fall, together with the absorption components of the lines of *H*, *Ti* II, *Fe* II, etc.

The radial velocities of the *H* and *He* I lines are collected in Table 6; all the Balmer lines with definite P Cygni characteristics have been included (from H_{15} to H_9), and they give very consistent results.

The lines of *Ti* II, *Fe* I, and [*Fe* II] are all very weak, and some identifications may be doubtful, but their presence may be regarded as very probable. The extreme weakness of [*Fe* II] and the absence of forbidden lines of any other element indicates that the P Cygni layer is rather dense or that its distance from the exciting nucleus is small.

In many respects this part of the spectrum is very similar to the present spectrum of BD+11°4673,[9] which also shows *Fe* I, *Ca* I, *Si* I, and *Si* II; but higher stages of excita-

TABLE 6

RADIAL VELOCITIES OF THE LINES OF P CYGNI TYPE

(In Km/Sec)

Lines Used	vEmission	vAbsorption	Differences
Balmer lines	+46.2	−37.2	83.4
λ 3889 *He* I	+50.1	−60.9	111
Other *He* I lines	+27	−53.8	80.8

tion are present in BD+11°4673. Of course, the comparison with a P Cygni type star which is single may be quite artificial, as the presence of the late-type companion may substantially distort the P Cygni layer. The dilution effect is apparent in the absorption component of *He* I 3889. This line, which arises from the metastable $2s^3S$ level, shows a fairly strong absorption component. The line λ 3965, which arises from the metastable $2s^1S$ level, is complicated by the strong neighboring line of [*Ne* III] 3967, but we believe that it has also a violet absorption line. In the series ($2p^3P^o$ — nd^3D) of *He* I, λ 4026 shows an absorption line of intensity 2, while λ 4472 shows one of intensity 1. The fact that these triplet lines are present at all in absorption proves that the dilution is not excessive. The dilution factor can hardly be less than 0.01, and we doubt that it is more than 0.1. The P Cygni type shell should, therefore, have a radius $r \sim 5R$.

The selectivity observed in the *Si* II spectrum is striking. The presence of the group λλ 3853.7–3856.0–3862.6 ($3s\,3p^2\,{}^2D$ — $3s^2\,4p\,{}^2P^o$) is certain, although the group λλ 4128–4130 ($3s^2\,3d\,{}^2D$ — $3s^2\,4f\,{}^2F^o$) is absent; this had been noticed by H. H. Plaskett. It is also observed in P Cygni itself and in BD + 11°4673.[9] It may be due to the fact that the lower level $3s\,3p^2\,{}^2D$, although not really metastable, is connected with the ground level $3s^2\,3p\,{}^2P^o$ by a weak transition (weak lines at λ 1817 and λ 1808). It should be noticed that the electron configuration of the ^2D level is $3s\,3p^2$, whereas all the other terms giving strong lines are due to the addition of one excited electron to the closed subshell $3s^2$.

VII. CONCLUSIONS

During the outburst of Z Andromedae in 1939 the only spectrum which could be observed was that of the P Cygni type expanding shell. The M spectrum, the spectrum of the nebula, and that of the nucleus were not visible. At the time of our observations the visual magnitude of Z Andromedae was 8.2.

In the summer of 1940, when the visual magnitude was 9.7, the P Cygni shell was still present, but the violet-absorption components were weaker and the emission spectrum

[31] On Plaskett's spectrograms the Balmer continuum was in emission. On a spectrogram which we have taken on January 5, 1941, the Balmer continuum is clearly in emission and the P Cygni features are no longer visible.

had changed from that corresponding to an A star to one corresponding to a B star. Its evolution resembled that of a slow nova and evidently approached the kind of spectrum which Plaskett observed in 1923–1926. The forbidden lines of [*Fe* II], which were strong on Plaskett's plates, were still very weak on our 1940 plates.

The velocity of expansion of this shell has been approximately 100 km/sec. Since about 450 days have elapsed since the beginning of the outburst, the shell must have expanded over a distance of about 10^9 km. But the observable spectrum of the shell may not come from the same layer if material is being fed into the expanding mass over an appreciable period of time. Hence, the value of 10^9 km represents the upper limit of our estimate for the present distance between the P Cygni type shell and the surface of the nucleus.

When the star's brightness had declined to magnitude 9.7, the M star, the nebula, and the nucleus were again present in the spectrum. To all appearances they had not changed since before the outburst. It is possible that they never did change appreciably during the outburst and that their absence in the fall of 1939 was caused solely by the brightness of the P Cygni shell which required relatively short exposures. A search for the strong nebular emission line *He* II 4686 on our best plates of last fall shows that it was not visible at that time, also that it would not have been complicated by blending with strong lines of the P Cygni spectrum. The very strong nebular line should have shown quite readily with the shorter exposure required for Z Andromedae last fall, provided it was not superposed over a strong continuous spectrum. Whether it would still have been visible on top of the continuous spectrum is difficult to decide, but we have the impression that the line was really weaker last fall.

It is of interest to compute the relaxation time, τ, considered by Grotrian.[32] If we suppose that the ultraviolet exciting radiation of the nucleus was completely extinguished by the dense P Cygni shell in 1939 and that the nebular radiation had ceased completely, then τ would measure the length of time a pure hydrogen nebula would require to return to within 1.67 mag. of the final (normal) brightness. We follow Grotrian, but assume for the radius of the nucleus

$$R^* = 0.3R\odot ,$$

$$T^* = 70{,}000^\circ .$$

We also assume, following Menzel, that the

$$\text{Number of electrons per cm}^3 = 10^6 .$$

Using Cillié's data for hydrogen, we find for the volume of the nebula

$$V = 10^{48}\text{cm}^3$$

and

$$\tau \sim 2 \times 10^6 \text{ sec} \sim 3 \text{ or } 4 \text{ weeks} .$$

This is quite consistent with the observations, if we assume that the P Cygni shell in August, 1940, was completely transparent to the ionizing radiation.

The remarkable similarity of the nebular spectrum before and after the outburst suggests that its distance from the nucleus is great compared with the radius of the P Cygni type shell. The best estimate we can get for the latter depends upon the dilution factor:

[32] *Zs. f. Ap.*, **13**, 228, 1937.

$r = 5R^*$. The radius of the nucleus is not known. But all available evidence points to a radius R^* for a nova-like object which is considerably smaller than the radius of the sun.[33] If we adopt $R^* = 0.3R\odot$, the radius of the P Cygni type shell would be about $1.5R\odot$ or, roughly, 10^6 km. This is much smaller than the upper limit derived from the velocity of expansion. We are inclined to believe that the phenomenon cannot be treated as a single, thin layer which expands with a velocity of 100 km/sec. This is not surprising, since in all normal P Cygni type stars we are already accustomed to think of a continuous process of ejection. Once we accept the order of magnitude suggested for R^*, the small radius of the P Cygni shell follows from the dilution effect and from the weakness of the forbidden lines.

The radius of the nebula remains unknown. But the order of its size may be inferred from the estimate of the volume which we have made previously:

$$V = 10^{48}\text{cm}^3 .$$

If the entire sphere were occupied, we should find for the radius

$$r_{\text{nebula}} = 10^{16}\text{cm} = 10^{11}\text{km} .$$

This is of the same order of magnitude as the radius of the forbidden [*Fe* II] nebula which surrounds the B-type companion of α Scorpii.[34] This nebula, located at a distance of 100 parsecs, has a radius of 3″.

The entire picture of the system agrees well with that which results from Kuiper's dynamical theory[35] of binaries, such as β Lyrae, WY Gem, etc. The late-type component of Z Andromedae must be a supergiant, and its outer atmosphere may have a radius which is considerably larger than that determined with the interferometer for α Orionis and α Scorpii. It is entirely possible that the nebular material of Z Andromedae is concentrated within the limiting surface computed by Kuiper.

We are indebted to Professor Leon Campbell of the Harvard Observatory for information concerning the light-curve of Z Andromedae, and to Dr. D. M. Popper for some of the spectrograms taken last winter.

McDonald Observatory
and
Yerkes Observatory
September 1940

[33] We are indebted for this suggestion to Dr. G. P. Kuiper.

[34] *Ap. J.*, **92**, 316, 1940.

[35] *Ap. J.*, **93**, 133, 1941.

REVIEWS

Atlas of Spectra of Nova Herculis, 1934. By F. J. M. STRATTON and W. H. MANNING. Introduction + 16 unbound plates. Cambridge: Cambridge University Press, 1939. 25*s*.

The *Atlas* represents a selection of spectrograms from twenty-six observatories, so chosen that the period of time from the outburst of the nova in December, 1934, to the drop in April, 1935, is covered as uniformly as possible.

The authors have enlarged all spectrograms to the same scale; this has resulted in a spottedness in the appearance of the reproductions where spectra of high and low dispersion are situated near each other. It is, however, at best a difficult problem to render homogeneous reproductions of spectrograms of widely different dispersions, and in particular in the case of as evanescent an object as a nova we are fortunate in having a series of this quality and completeness.

The *Atlas* was published under the auspices of the International Astronomical Union.

W. W. M.

An Introduction to Astronomy. By ROBERT H. BAKER. 2d ed. New York: D. Van Nostrand Co., 1930. Pp. 315. $3.00.

The chapters on galactic and extragalactic structure have been entirely re-written for the second edition of this abbreviated version of Professor Baker's well-known textbook. The author has also introduced numerous minor alterations in the text and has given space to the most important advances during the past few years.

ERRATUM
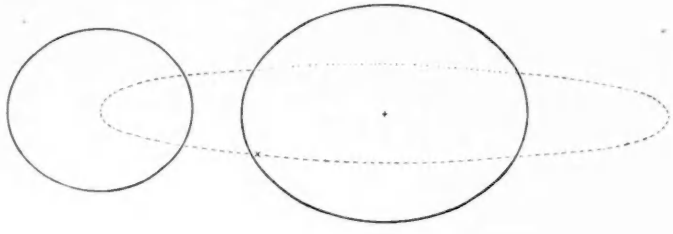
The small circle in the lower right-hand corner of Figure 1 of the article by Z. Kopal on page 100 of the January, 1941, issue was inadvertently omitted. The correct figure is reproduced herewith.